

GPR55 as a novel target in disease control of multiple sclerosis

**Barts and the London School of Medicine and Dentistry
Queen Mary University of London, United Kingdom**

Sofia Sisay

DEDICATION

I would like to dedicate this thesis to my Mother

ACKNOWLEDGEMENTS

I would like to thank to all those who have supported me throughout my PhD studies. I am sincerely thankful to my supervisors Prof. David Baker, Dr Greg Michael, Dr. Samuel Jackson and Gavin Giovannoni for their continuous guidance and support. In particular, I would like to express my gratitude to Prof. David Baker for his expertise, mentoring and patience throughout my PhD studies.

I would like to thank Andy Irving (University of Dundee) for his assistance with signalling assays and for providing GPR55 antibodies. I would also like to thank Dr. Dave Selwood (The Wolfson Institute for Biomedical Research, UCL) for providing VSN16R. I would like to thank Dr. Gareth Pryce for helping me with EAE experiments.

It has been a pleasure to work with everyone in the Neuroimmunology Research Group (Blizard Institute, Queen Mary University of London) who are a friendly and enthusiastic team to work with.

I would also like to thank The Multiple Sclerosis Society of Great Britain and Northern Ireland for funding this PhD project.

Avslutningsvis önskar jag framföra mitt tack till min familj, min släkt och mina vänner som på olika sätt har uppmuntrat mig under resans gång. Framförallt vill jag tacka Priya, Daniel, Mulugeta, Haddy, Weini och Monica för all uppmuntran och stöd under mina studier.

TABLE OF CONTENTS

DEDICATION	2
ACKNOWLEDGEMENTS	3
TABLE OF CONTENTS.....	4
LIST OF FIGURES	8
LIST OF TABLES.....	10
LIST OF SUPPLEMENTARY FIGURES.....	11
ABBREVIATIONS	12
ABSTRACT.....	15
CHAPTER 1 Introduction	16
1.1 Cannabinoids and Cannabinoid receptors	16
1.1.1 Cannabinoid CB ₁ and CB ₂ receptor ligands	17
1.1.2 Endocannabinoid system	20
1.2 Non-CB ₁ /non-CB ₂ receptors possibly related to the cannabinoid system	21
1.2.1 GPR119.....	21
1.2.2 GPR18.....	21
1.2.3 GPR35.....	22
1.3 G-protein coupled receptor 55(GPR55)	23
1.3.1 GPR55.....	23
1.3.2 Distribution of GPR55	24
1.4 Putative GPR55 ligands, endocannabinoids and cannabinoids	24
1.4.1 Anandamide.....	25
1.4.2 2-Arachidonoyl Glycerol.....	25
1.4.3 Tetrahydrocannabinol.....	25
1.4.4 Rimonabant.....	26
1.4.5 CP55, 940	26
1.4.6 WIN 55,212-2	26

1.4.7 Cannabidiol	27
1.4.8 Abnormal cannabidiol.....	27
1.4.9 O-1602.....	27
1.4.10 O-1918.....	28
1.4.11 Lysophosphatidylinositol	28
1.4.12 Other ligands.....	28
1.5 GPR55 signalling and intracellular mechanisms	30
1.6 Biological function of GPR55.....	30
1.7 GPR55 and cancer	31
1.8 Multiple sclerosis (MS).....	32
1.8.1 Pathogenesis of MS.....	35
1.8.2 MS therapies	36
1.8.3 Cannabis and MS.....	39
1.8.4 Spasticity, cause and incidence.....	39
1.9. Anti-spastic drugs and mechanisms.....	39
1.10 Cannabinoids in Spasticity	40
1.10.1 Symptomatic control.....	40
1.11 3-(5-dimethylcarbamoyl-pent-1-enyl)-N-(2-hydroxy-1-methyl-ethyl)benzamide (VSN16).....	43
1.11 AIMS AND OBJECTIVES.....	45
CHAPTER 2 Material and Methods	46
2.1 Mice	46
2.2 PCR	46
2.3 Antibody production	52
2.4 Enzyme Linked Immunosorbent Assay (ELISA)	53
2.5 Antibody isotyping ELISA	54
2.6 Western blotting.....	54
2.7 Immunofluorescence	54
2.8 cAMP Response Element-binding Protein staining.....	55

2.9 Phalloidin staining.....	55
2.10 Flow cytometry	55
2.11 Calcium signalling.....	56
2.12 Quantitative PCR (qPCR)	56
2.13 ³⁵ S Oligonucleotide in <i>situ</i> hybridization.....	60
2.14 Non-Radioactive <i>In situ</i> Hybridization (NR-ISH).....	62
2.15 EAE	63
2.16 Spastic measurement.....	66
2.17 Flow cytometry analysis-surface and cytokine staining	67
2.18 MOG and Con A proliferation assay.....	68
CHAPTER 3 Molecular characterization of GPR55 knockout mice.....	70
3.1 Introduction	70
3.2 Results.....	73
3.2.1 Genetics of GPR55 knockout mice	73
3.4 Discussion.....	77
CHAPTER 4 Production of GPR55 reactive antibodies and characterization of astrocytoma cell lines	78
4.1 Introduction	78
4.2 Results.....	80
4.3 Discussion.....	90
CHAPTER 5 Expression profile of GPR55 mRNA levels in various tissues	96
5.1 Introduction	96
5.2 Results.....	100
5.3 Discussion.....	107
CHAPTER 6 Immune function of GPR55 in Neuroinflammation	109
6.1 Introduction	109
6.2 Results.....	111
6.3 Discussion.....	129

CHAPTER 7 Spasticity	133
7.1 Introduction	133
7.2 Results.....	135
7.3 Discussion.....	147
CHAPTER 8 Final conclusions	149
APPENDIX Supplementary data	188

LIST OF FIGURES

Figure 1.1 Structure of CB ₁ and CB ₂ receptors.....	18
Figure 1.2 Structures of cannabinoid agonists	19
Figure 1.3 The course of multiple sclerosis	34
Figure 2.1 GPR55 gene (Gpr55 gene) deletion construct	50
Figure 2.2 Clinical Disease Course of Chronic Relapsing Experimental Allergic Encephalomyelitis.....	65
Figure 2.3 Figure 2.3 Protocol of spastic measurement	66
Figure 2.4 Limb stiffness.....	67
Figure 3.1 GPR55 knockout targeting strategy.....	72
Figure 3.2 GPR55 knockout targeting southern data	73
Figure 3.3 Genotyping-PCR Detection of GPR55 Alleles using the polymerase chain reaction	74
Figure 3.4 Genotyping-PCR Detection of GPR55 Alleles using the polymerase chain reaction	75
Figure 4.1 Detection of GPR55 Alleles using the novel designed polymerase chain reaction	79
Figure 4.2 Antibody isotyping	81
Figure 4.3 CREB activation	82
Figure 4.4 Phalloidin staining	83
Figure 4.5 Calcium signaling	84
Figure 4.6 Immunofluorescence-GPR55 antibody staining	85
Figure 4.7 GPR55 rabbit polyclonal antibody	86
Figure 4.8 Hybridomas	87
Figure 4.9 Western blotting	88
Figure 4.10 Flow cytometry	89
Figure 5.1 GPR55 standard curve: Amplification of a GPR55 amplicon	99
Figure 5.2 GPR55 standard curve: standard curve samples run on agarose	100
Figure 5.3 GPR55 mRNA levels.....	101
Figure 5.4 In situ hybridization was used for detection of GPR55 mRNA levels in GPR55 transfected cell line (E1 DBT), non-transfected (DBT) and mouse brain WT and KO tissues.....	102
Figure 5.5 Non-radioactive in situ hybridization in the testis	103
Figure 5.6 Non-radioactive in situ hybridization in WT BDT and E1 (GPR55) DBT cell lines	104
Figure 6.1 Immunophenotyping of lymphocytes from naïve C57BL/6.GPR55 ^{-/-} and C57BL/6 ^{+/+} mice.....	111
Figure 6.2 Immunophenotyping of blood lymphocytes from naïve C57BL/6.GPR55 ^{-/-} and C57BL/6 ^{+/+} mice	112

Figure 6.3 Spleen and blood monocytes and dendritic cells from C57BL/6.GPR55 ^{-/-} and C57BL/6 ^{+/+} mice.....	113
Figure 6.4 Thymus and lymph node T-cell immunophenotypes	114
Figure 6.5 Con A and MOG 35-55 proliferation assays	115
Figure 6.6 Experimental autoimmune encephalomyelitis	116
Figure 6.7 Immunophenotyping of spleen cells from in vivo and/or in vitro MOG stimulated C57BL/6.GPR55 ^{-/-} and C57BL/6 ^{+/+} mice	118
Figure 6.8 IL-4 cytokine responses in T- and B-cells from MOG stimulated C57BL/6.GPR55 ^{-/-} and C57BL/6 ^{+/+} mice	119
Figure 6.9 IL-17A cytokine responses in T- and B-cells from MOG stimulated C57BL/6.GPR55 ^{-/-} and C57BL/6 ^{+/+} mice	120
Figure 6.10 IFN- γ cytokine responses in T- and B-cells from MOG stimulated C57BL/6.GPR55 ^{-/-} and C57BL/6 ^{+/+} mice	121
Figure 6.11 IL-10 cytokine responses in T- and B-cells from MOG stimulated C57BL/6.GPR55 ^{-/-} and C57BL/6 ^{+/+} mice	122
Figure 6.12 Fox 3P responses in T- and B-cells from MOG stimulated C57BL/6.GPR55 ^{-/-} and C57BL/6 ^{+/+} mice	123
Figure 6.13 CFSE proliferation assay.....	124
Figure 6.14 Experimental autoimmune encephalomyelitis in ABH mice.....	125
Figure 6.15 Relapse remitting experimental autoimmune encephalomyelitis	126

LIST OF TABLES

Table 1.1 GPR55 agonists and antagonists.....	29
Table 1.2 Symptomatic treatments in MS.....	41
Table 2.1 PCR components for GPR55- specific primers.....	48
Table 2.2 PCR components for Neomycin primers.....	49
Table 2.3 PCR components for multiplex PCR with primers specific for GPR55 and Neomycin.....	51
Table 2.4 Reference gene GAPDH.....	57
Table 2.5 Reference gene 36B4.....	58
Table 2.6 Quantitative PCR components for GPR55.....	59
Table 2.7 Intracellular cytokine and β -actin reference gene primers.....	69
Table 2.8 Quantitative PCR components for cytokines.....	69
Table 5.1 Mouse GPR55 mRNA levels.....	94
Table 5.2 Human GPR55 mRNA levels.....	96
Table 5.3 Human GPR55 mRNA levels in cell lines.....	97
Table 5.4 Reference genes GAPDH and 36B4.....	98
Table 6.1 Function of GPR55 in Neuroinflammation-C57BL/6 mice.....	115
Table 6.2 Function of GPR55 in Neuroinflammation in ABH mice.....	125
Table 7.1 Physiochemical properties of compounds.....	138
Table 7.2 VSN16R Does not induce weight loss following repeated administration.....	140

LIST OF SUPPLEMENTARY FIGURES

Supplementary Figure 1: TG0039 Project Materials- GPR55 mouse deletion sequence.....	188
Supplementary Figure 2A: FACS raw data –immunophenotyping of naïve animals	199
Supplementary Figure 2B: FACS raw data –immunophenotyping of naïve animals	200
Supplementary Figure 2C: FACS raw data –immunophenotyping of naïve animals	201
Supplementary Figure 2D: FACS raw data –immunophenotyping of naïve animals	202
Supplementary Figure 2E: FACS raw data –immunophenotyping of naïve animals	203
Supplementary Figure 2F: FACS raw data –immunophenotyping of naïve animals	204
Supplementary Figure 3: FACS raw data – IFN γ and IL-10 cytokine responses in T- and B-cells from MOG in vivo stimulated C57BL/6.GPR55 $^{-/-}$ and C57BL/6 $+/+$ mice	205
Supplementary Figure 4: FACS raw data – IFN γ and IL-10 cytokine responses in T- and B-cells from MOG in vivo and in vitro stimulated C57BL/6.GPR55 $^{-/-}$ and C57BL/6 $+/+$ mice:.....	206
Supplementary Figure 5: FACS raw data – IL-4 and IL-17A cytokine responses in T- and B-cells from MOG in vivo stimulated C57BL/6.GPR55 $^{-/-}$ and C57BL/6 $+/+$ mice.....	207
Supplementary Figure 6: FACS raw data – IL-4 and IL-17A cytokine responses in T- and B-cells from MOG in vivo and in vitro stimulated C57BL/6.GPR55 $^{-/-}$ and C57BL/6 $+/+$ mice.....	208
Supplementary Figure 7: FACS raw data – CFSE proliferation assay	209
Supplementary Figure 8: FACS raw data – Fox 3P responses in T- and B-cells from MOG stimulated C57BL/6.GPR55 $^{-/-}$ and C57BL/6 $+/+$ mice.....	210
Supplementary Figure 9: Experimental autoimmune encephalomyelitis in CB2 knockout animals.....	211

ABBREVIATIONS

Abn-Cbd	Abnormal cannabidiol
AP	Acute pancreatitis
ABHD6 and ABHD12	Alpha-beta-hydrolase domain 6 and 12
Anandamide	N-arachidonylethanolamine
2-AG	2-Arachidonoyl glycerol
β arr2	β -arrestin2
BBB	Blood:Brain:Barrier
BSA	Bovine serum albumin
cAMP	Cyclic adenosine monophosphate
CBD	Cannabidiol
CB	Cannabinoid
CB ₁	Cannabinoid receptor 1
CB ₂	Cannabinoid receptor 2
CB ₃	Cannabinoid receptor 3
CD	Cluster of differentiation
CFA	Complete Freund's Adjuvant
CFSE	Carboxyfluorescein succinimidyl ester
CNS	Central nervous system
CREAE	Chronic relapsing experimental allergic encephalomyelitis
CREB	cAMP Response Element-binding Protein
DAG Lipase	Sn-1-diacylglycerol lipases (DAGL α and DAGL β)
DBT	murine Delayed Brain Tumor
DEPC	Diethylpyrocarbonate
DIG	Digoxigenin
dH ₂ O	Distilled H ₂ O
DMEM	Dulbecco's modified eagle medium
DTT	Dithiothreitol
EAE	Experimental autoimmune encephalomyelitis
EBV	Epstein Barr virus
ECL	Chemiluminescence
ELISA	Enzyme linked immunosorbant assay
ERK	Extracellular signal-regulated kinase
FAAH	Fatty acid amide hydrolase

FABP	Intracellular fatty acid binding proteins
FITC	Fluorescein isothiocyanate
GAPDH	Glyceraldehyde-3-phosphate dehydrogenase
GPCR	G protein-coupled receptor
GPR55	G-coupled receptor 55
GDP	Guanine diphosphate
GTP	Guanine triphosphate
HAT	hypoxanthine-aminopterin-thymidine
HEK	Human embryonic kidney
HHV6	Human herpesvirus type 6
HP	horseradish peroxidase
HSV	Herpes simplex
HT	hypoxanthine-thymidine
IL	Interleukin
IP3	Inositol triphosphate
KOMP	Knockout mouse project
LPI	Lysophosphatidylinositol
MAB	Maleic Acid Buffer
MAG lipase	Monoacylglycerol lipase
MAPK	Mitogen-activated protein kinase
MECA	Melancortin, endothelial, differentiation gene, cannabinoid, adenosine
MHC	Major histocompatibility complex
MMP	Matrix metalloproteinases
MOG	Myelin oligodendrocyte glycoprotein
MRI	Magnetic resonance imaging
mRNA	Messenger ribonucleic acid
MS	Multiple sclerosis
MUSEC	Multiple Sclerosis and Extract of Cannabis
NAGly	N-arachidonoyl glycine
NAPE-PLD	N-acyl-phosphatidylethanolamine selective phospholipase D
OEA	Oleoylethanolamide
PFA	Paraformaldehyde
PEA	Palmitoylethanolamide
PEG	Polyethylene glycol
PLA ₁	Phospholipase A ₁

PLC	Phospholipase C
PBMC	Peripheral Blood Mononuclear Cell
PPMS	Primary progressive multiple sclerosis
PTX	<i>Bordetella pertussis</i> toxin
RhoA	Ras homolog gene family, member A
RPMI	Roswell Park Memorial Institute
RRMS	Relapsing-remitting multiple sclerosis
SD	Standard deviation of the mean
SEM	Standard error of the mean
SPMS	Secondary progressive multiple sclerosis
TIGM	Texas A&M Institute for Genomic Medicine
TPA	Phorbol ester 12-O-tetradecanoylphorbol-13-acetate
TBE	Tris/Borate/EDTA
THC	Δ^9 -Tetrahydrocannabinol
TE	Tris-EDTA
TMB	3,3',5,5'-Tetramethylbenzidine
TNF- α	Tumour necrosis factor α
VZV	Varicella zoster virus
WB	Western Blotting
q-pcr	Quantitative polymerase chain reaction

ABSTRACT

Multiple sclerosis (MS) is a neurodegenerative disease associated with immune attack of the central nervous system (CNS) leading to neuronal and axonal loss. This affects neurotransmission accumulating residual disability and the development of neurological signs such as spasticity. Numerous studies have reported a beneficial role of cannabinoids in alleviating symptoms associated with neurological damage. The endocannabinoid system has been shown to control experimental spasticity in experimental autoimmune encephalomyelitis (EAE) an animal model of multiple sclerosis (MS). The orphan G-protein coupled receptor 55 (GPR55) has been identified as a functionally –related cannabinoid receptor known to be stimulated by lysophosphatidylinositol. In the current study a novel GPR55 gene knockout mouse and GPR55-transfected cell line was obtained and characterised and the function and distribution of GPR55 was analyzed. Due to the lack of GPR55 specific antibodies, we attempted to generate GPR55-specific monoclonal antibodies in GPR55 knockout mice, however none of these reacted only specifically to the native protein. As alternatives to antibodies, GPR55 mRNA levels were quantified using quantitative polymerase chain reaction (qPCR) and *in situ* hybridization.

The GPR55 knockout mice on the C57BL/6 mouse background failed to generate an autoimmune response during EAE in an initial experiment suggesting that GPR55 controls immune function. Disease was variable in the C57BL/6 mice and EAE was induced in the GPR55 knockout mice on the ABH background and animals developed spasticity. VSN16R is a drug that has shown to inhibit experimental spasticity and binds specifically to GPR55, without the typical side effects associated with cannabis. This compound was found to be an allosteric modulator of GPR55. Animals were treated with VSN16R however the anti-spastic effect remained in the GPR55 knockout mice. Hence, the effect of VSN16R is not mediated by GPR55 in EAE and a novel target needs to be identified.

CHAPTER 1

Introduction

1.1 Cannabinoids and Cannabinoid receptors

The Asian hemp plant *Cannabis sativa* belongs to the family Cannabaceae and contains at least 60 active compounds (Gaoni & Mechoulam., 1964). Despite the fact the plant was discovered many thousands of years ago the major active ingredient of cannabis, Δ^9 tetrahydrocannabinol (THC), was only isolated in 1964 (Brown *et al.*, 2009; Gaoni *et al.*, 1964). After the discovery of the structure of THC there was a debate on whether the drug acted on specific receptors (Brown *et al.*, 2009). However, by using high affinity synthetic chemical autoradiography with radioactively labeled compounds distinct tissue distributions suggestive of an activity of a receptor was identified (Howlett *et al.*, 2002; Howlett *et al.*, 2010). This debate ended in 1990 when the cannabinoid receptor 1 (CB₁) was cloned from a cDNA library of rat cortex (Matsuda *et al.*, 1990). The CB₁ gene is located at chromosome 6q14-q15 and encodes a 472 amino acid residue (Figure 1.1) in humans. The CB₁ receptor is the most abundant G protein coupled receptor (GPCR) in the CNS and has been found to be expressed at high levels in the hippocampus, basal ganglia, cerebral cortex, amygdala, and cerebellum (Glass *et al.*, 1997a; Herkenham *et al.*, 1990; Tsou *et al.*, 1998). The distribution of the CB₁ receptor correlates with the documented effects of cannabinoids including cognitive impairment, memory, motor coordination and induced sign of analgesia (Howlett *et al.*, 2002). The CB₁ receptor is also expressed in other peripheral organs including spleen and tonsils (Galieue *et al.*, 1995; Glass *et al.*, 1997a; Herkenham *et al.*, 1990). CB₁ receptors are located notably presynaptic where they mediate inhibition of ongoing release of a number of different excitatory and inhibitory neurotransmitters (Howlett *et al.*, 2002; Howlett *et al.*, 2010; Wilson *et al.*, 2002). Shortly after the discovery of the CB₁ receptor a second cannabinoid receptor 2 (CB₂) was cloned from human promyelocytic leukaemia cells (Munro *et al.*, 1993). Human CB₂ gene is located at chromosome 1p36.11 and encodes a 360 amino acid residue (Figure 1.1). The CB₂ receptor only shares an amino acid sequence homology of 44% to the CB₁ receptor throughout the total protein (Munro *et al.*, 1993). Most studies indicate a restricted expression profile of CB₂ receptors to the periphery and in lymphoid organs (Munro *et al.*, 1993). Although some studies have suggested neuronal expression of CB₂ receptor this has been inconsistent (Howlett *et al.*, 2002; Nunez *et al.*, 2004). For example, it has been reported that CB₂ receptors can also be expressed on CNS microglial cells under inflammatory conditions (Nunez *et al.*, 2004). CB₂

receptors can modulate immune cell migration and cytokine release both outside and within the brain upon activation (Pertwee, 2005a).

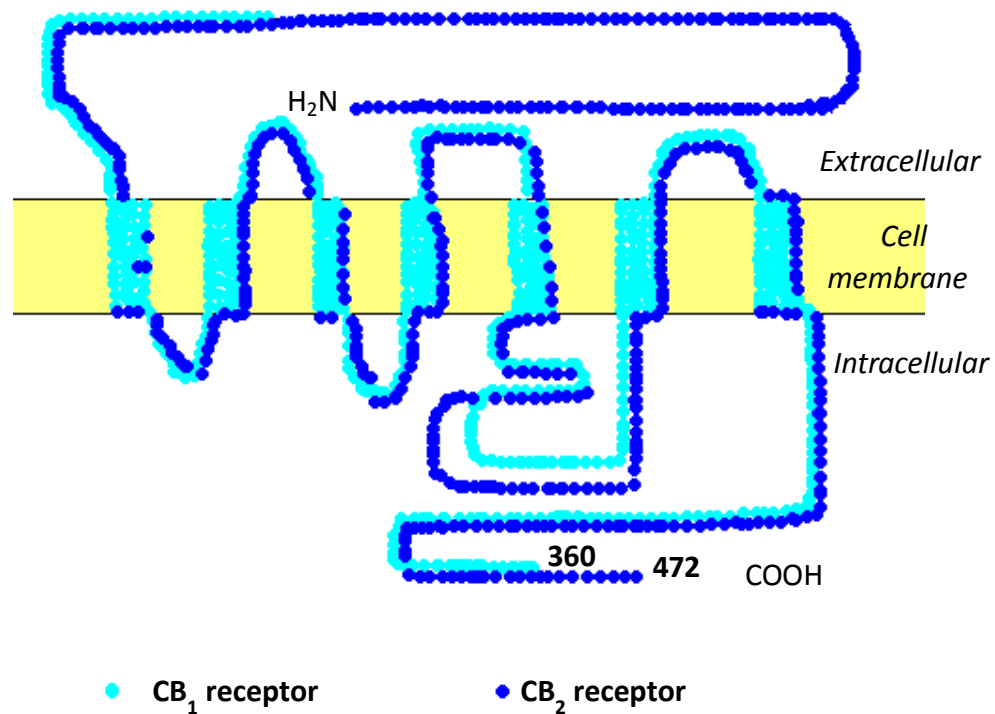
Both receptors belong to a family of G protein-coupled receptors. The receptors are predicted to be composed by seven membrane domain helices, an extracellular N-terminus and an intracellular C-terminus. The heterotrimeric G proteins that predominantly interact with GPCR consist of α , β and γ subunits (Fredriksson *et al.*, 2003). The GPCR main function is to transduce extracellular stimuli into intracellular signals. The receptors are activated by many extracellular ligands including neurotransmitters, lipids, proteins, hormones and chemokines (Kroeze *et al.*, 2003). A conformational change of the receptor occurs upon ligand binding to the GPCRs. Upon G protein complex interaction with an active receptor the GDP (guanine diphosphate) bound to the α subunit is exchanged for GTP (guanine triphosphate) and dissociated from the β/γ subunit. This in turn can lead to the activation of an associated G-protein and depending on the type of G-protein the receptor is coupled to a range of downstream signalling pathways can be activated (Kroeze *et al.*, 2003). CB₁ and CB₂ receptors signalling through G_{i/o} is recurrently exploited in the *in vitro* assays for cannabinoid receptor agonism, ³⁵S GTPγS binding assay and the cyclic adenosine monophosphate (cAMP) assay, used to detect cannabinoid activity (Howlett *et al.*, 2002). CB₁ and CB₂ receptors inhibit adenylyl cyclase and activate mitogen-activated protein kinase (MAPK) activity through their binding to G_{i/o} proteins (Felder *et al.*, 1995; Howlett *et al.*, 1984; Kobayashi *et al.*, 2001) and are *Bordetella pertussis* toxin (PTX) –sensitive (Howlett *et al.*, 2002). In addition CB₁ receptors can signal through G_s proteins (Glass *et al.*, 1997b). Furthermore CB₁ receptors are coupled to calcium channels, inwardly rectifying potassium channels and other ion channels (Howlett *et al.*, 2002; Howlett *et al.*, 2010; Mackie *et al.*, 1995). CB₁ receptors also have one or more allosteric sites that can be targeted by ligands in a manner that augments or inhibits the activation of this receptor by direct agonists (Howlett *et al.*, 2002; Price *et al.*, 2005).

1.1.1 Cannabinoid CB₁ and CB₂ receptor ligands

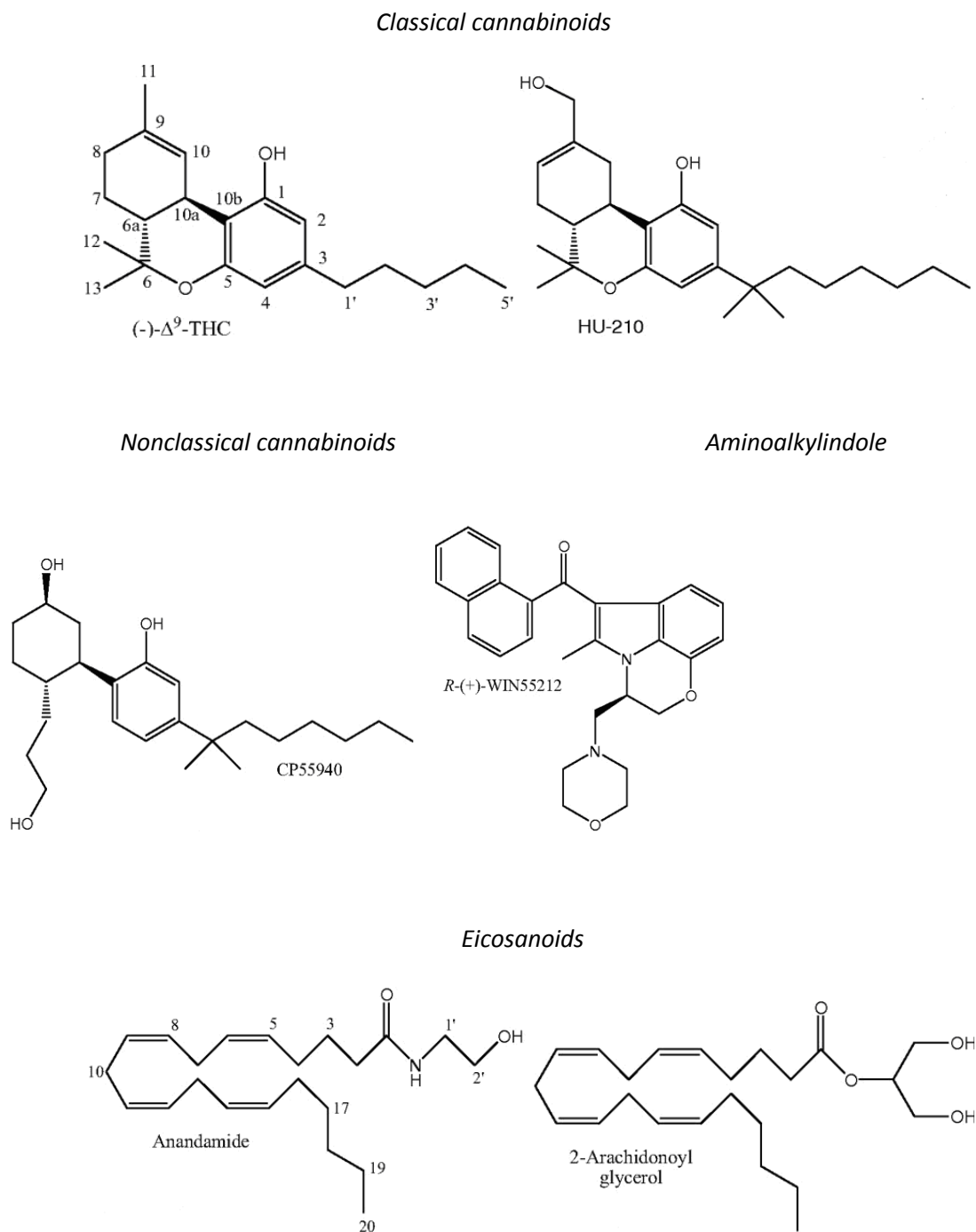
Although cannabinoids were originally defined to describe the dibenzopyran compounds within the cannabis plant, this definition has been extended to any compounds that bind to the cannabinoid receptors (Figure 1.2) (Howlett *et al.*, 2002). Cannabinoid agonists are currently classified in four major groups according to their chemical structures: *classical*, *nonclassical*, *aminoalkylindole* and *eicosanoid* (Howlett *et al.*, 2002). The *classical* group consists of dibenzopyran derivatives and includes Δ⁹-THC the major psychoactive substance in the plant cannabis and compounds such as HU-210 a synthetic analogue of THC (Pertwee, 2005b). The *non-classical* group consists of bicyclic and tricyclic analogues of THC that lack the pyran ring and

includes the synthetic compound CP55,940 (Pertwee, 2005b). *Aminoalkylindole* structures differ distinctly from the classical and non classical cannabinoid agonists one example is WIN 55,212-2, which is a commonly used synthetic research tool (Pertwee, 2005b). The two most studied *eicosanoids* are the endocannabinoids anandamide (*N*-arachidonyl ethanolamine) and 2-arachidonylglycerol (2-AG).

Figure 1.1 Structure of CB₁ and CB₂ receptors



The cannabinoid receptors CB₁ (472 amino acid) and CB₂ (360 amino acid) belong to a family of seven transmembrane receptors with an extracellular N-terminus and an intracellular C-terminus. Each dot represents an amino acid residue (adapted from <http://www.hampapartiet.se/cb1cb2.htm>).

Figure 1.2 Structures of cannabinoid agonists

Structures of cannabinoid receptor agonists that is relatively non-selective for either CB₁ or CB₂ receptors (Pertwee, 2005).

1.1.2 Endocannabinoid system

Endogenous cannabinoid receptor agonists from mammalian tissues were discovered after the cloning of the CB₁ receptor. The two most studied endocannabinoids are anandamide and 2-AG. Anandamide is a natural fatty acid originally isolated from porcine brain (Devane *et al.*, 1992; Melck *et al.*, 1999) and has the ability to bind to and activate CB₁ and CB₂ with a similar potency (Lauckner *et al.*, 2008). The endocannabinoid system regulates signalling between neurons and endocannabinoid ligands and act in a retrograde manner (Howlett *et al.*, 2002; Howlett *et al.*, 2010; (Wilson *et al.*, 2001). Endocannabinoids are derivatives of arachidonic acid that are generated by post-synaptic neurons “on demand” in response to elevations of intracellular calcium resulting from depolarization induced opening of voltage controlled Ca²⁺ channels (Di Marzo *et al.*, 2005; Howlett *et al.*, 2004; Piomelli, 2003). Upon release from the post-synaptic membrane the endocannabinoids diffuse retrogradely across the synapse and this in turn activates the pre-synaptic CB₁ receptors to decrease release of either excitatory or inhibitory transmitters (Howlett *et al.*, 2002; Howlett *et al.*, 2010; Katona *et al.*, 2012). Endocannabinoids appear to be released ‘on demand’ from membrane precursors via multi-step enzymatic pathways upon augmented intracellular calcium after neuronal activation or via stimulation of metabotropic receptors coupled to Gq/11 proteins (Kammermeier *et al.*, 2003). Metabotropic glutamate receptors (mGluRs) have shown to modulate neuronal excitability and transmitter release (Katona *et al.*, 2012). Anandamide can be synthesized through a number of pathways (Battista *et al.*, 2012). N-acyl-phosphatidylethanolamine selective phospholipase D (NAPE-PLD) is considered the major enzyme responsible for the synthesis of anandamide (Okamoto *et al.*, 2009). However, another group have demonstrated that NAPE-PLD deficient mice did not show altered anandamide expression levels compared to wildtype littermates, suggesting that anandamide can also be synthesized through other pathways (Leung *et al.*, 2006). Synthesis of 2-AG is generated via phospholipase C (PLC) mediated hydrolysis of NAPE (Di Marzo, 2008) followed by the activity of the sn-1-diacylglycerol lipases (DAGL α and DAGL β) (Bisogno *et al.*, 2003; Di Marzo, 2008; Wang *et al.*, 2009; Yoshida *et al.*, 2006). Regulation of 2-AG production was recently reported in a study where DAGL α and DAGL β knockout mice were generated (Gao *et al.*, 2010; Tanimura *et al.*, 2010). The main route of synthesis for 2-AG was found to be mediated by DAGL α and retrograde endocannabinoid induced signalling was lost in DAGL α knockout mice. Additionally, adult neurogenesis in both DAGL α and β knockout mice was reduced, compared to wildtype littermates (Gao *et al.*, 2010). 2-AG can also be produced via phospholipase A₁ (PLA₁) hydrolysis of phosphoinositol precursors (Di Marzo, 2008). Endocannabinoids are enzymatically degraded once they have entered the cell. Anandamide and 2-AG are both substrates for fatty acid amide

hydrolase (FAAH) (Cravatt *et al.*, 2001). FAAH is the major degradative enzyme of anandamide *in vivo* whereas 2-AG is degraded by monoglycerol lipase (MAG lipase) and two novel serine hydrolases alpha-beta-hydrolase domain 6 and 12 (ABHD6 and ABHD12) (Blankman *et al.*, 2007; Dinh *et al.*, 2002; Dinh *et al.*, 2004). Intracellular fatty acid binding proteins (FABPs) have been reported to act as carriers for anandamide thereby facilitating its degradation by FAAH (Kaczocha *et al.*, 2009).

Endocannabinoids have been implicated in a number of physiological functions. One of the important roles of the endocannabinoid system is to maintain homeostasis. Altered levels of endocannabinoids have been associated with a number of disorders including pain and inflammation, immunological and neurological conditions and obesity (Andre *et al.*, 2010; Eckel *et al.*, 2005). In obesity, caused by high-fat food intake, upregulated levels of endocannabinoids has shown to be associated with an increased risk for cardiovascular and associated metabolic diseases. A pharmacological blockade of the system could therefore be used for treatment of obesity (Di Marzo, 2008; Eckel *et al.*, 2005). Indeed, the CB₁ receptor antagonist SR141617A (rimonabant) was licenced for the control of dietary intake in obesity, before its withdrawal due to adverse neurobehavioural effects, anxiety, depression and suicidal tendency (Eckel *et al.*, 2005; Pertwee, 2005a).

1.2 Non-CB1/non-CB2 receptors possibly related to the cannabinoid system

1.2.1 GPR119

GPR119 is an intronless GPCR that belongs to the MECA (melancortin, endothelial differentiation gene, cannabinoid, adenosine) group of receptors (Fredriksson *et al.*, 2003). The GPR119 gene is located to chromosome Xq26.1 and encodes a 335 amino acid GPCR in humans (Fredriksson *et al.*, 2003). The receptor is phylogenetically related to cannabinoid receptors and fatty acid amides such as N-oleoyl dopamine, oleoyl ethanolamide, palmitoyl ethanolamide and anandamide bind to GPR119 (Overton *et al.*, 2006). The receptor is expressed in the pancreas, where it is thought to be involved in the control of glucose-dependent insulin release, and in gastrointestinal organs (Lauffer *et al.*, 2008).

1.2.2 GPR18

The GPR18 gene is located to chromosome 13q32.3 and encodes a 331 amino acid GPCR (Gantz *et al.*, 1997; Pertwee *et al.*, 2010). The receptor has been found to be expressed in the lymphoid organ such as spleen, thymus and in peripheral lymphocytes (Gantz *et al.*, 1997; Kohno *et al.*,

2006). N-arachidonoyl glycine (NAGly) is an endogenous lipid that is structurally similar to anandamide. However, NAGly does not activate cannabinoid receptors. NAGly has been shown to induce intracellular calcium mobilization in GPR18-transfected cells (Kohno *et al.*, 2006). GPR18 cells have been found to be PTX-sensitive in the same study suggesting G_i coupling. Anandamide has vasoactive effects on the vasculature independent of CB₁ and CB₂ (Howlett *et al.*, 2002). GPR18 is expressed on the vasculature and immune cells and has been reported to be a vasculature target (Parmar, 2009). GPR18 has also been suggested to be a receptor for abnormal cannabidiol (Abn-Cbd). However, there is currently no data showing the activation of the receptor by CB₁ or CB₂ receptor ligands (Kohno *et al.*, 2006).

1.2.3 GPR35

The GPR35 gene is located to chromosome 2q37.3 and encodes a protein of 309 amino acids (O'Dowd *et al.*, 1998). GPR35 expression has been detected in the rat intestine and mainly in mouse spleen, lymph nodes, small intestine, lung, colon, pancreas, stomach, trachea, adipose and brain. High levels of human GPR35 were also detected in small intestine, colon, spleen, peripheral leucocytes and low levels in stomach, adipose and thymus (O'Dowd *et al.*, 1998; Wang *et al.*, 2006). The metabolite kynurenic acid has been reported as an endogenous ligand for GPR35. GPR35 transfected cells have been shown to be activated by kynurenic acid, no response was seen in vector transfected cells (Wang *et al.*, 2006). Kynurenic acid has been shown to elicit calcium mobilization and inositol phosphate production in a GPR35-dependent manner (Wang *et al.*, 2006). Kynurenic acid has also been shown to stimulate [³⁵S] GTPγS binding in a GPR35-dependent manner and induce internalization of GPR35, this effect was abolished by pre-treatment with PTX suggesting that GPR35 activation by kynurenic acid couples to a PTX-sensitive $G_{i/o}$ pathway (Wang *et al.*, 2006). Kynurenic acid did not activate around 40 other GPCRs including GPR55 (Wang *et al.*, 2006). As GPR35 shares sequence similarity with GPR55 the effect of several cannabinoid ligands has been examined. THC has shown to induce calcium levels in a GPR35 transfected cell line and not in the vector-transfected cells (Oka *et al.*, 2010). In contrast, the ligands CP55940, WIN55212-2 and AM251 did not evoke a response in any of the cell lines (Oka *et al.*, 2010).

1.3 G-protein coupled receptor 55(GPR55)

1.3.1 GPR55

The biological activity of certain cannabinoids and atypical cannabinoids, cannabinoids that do not mediate their effects through CB₁ or CB₂ receptors, as shown in CB₁ or CB₂ deficient mice has prompted some people to hypothesize the existence of a third cannabinoid receptor (CB₃). However, the human genome has been sequenced and there are no highly structurally-related receptors present. This suggests that if present the putative CB₃ is more likely to be functionally related than structurally-related. The orphan receptor G-coupled receptor 55 (GPR55) was identified as a novel cannabinoid receptor in 2006 based on data in the patent literature relating to ligand binding (Baker *et al.*, 2006b). Human GPR55 was cloned in 1999 through an expressed sequence database by conducting homology searches of the amino acid sequences of known G-protein coupled receptors. The orphan receptor belongs to group δ of rhodopsin-like class A receptors (Fredriksson *et al.*, 2003). The gene was mapped to chromosome 2q37 and encodes a 319 amino acid protein in humans (Sawzdargo *et al.*, 1999). Mouse and Rat GPR55 mRNA have been described to be 75-78% identical to human GPR55 (Ryberg *et al.*, 2007). GPR55 however only shares a sequence homology of 13.5% with CB₁ and 14.4% with CB₂ (Baker *et al.*, 2006b). The association of GPR55 with cannabinoids was first described in a patent from GlaxoSmithKline where the interaction was demonstrated in a yeast expression system (Baker *et al.*, 2006). In this system yeast cells expressing human GPR55 were shown to be activated by the CB₁ antagonists AM251 and SR141716A at micro molar concentrations (Brown *et al.*, 2001). A subsequent patent from AstraZeneca (Drnotta *et al.*, 2004) described the binding of GPR55 transfected human embryonic kidney (HEK) cell membranes of the cannabinoid ligands CP55940 and SR141716A and anandamide whereas WIN55212-2 did however not show binding to GPR55 in the same assay (Ryberg *et al.*, 2007). Human GPR55 mRNA has been detected in different parts of the brain, mainly in the caudate nucleus and putamen as shown by Northern blot analysis and *in situ* hybridization (Sawzdargo *et al.*, 1999) and in lymphoid organs such as spleen and thymus (Oka *et al.*, 2009). GPR55 mRNA has been detected in rat hippocampus, thalamic nuclei and in the midbrain (Sawzdargo *et al.*, 1999). Mouse GPR55 mRNA is expressed in the adrenal glands, large dorsal root ganglions (DRG), frontal cortex, striatum, jejunum, ileum, colon and testis (Ryberg *et al.*, 2007). GPR55 and CB₁ receptors have been shown to form heterodimers and can alter each others signalling capacities in HEK293 cells. Co-expression of the receptors has been shown to inhibit GPR55-mediated transcription factor activation, such as nuclear factor of activated T-cells and serum response element, as well extracellular signal-regulated kinase (ERK) 1/2 activation.

Whereas GPR55-mediated signalling was inhibited in the presence of the CB₁ receptor; this effect was not seen when the CB₁ receptor was inactive. However, the signalling properties of the CB₁ were enhanced in the presence of GPR55 (Kargl *et al.*, 2012). Recently the ligand binding properties of GPR55 were analyzed by applying homology modelling. An amino acid residue Lys80 was found to be crucial in GPR55 ligand recognition through a critical hydrogen bonding interaction with the docked ligands (Elbegdorj *et al.*, 2012).

1.3.2 Distribution of GPR55

The distribution of GPR55 has been confirmed from *in situ* hybridization or quantitative polymerase reaction (qPCR). There has been few studies reported using antibody staining. Here it has been reported that GPR55 is expressed on dorsal root ganglion, spinal cord and peripheral nerve (Sanudo-Pena *et al.*, 1999). Whilst this did appear to be selective for the target, it has been a common problem in cannabinoid biology that polyclonal antibodies are non-specific or need to be diluted exceptionally to obtain an apparent signal or there is significant batch variability. This has been the common with CB₁ specific antibodies (Egertova *et al.*, 2000; Grimsey *et al.*, 2008) and notably with CB₂- specific antibodies, which have contributed to the confusion of the expression of CB₂ in the nervous system. (Howlett *et al.*, 2002; Nunez *et al.*, 2004). The influence of dilution and specificity should be avoided if using monoclonal antibodies. However, because there is evolutionary conservation amongst species animals may be immunologically tolerant to targets. However gene knockout animals have not seen their targets and thus could prove a source to make monoclonal antibodies.

1.4 Putative GPR55 ligands, endocannabinoids and cannabinoids

The identification of GPR55 as a putative cannabinoid receptor (Baker *et al.*, 2006) prompted investigation of this receptor. GPR55 has also been found to be stimulated by endogenous, plant-derived and synthetic cannabinoid ligands (Drumota 2004; Ryberg *et al.*, 2007). However it is now clear that the ligand binding profile of chemicals to GPR55 is complex and inconsistent (Ross, 2009). In order to resolve the inconsistencies in classification of various agonists, a β -arrestin reporter assay has been used as the readout. The readout of the assay corresponds to early events of receptor activation compared to other employed assays where the downstream signalling pathways have been observed (Kapur *et al.*, 2009). β -arrestins are intracellular proteins that bind and desensitize activated GPCR thereby forming stable receptor/arrestin signalling complexes (Oka *et al.*, 2009). Upon ligand/agonist binding the β -arrestins are relocated to the activated membrane-bound receptor thereby representing early intracellular events. Alterations in β -

arrestin2 (β arr2) distribution and GPR55 receptor internalization following activation by lysophosphatidylinositol (LPI), the most potent GPR55 agonist, were assessed and the authors demonstrated that anandamide modulated agonist-mediated recruitment of β arr2 (Kapur *et al.*, 2009). No evidence of anandamide-dependent GPR55 receptor internalization on its own induced β arr2 trafficking in GPR55 U2OS cells (Kapur *et al.*, 2009).

1.4.1 Anandamide

Anandamide has demonstrated a higher potency for GPR55 than for CB₁ or CB₂ in a [³⁵S] GTP γ S binding assay (Ryberg *et al.*, 2007). Several other groups have used calcium mobilization assays and demonstrated similar or lower potency for anandamide at GPR55 compared to CB₁ or CB₂ (Lauckner *et al.*, 2008; Waldeck-Weiermair *et al.*, 2008). In contrast to the CB₁ and CB₂ receptors, stimulation by the agonist anandamide did not increase GPR55 mediated ERK1/2 phosphorylation in GPR55 transfected HEK293 cells (Kapur *et al.*, 2009; Lauckner *et al.*, 2008; Waldeck-Weiermair *et al.*, 2008). Previous studies have reported that anandamide exerts anti-proliferative effects on cholangiocarcinoma independent of any known cannabinoid receptors (DeMorrow *et al.*, 2007). However, since the identification of GPR55 the role of the receptor has now been evaluated (Huang *et al.*, 2011). Treatment with anandamide has shown to reduce cholangiocarcinoma cell proliferation *in vitro* and *in vivo* and this effect was not seen when the receptor was knockout down (Huang *et al.*, 2011). Recent studies have shown that anandamide can act as a partial agonist; enhancing the agonist effect at low concentrations and inhibiting it at high concentrations (Sharir *et al.*, 2012).

1.4.2 2-Arachidonoyl Glycerol

2-AG has been reported to be a GPR55 agonist in [³⁵S] GTP γ S binding assay using GPR55 transfected HEK293 cells at a concentration of 3nM (Ryberg *et al.*, 2007). In contrast, other studies have demonstrated the lack of effect by 2-AG on calcium mobilization in GPR55 transfected HEK293 cells (Lauckner *et al.*, 2008). An alteration in ERK1/2 phosphorylation was not observed in the GPR55 transfected cell lines HEK293 and U2OS nor did the endocannabinoid affect GPR55 receptor internalization or β -arrestin recruitment (Kapur *et al.*, 2009; Yin *et al.*, 2009). GPR55 expression has been shown to increase in human blood neutrophils upon activation by 2-AG (Balenga *et al.*, 2011a).

1.4.3 Tetrahydrocannabinol

THC has shown to act as a GPR55 agonist in the [³⁵S] GTP γ S binding assay using GPR55 transfected HEK293 cells (Ryberg *et al.*, 2007). THC mediated effect on GPR55 receptor internalization or β -

arrestin recruitment was however again absent (Kapur *et al.*, 2009; Yin *et al.*, 2009). Increased intracellular calcium levels have been observed in GPR55 transfected HEK cells and dorsal root ganglion neurons upon treatment with THC (Lauckner *et al.*, 2008).

1.4.4 Rimonabant

The CB₁ receptor antagonist SR14617A (rimonabant) was developed as an anti-obesity drug. Inconsistent data has been reported regarding the activity of rimonabant at GPR55. GPR55 antagonism has been reported in GPR55-transfected HEK293 cells at micromolar levels (Lauckner *et al.*, 2008). An agonist activity has been reported for rimonabant in which the compound has shown to mediate calcium mobilization in GPR55-transfected HEK293 cells (Henstridge *et al.*, 2009). GPR55 activation by rimonabant has also shown to downregulate the receptor via GPCR-associated sorting protein-1 (Kargl *et al.*, 2011).

1.4.5 CP55, 940

CP55,940 exerts high affinity for CB₁ and CB₂ receptors and a similar potency has been shown for the ligand at GPR55 when using the [³⁵S]-GTPγS binding assay (Ryberg *et al.*, 2007). In ERK1/2 activation or calcium mobilization GPR55 assays no agonistic activity was demonstrated by CP55,940 (Lauckner *et al.*, 2008; Oka *et al.*, 2007). CP55,940 has also shown to act as an antagonist/partial agonist at low micro molar concentrations by inducing the blocking of GPR55 internalization, the formation of β-arrestin GPR55 complexes and the phosphorylation of ERK1/2 (Kapur *et al.*, 2009). CP55940 has been shown to modulates cytokine rat mRNA expression in cerebellar granule cells however, this has shown to be a GPR55 receptor-independent mechanism (Chiba *et al.*, 2011).

1.4.6 WIN 55,212-2

WIN 55,212-2, a structural analogue of the aminoalkylindole JWH015, has demonstrated a CB₁ independent inhibition of glutamatergic neurotransmission suggesting a novel cannabinoid sensitive receptor in mouse hippocampus (Hajos *et al.*, 2001). The ability of the cannabinoid receptor radioligand [³H]-WIN55, 212-2 to bind to membranes prepared from the HEK293 cells GPR55 transfected cells has been examined. However, no detectable binding was observed when using 50 nM of [³H]-WIN55, 212-2 (Kapur *et al.*, 2009; Ryberg *et al.*, 2007). The lack of activity of WIN55, 212-2 at GPR55 has been consistent.

1.4.7 Cannabidiol

Cannabidiol is the major non psychoactive compound of cannabis (Mechoulam *et al.*, 2007). The stimulation of [³⁵S]-GTPγS by anandamide in GPR55 transfected HEK293 cells has been demonstrated to be antagonized by CBD (Ryberg *et al.*, 2007). The phytocannabinoid has however demonstrated low affinity for CB₁ and CB₂ receptors (Drmota 2004; Ryberg *et al.*, 2007). It has also been reported to act as a GPR55 antagonist in human osteoclasts using an ERK1/2 phosphorylation assay (Whyte *et al.*, 2009). CBD has recently been shown to have an anti-inflammatory role in acute pancreatitis (AP) that might be GPR55 related (Li *et al.*, 2013).

1.4.8 Abnormal cannabidiol

The GPR55 receptor has also been postulated to be an endothelial receptor possibly responsible for mediating the vasodilatory effects induced by atypical cannabinoids such as Abn-Cbd (Ryberg *et al.*, 2007). Although Abn-Cbd lacks significant affinity for CB₁ and CB₂ receptors (Drmota 2004; Ryberg *et al.*, 2007) it has shown to stimulate [³⁵S]-GTPγS binding in GPR55 transfected cells (Johns *et al.*, 2007; Ryberg *et al.*, 2007). The atypical cannabinoid however failed to induce GPR55-modulated βarr2 redistribution (Kapur *et al.*, 2009) nor did the ligand induce GPR55 mediated ERK1/2 activation (Oka *et al.*, 2007). The ligand did not affect calcium mobilization in GPR55 transfected HEK293 cells (Lauckner *et al.*, 2008).

1.4.9 O-1602

O-1602, an analogue of Abn-Cbd was synthesized in order to study structural requirements for the vasodilator activity of Abn-Cbd. The analogue has shown to be active in vasorelaxation (Ho *et al.*, 2004; Jarai *et al.*, 1999) and has shown to stimulate [³⁵S]-GTPγS binding in GPR55 transfected cells (Johns *et al.*, 2007; Ryberg *et al.*, 2007). O-1602 causes vasodilatation and hypotension but does not bind to either CB₁ or CB₂ receptors. Although GPR55 is activated by O-1602 it does not appear to mediate the vasodilator effects of this agent (Johns *et al.*, 2007). The analogue has demonstrated to promote GPR55 mediated ERK1/2 phosphorylation in human osteoclasts (Whyte *et al.*, 2009). In contrast, O-1602 failed to induce GPR55-modulated βarr2 redistribution (Kapur *et al.*, 2009). O-1602 has recently been demonstrated to be involved in reducing nociception in a rat model of acute arthritis mediated by GPR55 (Schuelert *et al.*, 2011).

1.4.10 O-1918

The Abn-Cbd analogue 1,3-Dimethoxy-5-methyl-2-[(1*R*,6*R*)-3-methyl-6-(1-methylethenyl)-2-cyclohexen-1-yl]benzene (O-1918), which is a stereoisomer of O-1602, has shown to inhibit vasorelaxation induced by anandamide (Offertaler *et al.*, 2003). The analogue can also antagonize vasorelaxation induced by the GPR55 agonists virodhamine (Ho and Hiley, 2004) and oleamide (Hoi *et al.*, 2006). O-1918 has also been shown to abolish an anti-nociceptive effect induced by a GPR55 agonist in an arthritis rat model (Schuelert *et al.*, 2011). Also, in the same study O-1918 was reported to be a GPR18 and BK (Big potassium) calcium channel antagonist (Schuelert *et al.*, 2011).

1.4.11 Lysophosphatidylinositol.....

GPR55 was recently reported as a lysophosphatidylinositol (LPI) receptor as it has consistently been shown to be stimulated by the agonist (Anavi-Goffer *et al.*, 2012; Henstridge *et al.*, 2009; Kotsikorou *et al.*, 2011; Lauckner *et al.*, 2008; Oka *et al.*, 2007). LPI is an acidic lysophospholipid and is thought to be a result of degradation of phosphatidylinositol by phospholipase A (PLA)(Oka *et al.*, 2009; Pineiro *et al.*, 2012). LPI has shown to stimulate [³⁵S] GTPγS binding to GPR55 expressing cell membranes (Oka *et al.*, 2007). It has also been reported that LPI can activate ERK1/2 phosphorylation in GPR55 transfected HEK293 cells and U2OS cell lines (Kapur *et al.*, 2009; Oka *et al.*, 2007). In addition, LPI has been shown to be an agonist when using GPR55 receptor internalization or β-arrestin recruitment assays (Henstridge *et al.*, 2009; Kapur *et al.*, 2009; Yin *et al.*, 2009). The endogenous compound 2- arachidonoyl lysophosphatidylinositol has recently been demonstrated to activate GPR55 in HEK293 cells more potently than LPI suggesting that this ligand might be the most potent GPR55 agonist (Oka *et al.*, 2007).

1.4.12 Other ligands

The GPR55 receptor has also been shown to be stimulated by the cannabinoid receptor agonists, noladin ether and virodhamine and non CB₁/CB₂ receptor ligands such as the anti-inflammatory compound palmitoylethanolamide (PEA) and oleoylethanolamide (OEA) in the [³⁵S]-GTPγS binding assay (Drnosta 2004; Ryberg *et al.*, 2007). Although some CB₁ and CB₂ cannabinoid ligands that bind to GPR55 there are other distinct chemical classes which like LPI do not recognize CB₁ and CB₂ receptors however these have shown to bind to GPR55 (Zhao *et al.*, 2012).

Using the β-arrestin recruitment assay a library screen of 290,000 compounds was performed in the NIH Molecular Libraries program (by the Sanford-Burnham Center for Chemical Genomics) (Heynen-Genel *et al.*, 2010a; Zhao *et al.*, 2012). Three potent and selective agonists for GPR55 were

identified: piperazine, ML184 (2440433) with 263 nM potency, tricyclic triazoloquinoline, ML185 (CID1374043) with 658 nM potency and morpholinosulfonylphenylamide, ML186 (CID15945391) with 305 nM potency (Table 1.1) (Heynen-Genel *et al.*, 2010a). All agonists had between 48-120 fold selectivity against GPR35, CB₁ and CB₂ (Heynen-Genel *et al.*, 2010a). Three antagonists for GPR55 have also been identified: piperadinyloxadiazolone, ML191 (23612552) with 160 nM potency, thienopyrimidine, ML192 (CID1434953) with 1080 nM potency; and quinoline aryl sulfonamide, ML193 (CID1261822) with a 221 nM potency (Table 1.1)(Heynen-Genel *et al.*, 2010b). All antagonists had between 27- 145 fold selectivity against GPR35, CB₁ and CB₂ (Heynen-Genel *et al.*, 2010b). All agonists and antagonists were involved in activating downstream responses of ERK phosphorylation and PKC β II translocation (Heynen-Genel *et al.*, 2010a; Heynen-Genel *et al.*, 2010b).

TABLE 1.1 *GPR55 agonists and antagonists*

GPR55 AGONISTS	POTENCY ¹	GPR55 ANTAGONISTS	POTENCY ²
piperazine, ML184 (2440433)	263 nM	piperadinyloxadiazolone, ML191 (23612552)	160 nM
tricyclic triazoloquinoline, ML185 (CID1374043)	658 nM	thienopyrimidine, ML192 (CID1434953) with	1080 nM
morpholinosulfonylphenylamide, ML186 (CID15945391)	305 nM	quinoline aryl sulfonamide, ML193 (CID1261822)	221 nM

GPR55 agonists¹ and antagonists². The potency (EC₅₀) of the compounds have been reported previously (Heynen-Genel *et al.*, 2010a; Heynen-Genel *et al.*, 2010b).

GSK494581A belongs to a series of benzoylpiperazines initially reported to act as inhibitors of the glycine transporter subtype 1 (Brown *et al.*, 2011). One of the benzoylpiperazines GSK575594A has been identified as a GPR55 ligand with 60-fold selectivity for the receptor. This ligand is similar to ML184 (CID2440433) (Zhao *et al.*, 2012). The benzoylpiperazine agonists has shown to activate human not rodent GPR55 (Brown *et al.*, 2011).

Recently a molecular model of GPR55 was derived in which interaction of the recently identified GPR55 agonists CID1792197, CID2440433 (ML184) and CID1172084 (ML185) ligands was examined. An important residue for agonist activation of GPR55 was identified and the three ligands resembled LPI and not cannabinoid ligands (Kotsikorou *et al.*, 2011). To date, no low nanomolar potency ligands have been shown for GPR55 and no radioligands have been discovered

to characterize binding at this receptor making it a hurdle to identify ligand binding properties (Zhao *et al.*, 2012). Unfortunately, these recently identified GPR55 specific ligands were synthesized after initiation of our experiments and were unavailable for this study.

1.5 GPR55 signalling and intracellular mechanisms

GPR55 signalling promote receptor coupling to multiple signalling pathways and is linked to heterotrimeric G proteins (Ryberg *et al.*, 2007). GPR55 has been shown to use G_q , G_{12} , $G_{\alpha_{13}}$ for signal transduction that mediates activation of members of the Rho family of GTPases including rhoA, cdc42 and rac1 (Henstridge *et al.*, 2009; Lauckner *et al.*, 2008). RhoA has been reported to be involved in regulation of the actin cytoskeleton (Lauckner *et al.*, 2008; Waldeck-Weiermair *et al.*, 2008). LPI has shown to induce a rapid phosphorylation of ERK (extracellular signal-regulated kinase) in the MAPK/ERK (mitogen-activated protein kinase) signal transduction pathway in GPR55 transfected HEK293 cells (Oka *et al.*, 2007). In another study LPI induced the rapid phosphorylation of p38 MAPK in GPR55 expressing cells, this effect was absent in the vector transfected cells. MAPK p38 is involved in responses for cellular stresses such as activation of proinflammatory cytokines, heat shock, osmotic stress and regulation of cellular activities such as gene expression, differentiation and apoptosis (Pearson *et al.*, 2001).

1.6 Biological function of GPR55

At the time of initiation of this project the biological role of GPR55 was unclear. The role of GPR55 in hyperalgesia associated with inflammatory and neuropathic pain has been suggested from studies in GPR55 knockout mice. GPR55 knockout mice showed no mechanical hyperalgesia following partial nerve ligation when compare to wildtype mice (Staton *et al.*, 2008). An increase in the anti-inflammatory cytokines interleukin (IL) four and IL-10 was seen in the genetically modified mice after administration of Freund's adjuvant compared to wild type littermates suggesting a protective role in inflammation induced pain (Staton *et al.*, 2008).

GPR55 has been suggested to play a role in bone metabolism as it has been demonstrated that mice lacking CB_1 and CB_2 receptors have abnormal bone phenotypes (Idris *et al.*, 2008; Ofek *et al.*, 2006). Recently, GPR55 mRNA were detected in human and mouse osteoblasts and osteoclasts generated from macrophage colony-stimulating factor-dependent monocytes. The synthetic agonist O-1602 was used to investigate the role of GPR55 in osteoclast formation. It was found that O-1602 did not affect the formation of human osteoclast *in vitro*. In contrast the GPR55 antagonist CBD increased the total human osteoclast number which is consistent with the theory

that GPR55 plays an inhibitory role in osteoclastogenesis. Mouse osteoclast formation *in vitro* was however inhibited by O-1602 and LPI whereas the inhibitory effect was antagonized by CBD. The inhibitory effect was absent in GPR55 knockout mice (Whyte *et al.*, 2009).

Increased LPI levels have been found in obese patients (Moreno-Navarrete *et al.*, 2012). The same study also demonstrated higher GPR55 levels in diabetic patients compared with control group (Moreno-Navarrete *et al.*, 2012). Other studies have shown that activation of GPR55 by O-1602 promotes the increase of glucose stimulated insulin secretion in isolated rat pancreatic islets (Romero-Zerbo *et al.*, 2011). *In vivo* activation of GPR55 by O-1602 increases insulin levels in rats suggesting a role for GPR55 in endocrine pancreatic function (Lipina *et al.*, 2012; Moreno-Navarrete *et al.*, 2012; Romero-Zerbo *et al.*, 2011).

Numerous studies have reported that endocannabinoids and phytocannabinoids exert effects on intestinal contractility by inhibiting acetylcholine release from enteric neurons (Heinemann *et al.*, 1999; Roth, 1978). The atypical cannabinoid O-1602 has shown to inhibit neurogenic contractions in the gut mediated by GPR55 independent of CB₁ and CB₂ receptors (Ross *et al.*, 2012).

GPR55 has been suggested to be the cannabinoid- binding receptor responsible for vasodilatation to atypical ligands such as Abn-cbd and O-1602 however the vasodilatory effect to both ligands were comparable in GPR55 knockout and wildtype mice (Johns *et al.*, 2007). O-1918 also showed similar inhibitory effects of the vasodilatation induced by Abn-cbd in both mouse strains (Johns *et al.*, 2007).

1.7 GPR55 and cancer

There is limited information available about the role of LPI ligand in humans but increased levels have however been shown in ascites fluid and blood plasma in people with ovarian cancer (Sutphen *et al.*, 2004; Xiao *et al.*, 2001). This has been linked to tumourogenesis and a role for GPR55 and LPI in modulation, orientation, polarisation of breast cancer cells was recently presented (Pineiro *et al.*, 2010). A highly metastatic breast cancer cell line MDA-MB-231 was found to express 30-fold higher levels of GPR55 compared to a lower metastatic breast cancer cell line hence suggesting a role for GPR55 in control of metastasis (Ford *et al.*, 2010). LPI stimulated [³⁵S]-GTPγS binding to membranes from the highly metastatic cell line and enhanced migration of the MDA-MB-231 cells. It was not possible to knockout the receptor in the MDA-MB-231 cell line therefore it remains to confirm the role of GPR55 as the receptor responsible for the effects of LPI (Ford *et al.*, 2010). More recently, it has been shown that GPR55 modulates cancer cell migration

and proliferation *in vitro*, and tumor growth in a xenograft-based model of glioblastoma (Andradas *et al.*, 2011; Ford *et al.*, 2010; Pineiro *et al.*, 2011).

GPR55 has been demonstrated to drive chemically-induced mouse skin tumour development. Wild-type mice were shown to have an increased papilloma and carcinoma formation, enhanced skin cancer cell anchorage-independent growth, invasiveness and tumorigenicity *in vivo*, compared to GPR55 knockout mice (Perez-Gomez *et al.*, 2012). While all the carcinomas in the GPR55 knockout mice were well differentiated, 22% of the carcinomas were found to be poorly differentiated in the wildtype mice (Perez-Gomez *et al.*, 2012). Higher GPR55 mRNA levels were also detected in the carcinomas compared to control mouse skin (Perez-Gomez *et al.*, 2012). TPA (phorbol ester 12-O-tetradecanoylphorbol-13-acetate), a proliferation inducing agent has been described to induce local inflammation when applied on mouse skin and causes an increased dermal cell population (Perez-Gomez *et al.*, 2012). An increase of inflammatory CD45 positive cells and cytokines including IL β 1 and TNF α has been observed in the dermis of wildtype and not in the GPR55 deficient mice (Perez-Gomez *et al.*, 2012). The lack of highly selective and high affinity reagents have hampered with the elucidation of the true biology of GPR55.

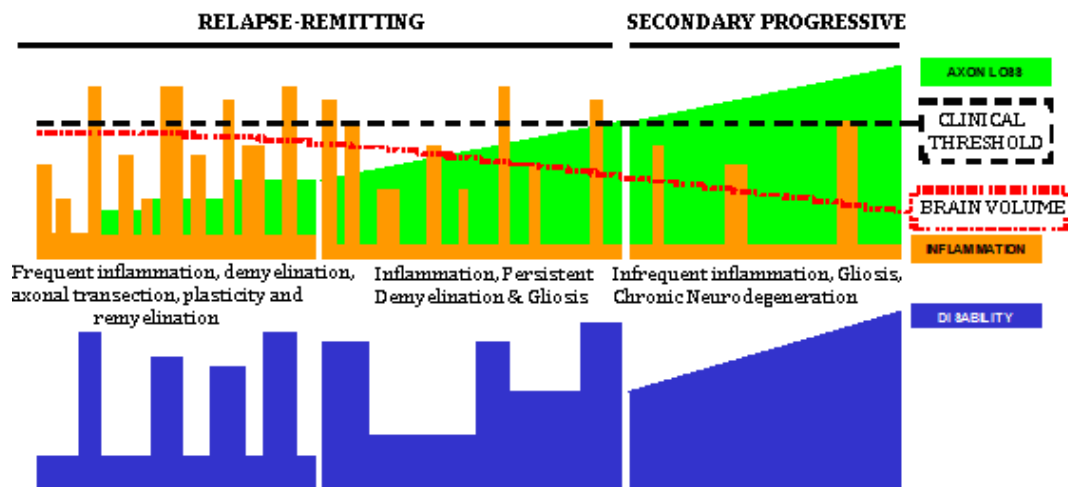
1.8 Multiple sclerosis (MS)

Multiple sclerosis (MS) is an immune-mediated demyelinating and neurodegenerative disease of the central nervous system (CNS). The disease is associated with repeated immune attack of the CNS leading to demyelination, axonal and neuronal loss thereby affecting normal neurotransmission (Compston & Coles., 2002; Compston & Coles., 2008). The symptoms vary depending on where demyelination and nerve loss occurs and leads to the development of neurological signs and symptoms including spasms, tremor, ataxia, weakness or paralysis, cognitive impairment and incontinence (Compston & Coles., 2002).

MS has an incidence of about 7 per 100,000 every year in the UK, however the incidence may be higher in certain areas of the UK and affect up to 1 in 170 in the Orkney islands (Visser *et al.*, 2012) and affects around 2.5 million individuals worldwide (Kurtzke, 1993). A total of 80% of non-benign MS patients present relapsing-remitting MS (RRMS) characterized by episodes of neurological deficits that develops into chronic secondary progressive MS (SPMS) (Figure 1.3) (Compston & Coles., 2002). Progressive disease from the onset is termed primary progressive and is presented in 10-15% of the patients and primarily affects the spinal cord and in some cases the optic nerve, cerebrum and cerebellum (Compston & Coles., 2002; Kurtzke, 1993). Depending on where the impaired saltatory conduction occurs different symptoms and signs will reflect the functional

anatomy. Magnetic resonance imaging (MRI) is a technique used to assess affected sites in MS. The cerebrum and the spinal cord are most frequently affected when assessed with MRI. A minimum of two attacks affecting more than one anatomical site separated in time is a diagnostic criteria required for clinically delineated MS. However, a combination of clinical presentation and MRI can be used as a diagnostic criteria (Compston *et al.*, 2008; Polman *et al.*, 2011). Other clinical features associated with the disease are findings of oligoclonal bands in 90% of cases (Compston *et al.*, 2002b). The aetiology of the disease remains unknown although epidemiological data indicate the involvement of environmental factors and genetic susceptibility (Dyment *et al.*, 2004). Globally, the risk of MS increases with distance north or south of the equator (Kurtzke, 1975). Immigrants that migrate from high-risk to low-risk areas in childhood are associated with a reduced risk of developing MS and *vice versa* (Hammond *et al.*, 2000). The disease is more common in northern Europeans and twice as common in women as in men (Compston *et al.*, 2002b). The incidence is also higher for relatives; (Compston *et al.*, 2002b). Although diagnosis of the disease is usually around 20-40 years old (McQualter *et al.*, 2007), 7% of patients are under 16 years old (Compston & Coles., 2002). Life expectancy for MS patients from disease onset is around 25 years although death may occur quickly within months or after many years. Average life expectancy is only reduced by about 7 years but the quality of life is significantly affected. A number of environmental factors have been investigated including infection, dietary factors, pollution and chemical agents. Viruses are among the most studied infectious agents related to MS pathogenesis. Suggested candidates have included Epstein Barr virus (EBV), Herpes simplex 1&2, Varicella zoster virus, Human Herpesvirus type 6 and reactivation of human endogenous retroviruses (Hauser *et al.*, 2006). There is strong evidence for a role of EBV where a late EBV infection and higher titres of a latent EBV antigen are associated with increased risk of developing MS. Individuals that have never been infected by EBV are associated with a low risk of developing MS (Hauser *et al.*, 2006)

Figure 1.3 *The course of multiple sclerosis*



An initial period of repeated inflammatory episodes results in blood: brain barrier dysfunction and in some occasions relapsing neurological deficit induced by persistent demyelination. This creates a chronic neurodegenerative microenvironment, seen by brain atrophy, which reaches a threshold beyond which clinical disease progresses unabated (adapted from Compston & Coles 2002).

Population studies have suggested an association between multiple sclerosis and alleles of the major histocompatibility complex (MHC) (Compston & Coles 2008). HLA type HLA-DR2 and in particular the allele HLA-DRB1*1501 has been linked to MS susceptibility (Barcellos *et al.*, 2003; Oksenberg *et al.*, 2004). To date over 50 non-MHC have been linked to susceptibility of MS (Wandstrat *et al.*, 2001). These are essentially all immune related. Other minor susceptibility loci include interleukin 2 and 7 receptors, the C-type lectin domain family 16 member A and the adhesion molecule CD58 (De Jager *et al.*, 2009). Vitamin D levels and sunlight exposure may provide a possible explanation for the association of latitude and MS risk (Pierrot-Deseilligny, 2009). Vitamin D affects the differentiation and function of cells in the immune system (Liblau *et al.*, 1995) and has shown to regulate HLA gene expression by a direct interaction with a functional vitamin D response element in the promoter region of HLA-DRB1 (Ramagopalan *et al.*, 2009). These results provide a mechanism linking genetic and environmental factors of MS susceptibility. Although vitamin D could influence disease course this could be *in utero* where vitamin D levels of the pregnant mother may influence immune development (Ebers, 2008; Dobson *et al.*, 2012). Over 50 other genetic variants have been linked to disease susceptibility which are largely linked to immune function (Kofler *et al.*, 2011; Sawcer *et al.*, 2011).

1.8.1 Pathogenesis of MS

The pathology of MS is complex and the sequence of events leading to initiation of disease remains to be confirmed. One of the major missions in MS research has been to establish the sequence of events that lead to the development of inflammatory plaque (lesions) (Raine, 1994). MS appears to be an immune-mediated disease initiated by the activation of autoreactive T cells, which leads to inflammatory events and myelin destruction, axonal loss, neurological deficit (Weiner, 2004) and activation of lymphocytes by exogenous pathogens or by nonspecific activation of T and B cells due structural homology between self-protein and a protein in the pathogen, a process called molecular mimicry (Steinman *et al.*, 2002).

MS is initiated by an unknown mechanism, which appears to initiate an inflammatory response where auto-reactive T cells are activated in the periphery and adhere to receptors on endothelial cells and migrate across the disrupted blood-brain barrier(BBB) (Compston *et al.*, 2008; Hauser *et al.*, 2006). The disruption of the BBB in MS has been shown using histology (Broman, 1964) and clinically using gadolinium enhanced MRI (Alnemri *et al.*, 1996) which detects active lesions in MS patients (Grossman *et al.*, 1986). CD11a/CD18 and CD49d/CD29 are integrins predominantly involved in leucocyte trafficking. CD11a/CD18 and CD49d/CD29 are expressed on lymphocytes and have been detected on leucocyte infiltration in MS lesions (Bo *et al.*, 1996). CD49d/CD29 binds the vascular cell adhesion molecule CD106 during an inflammatory response (Hauser *et al.*, 2006).After crossing the endothelial cell layer activated T cells must pass through the sub-endothelial basement membrane composed of type IV collagen, which is only found in basement membranes (Steinman *et al.*, 2002). Activated T cells then use enzymes like matrix metalloproteinases (MMP) that lyse the sub-endothelial basal lamina and allow the transmigration via a Rho-dependent pathway (Steinman *et al.*, 2002; Walters *et al.*, 2002). Type IV collagen has been shown to be particularly targeted by MMP 2 and 9, which are both detected in the CSF in MS (Steinman *et al.*, 2002). T cells that have crossed the blood brain barrier (BBB) are then reactivated by fragments of myelin antigens. Originally myelin proteins were considered the main candidates for initiation of MS, however other factors have also been implicated (Hauser *et al.*, 2006). The small heat shock-protein $\alpha\beta$ crystallin has been found to function as immunodominant myelin antigen when expressed at high levels in MS lesions (van Noort *et al.*, 1995). Antibodies against neurofascin, a cell adhesion molecule, have been suggested to mediate axonal injury in MS (Mathey *et al.*, 2007). Following the initial activation of myelin specific T cells and activation of the vasculature to upregulate adhesion molecules and chemokines a secondary wave of cells enter the CNS (Baker *et al.*, 2003). Upon an accumulation of T and B lymphocytes, plasma cells and

macrophages the immune response is enhanced by proinflammatory cytokines stimulation of naïve microglia (Compston & Coles., 2002). Th17 (T cells that produce IL-17) cells may cause damage to axons (Wu *et al.*, 2011) and there may be CD8 mediated killing of oligodendrocytes and neurons (Pierson *et al.*, 2012). A contact is then created between activated microglia and components of the oligodendrocyte-myelin unit allowing the delivery of toxic signals such as though tumour necrosis factor α (TNF- α) (Zajicek *et al.*, 1992). In acute demyelinating lesions axonal injury with transection has been observed; which correlates with T cell and microglial activation (Trapp *et al.*, 1998). This is known as the outside-in hypothesis of autoimmunity, however analysis of early MS lesions suggest that disease is an inside-out disease where early lesions occur before significant infiltration of T cells (Barnett *et al.*, 2004; Geurts *et al.*, 2010; Tsunoda *et al.*, 2002). At later secondary progressive stages areas of demyelination have been observed together with significant axonal and neuronal degeneration and it is now believed that progress in disability is due to neurodegeneration (Anderson *et al.*, 2008; Dutta *et al.*, 2011; Trapp, 1999). Remyelination is seen as shadow plaques and is mostly active during the acute inflammatory process and also involves phagocytic removal of myelin debris (Compston *et al.*, 2008). Remyelination of plaques has been observed in 20% of MS patients and is ongoing in grey matter lesions (Chang *et al.*, 2012; Patrikios *et al.*, 2006; Trapp, 2012). These 'pre-active' lesions contains clusters of microglia around the oligodendrocytes and occur in the grey and white matter, thus it is possible that the inflammatory response is recruited to clear the myelin debris. However it is clear that immunosuppression inhibits relapsing MS (Compston *et al.*, 2002a; Compston *et al.*, 2008). This implicates the immune system in this process. However, triggering events inside the CNS such as HERV activation in oligodendrocytes could trigger production of stress response that is recognized by peripherally recruited $\alpha\beta$ crystallin responsive cells (van Noort *et al.*, 2012)

1.8.2 MS therapies

Immunosuppressive therapies were primarily used to treat MS based on the assumption that MS is an autoimmune disease (Whitaker, 1994). Corticosteroids are currently used to treat relapses and modulate the duration of relapse in MS patients by suppressing important components of the immune system and vascular permeability (Tischner *et al.*, 2007). However, many of these treatments produce numerous side effects and are only partially effective in reducing disease severity (Thrower, 2009; Tischner *et al.*, 2007).

Anti-inflammatory and immunosuppressive therapies can provide beneficial effects on relapse rate and accumulation of disability early disease, however these do not appear to impact on disease progression (Confavreux *et al.*, 2004). The three main treatments for MS currently include:

first line and second line disease modifying therapy (DMT) for relapsing-remitting MS and symptomatic therapy (Dobson, 2013). The existing DMT therapies are aimed at modulating the immune response.

Beta interferons (IFN- β) were the initial drugs shown to be efficient in reducing the relapse rate (Hemmer *et al.*, 2005). These are now first line treatments in the UK based on costs and side effect potential. The immunomodulatory drugs interferon- β -1a and the non-glycosylated interferon- β -1b reduce the relapse rate in MS by about 30% and decrease disability accumulation (Capobianco *et al.*, 2008). Initially the interferons were mainly used for their anti-viral properties as viral infections are suggested to generate relapses (Hong *et al.*, 2002). Interferons have shown to act as antagonists of proinflammatory cytokines and have been suggested to down regulate MHC class II antigen expression, however the precise mechanism of action is unclear (Hall *et al.*, 1997). Approximately 3–30% of patients of IFN β -treated patients develop neutralising antibodies (NAbs) during treatment which impact negatively on the effect of the drug (Capobianco *et al.*, 2008). *Glatiramer acetate* (Copaxone) is another first line drug for treatment of relapsing remitting MS (Capobianco *et al.*, 2008). The drug is a polymer molecular mimic of a region of myelin basic protein and has demonstrated to suppress the relapse rate by about 30% (Flechter *et al.*, 2002). In addition the drug effects cytokine production and prevents presentation of autoantigens by monocytes and dendritic cells and may provoke active T cell suppression against MBP (Farina *et al.*, 2005; Neuhaus *et al.*, 2001). These are first line based on the lower costs and side-effect profile, which are restricted mainly to injection-site, reactions and flu-like symptoms in the case of beta interferons. Second-line drugs for MS treatment include monoclonal antibodies and small molecules, which are more potent but have more side-effects and considerably higher costs. The humanized monoclonal antibody (mAb) Natalizumab (*Tysabri*[®]) binds to the α 4-integrin (CD49d) component of adhesion molecules found on lymphocytes, monocytes, and eosinophils and prevents entry of immune cells into the CNS (Selewski *et al.*, 2010; Tsunoda *et al.*, 2007). Natalizumab can reduce the relapse rate by approximately 70% (Hutchinson *et al.*, 2009). Natalizumab however can be associated with hypersensitivity because it is an immunogenic protein and importantly about 2.77:1000 currently develop progressive multifocal leukoencephalopathy a disabling or fatal infectious demyelinating disease of the brain (Bloomgren *et al.*, 2012; Rice *et al.*, 2001; Yousry *et al.*, 2006). In fact this increases to 1 in 94 people on Natalizumab for more than 24 months who have previously been treated with immunosuppressants and are infected with the JC virus (Bloomgren *et al.*, 2012). *Mitoxantrone* is a cytotoxic agent with immunosuppressant properties and has shown to reduce the number of B cells, inhibit T cell function and augment T cell suppressor activity (Martinelli Boneschi *et al.*,

2005). The drug is associated with a more toxic effect than the interferons and is mainly used by patients with high relapse frequency and aggressive relapse disease; this causes cardiotoxicity and the development of cancer (Edan *et al.*, 1997; Mulroy *et al.*, 2012; Paul *et al.*, 2009). Natalizumab and mitoxantrone are drugs used as second- or third- line treatments (Brinkmann *et al.*, 2010).

Fingolimod (*Gilenya*[®], FTY720) is an oral drug that mediates modulation of sphingosine-1-phosphate receptors (Brinkmann *et al.*, 2010). Current research suggests that the action of FTY720 is mainly mediated by modulation of the sphingosine-1-phosphate receptors on the lymphocytes preventing exit of central effector cells from lymphoid tissue thereby reducing the infiltration of autoaggressive lymphocytes into the CNS (Brinkmann, 2009; Chun *et al.*, 2010). The drug has also been demonstrated to reduce astrogliosis in EAE (Choi *et al.*, 2010). Other recently developed drugs include Lemtrada[®], (Alemtuzumab, Campath-1H) which targets CD52 to deplete T and B cells and is undergoing regulatory approval (Buttmann, 2010; Goldenberg, 2012). Daclizumab is a humanized monoclonal antibody which targets CD25, a molecule which is involved in T cells activation and inhibits Natural killer cell function (Bielekova, 2012; Kaur *et al.*, 2012; Perry *et al.*, 2012). Ocrelizumab is a humanized anti-CD20 monoclonal antibody which depletes CD20 expressing B-cells (Lulu *et al.*, 2012). Although Cladribine, an oral drug that is a purine synthesis inhibitor which depletes peripheral lymphocyte levels, demonstrated significant efficacy and a relative safe profile in phase II and phase III studies compared to placebo, this drug was not granted regulatory approval in the EU or in the USA (Lulu *et al.*, 2012; Muir *et al.*, 2011). The company was requested to conduct a second phase III trial for cladribine and decided to stop manufacturing the drug due to costs and other factors. Other oral drugs that are licensed for use in MS include BG12 (Tecfidera[®]), Teriflunomide (Aubagio[®]) and Laquinimod (Limmroth, 2012; Papadopoulou *et al.*, 2012; Toubi *et al.*, 2012). BG12, a fumaric acid ester, decreases leucocyte infiltration through the BBB, it also activates antioxidant pathways such as nuclear factor (erythroid-derived 2)-like 2 (Nrf2-2) pathway thereby protecting against neuronal death and myelin injury (Limmroth, 2012; Nguyen *et al.*, 2009). Teriflunomide is a pyrimidine synthesis inhibitor that decreases T-cell proliferation by reducing activity of mitochondrial enzyme dihydro-orotate dehydrogenase which is required for DNA synthesis (Papadopoulou *et al.*, 2012). Laquinimod has demonstrated to have an immunomodulatory effect and inhibits T-cell and macrophage entry into the CNS; it also stimulates pro-inflammatory cells into shifting to anti-inflammatory cells (Toubi *et al.*, 2012). However, Laquinimod had low efficiency compared to the beta interferons but it have an effect on atrophy. There are no licensed drugs that inhibit either non-relapsing, gadolinium enhancing primary or secondary progressive disease. Importantly Alemtuzumab (Coles *et al.*,

1999a; Coles *et al.*, 1999b), Cladribine (Rice *et al.*, 2000) and bone marrow transplantation (Inglese *et al.*, 2004) that inhibit relapse but do not halt progression. This supports the concept of MS containing a neurodegenerative nature and component.

1.8.3 Cannabis and MS

Cannabis has been used for medical purposes for over thousands of years (Pertwee, 2009). The increased self-medication of this illegal drug has been reported in anecdotal reports especially by patients with multiple sclerosis (Fox *et al.*, 2012; Pertwee, 2002). Evidence of beneficial use of cannabis has now been shown in a number of clinical trials where treatment with cannabinoid agonists has been perceived to control symptoms including spasms, pain, spasticity and incontinence reported by the patients (Deutsch *et al.*, 2008; Kmietowicz, 2010; Novotna *et al.*, 2011; Pertwee, 2002; Pertwee, 2007).

1.8.4 Spasticity, cause and incidence

Spasticity appear to be among the symptoms resulting from injury to the upper motor neurons within the CNS (Adams *et al.*, 2005). The pathophysiology of spasticity remains poorly understood but it may reflect a loss of inhibitory circuitry in the spinal cord resulting in excessive levels of stimulatory signals. Under normal conditions inhibitory signals are directed via the corticospinal tract to the spinal cord but following injury causing damage to the corticospinal tract; this leads to excessive contraction of the muscles and in some cases even at rest (Adams *et al.*, 2005; Brown, 1994; Nielsen *et al.*, 2007). Spasticity is a common feature in MS and affects up to 84.3% of patients (Compston *et al.*, 2002b; Oreja-Guevara, 2012).

1.9. Anti-spastic drugs and mechanisms

Anti-spastic drugs are mainly used for management of spasticity observed in diseases affecting the upper motor neurons such as MS most of which exert their effects though centrally mediated mechanisms (Meleger, 2006). Baclofen is a GABA_B receptor agonist which act both presynaptically and postsynaptically (Meleger, 2006) leading to a decrease in the excitatory neurotransmitter release and neurotransmitters involved in transmission of nociceptive impulses such as the neuropeptide substance P (Hwang *et al.*, 1989). Baclofen is however associated with side effect such as sedation, depression hallucination and nausea (Meleger, 2006). Spasticity is decreased upon binding to GABAB receptors on presynaptic terminals of spinal interneurons; this results in hyperpolarization of the membrane leading to reduced calcium influx and release of the excitatory neurotransmitters, glutamate, and aspartate. Postsynaptic interactions with sensory afferent

terminals cause membrane hyperpolarization via a G-protein-coupled receptor causing to increases in potassium conductance thereby enhancing inhibition (Milanov, 1992). Dantrolene is a muscle relaxant that inhibits the release of calcium from the sarcoplasmic reticulum thereby uncoupling motor nerve excitation and muscle contraction. Dantrolene does not directly affect the CNS however it is associated with muscle weakness (Meleger, 2006). Botulinum toxin is a protein and neurotoxin produced by *Clostridium botulinum*, an anaerobic bacillus (Wheeler *et al.*, 2013). There are seven types of the toxin (A-G) which all block acetylcholine release bacillus (Wheeler *et al.*, 2013). Botulinum toxin exerts its effects by preventing calcium-dependent release of acetylcholine resulting in long duration flaccid paralysis of the muscle into which it is injected (Meleger, 2006; Wheeler *et al.*, 2013). Benzodiazepines such as diazepam have an anti-spasticity effect by acting on GABA_A receptors to hyperpolarize the cellular membrane; this increases presynaptic inhibition (Zafonte *et al.*, 2004). Tizanidine is a central acting adrenoceptor agonist that mainly affect spinal polysynaptic reflexes and is used for treatment of spasticity in MS (Coward, 1994; Kamen *et al.*, 2008). Compounds derived from *C. sativa* or cannabinoids are used for anti-nociception and muscle relaxation in people with MS (Zajicek, 2005; Zajicek *et al.*, 2003). Both Dronabinol/Marinol, (THC) and nabilone, a synthetic cannabinoid, have been used for treatment of pain and spasticity in MS (Smith, 2007).

1.10 Cannabinoids in Spasticity

1.10.1 Symptomatic control

There are many symptoms of MS that are controlled by different drugs (Table 1.1), however these are poorly controlled (Compston *et al.*, 2002a). In trials where the effect of smoked cannabis was monitored, and there were obvious cannabimimetic effects, it was possible to demonstrate benefit in a cross-over study (Corey-Bloom *et al.*, 2012). However, trials aimed at avoiding psychoactive effects have had more problems in demonstrating the beneficial effects of smoked cannabis.

Table 1.2 *Symptomatic treatments in MS*

Symptomatic treatments in MS (Compston <i>et al.</i> , 2002a; Goodman <i>et al.</i> , 2009)		
Site	Symptoms	Treatments
Brainstem	- Impaired speech and swallowing	Tricyclic anti-depressants
Cerebrum	- Depression	Antidepressants
Spinal cord	- weakness - stiffness - painful spasms -walking difficulties - spasticity	Tizandine baclofen dantrolene fampridine benzodiazepines intrathecal baclofen
Other	- Pain	Carbamazepine gabapentin
	- Fatigue	Amantadine

Lesion sites, syndromes, and symptomatic treatments in multiple sclerosis.

In experimental autoimmune encephalomyelitis (EAE), an animal model of MS, spasticity develops due to repeated neuroimmunological attack of the CNS that leads to loss of axons (Baker *et al.*, 2000; Baker *et al.*, 2001). In this animal model the stimulation of the cannabinoid receptors with agonists has shown to improve limb and tail spasticity (Baker *et al.*, 2000; Baker *et al.*, 2001; Pryce *et al.*, 2007). Treatment with the cannabinoid receptor antagonists, SR141716A, however worsened the spasticity in the animals (Baker *et al.*, 2000). Although CB₂ agonists had also been suggested as anti-spastic compounds these are also found to stimulate the CB₁ receptor and there is no evidence that CB₂ mediates any anti-spastic effect (Pryce *et al.*, 2007; Wilkinson *et al.*, 2003). CB₁ receptors and THC mediate the beneficial control of spasticity and modulate the adverse effects of cannabis (Pryce *et al.*, 2007). Numerous clinical trials have been undertaken on spasticity in MS (Novotna *et al.*, 2011; Rog, 2010; Wade *et al.*, 2006; Zajicek, 2005; Zajicek *et al.*, 2003; Zajicek *et al.*, 2011). In the Cannabinoids in Multiple Sclerosis (CAMS) trial the effects of Cannador

(2.5 mg THC: 1.25mg CBD), Marinol (synthetic delta-9-THC in oil 2.5 mg) or placebo on spasticity and other MS symptoms was examined. Overall patients reported that the drugs provided a significant improved effect on pain and muscle spasms (Zajicek *et al.*, 2003). The “Multiple Sclerosis and Extract of Cannabis” (MUSEC) study conducted between 06/2006 to 09/2008 confirmed the previous findings reported in the CAMS trial (Zajicek J., 2009). In this study 279 patient were treated with oral cannabis extract (2.5 mg THC: 1.25 mg CBD) or placebo for up to 12 weeks. Approximately 30% of the MS patients receiving oral cannabis extract compared to 15% in the placebo group reported relief of muscle stiffness and in some patients pain and sleep quality also improved (Zajicek J., 2009). In a recent phase III clinical trial MUSEC an extract from *C. sativa* (extraction medium ethanol 96%) in soft gelatine capsules, standardised on CBD (range 0.8-1.8 mg) and containing 2.5 mg D9- THC was used as the main cannabinoid (Cannador;)to study its efficiency for symptomatic relief of muscle stiffness and pain in adult patients with MS (Zajicek *et al.*, 2012). Approximately 30% of the patients reported that treatment with oral extract of *C. sativa* relieved muscle stiffness, body pain, spasms and improved sleep quality compared to 15% in the placebo group (Zajicek *et al.*, 2012).

The oromucosal administration allows a rapid absorption similar to smoking cannabis due to direct absorption into the systemic circulation avoiding both gastrointestinal absorption and first pass metabolism through the liver. Oromucosal administration allows a more accurate self-titration as minimal absorption by the oral route helps to minimize the variability of individual responses known to occur with other cannabinoids (Rog, 2010). Sublingual administration has shown to be a more rapid way of obtaining maximal plasma concentration compared to the oral route (Kappos *et al.*, 2008; Rog *et al.*, 2007). Sativex[®] (GW Pharmaceuticals Ltd., Salisbury, UK) is an oromucosal cannabis-based medicine that consists of approximately 1:1 ratio tetrahydrocannabinol (27 mg/ml) and CBD (25 mg/ml) with less than 10% of other cannabis-based compounds in an alcoholic solution (Whittle, 2001). In a recent randomized, double-blind study Sativex[®] has shown to improve spasticity in patients who had previously failed to respond sufficiently to other anti-spasticity medications (Novotna *et al.*, 2011). GW has previously achieved positive regulatory assessments in the UK, Spain, Germany, Italy, Denmark, Sweden, Austria, Canada, New Zealand and the Czech Republic and Sativex[®] has so far been approved / recommended for approval in eighteen countries for the treatment of spasticity (muscle stiffness/spasm) due to MS (<http://www.gwpharm.com>) (Oreja-Guevara, 2012). Recently GW announced that a further ten countries had now been recommended for approval under a Mutual Recognition Procedure including Belgium, Finland, Iceland, Ireland, Luxembourg, the Netherlands, Norway, Poland,

Portugal and Slovakia. A regulatory filing is also underway in Switzerland. Sativex[®] has also been approved for the treatment of cancer-related pain in Canada (Oreja-Guevara, 2012). Sativex[®] is frequently associated with mild to moderate side effects such as dizziness, drowsiness, fatigue and headache however these effects can be reduced by gradually increasing the dose of the drug (Sastre-Garriga et al., 2011).

There is accumulating evidence demonstrating the control of spasticity by the endocannabinoid system in the chronic relapsing EAE (CREAE) animal model. Firstly, an increase of endocannabinoid levels in areas of nerve damage and in spinal cord lesions in spastic EAE animals has been detected compared to EAE animals lacking spastic signs (Baker *et al.*, 2001). Augmented levels of endocannabinoids have also been identified in MS tissues suggesting that the endocannabinoid system controls irregular neurotransmission. Secondly, spasticity in EAE animals has shown to improve with administration of drugs that are considered to increase extracellular concentrations of endocannabinoids (Baker *et al.*, 2000; Pertwee *et al.*, 2000).

1.11 3-(5-dimethylcarbamoyl-pent-1-enyl)-N-(2-hydroxy-1-methyl-ethyl)benzamide (VSN16R)

It has been shown that cannabis can control symptoms of MS (Corey-Bloom *et al.*, 2012; Kmietowicz, 2010; Zajicek *et al.*, 2012). This supports earlier observations found in animals with EAE (Baker *et al.*, 2000; Baker *et al.*, 2012). As THC in cannabis and the CB₁ receptor mediate most of both the beneficial and adverse effects of cannabis (Baker *et al.*, 2012; Pryce *et al.*, 2007; Varvel *et al.*, 2005) an attempt was made to produce a CNS-excluded, CB₁ receptor agonist, that can control spasticity by controlling peripheral nerve transduction, yet avoid stimulation of CB₁ receptors cognitive centres of the brain (Pryce, 2010). One of these compounds (3-(5-dimethylcarbamoyl-pent-1-enyl)-N-(2-hydroxy-1-methyl-ethyl)benzamide) termed VSN16R was a water soluble (over 200mg/ml) molecule. The molecule has been found to be orally active with about 30% bioavailability and had a half-life of about 90 min and a C_{max} with 15-30min in mice (Pryce, 2010). The compound has been found to be highly potent *in vitro* and inhibits neurogenic contractions of the vas deferens at low nanomolar concentrations, and this action was inhibited by SR141617A and AM251, two CB₁ receptor antagonists (Pryce, 2010). VSN16R has been shown to inhibit spasticity in EAE at doses ≥1mg/kg i.v. and ≥5mg/kg p.o. that was maintained following repeated administration (Pryce, 2010). This occurred via a CB₁-independent mechanism as assessed by activity in CB₁^{-/-} mice. VSN16R has also failed to show any significant binding to a panel of over 70 different neurotransmitter receptors and ion channels, including CB₁ and CB₂ receptors (Pryce, 2010). It has been suggested that agonists and antagonists bind to different sites

of GPR55 (Elbegdorj *et al.*, 2012). However, interesting VSN16R failed to directly agonize or antagonize the GPR55 receptor in human GPR55-transfected cell lines. However, the action of GPR55 agonist-induced cell signalling was enhanced by VSN16R (Pryce, 2010). This suggested that VSN16R could be a novel, selective, allosteric modulator of GPR55 function. As all reported GPR55 agonists or antagonists have known additional specificities (Baker *et al.*, 2006a) and that the full extent of the endocannabinoid system remains to be elucidated, demonstration of action of pharmacological targets in gene-deficient mice is invaluable to in the validation process.

1.11 AIMS AND OBJECTIVES

The aims of this project is to investigate the role of GPR55 as a therapeutic target to treat spasticity.

The objectives of this project are;

1. Characterize the biology of GPR55.
2. Develop monoclonal antibodies against GPR55 as there are currently no commercially specific GPR55 antibodies available.
3. Identify the distribution profile of GPR55 in rodent tissue, with particular attention to the CNS and peripheral nervous system.
4. Identify the function of GPR55 during EAE in rodents, as it is hypothesized that GPR55 may be up-regulated during disease.
5. Investigate the effect of GPR55 deletion on VSN16R function.
6. Examine the role of the GPR55 in control of spasticity in EAE.

CHAPTER 2

Material and Methods

2.1 Mice

ABH mice were from stock bred at Queen Mary University of London (QMUL), were purchased from Harlan UK Ltd, Bicester, Oxon UK or were donated by UCB, Cambridge, UK or from stock held by Charles Rivers, Margate, Kent. C57BL/6 mice were purchased from Charles Rivers, UK or were from stock bred at QMUL. All animal studies were performed following the Animals (scientific procedures) Act 1986. Mice from in-house bred stock were maintained in a 12h light/dark cycle with controlled humidity and temperature and housed to standards appropriate to the ARRIVE guidelines as described previously (Al-Izki et al. 2012). Animals were fed RM-1E diet and water *ad libitum*.

2.1.1 GPR55 knockout mice

Mice, 129xC57BL/6.GPR55^{tm1Tigm}, expressing a GPR55 gene deletion construct were generated by Lexicon Inc. the and founder mice purchased from the Texas Institute of Genomic Medicine (TIGM Houston, Texas USA). A targeting vector was constructed to replace part of exon 2 of the GPR55 gene (containing the entire coding region) with a selection cassette (Fig. 2.2.1). Homologous recombination was carried out in 129SvEv^{Brd}-derived ES cells, followed by injection of targeted ES cells into blastocysts. The gene deletion map, primer sequence for detection of wild-type and other primers for the knockout targeting molecule and a male 129/C57BL/6.*Gpr55* gene knockout was supplied. These mice were quarantined and initially backcrossed with C57BL/6 mice and re-derived by caesarean section to remove pathogens. A breeding colony was established from a single male animal.

2.2 PCR

2.2.1 DNA extraction

Ear biopsies were removed from mice and DNA tissues samples were prepared following digestion at 56°C overnight in lysis buffer containing 487.5µl Nucleon™ reagent B (400mM TRIS, 60mM EDTA, 15mM NaCl, 150mM SDS 1% pH:8.0) and 12.5µl (20mg/ml) proteinase K (Invitrogen, Paisley, UK). Sodium perchlorate at a volume of 187.5µl (6M) (Sigma-Aldrich, Poole, Dorset, UK) was then added for deproteinization and the samples were incubated for 30 min at 60°C. A volume of 750µl

of chloroform was added and samples were vortexed for 10 min and centrifuged for 2 min at 478g. The aqueous phase was mixed with 1000µl (2 volumes) of ethanol to precipitate the DNA. Samples were mixed and centrifuged for 5 min at 478g. The supernatant was removed and the pellet was dried at 60°C for 10 min. Samples were dissolved in 200µl of distilled H₂O (dH₂O). A Qiagen DNeasy extraction kit from (Qiagen, Crawley, UK) was used for later experiments using the protocol provided by the manufacturer.

2.2.2 PCR 1&2 Genotyping

The following primers and polymerase chain reaction conditions as previously described were used (Johns *et al.*, 2007). The GPR55 sequences were following; GPR55 wild-type: DW1: 5'-TCTTCCCCCTGGAGATCTTT-3'; DW2: 5'-CTGGGAGAAAGGAGACCACA-3'; 30 cycles of 94°C (45 s), 58°C (45 s), and 72°C (45 s) generated an amplicon of 207 bp and the GPR55 knockout (Neomycin gene) (N-5', neomycin gene specific 5' primer: 5'-CCGGCCGCTTGGGTGGAGAGG-3' and N-3', neomycin gene specific 3' primer: 5'-TCGGCAGGAGCAAGGTGAGATGACA-3'; 30 cycles of 94°C (30 s), 68°C (30 s), and 72°C (30 s) generates an amplicon of 299 bp. The PCR components are shown in tables 2.2.1 and 2.2.2. Primers were from Sigma-Aldrich (Ltd, Poole, Dorset, UK). The DNA samples were screened by PCR using Qiagen PCR core kit reagents (Qiagen, Crawley, UK). Samples were run using a Peltier Thermal cycler PTC-225 (MJ Research, Harlow, UK).

New primers for detection of the different genotypes; wildtype, heterozygous and GPR55 knockouts were designed and synthesized (Sigma-Aldrich Ltd, Poole, Dorset, UK). The following primers were used; Forward 5'-TCTGGATTCATCGACTGTGG-3', Reverse1 5'-CTCCACAATCAAGCTGGTCA-3' WT 207bp, Reverse2 5'-GTCACCCATCCAGGTGATGT-3' Transgene 299bp. The cycling conditions for the PCR were following; 35 cycles of 94°C (30 s), 94°C for (30 s), 55°C for (30 s), 72°C (30 s), 72°C (120 s), 4°C (∞), generating an amplicon of 207 bp (GPR55) and 299 bp (Transgene, Neomycin). The DNA samples were screened by PCR using Qiagen PCR core kit reagents (Qiagen, Crawley, UK). The PCR components are shown in table 2.2.3. Samples were run using a Peltier Thermal cycler PTC-225 (MJ Research, Harlow, UK).

Table 2.1 *PCR components for GPR55- specific primers*

Initial concentration reaction components	Final concentration reaction components	Volume (μl)
dH ₂ O	dH ₂ O	27
10 x PCR Rxn buffer (Invitrogen, Paisley, UK) (Tris HCl [pH8.3], 50mM KCl)	10 x PCR buffer (Tris HCl [pH8.3], 50mM KCl)	5
50mM MgCl ₂ (Invitrogen, Paisley, UK)	2.5mM MgCl ₂	2.5
2.0mM dNTP (Invitrogen, Paisley, UK)	0.25mM dNTP	5
20μM <i>Forward DW1 primer</i> (Sigma-Aldrich Ltd, Poole, Dorset, UK)	1μM F DW1 primer	2.5
20μM <i>Reverse DW2 primer</i> (Sigma-Aldrich Ltd, Poole, Dorset, UK)	1μM R DW2 primer	2.5
1.25U/μl Taq Polymerase (Invitrogen, Paisley, UK)	0.0125U/μl Taq Polymerase	0.5
DNA sample	DNA sample	5
Total volume		50.00μl/reaction

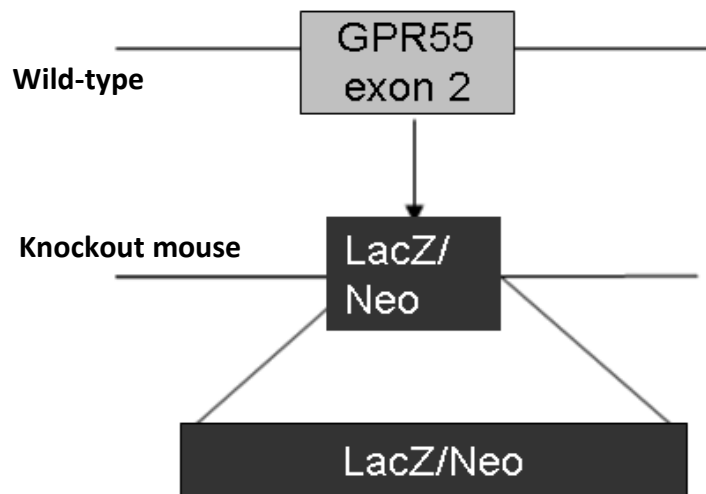
PCR components for master mix. Initial concentrations, final concentrations and volume of components required for PCR master mix to produce a final volume of 50μl per reaction.

Table 2.2 *PCR components for Neomycin primers*

Initial concentration reaction components	Final concentration reaction components	Volume (μl)
dH ₂ O	dH ₂ O	27
10 x PCR Rxn buffer (Invitrogen, Paisley, UK) (Tris HCl [pH8.3], 50mM KCl)	10 x PCR buffer (Tris HCl [pH8.3], 50mM KCl)	5
50mM MgCl ₂ (Invitrogen, Paisley, UK)	2.5mM MgCl ₂	2.5
2.0mM dNTP (Invitrogen, Paisley, UK)	0.25mM dNTP	5
20μM <i>Forward NEO5' primer</i> (Sigma-Aldrich Ltd, Poole, Dorset, UK)	1μM F NEO 5'primer	2.5
20μM <i>Reverse NEO3' primer</i> (Sigma-Aldrich Ltd, Poole, Dorset, UK)	1μM R NEO 3'primer	2.5
1.25U/μl Taq Polymerase (Invitrogen, Paisley, UK)	0.0125U/μl Taq Polymerase	0.5
DNA sample	DNA sample	5
Total volume		50.00μl/reaction

PCR components for master mix. Initial concentrations, final concentrations and volume of components required for PCR master mix to produce a final volume of 50μl per reaction.

Figure 2.1 *GPR55* gene (*Gpr55* gene) deletion construct



129/BL6.*Gpr55* knockout mice were obtained from TIGM. The coding sequence of GPR55 is deleted in the 129/BL6.*Gpr55* mice and replaced by LacZ/Neo. The animals were then backcrossed for two generations with C57BL/6 mice. As the knockout animals express LacZ/Neo, detection of this gene can be performed using PCR. The mouse GPR55 gene is located in chromosome 1(Ch1:87836112-87857630 bp). The deletion sequences are attached in the appendix (Supplementary Figure 1).

Table 2.3 *PCR components for multiplex PCR with primers specific for GPR55 and Neomycin*

Initial concentration reaction components	Final concentration reaction components	Volume (μl)
dH ₂ O	dH ₂ O	24.5
10 x PCR Rxn buffer (Invitrogen, Paisley, UK) (Tris HCl [pH8.3], 50mM KCl)	10 x PCR buffer (Tris HCl [pH8.3], 50mM KCl)	5
50mM MgCl ₂ (Invitrogen, Paisley, UK)	2.5mM MgCl ₂	2.5
2.0mM dNTP (Invitrogen, Paisley, UK)	0.25mM dNTP	5
20μM Forward GPR55 primer (Sigma-Aldrich Ltd, Poole, Dorset, UK)	1μM F GPR55 primer	2.5
20μM Reverse 1 GPR55 primer (Sigma-Aldrich Ltd, Poole, Dorset, UK)	1μM R1 GPR55 primer	2.5
20μM Reverse 2 GPR55 primer (Sigma-Aldrich Ltd, Poole, Dorset, UK)	1μM R2 GPR55 primer	2.5
1.25U/μl Taq Polymerase (Invitrogen, Paisley, UK)	0.0125U/μl Taq Polymerase	0.5
DNA sample	DNA sample	5
Total volume		50.00μl/reaction

PCR components for master mix. Initial concentrations, final concentrations and volume of components required for PCR master mix to produce a final volume of 50μl per reaction.

2.2.3 Gel electrophoresis

The PCR products were analyzed using gel electrophoresis at (120 volts) for 60-90 min. For each sample 18µl DNA was loaded with 3µl bromophenol blue loading buffer (Invitrogen, Paisley, UK). PCR products were analyzed by 2% agarose gel, 4g agarose (Fisher BioReagents, Loughborough, UK), in 20ml (10x) Tris/Borate/EDTA (TBE) buffer (Sigma, Poole, UK), 10µl ethidium bromide (Sigma-Aldrich, Poole, Dorset, UK) and 180ml dH₂O. A 50bp ladder (Invitrogen, Paisley, UK) was used as a reference. Gels were imaged on a luminescent imaging system (UVIdoc).

2.3 Antibody production

Fusion peptides corresponding to both the extracellular and intracellular domains of GPR55 were obtained from Dr Ken Mackie, University of Indiana, USA. Essentially uncharacterized cell lines overexpressing GPR55 in a mouse astrocytoma, murine Delayed Brain Tumor (DBT) E1 cell line, and non-transfected controls DBT were obtained from Dr. Nephi Stella (University of Washington, Seattle, USA). It has previously been reported that the untransfected DBT cell line does not express CB₁, CB₂ nor GPR55 receptors (Cudaback *et al.*, 2010).

GPR55 knockout mice (C57BL/6.*Gpr*^{-/-}) were immunized with GPR55-GST fusion peptides (vector pGEX-3X), including an amino terminus and C terminus full length mouse sequences and IC3 the third intracellular loop of the mouse protein or with the GPR55 transfected astrocytoma cell line E1. Immunization with cell lines for production of antibodies has previously been described (Croxford, 2010). The following sequences were used; NH: MSQPERDNCSFDSVCKLTRT, IC3: YRSIHILLRRPDSTEDWVQQRDTKGWVQKRAC and CT-FL: KEFRMRIKAHRPSTIKLVNQDTMVSRG. The spleen from immunized mice was fused with a plasmacytoma cell line NS-1 (Healey *et al.*, 1987) and hybridomas were screened using Enzyme-linked immunosorbent assay (ELISA) against the proteins used for immunization. Flow cytometry, immunostaining and Western blot of membrane lysates from GPR55-expressing cell lines was used to test the antibodies. The positive hybridomas were then antibody isotyped.

Dulbecco's modified eagle medium (DMEM) (Sigma-Aldrich, Poole, Dorset, UK) was prepared before fusion by adding 1% penicillin (Invitrogen, Paisley, UK) and 1% hepes (Sigma-Aldrich, Poole, Dorset, UK). The medium was kept at 37°C during the fusion. An aliquot of 10 ml of complete medium was transferred into a falcon tube. Immunized mice were then sacrificed and the spleen was removed and extracted with a syringe in a Petri dish. All centrifugation were made on the Thermo Fischer heraeus multifuge 3SR centrifuge order no: 75004371. The cell suspension was then transferred into a falcon tube and centrifuged for 5-10 min at 478g. This was also repeated

with the NS-1 cells. The supernatant was decanted and 10 ml of medium was added. This was repeated 3 times followed by a centrifugation at 478g. An aliquot of cell suspension was taken before the last wash in order to count the cells and the two cell types were mixed together and centrifuged for 5 min at 478g at a ratio of 5 lymphocytes: 1 NS-1 cell. The fusion was started by removing the supernatant. 1 ml of Polyethylene glycol (PEG) (Sigma-Aldrich, Poole, Dorset, UK) was added to the pellet during 1 min 30 s and the tube shaken at the same time and then left for 30 s. 1 ml of complete medium was then added during 1 min 30 s followed by adding 20 ml of medium during 2 min. The cell suspension was then left in a water bath for 5 min. After centrifugation for 5 min at 478g, the supernatant was removed and fresh complete medium was added. The cells were then left in a 37°C incubator for approximately 3 h. The cells were plated in a 96 well plate by adding 100 µl of cell suspension and 100 µl of complete medium in each well. The hybridomas were then grown in complete medium containing 1x hypoxanthine-aminopterin-thymidine (HAT) (Sigma-Aldrich, Poole, Dorset, UK). HAT was replaced by hypoxanthine-thymidine (HT) after two weeks and added to the cell medium for another two weeks. DMEM (Sigma-Aldrich, Poole, Dorset, UK) medium used for preparation of fusion contained Hepes (1%) (Sigma-Aldrich, Poole, Dorset, UK), penicillin streptomycin (1%) (Sigma-Aldrich, Poole, Dorset, UK). Complete medium used after fusion contained: (5%) Horse serum (Lonza, Cambridge, UK), (5%) foetal calf serum (Invitrogen, Paisley, UK), penicillin streptomycin (1%) (Sigma-Aldrich, Poole, Dorset, UK), sodium pyruvate (1%) (Sigma-Aldrich, Poole, Dorset, UK), L-glutamine (1%) (Lonza, Cambridge, UK), Insulin (1%) (Sigma-Aldrich, Poole, Dorset, UK), (0.1%) B-mercaptoethanol (Invitrogen, Paisley, UK) and 1x HAT (Sigma-Aldrich, Poole, Dorset, UK). Other components used were PEG (Sigma-Aldrich, Poole, Dorset, UK) and 1x HT (Sigma-Aldrich, Poole, Dorset, UK).

2.4 Enzyme Linked Immunosorbent Assay (ELISA)

96 well flat bottom culture plates were coated with 10 µg of peptides/fusion proteins and were incubated overnight at 4°C. The following day the plate was blocked with 1% bovine serum albumin (BSA) prepared in PBS for 1 h at 37°C. The plate was washed 4-5 times with PBS+0.1% tween following the addition of primary antibody, 100 µl serum from immunized animal or 100 µl supernatant from hybridomas, was added. The plate was incubated for a further 1 hour at 37°C. Once again 4-5 washes were done with PBS tween before the addition of anti-mouse horseradish peroxidase (HP) conjugated secondary antibody (DAKO, Cambridgeshire, UK) prepared at 1:1000 dilution. After an hour of incubation at 37°C the plate was washed 4-5 times and 100 µl of substrate 3, 3', 5, 5'-Tetramethylbenzidine (TMB) (Sigma-Aldrich, Poole, Dorset, UK), was added to each well. After the reaction turned blue it was stopped by addition of 50 µl of hydrochloric acid. The plate was then read at 450 nm using the KC-4 programme from (Biotek, Bedfordshire, UK).

2.5 Antibody isotyping ELISA

A 96 well plate was coated with 50µl of isotype-specific rat anti-mouse purified monoclonal antibodies including IgG1, IgG2a, IgG2b, IgG3, IgM, IgA, Igκ and Igλ diluted 1:50 in PBS. Plate was then incubated at 4°C overnight and washed 4x with 0.05% Tween-20 in PBS. 200µl blocking buffer, 10% BSA in PBS, was added to each well and incubated at RT for 30 min. 100µl of each supernatant from positive hybridomas was added to plate columns and incubate for 1 hour at RT. Plate was then washed 4x with 0.05% Tween-20 in PBS before adding 100 µl of 1/100 HP-labeled rat anti-mouse Ig mAb diluted in 10% BSA in PBS to each well and incubated at RT for 1 hour. Plate was then washed 6x with 0.05% Tween-20 in PBS and 100 µl of substrate solution was added to each well and the plate was read spectrophotometrically at 450 nm.

2.6 Western blotting

Western Blotting (WB) was carried out using protein samples from GPR55 transfected and non-transfected cells. 10µg of protein samples were loaded onto a 10% Tris HCl gel (Bio-Rad, Hertfordshire, UK). The samples were run for approximately 90 min at 120 volts using the Mini-Protean gel system apparatus from Bio-Rad. The gels were then transferred onto nitrocellulose membrane which was blocked overnight with 5% BSA at 4°C. The following day the membrane was washed with 1X PBS followed by incubation for 1 h at RT with supernatant from positive hybridomas diluted 1:100. The membrane was washed 4X with PBS after which the secondary antibody anti-mouse HP (DAKO, Cambridgeshire, UK) was added for 1 h at RT. Another 4X washes with PBS were done again before the addition of enhanced chemiluminescence (ECL) reagent (GE Healthcare, Buckinghamshire, UK, 17-0855-02) to the membrane. The membrane was then exposed for 1-2 min using a film (Kodak, Amersham Pharmacia Biotech, Bucks, UK, 17-0340-01).

2.7 Immunofluorescence

Immunofluorescence was performed on to staining the GPR55 transfected cells with non-transfected cells with the supernatant from positive hybridomas. Cells were seeded in a 24 well plate and let to grow for 3-4 days. Cells were washed 3 X 5min in PBS 0.1% tween and fixed with 4% paraformaldehyde (PFA) for 20 min. Cells were washed 3 x 5 min in PBS 0.1% tween. Cells were then blocked for 1 hour at room temperature (RT) with 1% BSA in PBS 0.1% tween. 200µl supernatant (or other ab) were then added per well at incubated for 1 h at RT. Cells were washed 3 x 5 min in PBS 0.1% tween after incubation and incubated with a 1:100 secondary antibody anti-mouse IgG (H+L) Fluorescein isothiocyanate (FITC) (other ab) for 2h at RT. Cells were washed 2 X 5 min in PBS 0.1% tween. The wells were cover slipped and viewed under a fluorescent microscope.

2.8 cAMP Response Element-binding Protein staining

Cells were grown onto cover slips in a 24 well plate for 48 h in RPMI media containing 10% FBS. Serum free medium was added to each well 24 h prior to experiment. Hepesbuffer (1x) was warmed in a 37°C CO₂ free chamber. Ligands were diluted in warm hepes and 1ml of ligands was added to each well. Cells were fixed with ice cold methanol pre-cold in a -20°C freezer and incubated in -20°C freezer for 10 min. Cells were then blocked with 5% milk diluted in hepes buffer for 20 min. Wells were then washed with hepes buffer and the cover slips were placed on parafilm. The cells were then stained with a primary CREB (cAMP Response Element-binding Protein) antibody (UPSTATE Cat no# 05-667 clone E9 Ms pCREB, Anti-phospho-CREB IgG1κ, 0.2mg/mg in dH₂O and glycerol) (Billerica, MA, USA) (1:1000) for 60 min at RT and kept in the dark followed by staining with a secondary ALEXA fluor 488 antibody (Invitrogen, Paisley, UK, Alexa fluor 488 donkey anti mouse A21202) (1/500) at RT for 30 min. Cells were washed with hepes buffer and analyzed on the LSM 510 confocal laser scanning microscope.

2.9 Phalloidin staining

Cells were grown onto cover slips in a 24 well plate for 48 h in RPMI media containing 10% FBS. Serum free medium was added to each well 24 h prior to experiment. Hepesbuffer (1x) was warmed in a 37°C CO₂ free chamber. Ligands were diluted in warm hepes and 1ml of ligands was added to each well and incubated for 30 min at 37°C. Cells were fixed with 4% PFA for 10 min. Cells were then blocked with 0.01% triton diluted in hepes buffer for 10 min. Wells were then washed with hepes buffer and the cover slips were placed on parafilm. The cells were then stained with Phalloidin (Texas-Red Phalloidin, (Invitrogen, Paisley, UK) (1:500) and incubated for 30 min. The cells were washed with hepes buffer and analyzed on the LSM 510 confocal laser scanning microscope.

2.10 Flow cytometry

Supernatant was taken from cell hybridomas and analyzed by flow cytometry. A total of 1x10⁶ cells/ml GPR55 transfected cells and non-transfected cells were used. PBS and supernatant from wells without hybridomas were used as a negative control and 100µl of supernatant from wells with hybridomas in 5% FBS in phosphate buffered saline (PBS). Cells were incubated with the antibodies for 30 min at 4°C and then washed with 5% FBS in PBS. Samples were then incubated with Alexa fluor 488 (Invitrogen, Paisley, UK) (1/100) for 30 min at 4°C. Samples were vortexed and incubated for a minimum of 10 min at RT and were analysed by flow cytometry (Becton Dickinson, Oxford, UK).

2.11 Calcium signalling

A 2mM stock solution of Fura 2-am solution was initially prepared in DMSO; 499.5µl DMSO was added to 1mg lyophilized Fura-2-am (ref: F0888, Sigma-Aldrich, Poole, Dorset, UK). A volume of 3µl of 2mM stock was added into a 15 ml falcon tube and followed by 1 ml of hepes buffer. The solution was then mixed well with a pipette and vortexed. Cells were grown onto cover slips in a 24 well plate for 48 h in RPMI media (Sigma-Aldrich, Poole, Dorset, UK) containing 10% FBS. Serum free medium was added to each well 24h prior to experiment start. Wells were washed with hepes buffer and 333µl of fura 2-am diluted in hepes was added per well. The cells were incubated for 60 min and then washed with hepes buffer and analyzed on the LSM 510 confocal laser scanning microscope.

2.12 Quantitative PCR (qPCR)

2.12.1 RNA extraction

Tissues were collected from mice and immediately immersed in liquid nitrogen or RNA later solution (Qiagen, Crawley, UK) and then stored at -80°C. RNA extractions were performed with an RNeasy mini kit (Qiagen, Crawley, UK). Tissues were initially weighed and approximately 30mg was used per sample. Tissues were homogenized in 600 µl lysis buffer either by using a mortar and pestle followed by trituration using a needle or by using a tissuelyser (Qiagen, Crawley, UK).

The lysates were then centrifuged for 3 min at 8000xg. The supernatants were then transferred by pipetting into a new micro centrifuge tube. One volume of 70% ethanol was added to the cleared lysate and mixed immediately by pipetting. Up to 700 µl of the sample was transferred to an RNeasy spin column placed in a 2 ml collection tube. If the sample volume exceeded 700 µl, aliquots were centrifuged for 15s at 8000xg in the same RNeasy spin column. The flow-through was discarded after each centrifugation. An amount of 700 µl of buffer RW1 (wash buffer containing ethanol and salts) was added to the RNeasy spin column and samples were centrifuged for 15 s at 8000xg and the flow-through was discarded. A total of 500 µl Buffer RPE (wash buffer containing ethanol and salts) was added to the RNeasy spin column and samples were centrifuged for 15 s at 8000xg. An additional wash with 500 µl Buffer RPE was added to the RNeasy spin column and samples were centrifuged for 2 min at 8000xg. The RNeasy spin column was then placed in a new 2 ml collection tube to eliminate any possible carryover of Buffer RPE. The RNeasy spin column was then placed in a new 1.5 ml collection tube and 30µl of RNase-free water was added directly to the spin column membrane to elute the RNA. Samples were then centrifuged for 15 s at 8000xg. The RNA concentrations in the samples were then spectrophotometrically measured (Nanodrop ND-1000) (Thermo Scientific, Ringmer, East Sussex, UK).

2.12.2 Reference genes: GAPDH and 36B4

The following primers were used for detection of GAPDH; forward 5'-GCCTTCTCCATGGTGGTGAA -3', reverse 5'-GCACAGTCAAGGCCGAGAAT -3'. SYBR green was used as a dye for detection of GAPDH. The following 36B4 primers and probe; forward 5'-AGATGCAGCAGATCCGCA -3', reverse 5'-GTTCTTGCCCATCAGCACC -3', 5'-HEX-CGCTCCGAGGGAAGGCCG -TAMRA-3' were tested as reference genes in the various mouse tissues. Quantitative PCR was performed in duplicates in 96-well reaction plates with the Applied Biosystems 7500 Real-Time PCR system (Applied Biosystems, Warrington, Cheshire, UK) and the cycling conditions for the qPCR were following; 95°C (10 min), 40 cycles of 95°C for (45 s), 60°C for (60 s). The PCR components for GAPDH are shown in table 2.5 and in table 2.6 for 36B4.

Table 2.4 *Reference gene GAPDH*

Initial concentration reaction components	Final concentration reaction components	Volume (μl)
dH ₂ O	dH ₂ O	5
2xTaqMan® Gene Expression Master Mix(Qiagen, Crawley, UK)	2 x Gene Expression Master Mix	10
10μM <i>Forward GAPDH primer</i> (Invitrogen, Paisley, UK)	0.5μM F GAPDH primer	1
10μM <i>Reverse GAPDH primer</i> (Invitrogen, Paisley, UK)	0.5μM R GAPDH primer	1
10μM <i>Taqman probe</i> (Invitrogen, Paisley, UK)	0.5μM Taqman probe	1
cDNA sample	cDNA sample	2
Total volume		20μl/reaction

PCR components for master mix. Initial concentrations, final concentrations and volume of components required for qPCR master mix to produce a final volume of 20μl per reaction.

Table 2.5 *Reference gene 36B4*

Initial concentration reaction components	Final concentration reaction components	Volume (μl)
dH ₂ O	dH ₂ O	5
2xTaqMan® Gene Expression Master Mix (Qiagen, Crawley, UK)	2 x Gene Expression Master Mix	10
10μM <i>Forward 36B4 primer</i> (Invitrogen, Paisley, UK)	0.5μM F 36B4primer	1
10μM <i>Reverse 36B4primer</i> (Invitrogen, Paisley, UK)	0.5μM R 36B4 primer	1
10μM <i>Taqman probe</i> (Invitrogen, Paisley, UK)	0.5μM Taqman probe	1
cDNA sample	cDNA sample	2
Total volume		20μl/reaction

PCR components for master mix. Initial concentrations, final concentrations and volume of components required for qPCR master mix to produce a final volume of 20μl per reaction.

2.12.3 Quantification of GPR55 mouse mRNA levels using qPCR

The following GPR55 primers and probe; 5'-CTATCTACATGATCAACTTGGCTGTTT-3', 5'-TGTGGCAGGACCATCTTGAA-3', 5'-FAM-CGATTACTGCTGGTGTCTCCCTCCC-TAMRA-3' were used for mRNA quantification as previously described (Ryberg *et al.*, 2007). Quantitative PCR was performed in duplicates in 96-well reaction plates with the Applied Biosystems 7500 Real-Time PCR system (Applied Biosystems, Warrington, Cheshire, UK) and the cycling conditions for the qPCR were following; 95°C (10 min), 40 cycles of 95°C for (45 s), 55°C for (45 s), 72°C (45s). The PCR components are shown in table 2.5.

Table 2.6 Quantitative PCR components for GPR55

Initial concentration reaction components	Final concentration reaction components	Volume (µl)
dH ₂ O	dH ₂ O	6.8
2xTaqMan® Gene Expression Master Mix(Qiagen, Crawley, UK)	2 x Gene Expression Master Mix	10
50µM Forward GPR55 primer (Invitrogen, Paisley, UK)	0.25µM F GPR55 primer	0.1
50µM Reverse GPR55 primer (Invitrogen, Paisley, UK)	0.25µM R GPR55 primer	0.1
100µM Taqman probe (Invitrogen, Paisley, UK)	5µM Taqman probe	1
cDNA sample	cDNA sample	2
Total volume		20µl/reaction

PCR components for master mix. Initial concentrations, final concentrations and volume of components required for qPCR master mix to produce a final volume of 20µl per reaction.

2.12.4 Standard curve

A GPR55 amplicon was designed, ctatct acatgatcaa cttggctgtt ttcgatttac tgctggtgct ctccctccca ttcaagatgg tcctgcaca 76bp, and was used for a standard curve in order to determine GPR55 mRNA levels in various tissues by qPCR.

2.13 ³⁵S Oligonucleotide in *situ* hybridization

Before starting the procedure all equipment was treated with 1 M NaOH then rinsed with dH₂O followed by a rinse with Diethylpyrocarbonate (DEPC) (Sigma-Aldrich, Poole, Dorset, UK) treated dH₂O. All other solutions were also treated with 1ml DEPC per litre of solution.

The following mouse GPR55 primers were designed and used for labeling:

Primer 1 mouse gpr55 pos: 424-457“gaggagagcaccagcagtaaatacgaaaacagcc”, primer 2 mouse gpr55 pos: 906-939“gcaatggtggagatgcaggctctctttgtaccc”and primer 3 mouse gpr55 pos: 1750-1783“cccattggctctgtcatgtctctattccacac”

2.13.1 Probe labeling

The isotype, ³⁵SdATP (1200Ci/mmol, Dupont/NEN#NEG-034) (PerkinElmer LAS, Beaconsfield, Bucks, UK), was thawed on ice for 30 min. The following was added to make 50µl reactions: 10µl of 5x tailing buffer (Promega, Southampton, UK), 29µl of dH₂O, 3µl of ³⁵S dATP(PerkinElmer LAS, Beaconsfield, Bucks, UK) , 4µl of oligonucleotide (Sigma-Aldrich, Poole, Dorset, UK) (4µl of 1pmol/µl stock) diluted in TE buffer (Tris-EDTA) and 4µl terminal deoxynucleotidyl transferase (Promega,Southampton,UK).The samples were vortexed and centrifuged briefly followed by an incubation at 37°C for 1-2 h. Separation of the samples was made on Pharmacia Sephadex G50 DNA grade columns (GE Healthcare,Buckinghamshire, UK, 17-0855-02). The samples were mixed and incubated at 37°C for 1-2 h. Excess liquid was then poured off and the columns were rinsed once with TE buffer pH 8.0. The bottom cap was then removed and filled with 3 ml of TE buffer and left to run though. The probe was added onto the column and 400µl TE buffer was added to the column. The eluate was discarded and an additional volume of 400µl equilibrium buffer was added to the column and collected in a 15ml falcon tube containing 5µl dithiotheitol (DTT) (Sigma-Aldrich, Poole, Dorset, UK). The activity in 2µl was then measured with a Beckman coulter liquid scintillation counter LS6000SC (Beckman Coulter LTD, High Wycombe, UK) and the probes were freeze dried.

2.13.2 Preparation of tissue sections

Frozen tissues were cut into 10µm sections onto superfrost slides (VWR International Ltd, Leicestershire, UK) and air dried for 30 min before storage in -80°C. Tissues were fixed for 5 min in 4 % Paraformaldehyde (PFA) in 0.1% phosphate buffer, pH 7.4 before prehybridization treatments.

2.13.3 Prehybridization

Sequential washes were made: 2x5 min in DEPC treated PBS, 1x10 min in triethanolamine (VWR International Ltd, Leicestershire)/acetic anhydride (Sigma-Aldrich, Poole, Dorset, UK) in DEPC PBS. Triethanolamine (3.75g in 250ml-0.1M/ acetic anhydride (625 μ l in 250ml-0.025M), x5 min in DEPC treated PBS, 1x2 min 70% ethanol diluted in DEPC water, 1x2 min 95% ethanol diluted in DEPC water, 1x2 min 100% ethanol diluted in DEPC water, 1x2 min in chloroform, 1x2 min 100% ethanol diluted in DEPC water, 1x2 min 95% ethanol diluted in DEPC water and slides were then air dried for 5-10 min.

2.13.4 Hybridization

The probe was resuspended in 2 ml of hybridization buffer (2X Denhardt's solution prepared from sigma stock 50x (Sigma-Aldrich, Poole, Dorset, UK), 4x Standard saline citrate (SSC), 3M NaCl 0.1M Tri-sodium citrate pH:7.0, 50% deionised formamide (Sigma-Aldrich, Poole, Dorset, UK), 10% dextran sulphate (Amersham Pharmacia Biotech, Bucks, UK, 17-0340-01) and heated for 5 min at 65°C then put on ice. A volume of 80 μ l was then applied to each slide and covered with a glass coverslip. The slides were incubated at 37°C overnight in a humidified chamber.

2.13.5 Washes

The following washes were made;

The coverslips were removed in 2xSSC with beta mercaptoethanol (1ml/250ml 2xSSC buffer), 2x15 min in 2xSSC/beta mercaptoethanol (Sigma-Aldrich, Poole, Dorset, UK) at 22°C in hood, 2x15 min in 1xSSC at 50°C in a water bath, 1x15 min in 0.2xSSC at 50°C in a water bath, 2x30 min in 1xSSC at 22°C, slides were dipped in 0.1 SSC to remove excess SSC, dipped in 70% ethanol for 10-20 seconds, dipped in 95% ethanol for 10-20 seconds and finally dipped in 100% ethanol for 10-20 seconds and air dried. Once dried, the slides were exposed to x-ray film (BIO-MAX MR-1) (PerkinElmer LAS, Beaconsfield, Bucks, UK) for 3-6 days. The development was performed in a darkroom using red Kodak no.2 filter (Amersham Pharmacia Biotech, Amersham Bucks, UK, 17-0340-01) with a bulb placed one meter from the slides. The slides were developed in Kodak D19 developer (Amersham Pharmacia Biotech, Bucks, UK) for 2.5 min and dipped in 0.5 acetic acid stop solution and then dipped 2x 5 min in 25-30% sodium thiosulfate solution. The slides were agitated every 30 second during the development and then rinsed in water for 6x10 min.

2.14 Non-Radioactive *In situ* Hybridization (NR-ISH)

Digoxigenin (DIG)-labeled antisense and sense cRNA probes were synthesized by *in vitro* transcription in the presence of DIG-labeling mix (Roche, Welwyn Garden City, Hertfordshire, UK) following the manufacturer's instruction and using ~1 µg of linearized template and T7 or SP6 RNA polymerase (New England Biolabs). The concentration and integrity of each RNA probe was analyzed by gel electrophoresis and spectrophotometrically (Nanodrop ND-1000) (Thermo Scientific, Ringmer, East Sussex, UK). For each probe, the transcription reaction resulted in ~10 µg of DIG-labeled RNA, which was diluted with DEPC-treated dH₂O to a concentration of 100 ng/µl, aliquoted, and stored at -80°C. All probes were used at a concentration of 800 ng/ml in hybridization buffer. Frozen sections were fixed in 4% PFA for 5 min and permeabilized with Proteinase K (Sigma-Aldrich, Poole, Dorset, UK), 5 µg/ml in 100mM Tris HCl pH 7.5 and 50mM EDTA, pH 8.0 for 10 min at 37°C. Post fixation was made in PFA for 5 min. After washes in PBS-0.1% Tween-20 (T-PBS) (Sigma-Aldrich, Poole, Dorset, UK), slides were acetylated in T-PBS containing 0.25% acetic anhydride and 0.1% triethanolamine (pH 8.0) for 10 min at room temperature (RT). Finally, sections were prehybridized at 57°C in hybridization buffer. After 1 h of pre-hybridization the probes were thawed on ice and 8 µl probe was denatured in a 95 °C water-bath for 5 min then resuspended in 1ml of hybridization buffer. A volume of 400 µl of hybridization buffer containing the probes was added to each slide and slides were covered by parafilm (VWR International Ltd, Leicestershire). The hybridization reaction was allowed to proceed for about 17 h at 57°C. After hybridization, the sections were washed in decreasing concentrations of SSC (2X, 1X, 0.2X and 0.05X, where 2X is 0.3M sodium chloride and 0.03M sodium citrate, pH 7.0) at 65°C for 15 min each. The slides were then washed in STE buffer (0.5M NaCl, 10mM Tris pH 7.5, 5mM EDTA) for 10 min at RT followed by treatment with Rnase A (Sigma-Aldrich, Poole, Dorset, UK) (25 µl of 20mg/ml stock in 50 ml of STE buffer) for 30 min at 37°C. After washing the slides twice with Maleic Acid Buffer (MAB) pH:7.5 (0.1M maleic acid, 0.15 NaCl, pH 7.5) they were incubated overnight at 4°C with anti-digoxigenin (DIG) alkaline phosphatase-Fab fragments (Roche, Hertfordshire, UK) diluted to 1:2000 with 0.5% Blocking Reagent (Roche, Hertfordshire, UK) in MAB/0.1% Tween 20. After two washes with T-PBS the slides were equilibrated in alkaline buffer (100mM Tris pH 9.5, 100mM NaCl, 50mM MgCl₂, 1% Tween-20) for 10 min before being incubated at RT with Nitro blue tetrazolium chloride/5-Bromo-4-chloro-3-indolyl phosphate, toluidine salt (NBT/BCIP) (Roche, Hertfordshire, UK) in alkaline buffer supplemented with levamisole (1 drop/5ml) (Vector laboratories, Inc, Burlingame, CA 94010-2206). Sections were checked every hour until adequate staining was achieved. Sections were finally washed in 3x for 5 min with T-PBS and mounted with a glycerol-PBS (1:8) based mounting medium.

2.15 EAE

2.15.1 EAE in C57BL/6 mice

The procedure of EAE in C57BL/6 mice was similar except that the spinal cord homogenate is replaced with 200µg synthetic peptide amide corresponding to the 35-55 amino acid residues of mouse myelin oligodendrocyte glycoprotein MOG35-55 made as a peptide amide (Sigma, Poole, UK). In subsequent experiments pre-prepared MOG35-55 in Freund's adjuvant was purchased from Hooke Laboratories, Lawrence, MA, USA).

2.15.2 EAE in ABH mice

20ml syringes (Becton Dickinson, Oxford, UK) were to make up the solution (i.e. multiples of 20ml). Firstly a stock solution was prepared (stock A), consisting of 4ml incomplete Freund Adjuvant (Difco, Becton Dickinson, Oxford, UK), 16mg *Mycobacterium tuberculosis* H37Ra and 2mg *M. butyricum* (Difco, Becton Dickinson, Oxford, UK), in a 5ml Bijou (Sterilin, Caerphilly, UK). This was kept for no longer than 1 month at 4°C. Stock mycobacteria were stored at -70°C. Once a vial was opened it was stored in fridge/freezer. If the incidence of EAE dropped to about 50% it was usually that the *M. tuberculosis* had lost its potency and needed replacing. Complete adjuvant: Freund's adjuvant was prepared by adding 11.5ml adjuvant incomplete Freund's adjuvant to 1ml stock A that was vortex-mixed before use.

The plunger from a 20ml syringe was removed and the barrel was plugged with a stopper cap (Scientific Laboratory Supplies, Nottingham, UK). 5ml sterile PBS was added and 33mg of freeze dried spinal cord homogenate (6.6mg/ml). This was mixed and then 5ml of Complete Freund's adjuvant was added (see above). The syringe was sealed with parafilm and vortexed. A retort stand, boss and clamp was used to hold the 20ml syringe in place with the water level reaching the level of the adjuvant (containing a drop of detergent) in a waterbath sonicator (Branson Ultrasonicator, Sigma, UK) and sonicated for 10 min to thicken the mixture and dissociate the spinal cord homogenate. The adjuvant was vortexed and placed on ice to cool. A 1ml syringe (Becton Dickinson, Oxford, UK) was inserted into the 20ml syringe and the adjuvant was pumped using the 1ml syringe until it had thickened sufficiently that the solution did not disperse when a drop was added to water. The plunger was inserted into the 20ml syringe and the syringe was tapped on the bench such that the content moved towards the plunger and then the syringe cap was removed. A long (6cm) large bore needle was fixed to the syringe and inserted into 1ml syringes with plungers pulled out to the 1ml mark. The syringe was filled to 1ml and the barrel of the 1ml syringe was wiped with tissue paper to remove any excess adjuvant. A 16mm 25g needle

(Becton Dickinson, Oxford, UK) was fixed to the 1 ml syringe. With the tip of the needle cover on the bench, the syringe was pushed very firmly onto the needle.

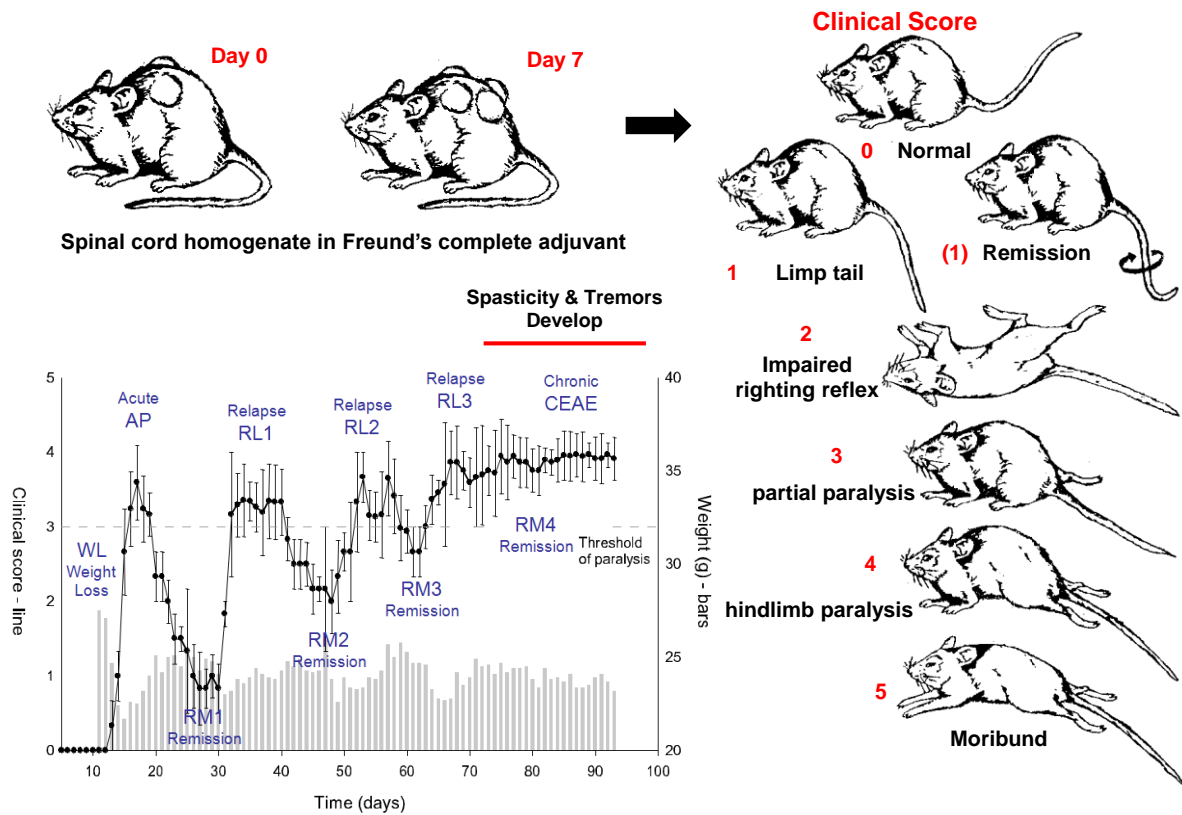
2.15.3 Injection of animals

Disease was typically induced in 6-8 week male and or female mice. Mice were held at the nape of the neck between thumb and forefinger. The tail was held with the right hand with thumb and forefinger (tips facing the head) and the mouse was placed on the top of a wire mouse cage. The skin of the dorsal surface of the flank was lifted with thumb and forefinger (left hand) and the needle was inserted (facing towards the head) subcutaneously into the mouse. 0.15ml of adjuvant was injected into the right flank and another 0.15ml was injected into the left flank. This was day 0. The procedure was repeated one week later (day 7). Injections were below, more posterior to the original injections. EAE ABH disease developed at around day 14-15 (Baker *et al.*, 1990; Amor *et al.*, 1994). A relapse could be induced about 7-8 days after a further injection of neuroantigen in Freund's complete or incomplete adjuvant (O'Neill *et al.* 1991). ABH mice did not require the injection of *Bordetella pertussis* toxin (Sigma, Poole, UK), however, MOG-induced disease in C57BL/6 mice typically required the co-administration of 0.1ml of 200ng *B. pertussis* toxin in PBS on day 0 and day 7.

2.15.4 Chronic Relapsing experimental autoimmune encephalomyelitis (CREAE)

Chronic relapsing experimental autoimmune encephalomyelitis (EAE) is an animal disease model of MS most commonly used to study autoimmune function. The disease displays relapsing-remitting episodes of neurological deficit similar to the most common form of MS (Baker *et al.*, 2000). The control of signs of disease and neuroprotection by cannabinoids has been in CREAE (Baker *et al.*, 2000).

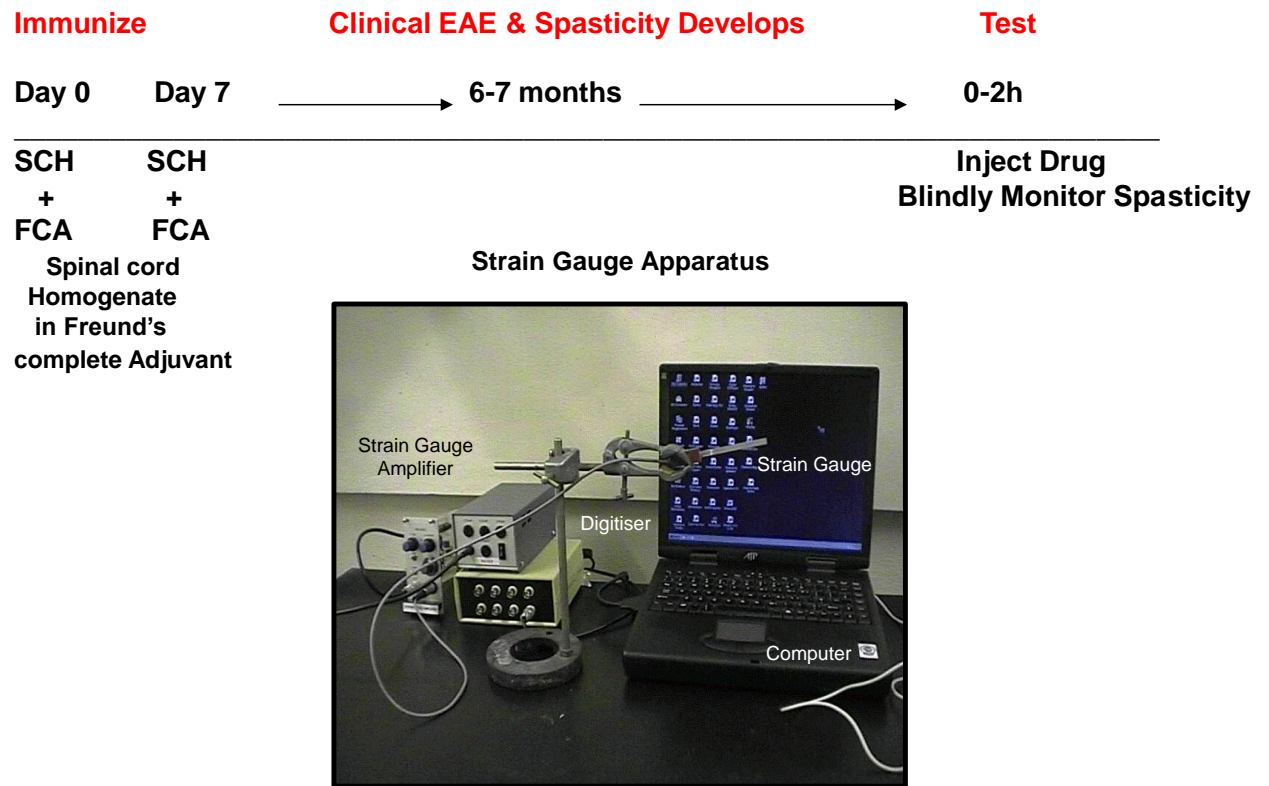
Figure 2.2 *Clinical Disease Course of Chronic Relapsing Experimental Allergic Encephalomyelitis*



Disease was induced in 6-8 week male and or female ABH mice. The animals were injected with spinal cord homogenate in Freund's complete at day 0 and day 7. Animals were weighed and scored daily from day 11 onwards. At approximately day 13, mice lost more than 1.5g of weight overnight. Weight loss continued for a few days. On about day 16, clinical signs start. This was ascending paralysis that started with the tail. This was scored as follows: Normal = 0 Fully flaccid tail = 1. Tail is completely paralysed. Impaired righting reflex. = 2. When turned on back, the animal does not right itself. Hindlimb paresis = 3. Significant loss of motor function of the hindlimbs, characterized by hindlimb gait disturbance. Complete hindlimb paralysis = 4. Both hind limbs drag. Moribund/Death = 5. If forelimbs became paralysed or at a weight loss limit of about 35% from the day 10 the animal was

2.15.5 Rotorod Activity Monitoring

Motor control and coordination was assessed on an accelerating (4 – 40 rpm. 12rpm/50s) RotaRod treadmill (ENV-575M. Med Associates Inc, St. Albans, VT, USA), during the remission phases of the disease, over a maximum 5 minute observation period. The trial was terminated when the mouse either fell from the RotaRod spindle or if the mouse failed to tolerate the revolving drum shown by holding onto the RotaRod spindle rod for two consecutive turns.

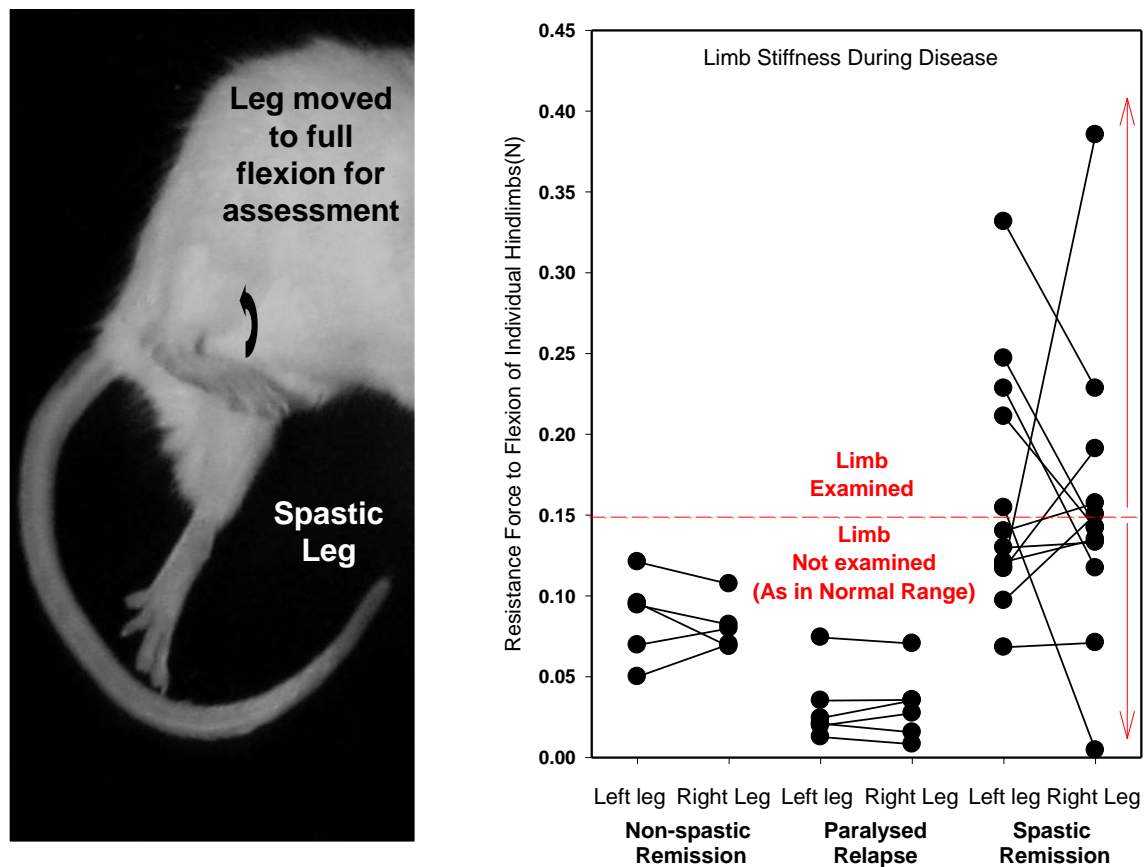
Figure 2.3 *Protocol of spastic measurement*

2.16 Spastic measurement

Following EAE induction and the development of chronic relapsing EAE, spasticity typically developed after 2-3 relapses, about 80-100 days post-induction (Baker *et al.*, 2000). This was assessed during remission from active paralytic episodes by the force required to bend the hind limb to full flexion against a strain gauge (Baker *et al.*, 2000). Mice were selected on the basis of mice visually showing spasticity. Limbs that were flexed were not measured. Animals were randomly assigned to treatment or vehicle and monitoring was performed blinded to treatment or nature of the genotype. The limb was extended two-three times and then the limb was gently pressed against a strain gauge to full flexion. The measurement of left then right hindlimbs was repeated typically 5 times per time point. Analogue signals were amplified and then digitized and captured using a DAQcard 1200 PCMCIA card (National Instruments Austin, TX, USA) and Acquire V1 software (D. Buckwell, Institute of Neurology, UCL) on the Windows™ XP platform. Limbs with a resistance to flexion force or with a resistance less than 0.15N were excluded from the analysis (Figure 2.3). The data were analyzed using Spike 2 software (Cambridge Electronic Design, UK) and a mean score for each limb at each time point was calculated and forces were converted to Newtons. The results represent the mean \pm SEM resistance to flexion force (N) or individual limbs,

which were compared using repeated measures analysis of variance or paired t tests using SigmaStat software (Figure 2.4) (Baker *et al.*, 2001). Groups contained a minimum of 5 animals per group, where analysis of both limbs would give over 80% power to detect a 25% change at a significance level of $P=0.05$

Figure 2.4 *Limb stiffness*



2.17 Flow cytometry analysis-surface and cytokine staining

Mice were killed by CO_2 overdose or by cervical dislocation and leukocytes from blood and spleen were collected under sterile conditions. Large spleen fragments were initially removed by passing the cell suspension through a nylon mesh on a 50 ml falcon tube and the cells were recovered by centrifugation for 5 min at 478g. Erythrocytes from the spleen cell suspension and from the blood were then lysed with a hypotonic ammonium chloride red blood cell lysis buffer (eBioscience Ltd, Hatfield, UK) for 5 min at room temperature and the reaction was then stopped by adding 20ml of 1x PBS. The pellet was then resuspended by gentle vortexing. Cells were then counted in a Neubauer chamber, based on the trypan blue exclusion, for viability discrimination. Cells were then diluted at 2×10^6 cells/ml in staining buffer (1xPBS 2% FCS) and a total of 200,000 cells were then added to each FACS tube (ref: 352058, BD, Oxford, UK). Cells were then incubated with

various surface antibodies (T-cell CD3, CD4, CD8, B-cell CD19, Dendritic cell CD11c, early T-cell CD25, CD44, and Monocyte F4/80 markers) and intracellular cytokines IL-2, IL-4, IL-10, IL-17A and IFN- γ diluted 1:100 per tube and incubated for 30 min in the dark at 4°C or on ice. A transcription factor FOX3P was also used to identify regulatory T cells. After incubation 3 ml of staining buffer was added to each tube. Tubes were then centrifuged at 478g 5 min at 4°C. After centrifugation pellets were resuspended in 300 μ l of staining buffer. Samples were then read on a LSRII flow cytometer (Becton Dickinson, Oxford, UK).

2.17.1 Flow cytometry analysis-CFSE staining

Leukocytes were obtained as previously mentioned (2.16) and washed in 1x PBS and resuspended in a concentration of 2 x10⁶ cells/ml. A final concentration of 5 μ M CFSE was then added and incubated at 37°C for 10 minutes. One volume of ice-cold FCS was then added to quench the staining and cells were then washed twice in staining buffer (1xPBS 2% FCS) and then incubated for 4 days. Samples were then read on a LSRII flow cytometer (Becton Dickinson, Oxford, UK).

2.17.2 Intracellular cytokine staining-QPCR

The following primers were used for intracellular cytokine staining (Table 2.7) Quantitative PCR was performed in duplicates in 96-well reaction plates with the Applied Biosystems 7500 Real-Time PCR system (Applied Biosystems, Warrington, Cheshire, UK) and the cycling conditions for the qPCR were following; 95°C (15 min), 40 cycles of 94°C for (45 s), 58°C for (45 s), 72°C (40s). The PCR components are shown in table 2.8.

2.18 MOG and Con A proliferation assay

C56BL/6.GPR55 knockout and heterozygous littermates were immunized with MOG peptide in Freund's adjuvant on day 0 and were injected with 200ng of B. pertussis toxin on day 0 and 1. Leukocytes were collected on day 9 and re-stimulated *in vitro* with MOG peptide at concentrations 1 μ g or 10 μ g for 72h (*see methods 2.15.1, 2.15.2*). Leukocytes from naïve GPR55 knockout and wildtype mice were also collected and stimulated with Con A for 48h. A total of 300,000 cells were then resuspended in a final volume of 100 μ l of RPMI 10% FCS and plated in 96 well-plates. A total of 0.5 units of ³H Thymidine (PerkinElmer LAS, Beaconsfield, Bucks, UK) was added to each well and cells were incubated during for 24hr at 37°C in 5%CO₂. Cells were then harvested (TOMTEC MACH III M CELL HARVESTER 96, Warwick, UK) and analysed on a counter (Wallac 1450, Microbeta plus Liquid Scintillation Counter, Cambridgeshire, UK).

Table 2.7 Intracellular cytokine and β -actin reference gene primers (Zhu et al., 2013)

IL-2	sense	5'-GCATGTTCTGGATTGACTC-3'
	antisense	5'-CAGTTGCTGACTCATCATCG-3'
IL-4	sense	5'-CAAACGTCCTCACAGCAACG-3'
	antisense	5'-CTTGGACTCATTATGGTG-3'
IL-10	sense	5'-GGTTGCCAAGCCTTATCGGA-3'
	antisense	5'-ACCTGCTCCACTGCCTTGCT-3'
IL-17A	sense	5'-AGCGTGTCCAAACACTGAGG-3'
	antisense	5'-CTATCAGGGTCTTCATTGCG-3'
IFN- γ	sense	5'-CCATCAGCAACAACATAAGC-3'
	antisense	5'-AGCTCATTGAATGCTTGGCG-3'
β -actin	sense	5'-AATCGTGCGTGACATCAAAG-3'
	antisense	5'-ATGCCACAGGATTCCATACC-3'

Table 2.8 Quantitative PCR components for GPR55

Initial concentration reaction components	Final concentration reaction components	Volume (μ l)
dH ₂ O	dH ₂ O	7.4
2x SYBR green Master Mix (Invitrogen, Paisley, UK)	2 x SYBR green Master Mix	10
10 μ M Forward cytokine primer (Invitrogen, Paisley, UK)	0.15 μ M F cytokine primer	0.3
10 μ M Reverse cytokine primer (Invitrogen, Paisley, UK)	0.15 μ M R cytokine primer	0.3
cDNA sample	cDNA sample	2
Total volume	20μl/reaction	

CHAPTER 3

Molecular characterization of GPR55 knockout mice

3.1 Introduction

GPR55 knockout animals have previously been used in order to establish whether the receptor is responsible for the effects of certain atypical cannabinoids (Johns *et al.*, 2007). The existence of a novel unidentified atypical cannabinoid receptor in the cardiovascular system was suggested from previous studies on the Abn-cbd and its analogue O-1602 (Johns *et al.*, 2007). Earlier studies have demonstrated vasodilator effects of the atypical cannabinoids Abn-cbd and O-1602 (Begg *et al.*, 2005; Jarai *et al.*, 1999; Offertaler *et al.*, 2003) thought to be mediated by a new “cannabinoid-like” receptor (Jarai *et al.*, 1999). Other reports have proposed that GPR55 interacts with endocannabinoids and synthetic cannabinoids that are thought to have an effect at an unknown cannabinoid receptor (Baker *et al.*, 2006a). Also, Greasley from an AstraZeneca group reported that GPR55 knockout mice were hypertensive in an unpublished talk at the Meeting of the British Pharmacological Society in 2006 (Hiley *et al.*, 2007).

As a result to previous findings, a study was used to determine whether GPR55 is the cannabinoid-binding receptor mediating vasodilator effects to atypical cannabinoids such as Abn-cbd and O-1602 (Johns *et al.*, 2007). In that study, GPR55 deficient mice were compared with wildtype littermates in order to investigate the potential cardiovascular role of the orphan receptor (Johns *et al.*, 2007). Baseline arterial blood pressure and baseline heart rate were found to be similar in the GPR55 deficient and wildtype mice and the arterial pressure was rapidly lowered upon administration of the Abn-Cbd in both mouse strains (Johns *et al.*, 2007). In addition, O-1602 was used to determine whether GPR55 mediated its vasodilatation in mesenteric arteries. The vessels from both strains were initially pre-treated with phenylephrine, a selective α_1 -adrenergic receptor agonist that increases blood pressure, and then treated with O-1602; both strains were found to have similar vasodilator responses upon treatment with the agonist (Johns *et al.*, 2007). Analysis of blood pressure of the mice used in this study failed to demonstrate any influence (<http://www.informatics.jax.org/external/ko/lexicon/261.html>).

A role for GPR55 in pain regulation was reported by Staton *et al.* in 2008. GPR55 deficient mice, previously used by another group, were used to further characterize the mice (Johns *et al.*, 2007; Staton *et al.*, 2008). Phenotypic analysis were performed including behavior in cage, posture, body weight, age of eye opening and general appearance comparing the GPR55 deficient mice with

wildtype mice (Staton *et al.*, 2008). Rotarod, a motor co-ordination and stamina test, and hot-plate tests were also used in order to determine if GPR55 deficient mice displayed any motor or nociception deficits (Staton *et al.*, 2008). Blood cell phenotypes were also evaluated in this study and no significant differences were found in monocyte, neutrophil, cytotoxic T-cell or T-helper cell populations (Staton *et al.*, 2008). The GPR55 knockout mice demonstrated a lack of mechanical hyperalgesia following subplantar injection of Freund's adjuvant in the left hind paw and upon sciatic nerve ligation (Staton *et al.*, 2008). Cytokine analysis demonstrated elevated levels of the anti-inflammatory cytokines IL-4, IL-10 and IFN- γ in the paw samples from GPR55 knockout mice compared to wild-type mice (Staton *et al.*, 2008).

GPR55 has also been suggested to play a role in glucose homeostasis as the activation of the receptor in islets of Langerhans by the agonist O-1602 led to increased levels of intracellular calcium and insulin secretion in wildtype animals. This effect was reported abolished in the GPR55 deficient mice (Romero-Zerbo *et al.*, 2011). GPR55 has also shown to play a role in bone physiology where the bone formation in GPR55 male knockout mice was abnormal compared to wild-type littermates (Whyte *et al.*, 2009).

No significant differences have been observed in most studies when comparing GPR55 knockout males and females however there are a few exceptions. GPR55 knockout females have been reported to show significant reduced withdrawal latency in the hot plate test at 50°C when compared to male littermates (Staton *et al.*, 2008). Although an abnormal bone formation was seen in the male knockout mice, this malformation was absent in the female littermates (Whyte *et al.*, 2009).

In order to characterize and investigate the role of the GPR55 we obtained GPR55 knockout animals. A panel of mice, 129xC57BL/6.GPR55^{tm1Tigm}, expressing a GPR55 gene deletion construct were generated by Lexicon Inc. /Texas Institute of Genomic Medicine (TIGM) using gene targeting or gene trap mutations (Informatics, 2012). The GPR55 knockout animals were further bred onto the C57BL/6 background and a colony was established in order to obtain enough animals for our experiments. The use of the animals allowed us to examine the function and role of GPR55 by comparing GPR55 deficient mice with wild-type littermates. The use of these GPR55 knockout mice has been previously reported by (Wu *et al.*, 2010a). We were initially provided with a PCR protocol and primer sets from TIGM however these tools gave inconsistent pcr results with faint bands showing false negative results hence wrong genotype therefore new primers were designed. In this chapter the genotype of our GPR55 mouse was characterised. All the genetic

information regarding the GPR55 knockout mouse was provided by TIGM.

3.1.2 Methods

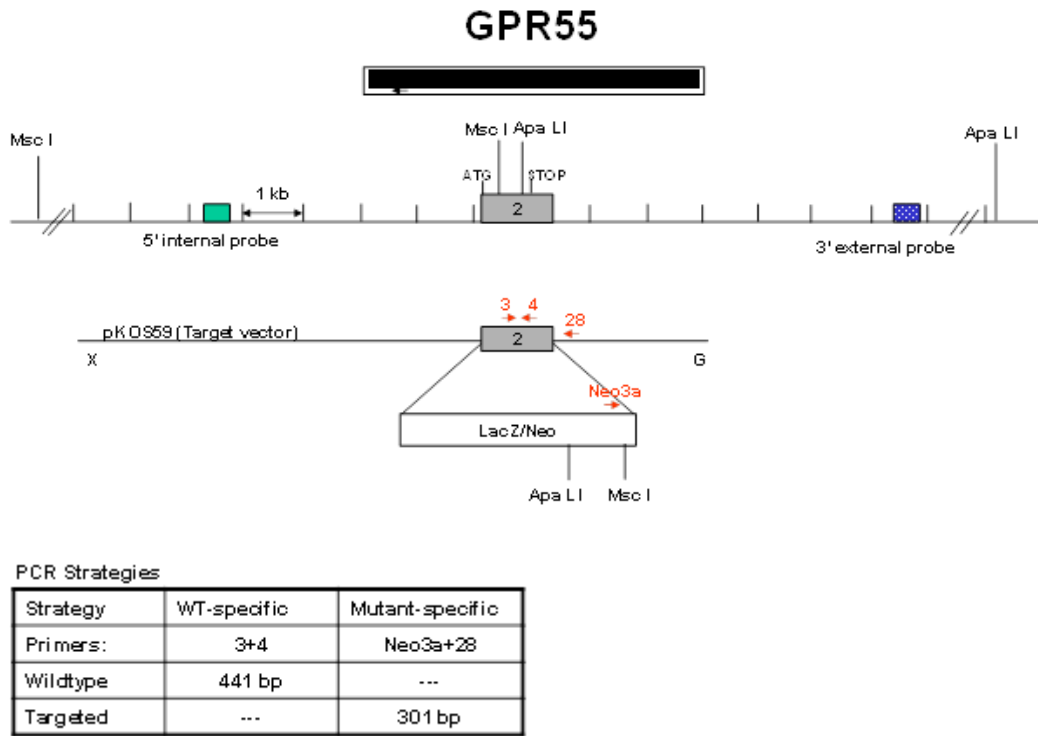
In this chapter PCR was used for genotyping of our animals (*see methods 2.2*).

3.2 Results

3.2.1 Genetics of GPR55 knockout mice

Founder uncharacterised mice were purchased from the Texas Institute of Genomic Medicine, as they became available. These were randomly generated as part of a commercial exercise to sell gene trapped mice by Lexicon Inc. Following a National Institute of Health initiative to generate gene knockouts of most genes, live mice and embryonic stem (ES) cells were purchased from Lexicon and Deltagen Inc and placed into repositories at markedly reduced costs (\$5,000) compared to original costs (\$24,000). These mice were funded for this project. All information and results regarding the GPR55 knockout targeting strategy was provided by TIGM (Figure 3.1, 3.2).. Briefly, gene targeting or gene trapping was performed in strain 129SvEv^{Brd}-derived embryonic stem (ES) cells. The chimeric mice were crossed with C57BL/6 mice in order to generate heterozygous animals. There were backcrossed onto C57BL/6 mice. The animals carrying the GPR55 mutant allele were intercrossed in order to generate wild type, heterozygous, and homozygous mutant animals (Informatics, 2012).

Figure 3.1 *GPR55 knockout targeting strategy*

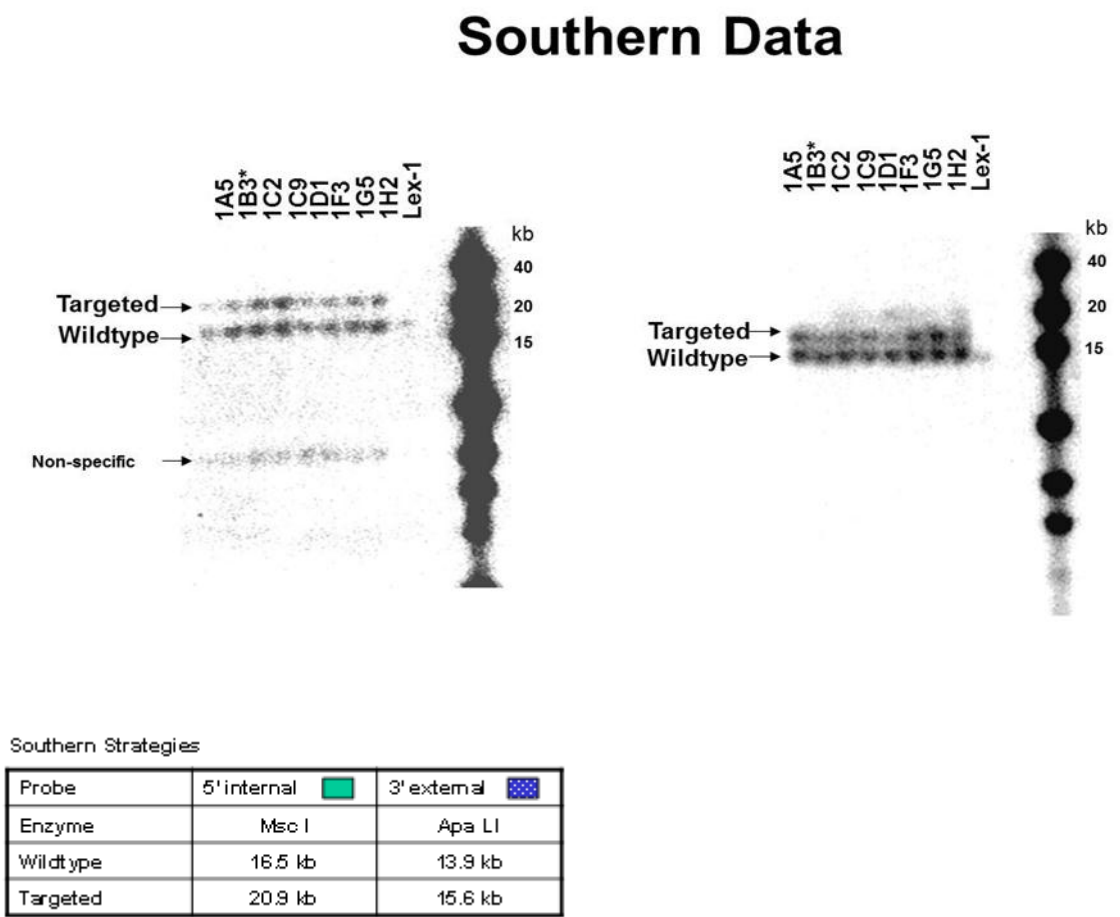


The 5' primer (5' – GCCATCCAGTACCCGATCC) and 3' primer (5' – GTCCAAGATAAAGCGGTTCC) was used for detection of the wildtype allele and 5' primer (5' – GCAGCGCATCGCCTTCTATC) and 3' primer (5' – TCAAGCTACGTTTTGGGTT) was used for identification of the mutant gene. Predicted size for the wildtype band was 441bp and for the mutant band 301bp. The following experiment was generated by TIGM.

3.3.2 Southern blot

Southern blot was performed in order to identify the GPR55 mutant clone. DNA was initially isolated, digested and then transferred to a membrane. The probes were then hybridized to the membranes and detected with autoradiography (Croning *et al.*, 2010).

Figure 3.2 GPR55 knockout targeting southern data

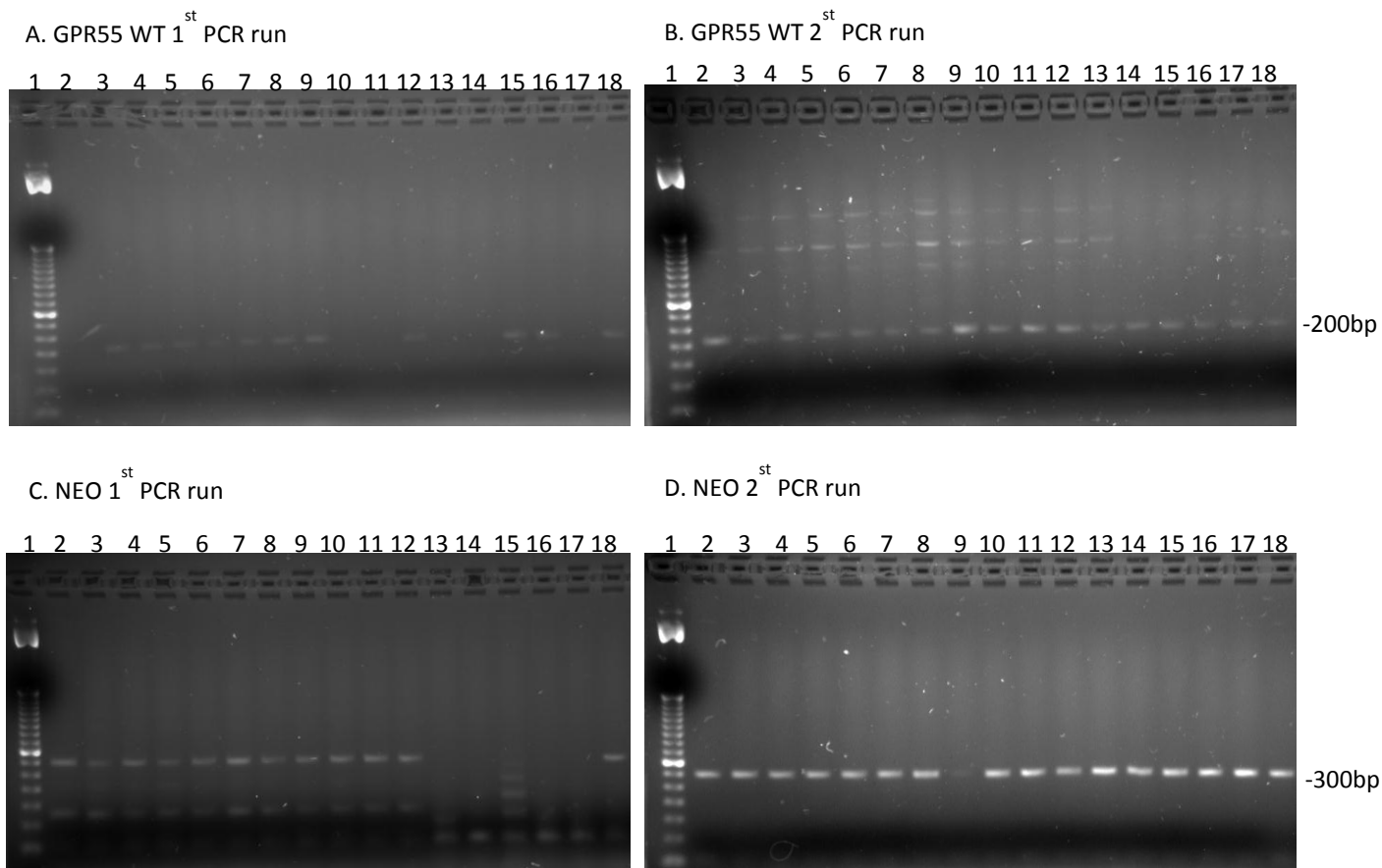


Detection of a GPR55 knockout ES clone was performed by Southern blotting. The 5' internal probes (5' – GGGCAGCCATGTTAGGAT and 5' – CTTCTGGCCTGTGGTACATA) and 3' external probes (5' – CTCTCACTTGCCAGCGACAC and 5' – CCATGGCAGGTCAGATAAGG) were used for detection of the GPR55 knockout clone. DNA from animals was digested using restriction enzymes Msc I and Apa LI. The predicted size of the wildtype internal band was 16.5kb and external band 13.9. The predicted size of the mutant internal band was 20.9kb and external band 15.6kb. The internal probe size corresponded to 387bp and the external probe size was 493bp. All data for the southern blot experiment was provided by Texas A&M Institute for Genomic Medicine.

3.3.3 Genotyping using two sets of primers

PCR protocol provided by TIGM had been previously tested in our lab and did not work therefore another PCR protocol and primer set described by Johns *et al.*, 2007 was used. Two separate PCR reactions were performed in order to detect the different genotypes and inconsistent results were often obtained (Figure 3.3). The GPR55 allele (wild-type) was detected in *Figures 3.3A,3.3B* and the mutant neomycin allele (NEO; GPR55 knockout) was detected in *Figures 3.3C* and *3.3D*. PCR reactions often had to be repeated due to inconsistencies and missing bands eg. in Figure 3.3A samples 10, 11, 13 and 14 were not detected however when PCR was repeated samples 10, 11, 13 and 14 were identified in Figure 3.3B. In Figure 3.3C samples 13, 14, 15, 16 and 17 were not detected and in Figure 3.3D sample 9 showed a very weak band.

Figure 3.3 Genotyping-PCR Detection of GPR55 Alleles using the polymerase chain reaction

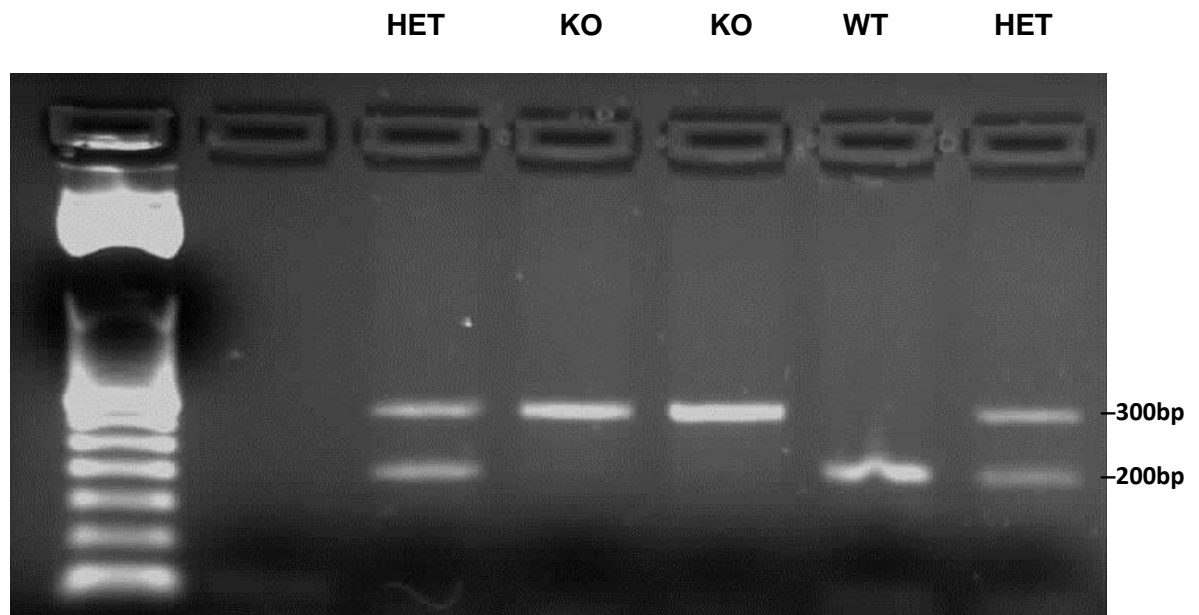


Earsnips from animals were taken for genotyping. DNA was prepared and amplified using PCR. The PCR products were subjected to 2% agarose gel electrophoresis and bands were detected using ethidium bromide. The GPR55 wildtype (WT) allele had a predicted size of 207bp band and the deletion allele had a predicted product size of 299bp. Band sizes were determined using a standard 50 base pair (bp) DNA ladder.

3.3.4 Genotyping using single pcr reaction

Due to inconsistencies using primers described by Johns et al., 2007 (Figure 3.3) new primers were designed (see methods 2.2.2). The newly designed PCR reaction allowed detection of both the wild-type GPR55 and the deletion allele, containing the neomycin resistance gene, within the cloning cassette that replaced GPR55 in a single PCR reaction. This was optimized to give robust detection so that the genotypes could be reliably confirmed in a single PCR reaction. This was used to identify the different genotypes: C57BL/6.GPR55^{+/+}, C57BL/6.GPR55^{+/-} and C57BL/6.GPR55^{-/-}.

Figure 3.4 Genotyping- *Detection of GPR55 Alleles using the novel designed polymerase chain reaction*



Earsnips from animals were taken for genotyping. DNA was prepared and amplified using PCR. This was subject to 2% agarose gel electrophoresis and bands were detected using ethidium bromide. The GPR55 wildtype (WT) allele had a predicted size of 209bp. The deletion allele had a predicted product size of 299bp which corresponds to size between the forward GPR55-related primer and the reverse primer detecting the inserted reporter (neomycin) gene. The heterozygous mice showed both bands around 209bp and 299bp. Band sizes were determined using a standard 50 base pair (bp) DNA ladder.

3.4 Discussion

The characterization of our animals was an important step in order to study the biology of GPR55. As GPR55 knockout animals had previously been become available as a part of the knockout mouse project (KOMP) to knockout all GCPR genes we could purchase the founder mice. The obtained animals were primarily backcrossed with C57BL/6 mice. Initially our group was supplied with primer sequences by TIGM in order to detect the wild type and mutant alleles and the PCR gave inconsistent results. Another PCR protocol was then tested also requiring two separate reactions as described by Johns et al., 2007. The PCR reaction with these sets of primers also often gave inconsistent results. Due to the varying results new primers were designed in order to optimize the PCR needed for the genotyping of our animals. The newly designed primer sequences and PCR allowed the detection of the different genotypes C57BL/6.GPR55^{+/+} (GPR55 WT), C57BL/6.GPR55^{+/-} (GPR55 heterozygous) and C57BL/6.GPR55^{-/-} (GPR55 knockout) in one single PCR reaction.

CHAPTER 4

Production of GPR55 reactive antibodies and characterization of astrocytoma cell lines

4.1 Introduction

The aims of this chapter were to generate GPR55 monoclonal antibodies and to characterize GPR55 transfected and control astrocytoma cell lines. One of the major issues for detection of the GPR55 receptor has so far been the lack or availability of specific antibodies. The development of GPR55 (monoclonal antibodies) reactive antibodies was initiated due to the failure to detect GPR55 in various assays using commercially purchased GPR55 polyclonal antibodies. One of the tested antibodies was purchased from Abcam (Cambridge, UK) and another one from GSK was obtained from A.Irving. Furthermore, others have found that most commercially available GPR55 polyclonal antibodies have failed to show specific GPR55 staining (A.Irving; Personal communication).

The advantage of polyclonal antibodies is the ability to detect multiple epitopes and that the polyclonal reagents are comparatively cheap and simple to produce compared to monoclonal antibodies. The use of larger animals also allows large volume of antibody rich serum however the disadvantage is that at some point the original batch needs to be replaced and that inevitability leads to problem of batch to batch variations. Differences in antibody titres and reactivity are common problems and polyclonal reagents in general suffer from a lack of reproducibility. Monoclonal antibodies, produced by a continuous antibody secreting B cell hybridoma clone, offer a reproducible supply of antibody with same specificity (Nelson *et al.*, 2000).

4.1.1 Material and Methods

In order to develop GPR55 antibodies GPR55 knockout mice (C57BL/6.*Gpr*^{-/-}) were immunized with GPR55-GST fusion peptides or with the GPR55 transfected astrocytoma cell line E1. The following peptide sequences were used; NH: MSQPERDNCSFDSVCKLTRT, IC3: YRSIHILLRRPDSTEDWVQQRDTKGWVQKRAC and CT-FL: KEFRMRIKAHRPSTIKLVNQDTMVSRG (*see methods 2.3*). In the absence of knowledge on the precise location of the GPR55 receptor in tissues it was important that a cell line was generated or obtained so that reactivity against native GPR55 could be assessed. The relatively uncharacterised astrocytoma mouse cell lines DBT (control) and E1 (mouse GPR55 transfected) were obtained from Dr. Nephi Stella. Functional activity of these cells was characterized using calcium signalling, CREB and Phalloidin assays.

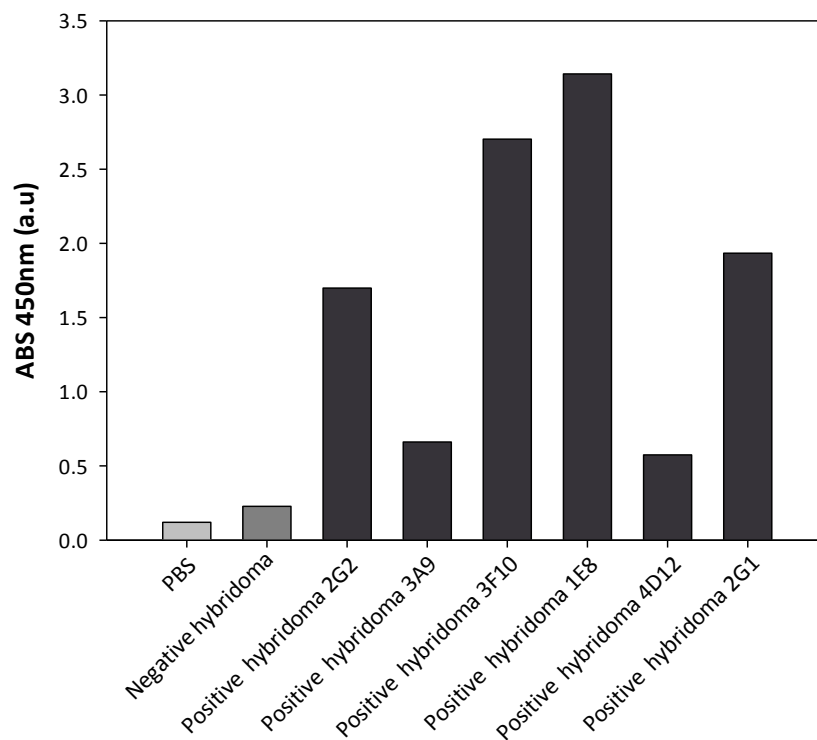
Hybridoma antibodies reactivity was tested using ELISA, immunofluorescence, western blotting and flow cytometry. Commercially purchased antibodies were also tested using immunofluorescence.

4.2 Results

4.2.1 GPR55 antibody production

Animals were immunized with a pool of GPR55-GST fusion peptides or with the GPR55 transfected astrocytoma cell line E1 and screened after 3-5 weeks in general. A total of 9 fusions were made and 520 hybridomas were screened out of which 40 were found positive against the immunizing peptides or cells by ELISA screening (Figure 4.1). The 40 hybridomas that reacted positive in the ELISA were also isotyped in order to indicate whether they may have been clonal however, all of the hybridomas except for one displayed reactivity against several isotypes (Figure 4.2). A total of 6 of these 40 hybridomas only showed reactivity against 1-3 isotypes and were selected to be further tested using different techniques (Figures 4.3, 4.5 and 4.10). Figure 4.1 demonstrates the antibody titres comparing negative controls with positive hybridomas after one fusion. As the antibodies failed to show specificity they were not further cloned by limiting dilution.

Figure 4.1 *Production of GPR55 antibodies*



C57BL/6.GPR55^{-/-} knockout animals were immunized with GPR55-GST fusion peptides or E1 cells in Freund's adjuvant and killed after 3-5 weeks. The spleen from the immunized animals was then fused with a NS-1 plasmacytoma cell line. Wells were screened daily and hybridomas were detected around one to two weeks after the fusion. Supernatants from hybridomas were then tested for reactivity against the GPR55-GST fusion peptides or E1 cells using ELISA. ELISA plates were coated with GPR55-GST fusion peptides or E1 cell protein followed by tissue culture supernatant and peroxidase conjugated anti-mouse immunoglobulin and activity was detected using the ABTS chromogen and H₂O₂. The absorbance was measured at 450nm for individual hybridoma.

4.2.2 Antibody isotyping

All 40 positive hybridomas were isotyped and due to most hybridomas expressed several isotypes only 6 hybridomas expressing less than 3 isotypes were selected for further analysis. This indicated that most hybridomas were not monoclonal. The grey highlighted wells correspond to positive isotype clones. Hybridoma 4D12 was found to be only one of hybridomas secreting a single isotype suggestive of clonality (Figure 4.2). The 6 selected hybridomas were further characterized (Figures 4.3, 4.5 and 4.10).

Figure 4.2 *GPR55 Antibody isotyping*

Isotype	PBS	2G2	2G1	3A9	3F10	1E8	4D12	Pos ctrl
IgG1	0.14	0.116	0.09	0.063	0.096	0.636	0.08	1.41
IgG2a	0.12	0.16	0.13	0.075	0.146	0.117	0.08	1.52
IgG2b	0.12	1.18	0.35	0.132	0.11	0.62	0.09	1.40
IgG3	0.27	0.123	1.09	1.526	0.757	1.546	0.86	1.33
IgM	0.10	1.279	0.12	1.386	1.785	0.06	0.18	1.41
IgA	0.12	0.113	0.17	0.078	0.096	0.112	0.11	1.51
Igκ	0.10	1.392	0.91	1.375	1.612	1.542	1.57	1.40
Igλ	0.12	0.097	0.14	0.079	0.06	0.563	0.15	1.45

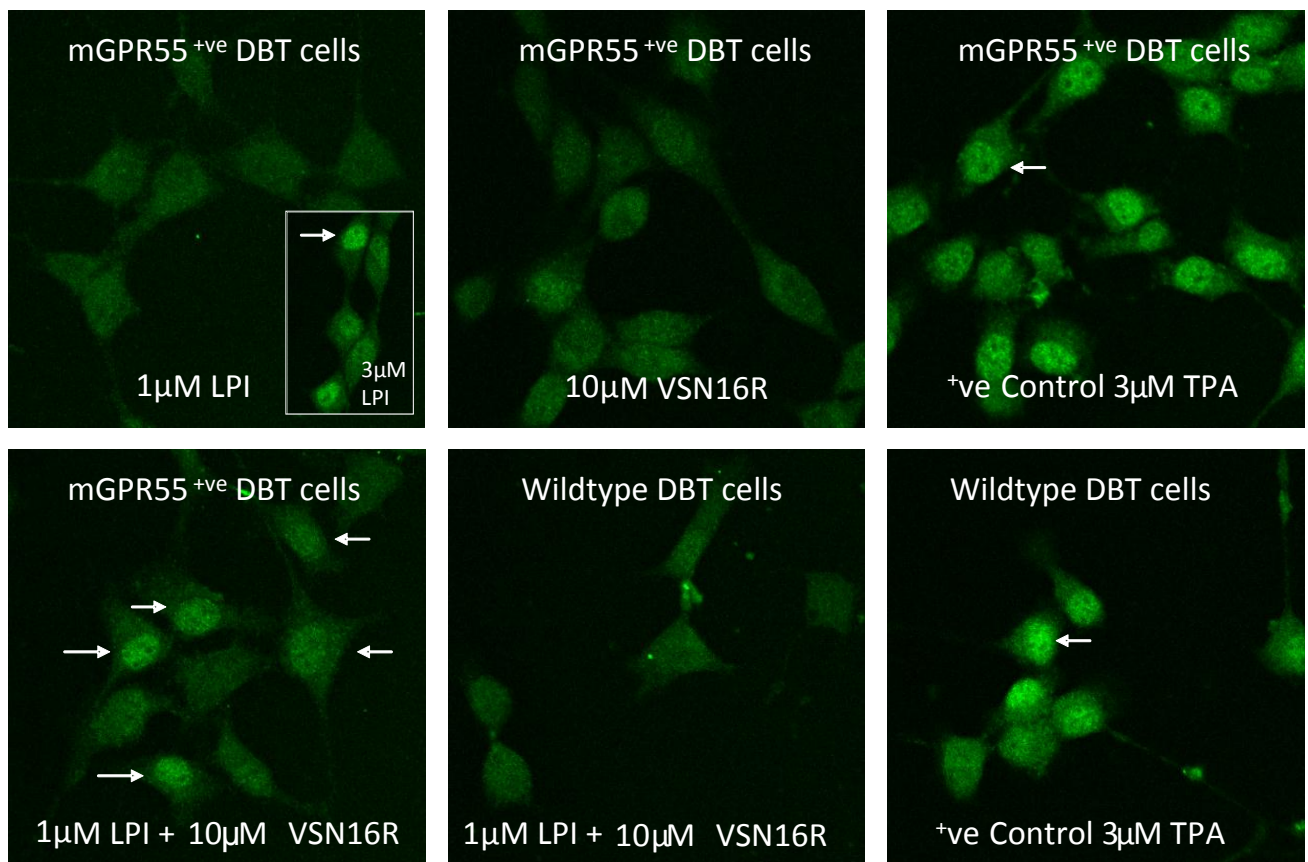
Supernatant from hybridomas that were tested positive against GPR55 peptides were isotyped. The positive wells were tested against isotype-specific rat anti-mouse IgG purified monoclonal antibodies. Briefly, the micro titre plates were coated with the anti-mouse purified monoclonal antibody isotypes including IgG1, IgG2a, IgG2b, IgG3, IgM and IgA followed by tissue culture supernatant and peroxidase conjugated anti-mouse immunoglobulin and activity was detected using the ABTS chromogen and H₂O₂. The absorbance was measured at 450nm for individual lines. The absorbance was measured at 450nm.

Whilst it was evident that some positive reactions to the immunizing peptides or homogenized cell proteins were detected using ELISA it was important to try and determine if these antibodies would react to native GPR55 and be useful for detection in tissues to determine distribution profile of the receptor. As this is an integral membrane G protein couple receptor, we decided to utilise a GPR55 expressing cell line. Rather than generating a line, one largely uncharacterised line was obtained from Dr Stella. This was functionally assessed using LPI as a GPR55 specific ligand; furthermore the influence of VSN16R, a putative GPR55 ligand was also tested on these cells.

4.2.3 GPR55 activation of cAMP Response Element-binding Protein (CREB)

Activation of the nuclear transcription factor CREB was analysed using the GPR55 agonist LPI, GPR55 modulator VSN16R and TPA proliferation agent was used as a positive control. At a concentration of $1\mu\text{M}$ of LPI on its own no activation of CREB was observed. There was also a lack of CREB activation when GPR55 transfected cells were treated with $10\mu\text{M}$ of VSN16R on its own. However, CREB activation was observed when GPR55-transfected cells were treated with either $3\mu\text{M}$ of LPI on its own or by combining $1\mu\text{M}$ of LPI with $10\mu\text{M}$ of VSN16R (Figure 4.3). There was no activity of these agents on non-transfected cells. Positive control showed nuclear localisation of pCREB.

Figure 4.3 CREB activation

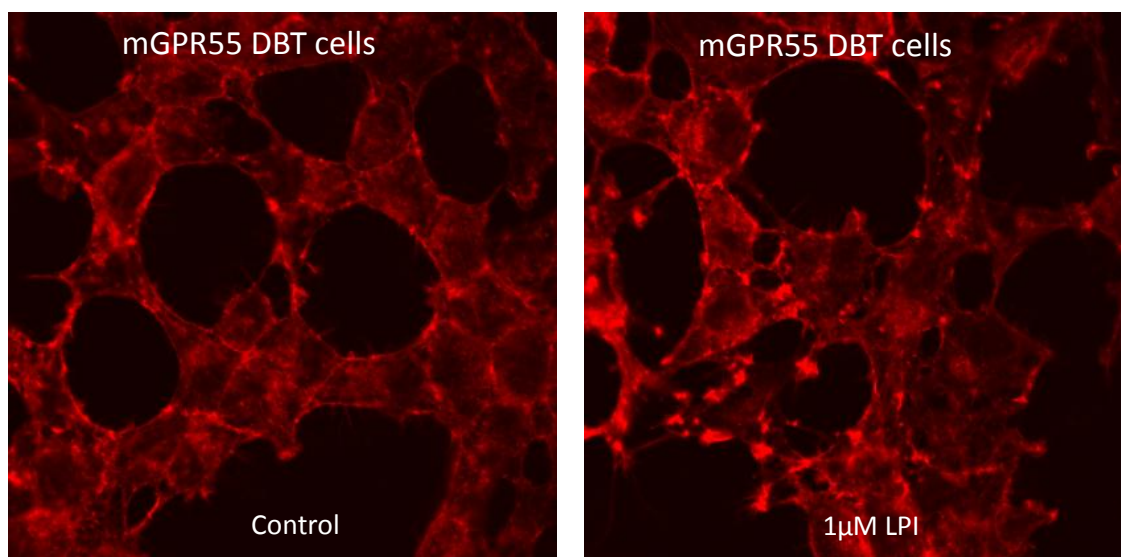


Cells grown on cover slips were initially fixed in ice cold methanol and incubated with mouse CREB primary antibody, Anti-phospho-CREB IgG1κ, 0.2mg/mg in dH₂O and glycerol) at 1:1000, and incubated for 60 minutes at RT. A secondary ALEXA fluor 488 antibody (Invitrogen, Alexa fluor 488 donkey anti-mouse A21202) at a concentration of 1:500 was then added and incubated for 30 minutes at RT. Cells were then analyzed using a LSM 510 confocal laser scanning microscope.

4.2.4 GPR55 mediated cytoskeletal rearrangement using phalloidin staining

The cytoskeleton is composed of intermediate filaments, actin filaments and microtubules. Phalloidin, a mushroom-derived toxin, is commonly used to label F-actin of the cytoskeleton. Phalloidin is labeled with various fluorophores and rhodamines are most commonly used as they are more resistant to photobleaching (Chazotte, 2010). Cytoskeletal rearrangement has previously been assessed by F-actin phalloidin staining (Balenga *et al.*, 2011a). In HEK transfected GPR55 cell lines stimulation by LPI caused RhoA mediated rearrangement of the actin cytoskeleton (Balenga *et al.*, 2011a). LPI has shown to promote neurite retraction and redistribution of F-actin in differentiated PC12 cells mediated by GPR55, G13 and Rho (Obara *et al.*, 2011). This effect was absent in undifferentiated PC12 cells (Obara *et al.*, 2011). Phalloidin was used to stain mouse GPR55 transfected DBT cell line. Upon stimulation with LPI a rearrangement of the actin cytoskeleton was observed. The LPI influence on actin re-arrangement indicates that GPR55 is expressed on the cell surface and is functionally active.

Figure 4.4 *Phalloidin staining*

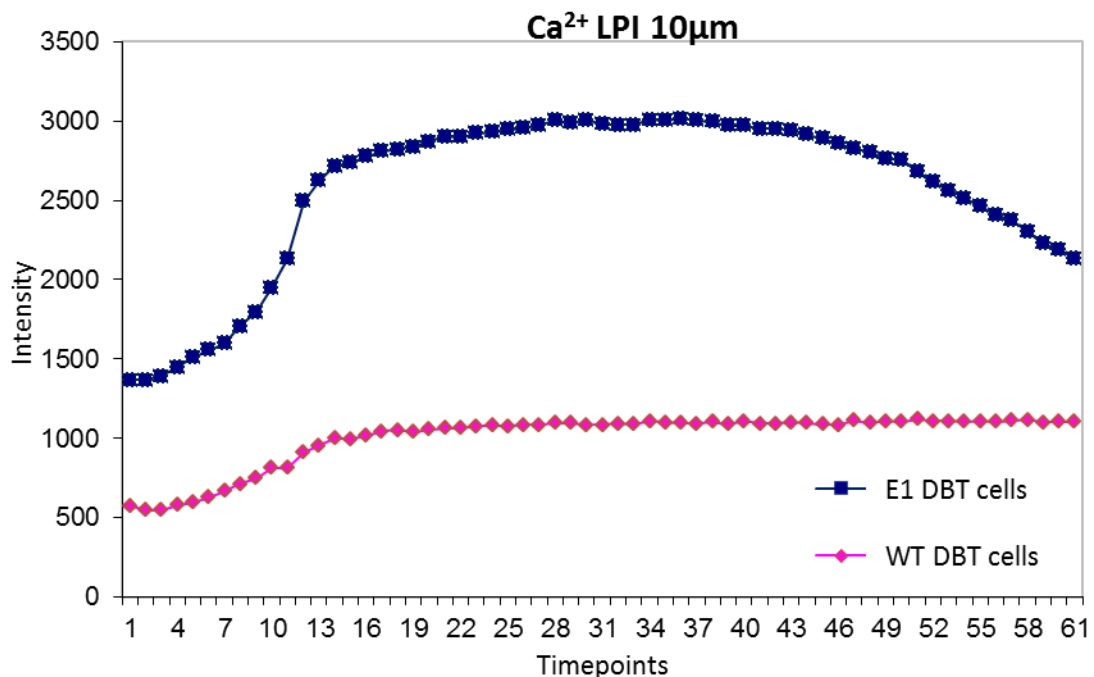


GPR55 transfected DBT cell line was grown on coverslips for 48 h at 37°C overnight. The cells were initially incubated in serum free medium for 30 min at 37°C for and then fixed with 4% PFA for 10 min at RT. Cells were then incubated with either vehicle or 1µM LPI and then stained with Phalloidin (1:500) 488 (Invitrogen, Paisley, UK).

4.2.5 GPR55 mediated calcium signalling

Fura-2-am ester is used to measure cellular calcium by fluorescence. Once added to the cells Fura-2-am crosses the cell membrane and the acetoxymethyl groups are detached by cellular esterases and restore the pentacarboxylate calcium indicator. The calcium induced fluorescence readings were measured at 340 nm and 380 nm in order to calculate calcium concentrations based 340/380 ratios fluorescence. The increase in calcium levels were measures at 61 time points for a period of 5 min. A significant increase of calcium levels were seen in the GPR55 transfected cell line (E1) compared to the untransfected cells (DBT) (Figure 4.5).

Figure 4.5 *Calcium signaling*

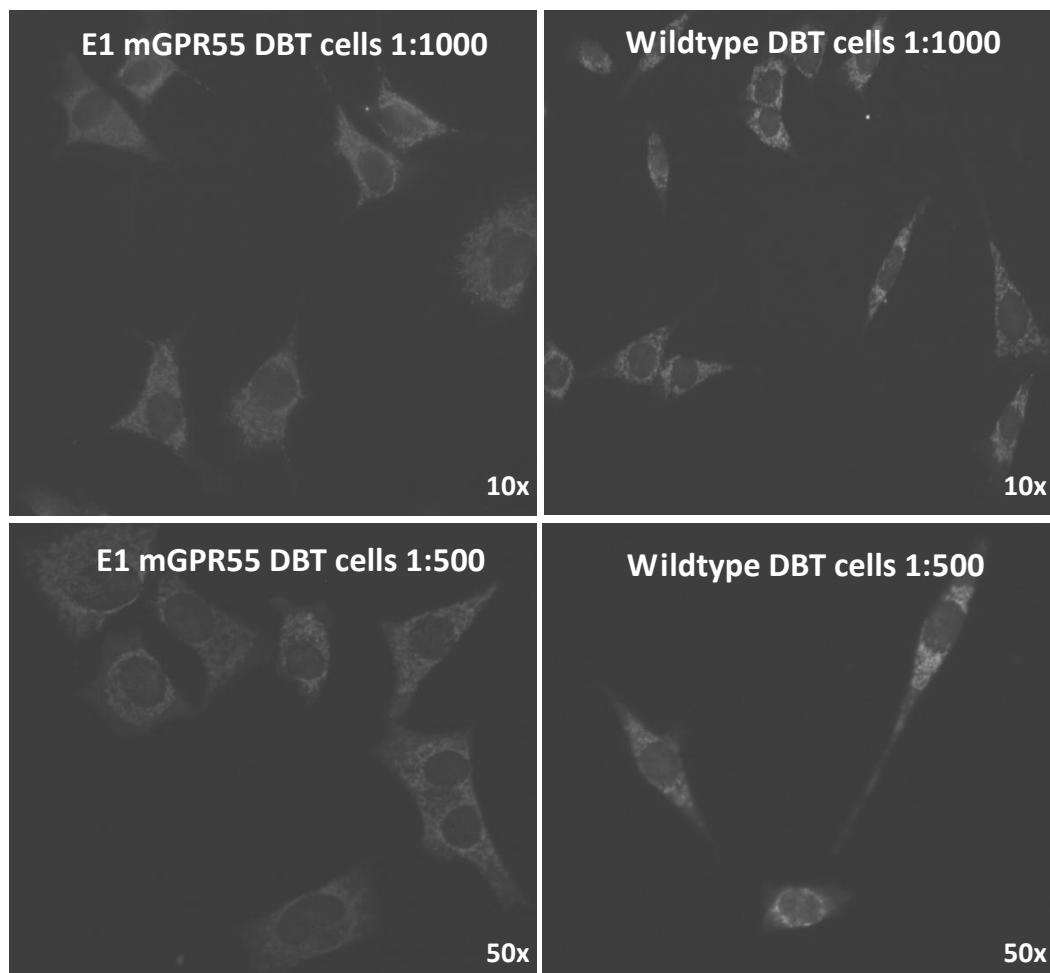


Cells were grown onto cover slips in a 24 well plate. Serum free medium was added to each well 24 hs prior to experiment start. Wells were washed with hepes buffer and fura 2-am diluted in hepes was added to each well. The cells were incubated for 60 min and then washed with hepes buffer and analyzed on the LSM 510 confocal laser scanning microscope. The results represent the fluorescence intensity (arbitrary units)

4.2.6 Immunofluorescence

Although numerous antibodies have been reported to detect GPR55 levels in cell lines and in rodent tissues most of the existing antibodies are probably non-specific and there is a need for reliable GPR55 specific antibodies (Henstridge *et al.*, 2011). The antibody used in the following experiment was purchased from Genetex (ref: GTX12700). The antibody shows similar staining patterns in both the GPR55 transfected and non-transfected cell line (Fig 4.6).

Figure 4.6 Immunofluorescence- GPR55 antibody staining

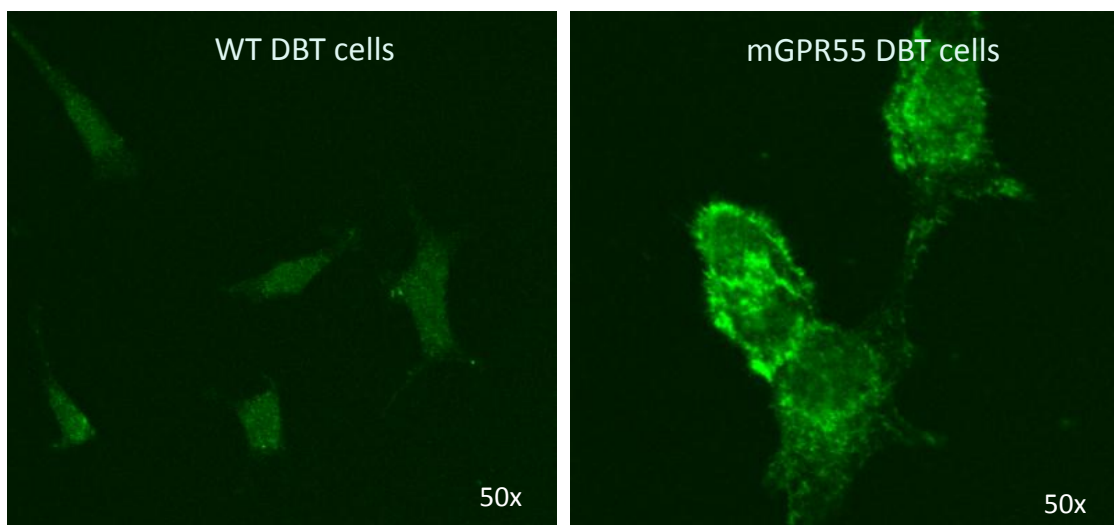


Cells were grown on coverslips in 24 well plates for 3-4 days. Cells were initially incubated with a primary antibody (1:1000) from Genetex (GTX12700). A secondary anti-rabbit IgG FITC antibody was then added. The coverslips were mounted on slides and analyzed using a fluorescent microscope.

4.2.7 GPR55 polyclonal antibody

I received an aliquot of a GPR55 polyclonal antibody from Dr A. Irving (University of Dundee). This was produced by Glaxosmithkline (Stevenage, UK) but unfortunately when their Neuroscience research group was being relocated from the UK to China the batch of anti-sera was lost. The polyclonal antibodies were used to stain mouse GPR55 transfected DBT cells and untransfected DBT cells. The antibodies were from a limited batch and as mentioned are no longer available therefore subsequent experiments could not be performed. The GPR55 transfected cells showed specific staining mainly in the cell membranes compared to the untransfected cells. These antibodies had previously been tested positive on GPR55-HEK (A.Irving, Dundee, personal communication). This data demonstrates that the GPR55 within the transfected cell is membrane associated.

Figure 4.7 *GPR55 rabbit polyclonal antibody*

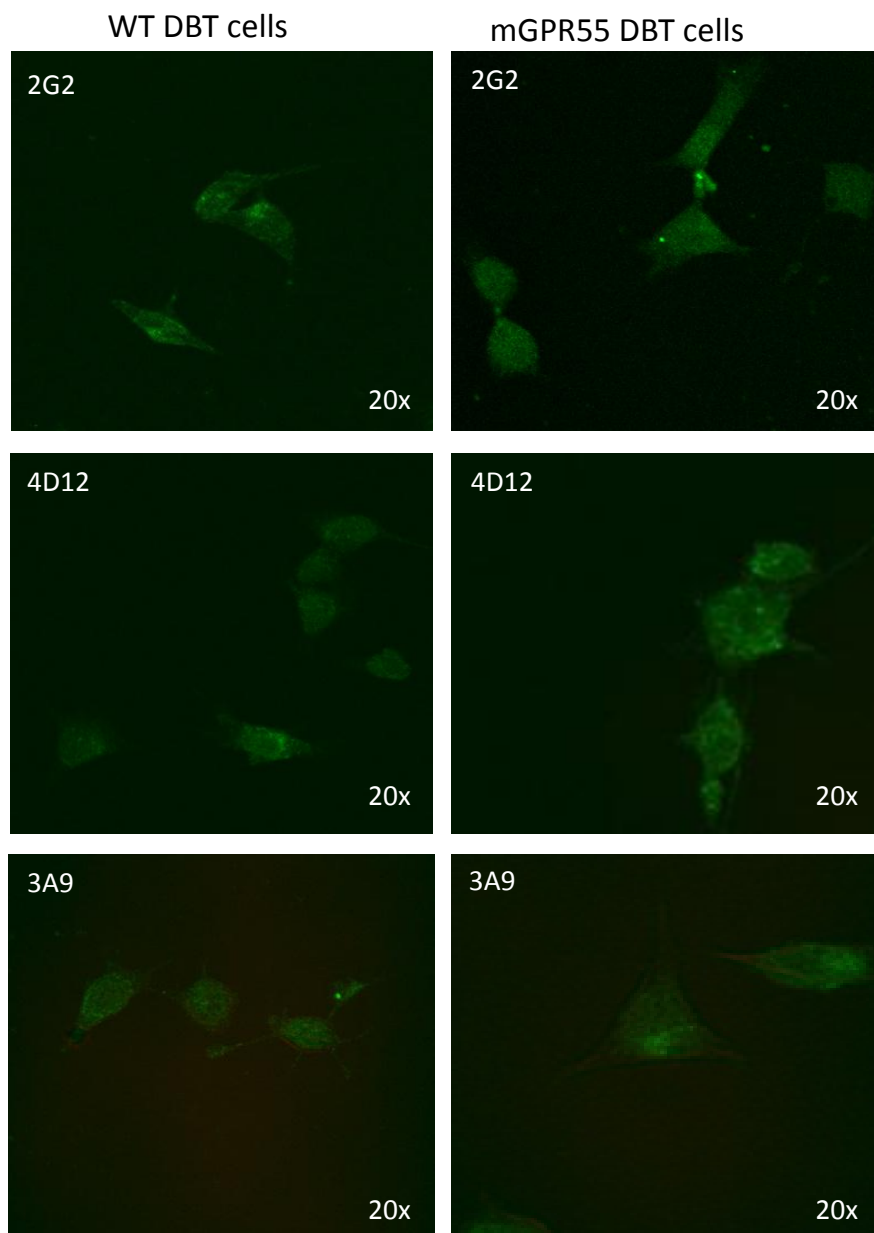


A GPR55 polyclonal antibody was used to stain mouse GPR55 transfected DBT cell line and untransfected DBT cell line. The cells were grown on coverslips for 48 h at 37°C overnight. Cells were then fixed in 4% PFA, 200 mM sucrose. Cells were then incubated with primary polyclonal GPR55 antibody for 1h (1:500). A secondary antibody was then added and cells were incubated for 30 min (Alexa fluor 488 donkey anti-rabbit IgG (H+L) 2mg/ml, A21206 (Invitrogen, Paisley, UK)).

4.2.8 Staining of cell lines with GPR55 hybridoma produced antibodies

A number of fusions were made and as mentioned before (4.2.2) six of the isotypic antibodies were selected to stain the wild-type DBT and GPR55 E1 DBT transfected cell lines. Staining pattern did not differ when comparing the the two cell lines and counting more than 50 cells per sample no consistent or specific differences in staining patterns was observed.

Figure 4.8 *Hybridomas*

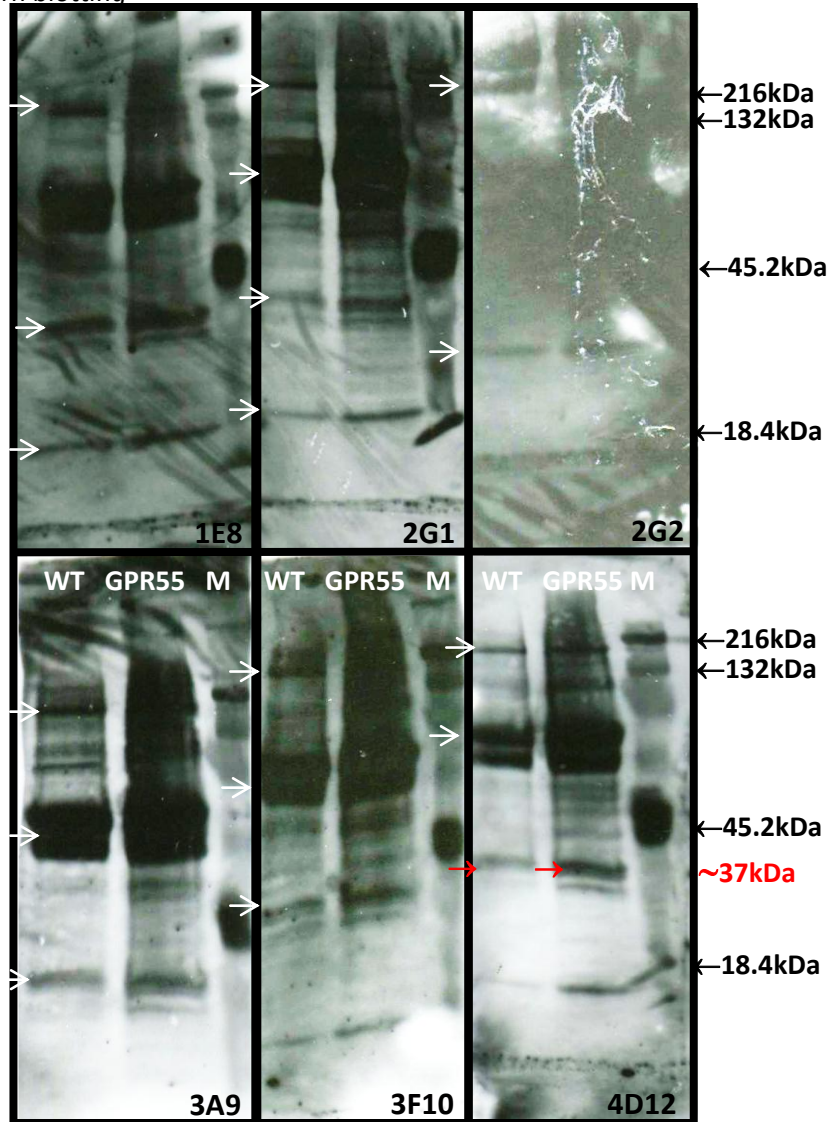


Cells were grown on coverslips in 24 well plates for 3-4 days. Cells were initially incubated with isotypic hybridomas. A secondary anti-mouse IgG FITC antibody was then added. The coverslips were mounted on slides and analyzed using a fluorescent microscope.

4.2.9 Western Blotting using GPR55 hybridoma produced antibodies

Western blotting performed using protein samples prepared by homogenizing GPR55 transfected and non-transfected cells (*see methods 2.6*). An amount of 10µg of protein samples were loaded onto the gels and as mentioned before (4.2.2) 6 selected hybridomas were used to stain the gels. The hybridoma antibody staining showed multiple bands also at the predicted correct band size for GPR55 seen especially in the blot using 4D12 antibody. A stronger band was seen in the GPR55 transfected cell line compared to the untransfected cell line.

Figure 4.9 *Western blotting*

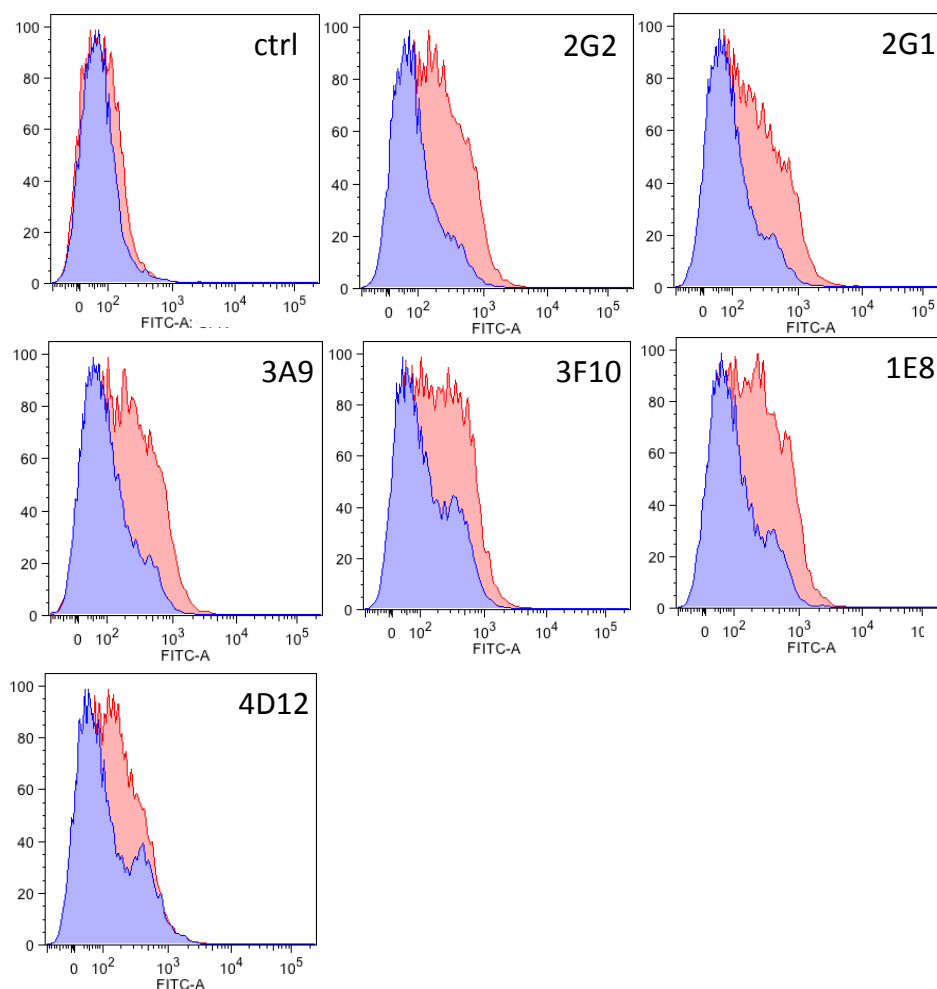


Protein samples were initially prepared by homogenizing GPR55 transfected and non-transfected cells. The gels were loaded with 10µg of protein and transferred onto nitrocellulose membranes. The membranes were then incubated with supernatants from the positive hybridomas diluted 1/100. The membranes were then incubated with a secondary antibody, anti-mouse IgG horseradish peroxidase, and later developed using ECL reagent. All hybridomas however demonstrated multiple unspecific bands (white arrows). The results were compared with a prestained kaleidoscope standard (Bio-Rad Laboratories Ltd, Hertfordshire, UK). A potential positive band can be detected around 37KDa

4.2.10 Flow cytometry with GPR55 hybridoma produced antibodies

As mentioned before (4.2.2) the supernatants from the 6 selected hybridomas were used to stain GPR55 transfected cells and non-transfected cells in flow cytometry. All the hybridomas showed weak positive reactivity against the GPR55 transfected cells compared to untransfected cells as shown in Fig. 4.10. The blue peaks represent the untransfected cells and the pink peaks the GPR55 transfected cells. PBS was used as a control.

Figure 4.10 Flow cytometry



Supernatant collected from positive hybridomas was analyzed by flow cytometry. A total of 1×10^5 cells per tube were used. PBS and supernatant from wells without hybridomas were used as a negative controls and 100 μ l of supernatant from wells with positive hybridomas. Cells were incubated with the antibodies for 30 min at 4°C followed by an incubation with Alexa fluor 488 (Invitrogen, Paisley, UK) (1/100) for 30 min at 4°C. Samples were then vortexed and incubated for a minimum of 10 min at RT and were analyzed by LSRII flow cytometry (Becton Dickinson, Oxford, UK).

4.3 Discussion

Following the production of hydridomas obtained by the fusion of splenocytes from GPR55 knockout mice immunised with GPR55 fusion peptides and GPR55 transfected cell line with the NS-1 plasmacytoma cell line a number of antibody secreting hybridomas were produced that recognised the immunizing peptides/cells in the ELISA assay. Although over 520 hybridomas were tested and 40 were found to react to the immunizing peptides/cells only 6 of these were selected for further analysis. This was due to the fact that most of the antibodies secreted by the hybridomas were tested positive to several or all of the different isotypes including IgG1, IgG2a, IgG2b, IgG3, IgM and IgA. The development of an IgG monoclonal antibody is desirable as IgG antibodies have higher affinity for their target than for instance IgM antibodies. IgG antibodies are also more commonly used in various assays, due to their specificity, including ELISA, WB and immunohistochemistry and since IgG and not IgM antibodies bind to protein A and G they can also be used for assays such as immunoprecipitation (Uma Devi *et al.*, 2001). However, in addition to the problem of generating clonal antibodies, it was important to use a mouse GPR55 expressing cell line to test the ability of antibodies to react with native protein. One was obtained through a collaboration and were first functionally characterised

In order to characterize the obtained astrocytoma cell line, one of the functional assays used was based on prior studies in human transfected cell lines (Henstridge *et al.*, 2010). This assay was the CREB activation assay. We used a phospho-CREB primary antibody to stain mouse GPR55 transfected DBT cell line and untransfected DBT cell line after stimulation by either LPI and/or VSN16R. Interestingly, LPI on its own at lower concentrations (1 μ m) did not activate CREB nor did VSN16R at a higher concentration (10 μ m). This indicated that VSN16R is not acting as an agonist. However, by treating the GPR55 transfected cell lines with 1 μ m LPI and 10 μ m VSN16R activation of CREB was observed. This may suggest that VSN16R functions as a GPR55 allosteric modulator upon co-stimulation with other ligands/agonists rather than being a direct agonist. Previous studies have reported that the GPR55 agonist LPI activates ERK MAP-kinase pathway, Ca²⁺ and CREB in cell lines. VSN16R has previously been demonstrated to relax mesenteric arteries and this influence was modified by GPR55 ligands (Baker *et al.*, 2006b; Hoi *et al.*, 2007a; Ryberg *et al.*, 2007).

Another method to functionally characterise the cell lines was to detect downstream GPR55-cell signalling via RhoA as it influences actin cytoskeleton rearrangement. Phalloidin was used to stain actin in mouse GPR55 transfected DBT cell line and untransfected DBT cell line. Stimulation caused cytoskeletal morphology rearrangement in the GPR55-transfected cell line upon stimulation with

1 μ M of LPI. Earlier studies have demonstrated GPR55, G13 and Ras homolog gene family, member A (Rho A) mediated rearrangement of the actin cytoskeleton in GPR55 transfected cell line upon stimulation by LPI (Balenga *et al.*, 2011a; Obara *et al.*, 2011).

Another assay that is responsive to GPR55 stimulation is calcium flux assays (Hoi *et al.*, 2007, Henstridge *et al.*, 2010). In our calcium assay LPI, at higher levels, 10 μ M, induced augmented intracellular Ca²⁺ levels in the GPR55 transfected cells compared to the untransfected cells. At a lower concentration of LPI, 1 μ M, no significant difference in levels of calcium was observed when comparing the two cell lines. Consistent with previous findings LPI (10 μ M) induced intracellular Ca²⁺ release was increased in GPR55 transfected cells compared to non-transfected cells (Waldeck-Weiermair *et al.*, 2008); this response was attenuated in cells treated with GPR55 siRNA or SR141716A (Bondarenko *et al.*, 2010; Lauckner *et al.*, 2008; Waldeck-Weiermair *et al.*, 2008).

Although current knowledge involving the downstream signalling pathways of GPR55 are limited compared to CB₁ and CB₂ the activation of GPR55 by agonists has been shown to activate the small GTP binding proteins Rho A, Cdc42, and Rac1 (Idris *et al.*, 2010; Ryberg *et al.*, 2007). Activation of the receptor has also shown to trigger activation of the ERK/MAPK signalling, provoke release of intracellular calcium through activation of phospholipase C and to activate nuclear factor of activated T-cells (NFAT) through alterations of intracellular calcium (Balenga *et al.*, 2011a; Henstridge *et al.*, 2009; Henstridge *et al.*, 2010; Idris *et al.*, 2010; Kapur *et al.*, 2009; Lauckner *et al.*, 2008; Oka *et al.*, 2007; Ross, 2009). Studies suggest that GPR55 is also coupled to G12/13 and activation of the receptor causes Ca²⁺ mobilization (Ho, 2010; Ross, 2009; Waldeck-Weiermair *et al.*, 2008). Increases in intracellular Ca²⁺ levels upon GPR55 activation by the cannabinoid ligands THC and JWH015 have been observed in dorsal root ganglion neurons and in GPR55 transfected HEK293 cells (Kapur *et al.*, 2009; Lauckner *et al.*, 2008). Other ligands such as LPI and its 2-arachidonyl analogue act as GPR55 agonists and have the capacity to induce calcium signalling upon activation of the receptor (Johns *et al.*, 2007; Kapur *et al.*, 2009; Oka *et al.*, 2007). In human endothelial cells the integrins $\alpha\beta$ 3 and α 5 β 1 have been reported to be involved in GPR55-mediated Ca²⁺ signalling by anandamide and O-1602 (Waldeck-Weiermair *et al.*, 2008). Although THC and anandamide activation of GPR55 demonstrated calcium alterations the endocannabinoid 2-AG had no effect (Barak *et al.*, 1997; Idris *et al.*, 2010). SR141716A has shown to act as an antagonist by reducing induced calcium rise by THC, JWH015 and methanandamide, a metabolically stable analogue of anandamide (Lauckner *et al.*, 2008). The same study demonstrated GPR55 mediated intracellular releases of calcium through G α_q , PLC, G α 12, RhoA and actin cytoskeleton (Henstridge *et al.*, 2009; Lauckner *et al.*, 2008). Using a reporter gene assay SR141716A has been shown to act as an agonist (Lauckner *et al.*, 2008) contradicting findings by

another study that found the ligand to act as an antagonist (Kapur *et al.*, 2009; Yin *et al.*, 2009). It is possible that some of these discrepancies relate to use of over-expressing cell lines. This may exhaust secondary messenger systems such that receptor stimulation may not give a similar signaling to that found in normal cells. Although our cell lines have been a useful tool to study the functions of the GPR55 receptor the untransfected cell line often had a background or baseline immunoreactivity/signaling (Figure 4.5, 4.6, 4.9 and 4.10).

Purchased antibodies were tested using immunofluorescence and one of the antibodies, from Genetex (ref: GTX12700), demonstrated similar staining patterns in both the GPR55 transfected and non-transfected cell line. This suggested lack of specificity. Another antibody from Glaxosmithkline was also tested and was found to show specific punctuation and staining pattern mainly in the outer cell membranes in the GPR55 transfected cells however this batch of antibody is no longer available. Antibodies produced by the 6 selected hybridomas were also tested against both cell lines using immunocytochemistry and overall similar background staining was detected in both cell lines when comparing over at least 50 cells per slide.

Although there are a number of reported polyclonal antibodies reactive to human GPR55 there is no evidence that these cross-react with mouse GPR55 and there are many of the batches of antibodies that do not produce consistent activity on human cells either. The Irving lab has tested over 11 batches without success (A.Irving, personal communication) and the Baker lab tested 3 antibodies without success before this project was initiated (D.Baker, personal communication). This lack of specificity has been a common finding with cannabinoid directed antibodies notably reacting with multiple proteins in CB₁ transfected and non-transfected cells on western blotting (Grimsey *et al.*, 2008). This may relate to the fact that GPCR are structurally similar receptors and are integral membrane proteins that will lack 3 dimensional conformations in solution. Likewise cannabinoid receptors are evolutionary conserved (Elphick, 2002). Mouse and human amino acid sequence CB₁ receptors are 97% identical (Abood *et al.*, 1997) and GPR55 is 75% identical (Ryberg *et al.*, 2007). Therefore it is likely that most animals are immunologically tolerant to their own protein and suggest that it will be difficult to make antibodies.

The information of GPR55 protein expression and functional significance in various physiological systems including the nervous system are at the moment limited. More research on the knockout mice and access to more antibodies and ligands will need to be evaluated in order to discover the function of the receptor in these systems (Henstridge *et al.*, 2011). A number of studies have demonstrated the use of GPR55 antibodies for staining various tissues and cell lines (Fonseca *et al.*, 2011; Henstridge *et al.*, 2011; Romero-Zerbo *et al.*, 2011). Different approaches have been

used to tackle the problems with the development of specific GPR55 antibodies. Henstridge *et al.* have demonstrated expression levels of GPR55 in HEK293 cells expressing a 3xhemagglutinin (HA) epitope tag at the N-terminus of GPR55 using a monoclonal HA antibody (Henstridge *et al.*, 2009). Other studies have also used an HA antibody for detection of GPR55 in human breast carcinoma cell line transfected with 3xHA-GPR55 (Ford *et al.*, 2010). Antibodies against the epitope were used in order to detect GPR55 surface levels in the cell line. The GPR55 expression levels in the cancer cell line were also knocked down using siRNA against GPR55 (Ford *et al.*, 2010). Commercially purchased antibodies from Ab-cam were used to detect GPR55 levels in human dermal micro vascular endothelial cells (Zhang *et al.*, 2010).

The orphan receptor has also been identified in rat uterine tissues throughout pregnancy using a commercial rabbit anti-rat GPR55 antibody. A rabbit IgG antibody was used as a control in the experiment (Fonseca *et al.*, 2011). HEK293 cells stably or transiently transfected with N terminus tagged GPR55 (FLAG-GPR55) were generated in order to study GASP-1 identified as a key regulator of the trafficking of GPR55. GPR55 protein expression was also determined by western blot analysis using a specific purchased GPR55 antibody (Kargl *et al.*, 2011). GPR55 expression levels in human cholangiocarcinoma cell lines were mainly found in the membrane and cytoplasm in the cell lines using a specific primary antibody (Genetex Inc. Irvine, CA) (Huang *et al.*, 2011). Using a reported “monoclonal” antibody (Caymen, Cat. no: 10224; Caymen Chemical, Ann Arbor, MI, USA) Lin *et al.*, 2011 found that GPR55 was localized mainly in the submucosa and myenteric plexus of the gut. The antibody used by Lin *et al.*, 2011 however was a polyclonal antibody and not a monoclonal antibody, according to the Caymen chemical website this must be a writing error by the authors. The authors demonstrated that GPR55 expression was found to be upregulated in the inflammatory intestine of rat suggesting that the activation of GPR55 may play a role in regulating intestinal function in pathophysiological conditions (Lin *et al.*, 2011). A rabbit anti-GPR55 antibody (Abcam, Cambridge, UK; cat. no. Ab41515) was used to stain mouse pancreatic cells from wildtype C57BL/6 and GPR55 knockout mice using immunofluorescence only demonstrated moderate staining in the pancreatic cells from the wildtype mice (Romero-Zerbo *et al.*, 2011). U2OS, an osteosarcoma cell line, stably transfected HA-GPR55E cells were pre-treated with an anti-HA antibody and then stimulated with the agonists virodhamine and AEA causing agonist-induced internalization of GPR55 (Sharir *et al.*, 2012). However, in the absence of knockout or knock-down experiments any reported activity of antibodies must be cautiously interpreted. This problem was evident with CB₂ receptor expression of nerve cells (Nunez *et al.*, 2004), which normally lack any evidence of receptor ligand binding in CB₁ knockout (Zimmer *et al.*, 1999) and lack of mRNA in nervous tissue (Munro *et al.*, 1993).

The initial antibodies produced to recognize CB₁ receptor in rodent brain and denatured CB₁ proteins on immunoblots were raised against the extracellular amine terminus (Grimsey *et al.*, 2008; Pettit *et al.*, 1998). Other CB₁ antibodies developed against the C-terminus of CB₁ have also been able to detect CB₁ receptors in rodent brain (Hajos *et al.*, 2000). Inconsistencies have also been demonstrated as in cases where initial antibody aliquots have previously worked as expected subsequent aliquots from the same sources failed to detect CB₁ receptors in brain sections (Grimsey *et al.*, 2008). Similar localization of CB₁ and CB₂ immunoreactivity in cerebellar cortex has also been identified (Gong *et al.*, 2006; Suarez *et al.*, 2008). CB₂ expression levels have also been detected in the rat cerebellum (Ashton *et al.*, 2006). The presence of CB₁ and CB₂ receptors has also been detected in the hippocampus of neonatal rats (Suarez *et al.*, 2009). Although CB₂ expression has also been identified in the hippocampus of adult rats the distribution profile shows a discrepancy, it is hypothesized that CB₂ expression changes during development until its final adult distribution (Gong *et al.*, 2006; Suarez *et al.*, 2009). CB₂ distribution in the peripheral and central nervous systems have been reported using different techniques and different groups have reported variable expression patterns of the receptor (Atwood *et al.*, 2010). The distribution profile of CB₁ receptor in wildtype compared to knockout animals is very different however CB₂ antibodies show a fainter but similar pattern in the CB₂ knockout animals compared to wildtype animals (Ashton, 2011). It has also been reported that attempts to identify CB₂ levels have also been a hurdle as there are currently no available highly specific CB₂ antibodies available (Onaivi *et al.*, 2012).

Western blot was used to investigate the specificity of the obtained hybridomas and all antibodies demonstrated unspecific binding relating to the target antigen and reacted with several proteins in both the GPR55 transfected and in the untransfected cell lines. However, in one of the antibody secreting hybridomas 4D12 a stronger band at the predicted size of GPR55 was detected in the GPR55 transfected cell line and a weak band in the untransfected cell line. Previous studies have also been performed where western blot analysis of liver and spleen homogenates from wildtype C57BL/6 mice showed 3 bands one at the expected size of 37 kDa and two other unspecific bands. The findings were explained by the authors as possible post-translational modifications of the receptor (Romero-Zerbo *et al.*, 2011). Although further optimization of the 4D12 hybridoma might have reduced the background staining, these experiments would be time consuming and almost one year of this study was focused on producing antibodies therefore alternative techniques such as *in situ* hybridization were instead used as shown in chapter 5.

FACS analysis was also used to determine the specificity of the hybridomas. Although minor differences were observed when comparing binding of the hybridomas to the wildtype DBT cells compared to the GPR55 transfected cells these low reactivities were comparable to isotype controls and not specific target antibody staining (Kiene *et al.*, 2012) (<http://www.mitosciences.com/PDF/flow-cytometry-protocol.pdf>).

CHAPTER 5

Expression profile of GPR55 mRNA levels in various tissues

5.1 Introduction

An aim of this chapter was to identify GPR55 levels in mouse tissues and in the astrocytoma cell line. Due to the lack of production of specific antibodies as mentioned in chapter 4 alternative techniques were applied to study mRNA levels of GPR55.

5.1.1 GPR55 mRNA levels

Mouse GPR55 mRNA (Table 5.1) levels have been detected in the adrenals, frontal cortex, ileum, jejunum, striatum and lower levels in the hypothalamus, brainstem, spleen, hippocampus and cerebellum (Ryberg *et al.*, 2007; Wu *et al.*, 2013). Background levels of GPR55 mRNA were detected in mouse adipose tissue (Ryberg *et al.*, 2007). GPR55 mRNA has also been found to be expressed in a primary mouse microglia and in the BV-2 mouse microglial cell line (McHugh *et al.*, 2010; Pietr *et al.*, 2009). In mice lacking the adipocyte hormone leptin, which causes increased food intake, and rats fed on high fat diet, significantly reduced GPR55 mRNA and protein levels were observed in the white adipose tissue when compared to lean littermates (Colombo *et al.*, 2002; Moreno-Navarrete *et al.*, 2012).

Table 5.1 Mouse GPR55 mRNA levels

GPR55 mRNA levels mouse tissues (Ryberg <i>et al.</i> , 2007; Henstridge <i>et al.</i> , 2011; Wu <i>et al.</i> , 2013)	
High expression levels	Low expression levels
Adrenals	Hypothalamus
Frontal cortex	Brainstem
Ileum	Spleen
Jejunum	Hippocampus
Striatum	Cerebellum

Previous studies have reported GPR55 mRNA in rat hippocampus, thalamic nuclei and in the midbrain (Sawzdargo *et al.*, 1999). GPR55 and also CB₁, CB₂, TRPV1 mRNA levels have also been detected in human proximal tubular (HK2) cells and in rat kidney (Jenkin *et al.*, 2010). GPR55 and CB₁ mRNA levels have also been detected in rat cerebellar granule cells (Chiba *et al.*, 2011). CB₁

mRNA and protein expression levels in the HK2 cells have also been detected by Lim *et al.*, 2010. GPR55 mRNA and protein levels have been detected in PC12 cells however no CB₁ or CB₂ mRNA expression was observed in the cell line (Obara *et al.*, 2011).

Human GPR55 expression levels have been detected in different parts of the brain, in lymphoid and in gastrointestinal organs (Table 5.2) (Brown *et al.*, 2003; Henstridge *et al.*, 2011; Oka *et al.*, 2009; Sawzdargo *et al.*, 1999). GPR55 have also been detected in the testis, myometrium and in cells including Peripheral Blood Mononuclear Cells (PBMC), lymphocytes and osteoclasts (Table 5.1)(Brown *et al.*, 2003; Henstridge *et al.*, 2011; Moreno-Navarrete *et al.*, 2012; Oka *et al.*, 2009; Whyte *et al.*, 2009). It was also reported that GPR55 is highly expressed in normal human breast adipose tissue and is present in visceral fat (Brown *et al.*, 2003). Levels of GPR55 mRNA have also been confirmed in human visceral (VAT) and subcutaneous adipose (SAT) tissues by another group (Moreno-Navarrete *et al.*, 2012). The same study also reported similar GPR55 mRNA levels in the liver when comparing obese or diabetic patients with healthy patients (Moreno-Navarrete *et al.*, 2012). GPR55 and CD14, a monocyte marker, were found to be expressed in adipocytes and in the stromal vascular fraction of fat tissues (Moreno-Navarrete *et al.*, 2012). GPR55 mRNA levels have also been detected in the spleen and thymus these findings lead the authors to explore the expression in lymphoblastoid cell lines (Oka *et al.*, 2007; Oka *et al.*, 2009). GPR55 expression was detected in IM-9 cells however no levels were identified in the Jurkat, Raji and Daudi cell lines (Oka *et al.*, 2009). GPR55 expression has been verified in a number of human cancer cell lines including ovary, prostate, pancreas, bile ducts, blood, brain, breast, cervix, skin and liver (Andradas *et al.*, 2011; Ford *et al.*, 2010; Henstridge *et al.*, 2011; Huang *et al.*, 2011; Pineiro *et al.*, 2011). GPR55 mRNA levels have also been detected in other human cell lines (Table 5.3) (Henstridge *et al.*, 2011).

5.1.2 Methods

In this chapter qPCR and *in situ* hybridization was used for detection of mRNA levels. To determine the tissue distribution, a GPR55 Taqman probe was used to examine the production of GPR55 mRNA in mouse tissues (*see methods 2.12.3*). The expression levels in the tissues were quantified using a GPR55 standard curve (*see methods 2.12.4*). In the first instance an analysis of tissue distribution was assessed compared with GPR55 deficient mice. Radioactive (*see methods 2.13*) and non-radioactive (*see methods 2.14*) *in situ* hybridization was also used to localize GPR55 expression in mouse tissues and in the E1 DBT and DBT cell lines.

Table 5.2 Human GPR55 mRNA levels

GPR55 mRNA levels in human tissues and cells	
High expression levels	Low expression levels
Brain: (Henstridge <i>et al.</i> , 2011) Regions in Brain: Putamen(Henstridge <i>et al.</i> , 2011) Striatum(Henstridge <i>et al.</i> , 2011) Nucleus Accumbens(Henstridge <i>et al.</i> , 2011) Caudate Nucelus (Henstridge <i>et al.</i> , 2011)	Brain: (Oka <i>et al.</i> , 2009) Regions in Brain: Caudate nucleus(Sawzdargo <i>et al.</i> , 1999) Putamen(Sawzdargo <i>et al.</i> , 1999) Hypothalamus(Henstridge <i>et al.</i> , 2011) Pituitary(Henstridge <i>et al.</i> , 2011)
Lymphoid organs: Spleen(Henstridge <i>et al.</i> , 2011; Oka <i>et al.</i> , 2009) Thymus (Oka <i>et al.</i> , 2009)	Lymphoid organs: Adenoid (Brown <i>et al.</i> , 2003)
Gastrointestinal organs: Ileum (Brown <i>et al.</i> , 2003) Small intestine (Oka <i>et al.</i> , 2009) Intestine(Henstridge <i>et al.</i> , 2011)	Gastrointestinal organs: Ileum (Brown <i>et al.</i> , 2003) Colon(Oka <i>et al.</i> , 2009) Stomach(Henstridge <i>et al.</i> , 2011)
Testis(Brown <i>et al.</i> , 2003; Oka <i>et al.</i> , 2009)	Liver (Moreno-Navarrete <i>et al.</i> , 2012)
Breast adipose(Brown <i>et al.</i> , 2003)	Visceral fat (Brown <i>et al.</i> , 2003; Moreno-Navarrete <i>et al.</i> , 2012) Fraction of visceral adipose: { - Adipocytes - Stromal vascular fraction (Moreno-Navarrete <i>et al.</i> , 2012)
Myometrium (Brown <i>et al.</i> , 2003)	Subcutaneous adipose (Moreno-Navarrete <i>et al.</i> , 2012)
Cells: Osteoclasts (Whyte <i>et al.</i> , 2009) Lymphocytes(Henstridge <i>et al.</i> , 2011) PBMC (Henstridge <i>et al.</i> , 2011)	Trachea (Oka <i>et al.</i> , 2009)
	Cervix (Oka <i>et al.</i> , 2009)
	Lung (Henstridge <i>et al.</i> , 2011; Oka <i>et al.</i> , 2009)
	Cells: Monocytes (Whyte <i>et al.</i> , 2009) Neutrophils(Henstridge <i>et al.</i> , 2011) Macrophages (Henstridge <i>et al.</i> , 2011) Platelets(Henstridge <i>et al.</i> , 2011) Bone marrow(Henstridge <i>et al.</i> , 2011)

Table 5.3 *Human GPR55 mRNA levels*

GPR55 mRNA levels human cell lines (Henstridge <i>et al.</i>, 2011)	
High expression levels	Low expression levels
NT-2 PRE Neuronal precursor derived tumor	CCF-STTG1 Astrocytoma
SAOS2 Sarcoma osteogenic	HS-2683 Neuronal glioma
	UT7-EPO Erythropoietin dependent leukemia
	HOS Osteosarcoma
	Prostate SMC Smooth muscle cells

5.2 Results

5.2.1 Reference genes

Glyceraldehyde-3-phosphate dehydrogenase (GAPDH) was initially tested as a reference gene; however, results showed variation in expression levels in different mouse tissues and was therefore not used. A second reference gene, acidic ribosomal phosphoprotein P0 (36B4), was also used for the GPR55 assay and this reference also demonstrated variations in expression levels in our study. However, the use of 36B4 as a reference gene for quantification of GPR55 mRNA levels in mouse tissues has previously been reported by another group (Ryberg *et al.*, 2007).

Table 5.1 *Reference genes GAPDH and 36B4*

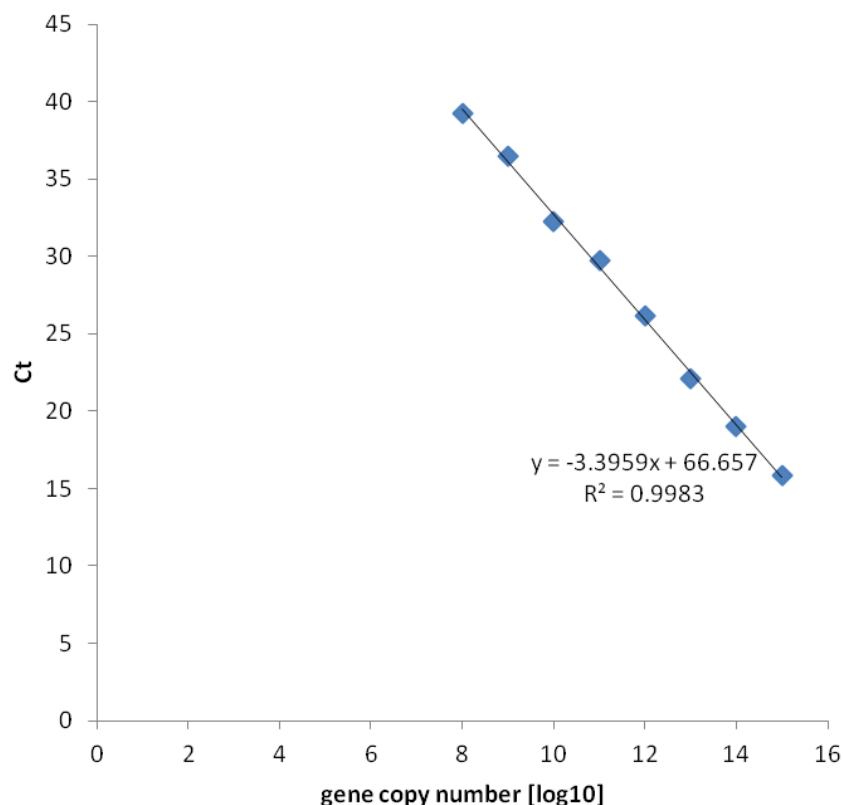
C56BL/6 mouse tissues	GAPDH (Ct)	36B4 (Ct)
WT Brain	18.3	26.3
WT Spleen	17.8	26.3
WT Testis	18.5	23.5
WT Pancreas	22.7	24.0

Various tissues were collected from GPR55 knockout and wild-type mice were taken for analysis of the reference genes GAPDH and 36B4. The reference gene expression levels were tested in the brain, spleen, testis and pancreas from 3 C57BL/6 mice. RNA extractions and cDNA synthesis were done on all tissues and cells and mRNA analysis was performed using qPCR. The Ct (threshold cycle) value represents the intersection between an amplification curve and a threshold line. The results represent the mean of GAPDH or 36B4 mRNA levels \pm SEM. n= 3 animals per group.

5.2.2 Standard curve for GPR55 template

As the reference genes varied in the different tissues it was decided to use a standard curve for quantification of the GPR55 mRNA levels. As mentioned previously (see methods 2.12.4) an amplicon of GPR55 was designed to make a standard curve. The efficiency (E) of PCR (slope) should be around 100% and corresponds to double the amount ($E=2$) for each cycle. Although an efficiency of 100% (100%) is ideal, a good reaction should have values between 90% and 110% corresponding to values between -3.58 and -3.10 (Larionov *et al.*, 2005). It was found that the efficiency was approximately -3.4.

Figure 5.1 GPR55 standard curve: Amplification of a GPR55 amplicon

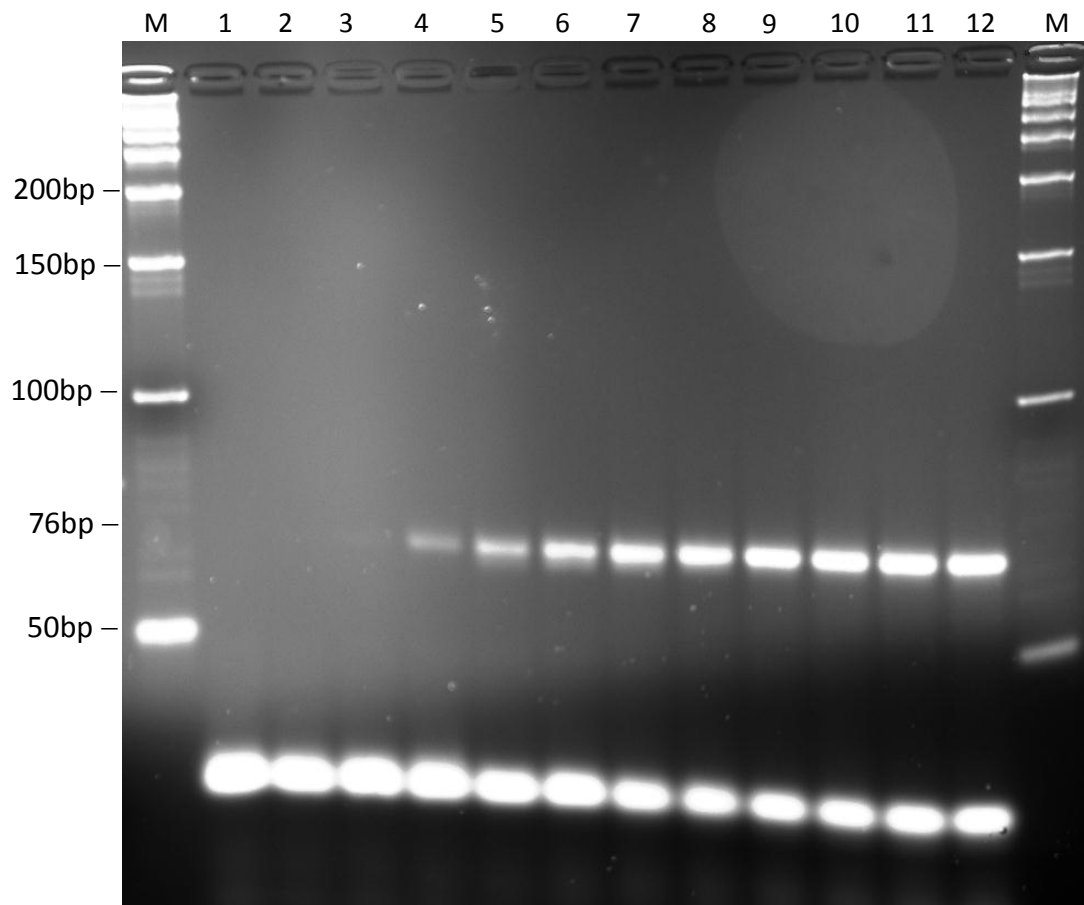


A 76bp GPR55 amplicon "ctatct acatgatcaa cttggctgtt ttcgatttac tgctggtgct ctccctccca ttcaagatgg tcctgccaca" was designed in order to make a standard curve. A series of dilutions were made and 8 different concentrations, 2×10^7 , 2×10^8 , 2×10^9 , 2×10^{10} , 2×10^{11} , 2×10^{12} , 2×10^{13} , 2×10^{14} , were selected to make the standard curve. The samples were amplified using qPCR. The various standard curve concentrations covered the different range of GPR55 mRNA levels from the various mouse tissues.

5.2.3 GPR55 Standard curve

The standard curve was run in duplicates in 96-well reaction plates and also run on an agarose gel in order to confirm the band size of the samples. The size of the samples corresponded to the predicted size of the designed amplicon at 76bp.

Figure 5.2 *GPR55 standard curve: standard curve samples run on agarose*

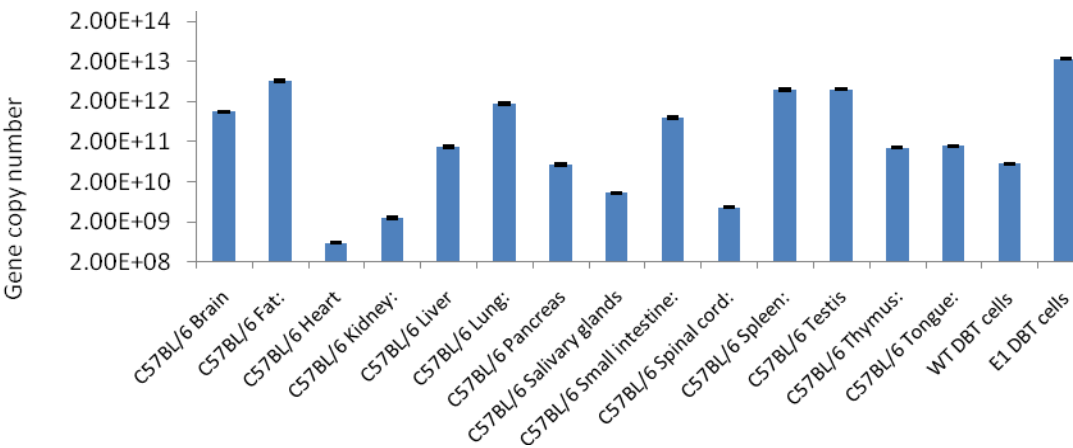


A 76bp GPR55 amplicon "ctatct acatgatcaa ctggctgtt ttcgatttac tgctggtgct ctccctcca ttcaagatg tctgccaca" was designed in order to make a standard curve. A series of dilutions were made and 12 different concentrations (gene copy numbers), 2×10^3 , 2×10^4 , 2×10^5 , 2×10^6 , 2×10^7 , 2×10^8 , 2×10^9 , 2×10^{10} , 2×10^{11} , 2×10^{12} , 2×10^{13} , 2×10^{14} , were run on the gel. The samples were amplified using qPCR. The various standard curve concentrations covered the different range of GPR55 mRNA levels from the various mouse tissues. The samples were amplified using qPCR. The reactions were then subject to 2% agarose gel electrophoresis and bands were detected using ethidium bromide. The GPR55 standard had a predicted size of 76bp. Band sizes were determined using a standard 50 base pair (bp) DNA ladder

5.2.4 GPR55 mRNA expression levels of in mouse tissues.

In order to determine the tissue distribution of GPR55, mRNA levels were prepared from a variety of different tissues. GPR55 mRNA levels were found expressed at higher levels in the brain, fat, liver, lung, small intestine, spleen, testis, thymus, tongue and in the GPR55 transfected cell line. Lower levels of GPR55 were detected in the heart, kidney, pancreas, salivary glands, and spinal cord and in the wild type cell line. The levels of GPR55 in KO tissues were comparable with control samples and did not produce appreciable levels of GPR55. The results suggested that DBT have low basal levels of GPR55.

Figure 5.3 GPR55 mRNA levels

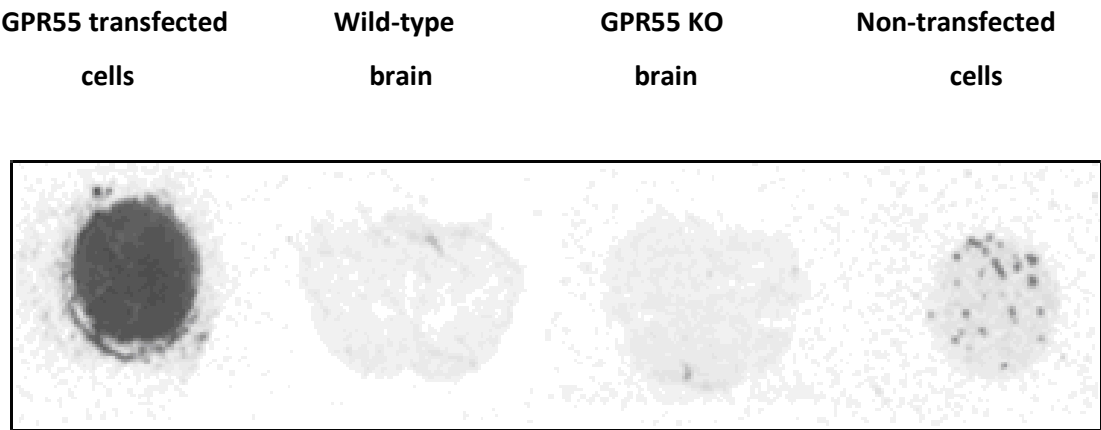


Various tissues were collected tissues from GPR55 KO and wild-type mice were taken for analysis of GPR55 mRNA levels. The mRNA levels of GPR55 in the GPR55 transfected cell line E1 DBT and WT DBT cells were compared to the levels in the tissues. RNA extractions and cDNA synthesis were performed on all tissues and cells and mRNA analysis was performed using qPCR. The mRNA expression levels of GPR55 receptor in mouse WT tissues was quantified using a GPR55 standard curve (Figure 5.1). The results represents the mean \pm SEM fold increase compared with the levels from KO mice (n=3/group).

5.2.5 Radioactive *In situ* hybridization

In situ hybridization using ³⁵S radioactive labeled probes was performed in order to localize specific mRNA sequences in tissue sections. This demonstrated marked expression in GPR55 transfected cells compared to non-transfected cells. However, this experiment showed no detectable expression of GPR55 in brain tissues. High levels of GPR55 were detected in the GPR55 transfected astrocytoma cell line.

Figure 5.4 *In situ* hybridization was used for detection of GPR55 mRNA levels in GPR55 transfected cell line (E1 DBT), non-transfected (DBT) and mouse brain WT and KO tissues

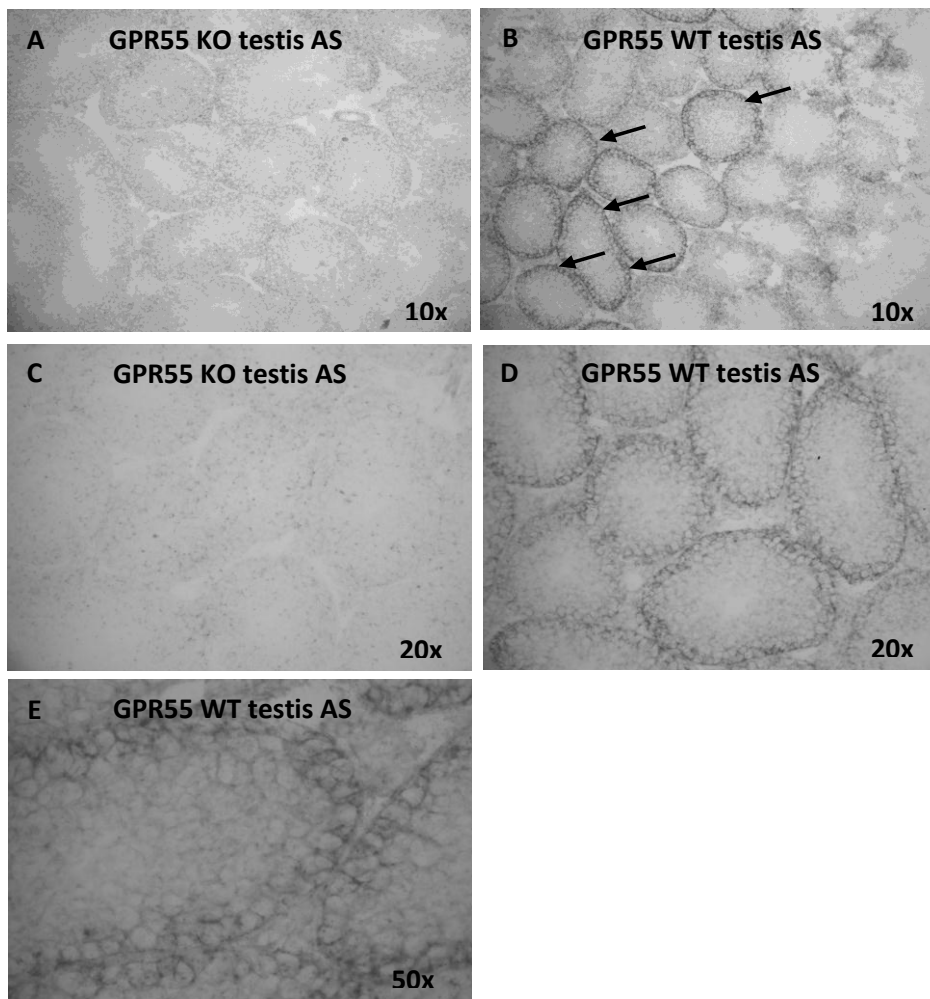


Cytospins with 2.5×10^6 cells per well were made from a *Gpr55* transfected astrocytoma cell line, the non-transfected astrocytoma cell line and 10µm cryostat sections from the brain of a wild-type and GPR55 KO mouse were made. Analysis of mRNA expression levels of GPR55 in the wild-type and GPR55 KO tissues was performed using *in situ* hybridization using a ³⁵S radioactive labeled GPR55 probe. Slides were coated in developing emulsion to detect activity. There was some signal in non-transfected cells and this probably represents background labelling.

5.2.6 Non-Radioactive *In situ* Hybridization (NR-ISH)-Digoxigenin (DIG)-labeled GPR55 RNA probe

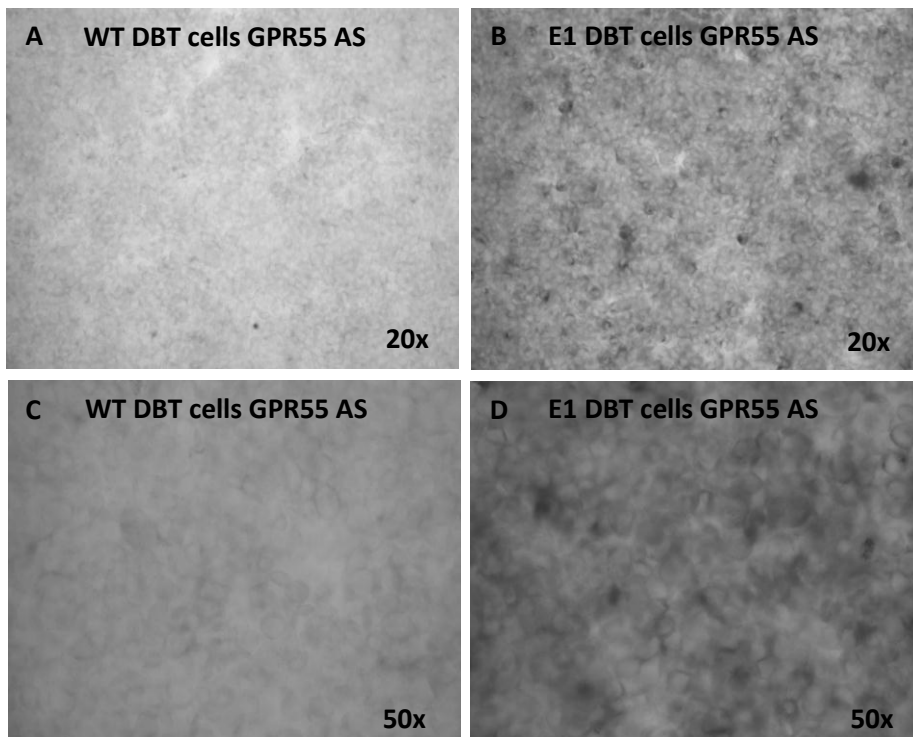
Due to the high background often observed in the *in situ* hybridization using radioactive labeled probes these were replaced by non-radioactive labeled probes to localize specific mRNA sequences in tissue sections. This was first investigated in the testis as qPCR analyses indicated that this tissue had a higher level of expression than in the brain as previously shown (Figure 5.3). Staining with the anti-sense (AS) GPR55 probe was mainly observed in the outer layer of the tubular wall in the wildtype testis (Figure 5.5) (arrows). A strong staining was observed in the GPR55 transfected E1 DBTcell line compared to the non-transfected WT DBT cell line (Figure 5.6). I did not get this approach to give a specific signal in the brain.

Figure 5.5 Non-radioactive *in situ* hybridization in the testis



Cryostat sections (10 μ m) from (A) a GPR55 KO mouse and (B) a wild-type mouse were prepared and fixed in 4% PFA. GPR55 mRNA was detected using *in situ* hybridization analysis using a non-radioactive AS DIG labeled, GPR55-specific probe. Digoxin was detected using specific antibody staining. This was incubated on the sections for 72h. Staining was mainly observed in the outer layer of the tubular wall in the wild-type testis (arrows).

Figure 5.6 Non-radioactive *In situ* hybridization in WT DBT and E1 (GPR55) DBT cell lines



A total of 2.5×10^6 cells per well were used from the *Gpr55* transfected E1 DBT cell line and the non-transfected WT DBT cell line. Cytopins were made and GPR55 mRNA was detected using *in situ* hybridization analysis using a non-radioactive AS DIG labeled, GPR55-specific probe. This was incubated on the sections for 72h.

5.3 Discussion

In the current study the tissue distribution of GPR55 was analyzed. A standard curve was used to quantify the levels of a GPR55 amplicon diluted at various concentrations. The CT values from the standard curve with known concentrations were used to correlate the different copy numbers. The efficiency of the PCR was 97% and was within the range of accepted values for a reaction at -3.3959 (5.2.2). Although other ways of quantifying mRNA levels using reference genes such as GAPDH and 36B4, would be an alternative to the standard curve, in our case the levels of the reference genes highly varied in the different tissues (Table 5.1)

High GPR55 levels were expressed in the E1 GPR55 DBT transfected cell line compared to the non-transfected DBT cell line. In the mouse tissues the highest levels of GPR55 were detected mainly in the spleen, testis and adipose tissues. Lower levels were seen in the heart, kidney, salivary gland and spinal cord.

Ryberg *et al.*, 2007 reported background levels of GPR55 mRNA in mouse adipose tissue. In this study high levels of GPR55 was found in mouse adipose tissue consistent with initial reports in a patent (Brown *et al.*, 2001). Substantial levels of GPR55 expression have also been reported in normal human breast adipose tissue and in visceral fat (Brown *et al.*, 2003). The authors in the same study however did not detect GPR55 levels in subcutaneous adipose tissues (Brown *et al.*, 2003). The various observations may be due to the use of different mouse strains or technical difficulties. Also, as the orphan receptor is expressed at seeming very low levels throughout most tissues compared to other targets such as CB₁ it could be due to insufficient technical sensitivity (Ryberg *et al.*, 2007).

Although human GPR55 expression levels have been detected in the caudate nucleus and putamen, no GPR55 expression levels were however detected in other parts of the brain including the hippocampus, thalamus, pons, cerebellum, frontal cortex of the brain or in the liver (Sawzdargo *et al.*, 1999). Expression of GPR55 and CD14 mRNA has also been observed in adipocytes and in the stromal vascular fraction of fat tissues; this might suggest that the receptor is present on monocytes, macrophages and lymphocytes (Moreno-Navarrete *et al.*, 2012).

In situ hybridization using radioactively labeled probes was performed to localize specific GPR55 mRNA sequences in tissue sections. So far, positive controls have been found to work, however problems with supply of batches of radioactivity have hampered attempts to detect GPR55. Due to the high background sometimes found in *in situ* hybridization using radioactive labeled probes the technique was replaced by *in situ* hybridization using non-radioactive labeled probes. Although the non-radioactive probes were used to detect GPR55 levels in the testis the technique was

however not sensitive enough to detect mRNA levels in any other tissue tested including spleen and brain. This demonstrates the insensitivity of the technique compared to qPCR (Figure 5.3). Likewise it also indicates that GPR55 is expressed at very low levels in tissues. Levels of GPR55 mRNA in the transfected cell lines were detected using both radioactive and non-radioactive *in situ* hybridization. However, some background punctate artifact staining was observed in the untransfected cell line but only in a few patches. This artifact staining was not observed in the untransfected cell line when using non-radioactive *in situ* hybridization.

A 10 fold difference in mRNA levels was observed when comparing GPR55 transfected cell lines with brain tissue and a 100 fold difference between the untransfected and transfected astrocytoma cell lines. The GPR55 mRNA levels in the testis were 5 fold less than in the transfected cell line or 5 times more than in the brain. Detection of mRNA levels in the brain using PCR and not when using *in situ* hybridization could be due to that the signal in the brain is distributed in many cells and therefore below detection levels.

CHAPTER 6

Immune function of GPR55 in Neuroinflammation

6.1 Introduction

The aim of this chapter was to investigate the function of the GPR55 receptor during EAE. We generated and genotyped GPR55 knockout mice on the C57BL/6 (chapter 1) background that were initially used for our EAE experiments. However, the EAE experiments on this strain showed inconsistencies in disease course. These animals were then backcrossed for over 11 generations onto the ABH background to generate fully congenic mice and this allowed us to investigate the function of GPR55 during EAE on the more stable background.

EAE is mainly used as an animal model of autoimmune, inflammatory diseases of the CNS and is the most common experimental model used to study MS (Constantinescu *et al.*, 2011; Farooqi *et al.*, 2010; Gold *et al.*, 2006; Steinman *et al.*, 2005). EAE can be induced in susceptible animal strains by active immunization with CNS-derived antigen such as spinal cord homogenate, myelin basic protein, proteolipid protein, MOG, myelin associated glycoprotein, infection with neurotropic viruses or with adoptive transfer of encephalitogenic myelin-reactive T cell lines (Denic *et al.*, 2011). Transgenic mouse EAE models which have a preponderance of myelin-specific T cell receptors have also been reported (Bettelli *et al.*, 2006; Ellmerich *et al.*, 2005; Friesen *et al.*, 2006). EAE is most commonly induced in mouse strains however the disease has been replicated in a wide range of species including chickens (Ranzenhofer *et al.*, 1958), dogs (Thomas *et al.*, 1950), goats (Lumsden, 1949), guinea pigs (Freund *et al.*, 1947), hamsters (Tal *et al.*, 1958) marmosets (Genain *et al.*, 1995), rabbits (Morrison, 1947), rats (Lipton *et al.*, 1952) and sheep (Innes, 1951).

EAE varies between animal species and strains from a chronic form of paresis in the C57BL/6 mice to a relapse-remitting disease that develops to secondary progression in ABH mice (Al-Izki *et al.*, 2012; Baker *et al.*, 2000). Whereas EAE in C57BL/6 mice is induced by immunization of MOG 35-55 peptide it is induced by immunization of spinal cord homogenate in complete Freund's adjuvant in ABH animals. However, immunization of ABH mice with MOG 35-55 peptide results in an immediate progressive chronic disease similar to that occurring in MOG35-55 peptide induced disease in C57BL/6 mice (Amor *et al.*, 2005).

EAE is characterized by a number of immunopathological and neuropathological mechanisms that lead to similar key pathological features of MS including inflammation, demyelination, axonal loss and gliosis (Constantinescu *et al.*, 2011). A perivascular infiltration of CD4⁺ T cells and macrophages has been observed mainly in the spinal cord during clinical episodes of neuroinflammation in ABH mice (Baker *et al.*, 1990; Butter *et al.*, 1991). This accumulation of immune cells correlates with severity of disease (Al-Izki *et al.*, 2012; Allen *et al.*, 1993; Baker *et al.*, 2000; Butter *et al.*, 1991). Demyelination is mainly observed during the relapse stage of the disease and rarely in the acute phase (Amor *et al.*, 2005; Baker *et al.*, 1990). An increased level of axonal degeneration in the spinal cord during EAE in ABH mice leads to the development of signs of neurological impairment such as decreased locomotor performance and clinical signs such as spasticity and tremor (Baker *et al.*, 2000).

Many of the current developed drugs used for treatment of multiple sclerosis have been assessed and validated on the basis of EAE studies (Constantinescu *et al.*, 2011; Farooqi *et al.*, 2010; Gran, 2007). While immunization with a known CNS antigen or antigens is used to develop EAE, the causative factor of MS remains unknown and there is no unique identified antigen in the human disease (Constantinescu *et al.*, 2011; Gran, 2007). The influence of GPR55 was unknown at the initiation of this project. EAE is known to be a largely CD4⁺ T cell induced disease (Mokhtarian *et al.*, 1984; O'Neill *et al.*, 1993). We aimed to detect phenotype and functional changes in immune cells *in vitro* and determine whether there was any influence of the genetic deletion on *in vivo* susceptibility to EAE.

6.1.1 Methods

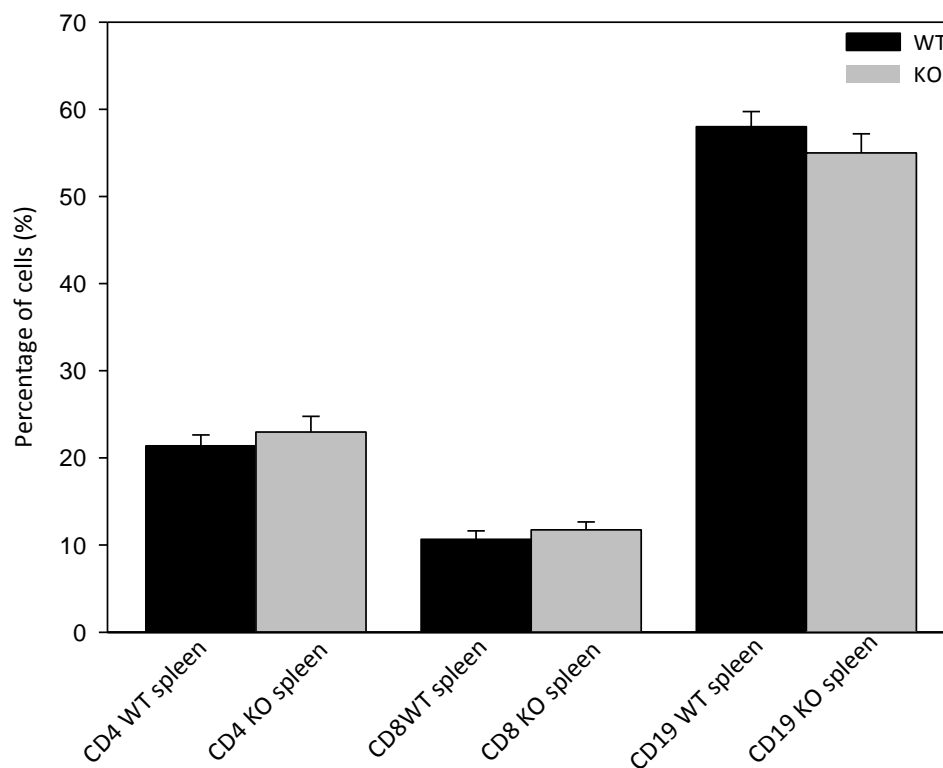
In this chapter EAE induced by either MOG35-55 peptide in C57BL/5 mice (*see methods 2.15.1*) or by spinal cord homogenate in mice on the ABH background (*see methods 2.15.2*). Immunophenotypical analyses were performed using flow cytometry and were used to characterize and compare the different strains, on the C57BL/6 background, in naïve state and after stimulation by MOG35-55 peptide (*see methods 2.16*). CFSE or radioactive proliferation assays using MOG35-55 peptide or Con A (*see methods 2.16.1*) were also performed. Cytokine profiling was analyzed using flow cytometry (*see methods 2.16*). Rotarod was used to measure neurological deficit in relapsing EAE in ABH mice (*see methods 2.15.5*).

6.2 Results

6.2.1 Immunophenotypes (Naïve T- and B-cells in spleen)

The immunophenotypes (T- and B-cells) of GPR55 KO mouse lymphocytes in spleen were compared with wild-type littermates in order to investigate potential differences. Analysis was performed by flow cytometry. Results displayed no significant difference between the two strains.

Figure 6.1 Immunophenotyping of lymphocytes from naïve C57BL/6.GPR55^{-/-} and C57BL/6 ^{+/+} mice

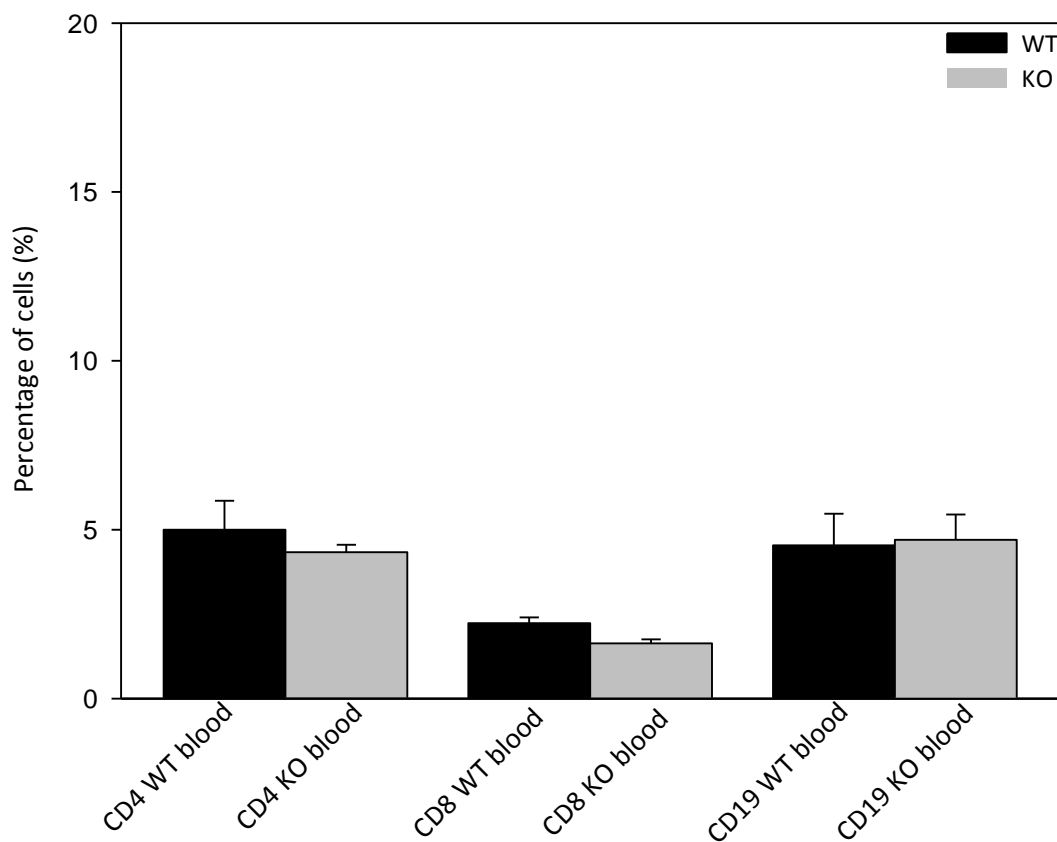


Naïve GPR55 knockout (C57BL/6.GPR55^{-/-}) and wildtype (C57BL/6 ^{+/+}) littermates were used for immunophenotyping. Leukocytes from spleen were collected and the cells were stained with various surface antibodies (T-cells CD4, CD8 and B-cells CD19) diluted 1:100. Samples were then read on a LSRII flow cytometer (Becton Dickinson, Oxford, UK).

6.2.2 Immunophenotypes (Naïve T- and B-cells in blood)

The immunophenotypes (T- and B-cells) of GPR55 KO mouse lymphocytes in blood were compared with wild-type littermates in order to investigate potential differences. Analysis was performed by flow cytometry. Results displayed no significant difference between the two strains.

Figure 6.2 Immunophenotyping of blood lymphocytes from naïve C57BL/6.GPR55^{-/-} and C57BL/6^{+/+} mice



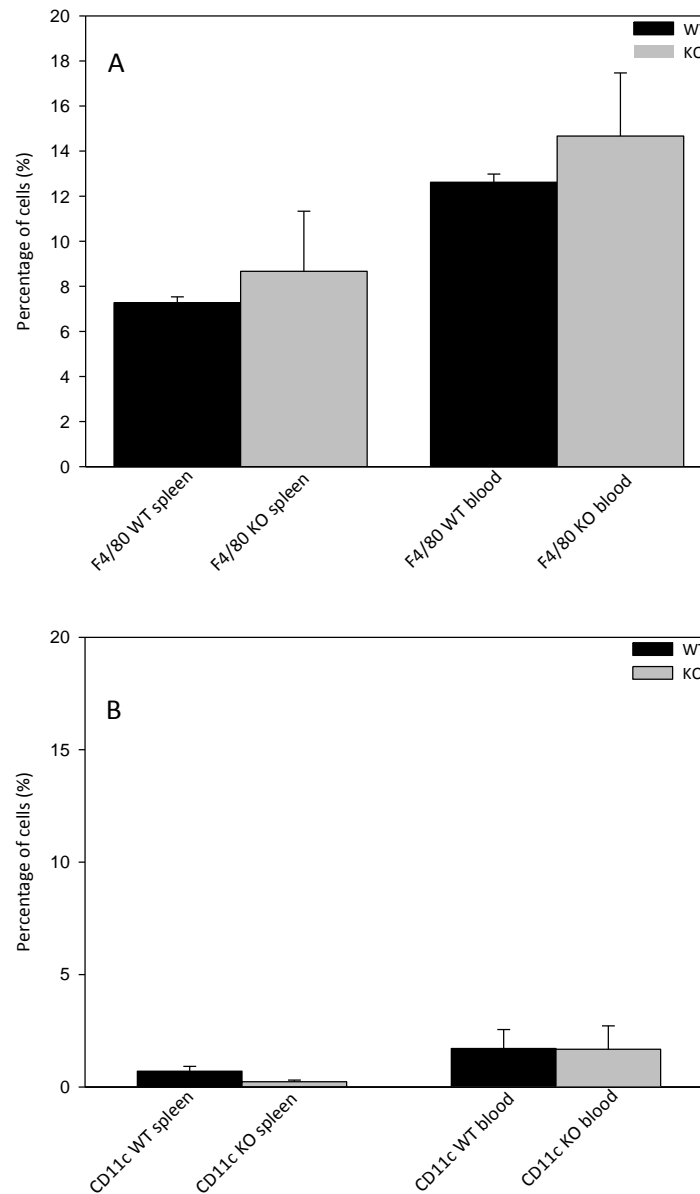
Naïve GPR55 knockout (C57BL/6.GPR55^{-/-}) and wildtype (C57BL/6^{+/+}) littermates were used for immunophenotyping. Leukocytes from blood were collected and the cells were stained with various surface antibodies (T-cells CD4, CD8 and B-cells CD19) diluted 1:100. Samples were then read on a LSRII flow cytometer (Becton Dickinson, Oxford, UK).

6.2.3 Immunophenotypes (Naïve monocytes and dendritic cells)

The immunophenotypes (Monocytes and dendritic cells) of GPR55 KO mouse leukocytes in spleen and blood were compared with wild-type littermates in order to investigate potential differences. Analysis was performed by flow cytometry. Results displayed no significant difference between the two strains. Markers for monocyte (F4/80) (Figure 6.3a) and dendritic cells (CD11c) (Figure 6.3b) were used.

Figure 6.3 Spleen and blood monocytes and dendritic cells from *C57BL/6.GPR55^{-/-}* and *C57BL/6^{+/+}*

mice

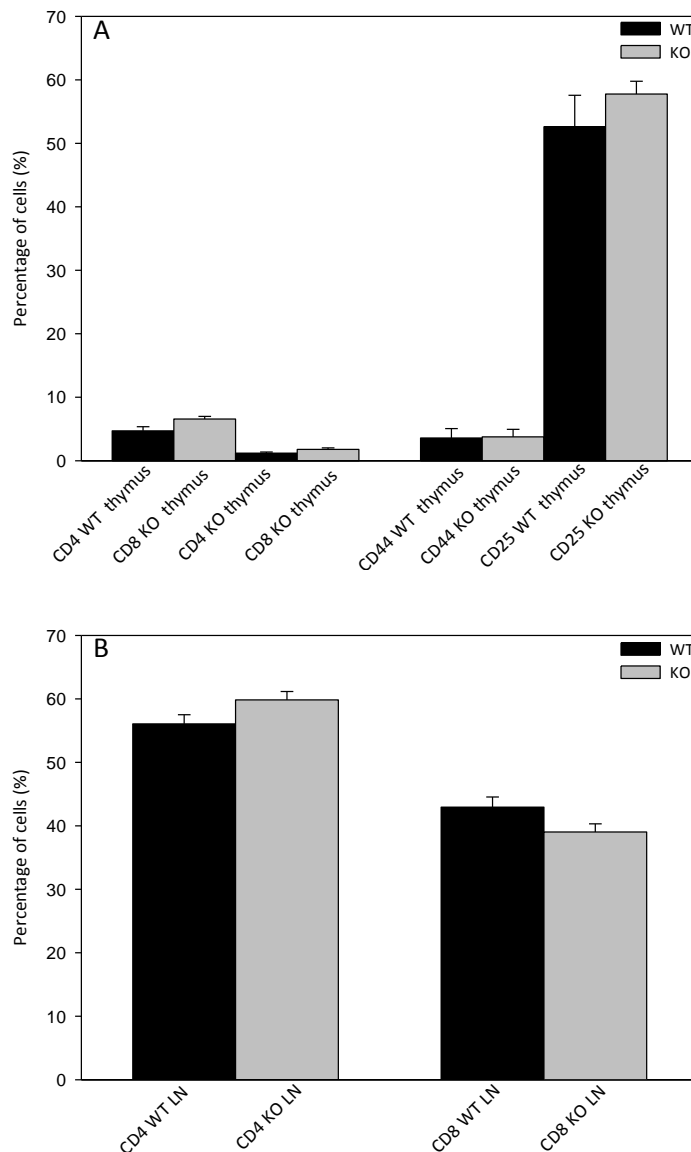


Naïve GPR55 knockout (*C57BL/6.GPR55^{-/-}*) and wildtype (*C57BL/6^{+/+}*) littermates were used for immunophenotyping. Leukocytes from blood were collected and the cells were stained with various surface antibodies (Monocyte-F4/80 and dendritic cell-CD11c markers) diluted 1:100. Samples were then read on a LSRII flow cytometer (Becton Dickinson, Oxford, UK).

6.2.4 Immunophenotypes (Naïve T- cells in thymus and lymph nodes)

Further analysis was performed to investigate T- cell immunophenotypes in the thymus (Figure 6.4A) and in the lymph nodes (LN) (Figure 6.4B) comparing GPR55 KO (C57BL/6) with wild-type animals. Early T-cell development markers CD25 and CD44 in the thymus were also investigated. No significant difference between the two strains was observed.

Figure 6.4 *Thymus and lymph node T-cell immunophenotypes*

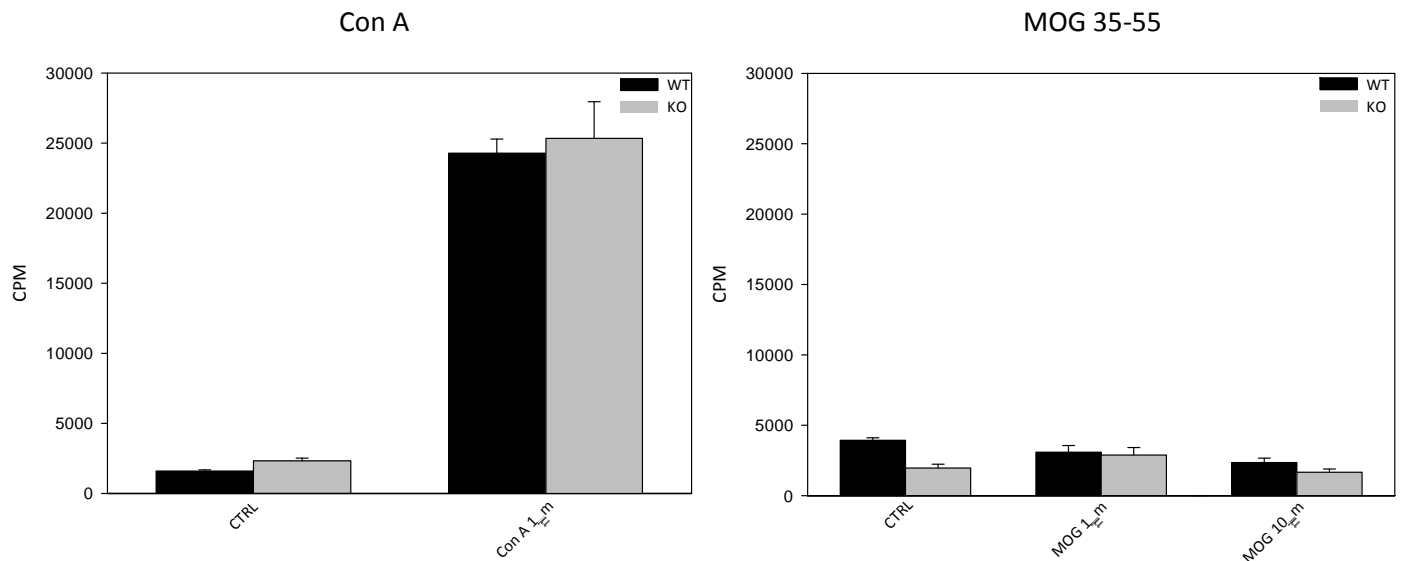


Naïve GPR55 knockout (C57BL/6.GPR55^{-/-}) and wildtype (C57BL/6^{+/+}) littermates were used for immunophenotyping. Cells from the thymus (Figure A) and lymph nodes (Figure B) were collected and stained with surface antibodies against T-cell markers CD4, CD8, early T-cell markers CD25, CD44 and were assessed by flow cytometry.

6.2.5 Stimulation of lymphocytes

Leukocytes (spleen) from GPR55 KO mice and wild-type littermates were isolated and stimulated with either the mitogen Concanavalin A (Con A) or MOG 35-55 peptide. Whilst cells responded to Con A there was essentially no specific proliferation in either wild-type or knockout animals in the cells stimulated with MOG 35-55 peptide.

Figure 6.5 Con A and MOG 35-55 proliferation assays

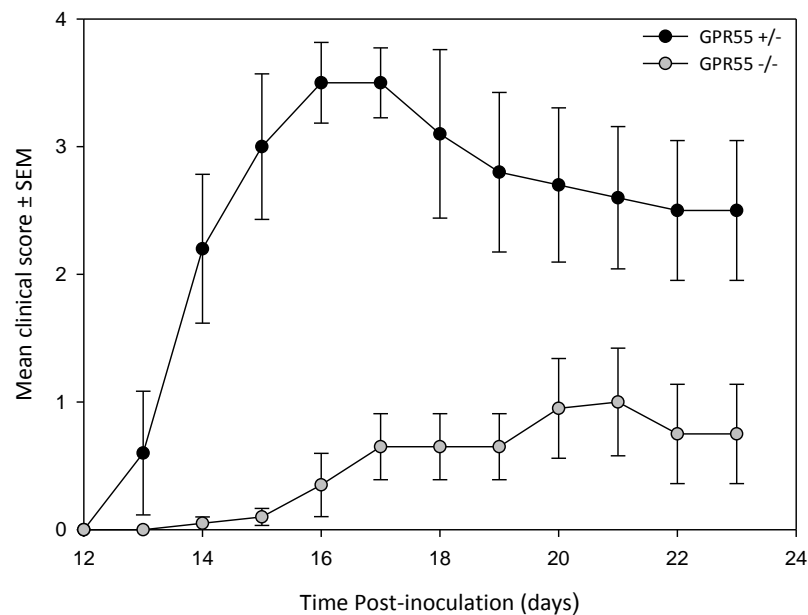


C56BL/6.*Gpr55* knockout and heterozygous littermates were immunized with MOG peptide in Freund's adjuvant on day 0 and were injected with 200ng of *B. pertussis* toxin on day 0 and 1. Splenocytes were collected on day 9 and re-stimulated *in vitro* with MOG peptide at concentrations 1 μ g or 10 μ g for 72h (Figure A). Splenocytes from Naïve GPR55 knockout and wildtype mice also collected and stimulated with Con A for 48h. A total of 300,000 cells were resuspended in a final volume of 100 μ l of RPMI 10% FCS and plated in 96 well-plates. After 24-48h a total of 0.5 units of 3 H Thymidine (PerkinElmer LAS, Beaconsfield, Bucks, UK) was added to each well and cells were incubated during for 24hrs at 37°C in 5%CO₂. Cells were then harvested (TOMTEC MACH III M CELL HARVESTER 96, Warwick, UK) and analysed on a counter (Wallac 1450, Microbeta Plus Liquid Scintillation Counter, Cambridgeshire, UK) (Figure B).

6.2.6 Function of GPR55 in Neuroinflammation-C57BL/6 mice

GPR55 knockout mice were generated by either backcross of C57BL/6.Gpr55^{-/-} with heterozygotes littermates or following a cross of heterozygote (C57BL/6.Gpr55^{+/-} x C57BL/6.Gpr55^{+/-}) mice. These were injected with MOG35-55 peptide in Freund's adjuvant. Results indicated that GPR55 knockout mice failed to generate an autoimmune response suggesting that GPR55 controls immune function (Figure 6.6, Table 6.1). The low susceptibility was also observed in additional experiments (n=4). There was a consistent lack of susceptibility in knockout animals but in some experiments the control groups failed to develop disease. The incidence and severity of disease was significantly reduced in the C56BL/6.GPR55^{-/-} knockout mice. *P<0.05

Figure 6.6 *Experimental autoimmune encephalomyelitis*



C56BL/6.Gpr55 knockout and heterozygous female littermates were immunized with MOG peptide in Freund's adjuvant on day 0 and 7 and were injected with 200ng of *B.pertussis* toxin on day 0 and 1. Animals were scored 0 = normal 1= limptail, 2= impaired righting reflex, 3= paresis and 4= complete hindlimb paralysis. The results represent the mean daily clinical score of animal ± SEM. n= 8-10 animals per group. Experiments were performed in collaboration with Dr. Gareth Pryce.

Table 6.1 *Function of GPR55 in Neuroinflammation-C57BL/6 mice*

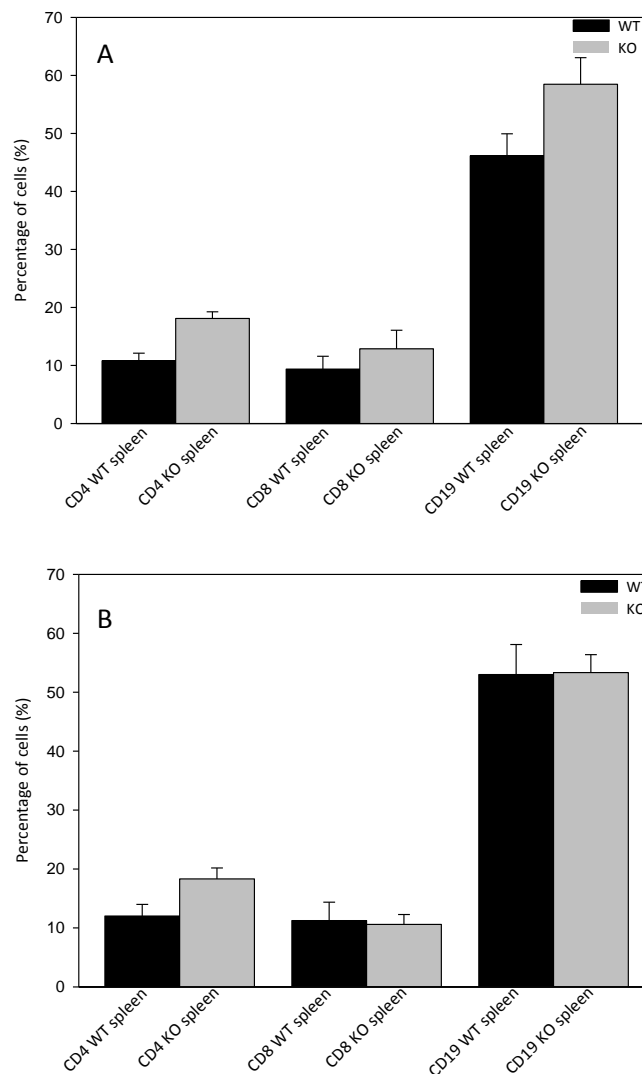
Mice	No. EAE	Mean EAE	Group Score \pm SEM	EAE Score \pm SEM	Day of Onset \pm SD
			All animals	Animals with Disease	
GPR55 ^{-/-} : Females	2/8		1.0 \pm 0.7	4.0 \pm 0.0	15 \pm 1.9
GPR55 ^{-/-} : Males	4/6		2.5 \pm 0.8	3.8 \pm 0.8	18 \pm 1.9
GPR55 ^{+/-} : Females	7/7		2.8 \pm 0.4	2.8 \pm 0.4	16 \pm 1.6
GPR55 ^{+/-} : Males	4/6		2.5 \pm 0.8	3.6 \pm 0.1	16 \pm 1.2
GPR55 ^{+/+} : Females	4/5		3.0 \pm 0.8	4.0 \pm 0.0	16 \pm 0.5
GPR55 ^{+/+} : Males	5/6		3.4 \pm 0.7	4.0 \pm 0.0	15 \pm 0.8

EAE was induced in GPR55 knockout (C57BL/6.GPR55^{-/-}), heterozygote (C57BL/6.GPR55^{+/-}) and wildtype (C57BL/6.GPR55^{+/+}) mice. These were immunized with MOG 35-55 peptide in Freund's adjuvant on day 0 and 7 and were injected with 200ng of *B.pertussis* toxin on day 0 and 1. Animals were scored 0 = normal 1= limptail, 2= impaired righting reflex, 3= paresis and 4= complete hindlimb paralysis. The results represent The mean maximum score for all animals within the group or the (EAE score) animals that got EAE n= 5-8 animals per groups. Experiments were performed in collaboration with Dr. Gareth Pryce.

6.2.7 Immunophenotypes (MOG 35-55 peptide stimulated T- and B-cells in spleen)

Immunophenotyping of naïve animals was previously done (Figure 6.1) and due to the observed reduced disease in the GPR55 (C57BL/6) knockout mice we decided to investigate the immunophenotypes post MOG stimulation. The immunophenotypes (T- and B-cells) of MOG 35-55 peptide stimulated GPR55 KO mouse lymphocytes in spleen were compared with wild-type littermates in order to investigate potential differences. Analysis was performed by flow cytometry. Results displayed no significant difference between the two strains.

Figure 6.7 Immunophenotyping of spleen cells from *in vivo* and/or *in vitro* MOG stimulated C57BL/6.GPR55^{-/-} and C57BL/6^{+/+} mice



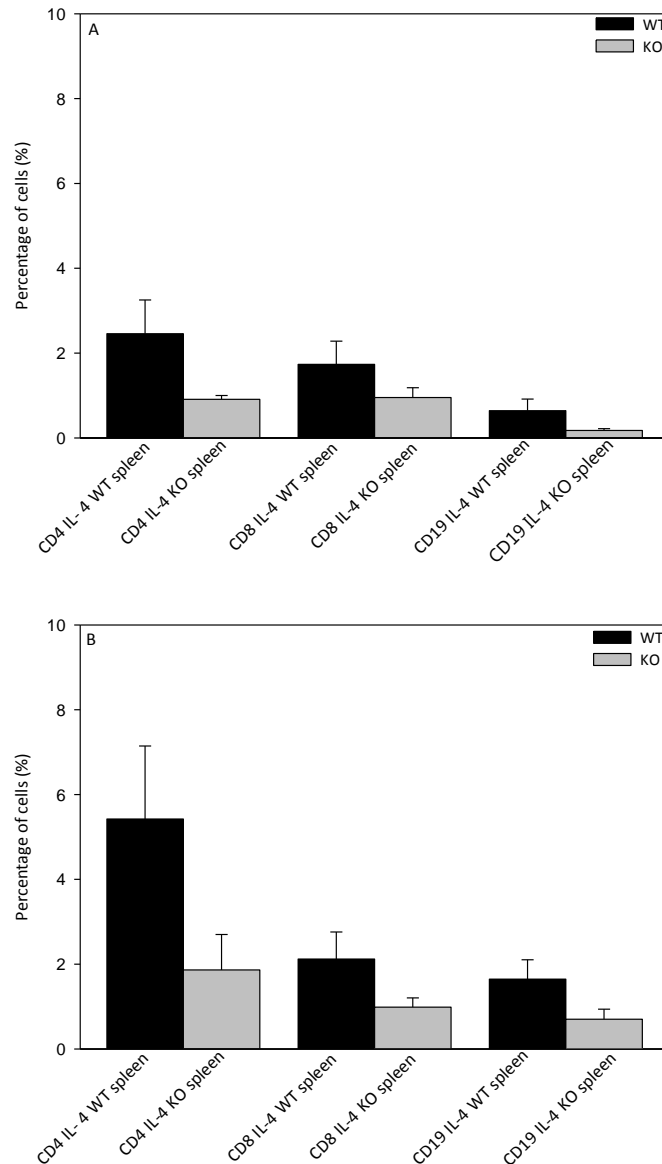
In vivo (A) and *in vitro* re-stimulated (10µg/ml) (B) MOG stimulated GPR55 knockout (C57BL/6.GPR55^{-/-}) and wild-type (C57BL/6^{+/+}) littermates were used for immunophenotyping. Leukocytes from spleen were collected and the cells were stained with various surface antibodies (T-cells CD4, CD8 and B-cells CD19) diluted 1:100. Samples were then read on a LSRII flow cytometer (Becton Dickinson, Oxford, UK).

6.2.8 IL-4 cytokine responses

The IL-4 cytokine response in T- and B-cells from MOG 35-55 peptide stimulated GPR55 KO mouse lymphocytes in spleen were compared with wild-type littermates in order to investigate potential differences. Analysis was performed by flow cytometry. Results displayed no significant difference between the two strains.

Figure 6.8 IL-4 cytokine responses in T- and B-cells from MOG stimulated *C57BL/6.GPR55^{-/-}* and

C57BL/6^{+/+} mice

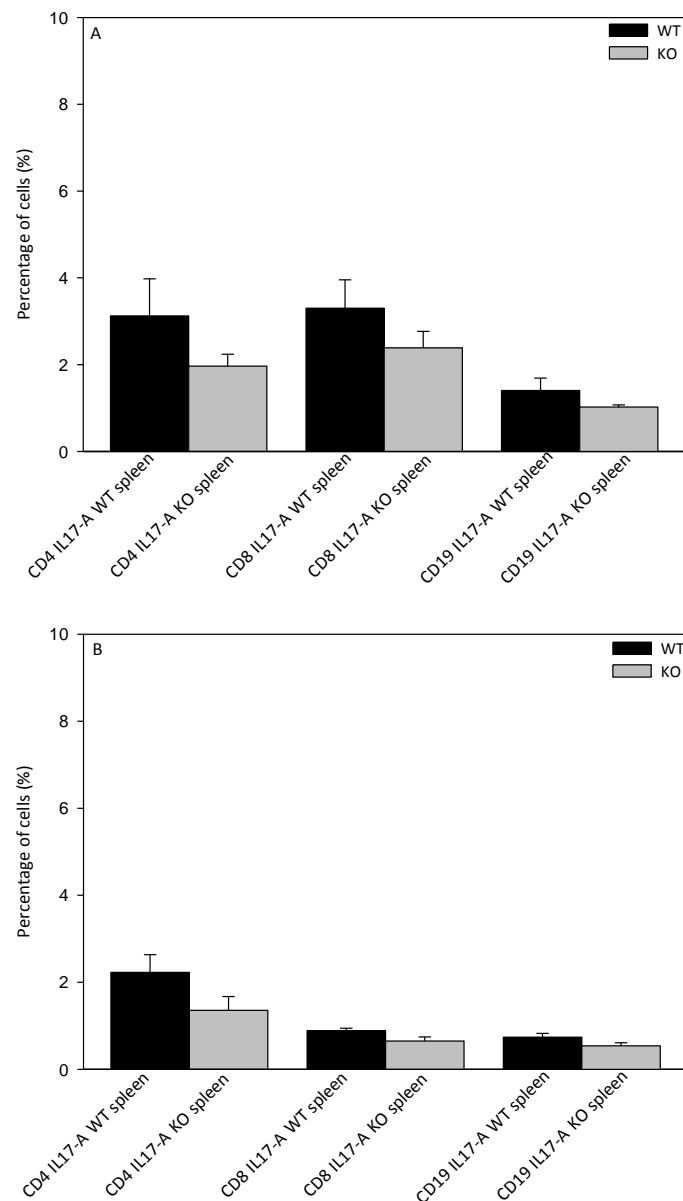


In vivo (A) and *in vitro* (10 μ g/ml) (B) MOG stimulated GPR55 knockout (*C57BL/6.GPR55^{-/-}*) and wild-type (*C57BL/6^{+/+}*) littermates were used for cytokine profiling. Lymphocytes from spleen were collected and the cells were stained with various surface antibodies/ T-cells markers CD4, CD8, CD19 and cytokine marker IL-4 diluted 1:100. Samples were then read on a LSRII flow cytometer (Becton Dickinson, Oxford, UK).

6.2.9 IL-17A cytokine responses

The IL-17A cytokine response in T- and B-cells from MOG 35-55 peptide stimulated GPR55 KO mouse lymphocytes in spleen were compared with wild-type littermates in order to investigate potential differences. Analysis was performed by flow cytometry. Results displayed no significant difference between the two strains.

Figure 6.9 IL-17A cytokine responses in T- and B-cells from MOG stimulated C57BL/6.GPR55^{-/-} and C57BL/6^{+/+} mice



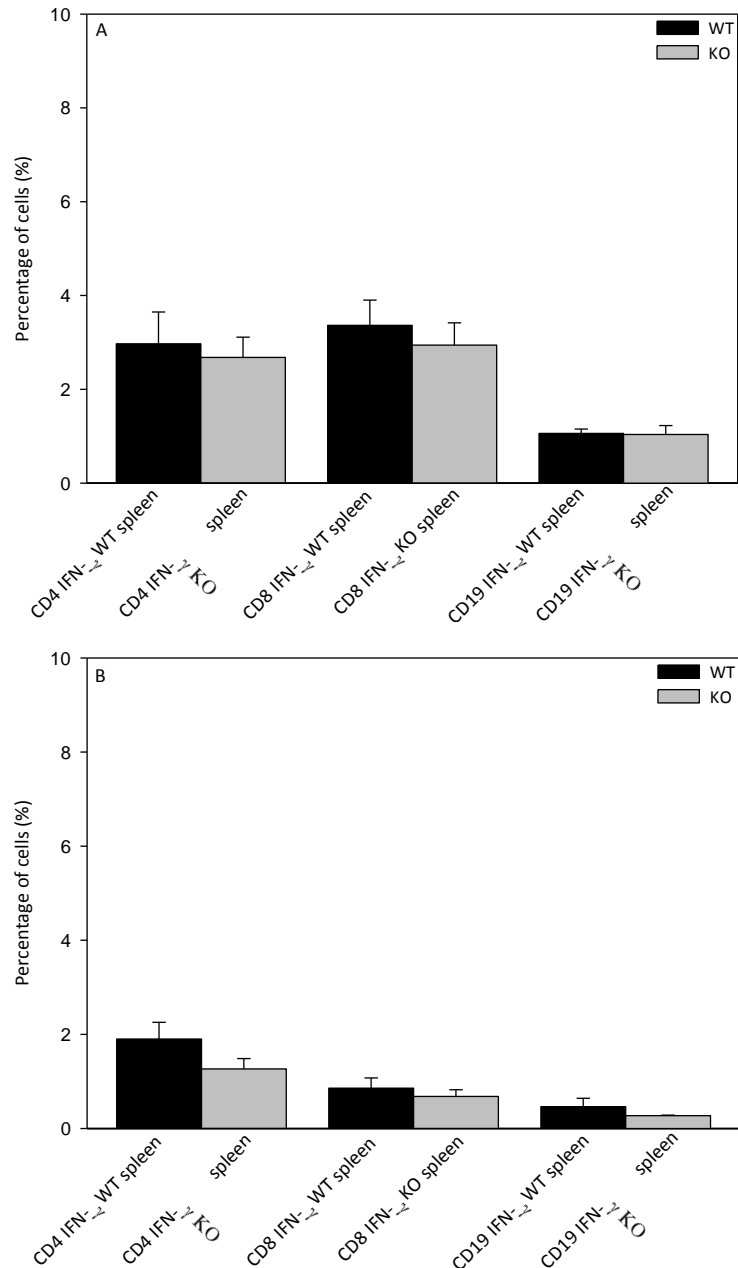
In vivo (A) and *in vitro* (10 μ g/ml) (B) MOG stimulated GPR55 knockout (C57BL/6.GPR55^{-/-}) and wild-type (C57BL/6^{+/+}) littermates were used for cytokine profiling. Leukocytes from spleen were collected and the cells were stained with various surface antibodies/ T-cells markers CD4, CD8, CD19 and cytokine marker and IL-17A diluted 1:100. Samples were then read on a LSRII flow cytometer (Becton Dickinson, Oxford, UK).

6.2.10 IFN- γ cytokine responses

The IFN- γ cytokine response in T- and B-cells from MOG 35-55 peptide stimulated GPR55 KO mouse lymphocytes in spleen were compared with wild-type littermates in order to investigate potential differences. Analysis was performed by flow cytometry. Results displayed no significant difference between the two strains.

Figure 6.10 IFN- γ cytokine responses in T- and B-cells from MOG stimulated C57BL/6.GPR55^{-/-} and

C57BL/6^{+/+} mice

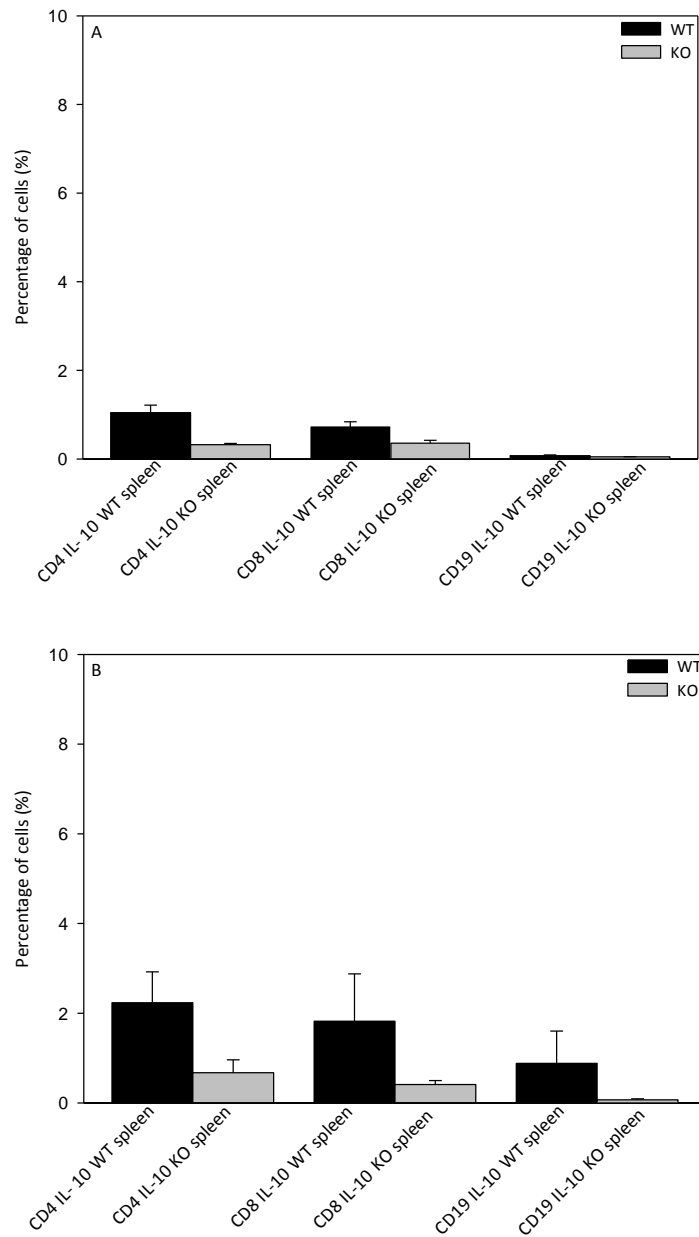


In vivo (A) and *in vitro* (10 μ g/ml) (B) MOG stimulated GPR55 knockout (C57BL/6.GPR55^{-/-}) and wildtype (C57BL/6^{+/+}) littermates were used for cytokine profiling. Leukocytes from spleen were collected and the cells were stained with various surface antibodies / T-cells markers CD4, CD8, CD19 and cytokine marker IFN- γ) diluted 1:100. Samples were then read on a LSRII flow cytometer (Becton Dickinson, Oxford, UK).

6.2.11 IL-10 cytokine responses

The IL-10 cytokine response in T- and B-cells from MOG 35-55 peptide stimulated GPR55 KO mouse lymphocytes in spleen were compared with wild-type littermates in order to investigate potential differences. Analysis was performed by flow cytometry. Results displayed no significant difference between the two strains.

Figure 6.11 IL-10 cytokine responses in T- and B-cells from MOG stimulated C57BL/6.GPR55^{-/-} and C57BL/6^{+/+} mice



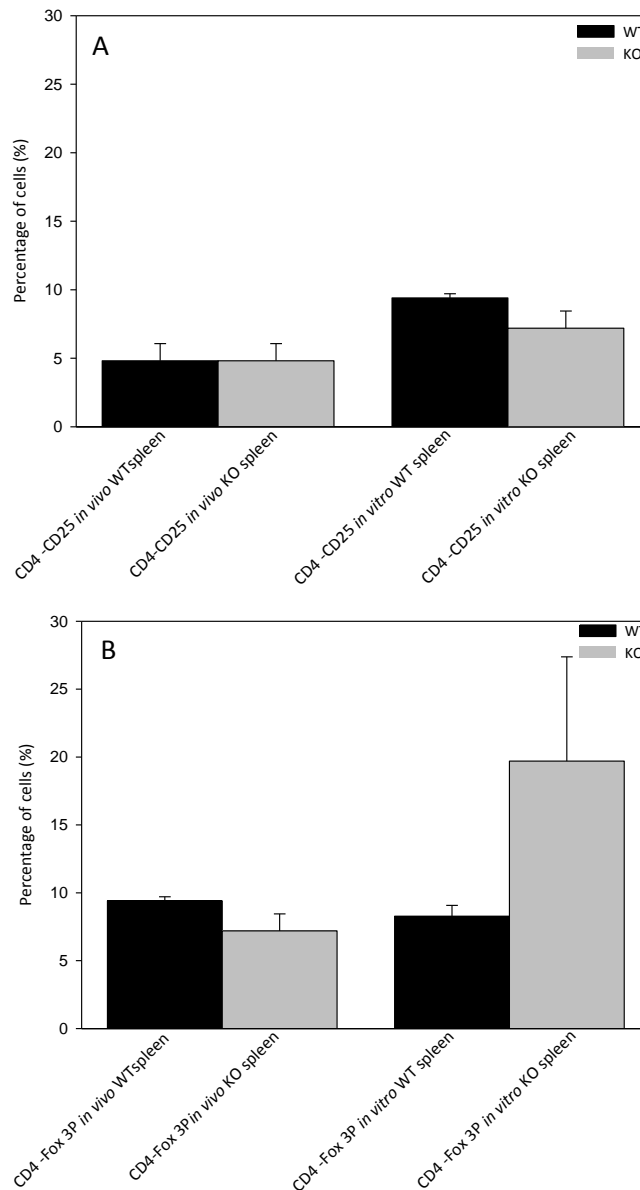
In vivo (A) and *in vitro* (10µg/ml) (B) MOG stimulated GPR55 knockout (C57BL/6.GPR55^{-/-}) and wildtype (C57BL/6^{+/+}) littermates were used for cytokine profiling. Leukocytes from spleen were collected and the cells were stained with various surface antibodies/ T-cells markers CD4, CD8, CD19 and cytokine marker IL-10 diluted 1:100. Samples were then read on a LSRII flow cytometer (Becton Dickinson, Oxford, UK).

6.2.12 Fox3P responses

The Fox3P responses in T- and B-cells from MOG 35-55 peptide stimulated GPR55 KO mouse lymphocytes in spleen were compared with wild-type littermates in order to investigate potential differences. The CD4 +FoxP3+CD25 markers were used to analyze regulatory T cells. Analysis was performed by flow cytometry. Results displayed no statistical significant difference between the two strains.

Figure 6.12 Fox 3P responses in T- and B-cells from MOG stimulated C57BL/6.GPR55^{-/-} and

C57BL/6^{+/+} mice

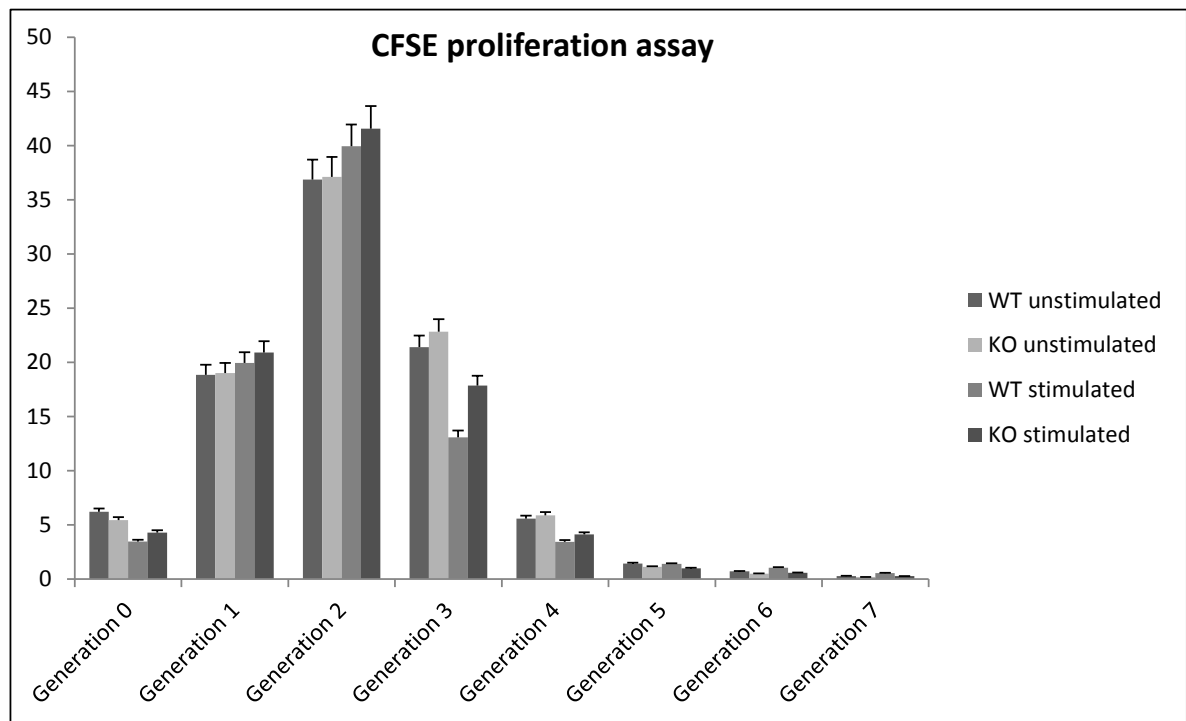


In vivo and *in vitro* (10µg/ml) MOG stimulated GPR55 knockout (C57BL/6.GPR55^{-/-}) and wild-type (C57BL/6^{+/+}) littermates were used for (A) CD4-CD25 and (B) CD4-Fox3P staining. Leukocytes from spleen were collected and the cells were stained with various surface antibodies CD4, CD25, and Fox3P diluted 1:100. Samples were then read on a LSRII flow cytometer (Becton Dickinson, Oxford, UK).

6.2.13 CFSE proliferation assay

Lymphocytes (spleen) from GPR55 KO mice and wild-type littermates were isolated and stimulated with MOG 35-55 peptide *in vivo* and re-stimulated *in vitro*. Proliferation was seen in both *in vivo* and in *in vitro* re-stimulated cells however no significant difference was seen between both groups. Also, proliferation did not differ when comparing lymphocytes from WT with knockout animals.

Figure 6.13 CFSE proliferation assay

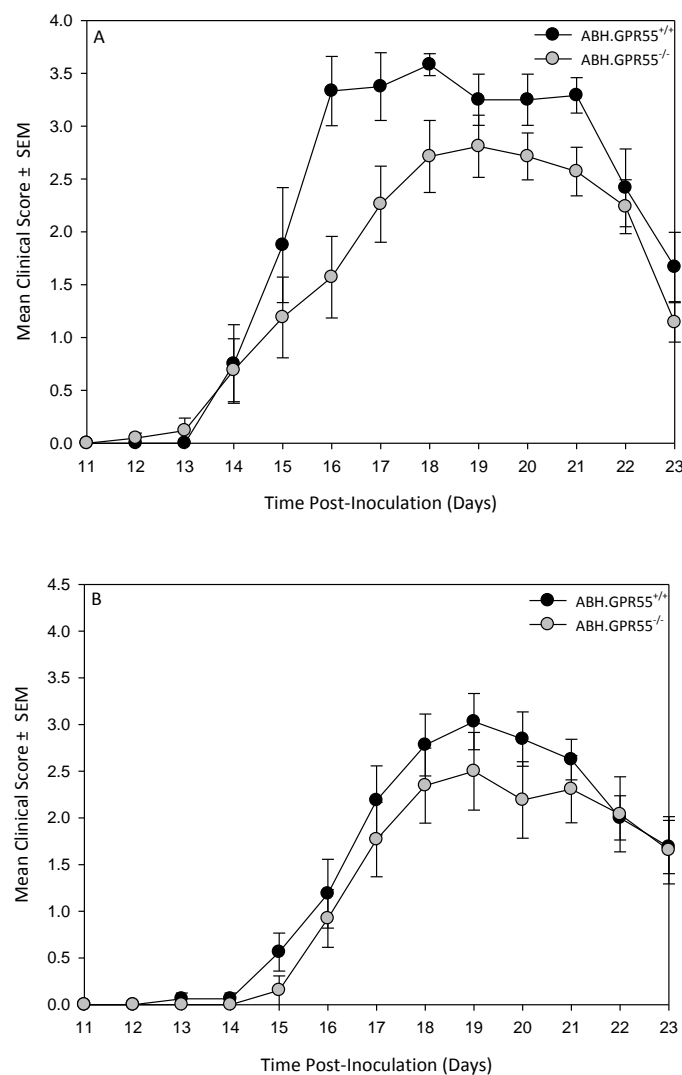


C56BL/6.*Gpr55* knockout and heterozygous littermates were immunized with MOG peptide 35-55 in Freund's adjuvant on day 0 and were injected with 200ng of *B. pertussis* toxin on day 0 and 1. Lymphocytes were collected on day 9 and left either unstimulated or were re-stimulated *in vitro* with MOG peptide at a concentrations of 10µg/mg for 72h. Lymphocytes were stained with CFSE (5µm) and incubated at 37°C for 4 days. Samples were then read on a LSRII flow cytometer (Becton Dickinson, Oxford, UK).

6.2.14 Function of GPR55 during experimental autoimmune encephalomyelitis in ABH mice

ABH.GPR55^{-/-} congenic mice were generated following a cross of GPR55 knockout mice on the C57BL/6 background (C57BL6.GPR55^{-/-}) with ABH wild-type mice for more than 11 generations. These were injected with spinal cord homogenate in Freund's adjuvant. The severity of the disease was marginally reduced in the GPR55 knockout mice on the ABH background during the acute phase particularly when comparing the female groups (Figure 6.14A: *females*; Figure 6.14B: *males* and Table 6.2).

Figure 6.14 *Experimental autoimmune encephalomyelitis in ABH mice*

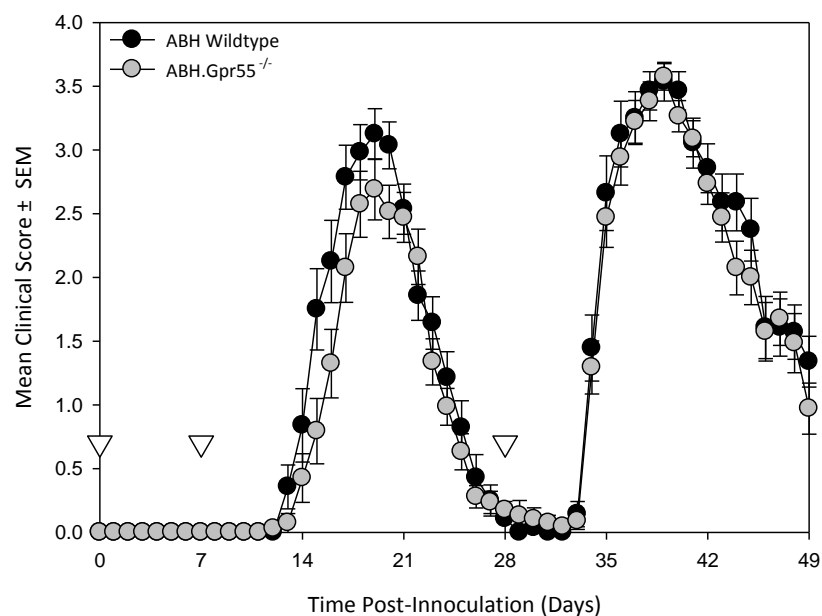


Males and female ABH.GPR55^{-/-} knockout and wild-type littermates were immunized with spinal cord homogenate in Freund's adjuvant on day 0 and 7. Animals were scored 0 = normal 1= limptail, 2= impaired righting reflex, 3= paresis and 4= complete hind limb paralysis. The results represent the mean daily clinical score of animal ± SEM. n= 8-10 animals per groups.

6.2.15 Function of GPR55 during relapse remitting EAE in ABH animals

The initial acute phase of disease is largely inflammatory, without much demyelination or axonal damage. However, relapsing disease is associated with greater neurological damage, which allows neuroprotective effects to be monitored (Al-Izki et al. 2012). EAE induced in ABH mice were monitored for more than 50 days. As noted results showed a marginally reduced disease during first attack (Figure 6.14, 6.15) however, this difference was not seen during the first relapse.

Figure 6.15 *Relapse remitting experimental autoimmune encephalomyelitis*



Male and female ABH.GPR55^{-/-} knockout (n=34) and wild-type littermates (n=28) were immunized with spinal cord homogenate in Freund's adjuvant on day 0 and 7 and day 28 (inverse triangles). Animals were scored 0 = normal 1= limptail, 2= impaired righting reflex, 3= paresis and 4= complete hindlimb paralysis and 5= moribund/death. The results represent the mean daily clinical score of animal ± SEM.

Table 6.2 *Function of GPR55 in Neuroinflammation in ABH mice*

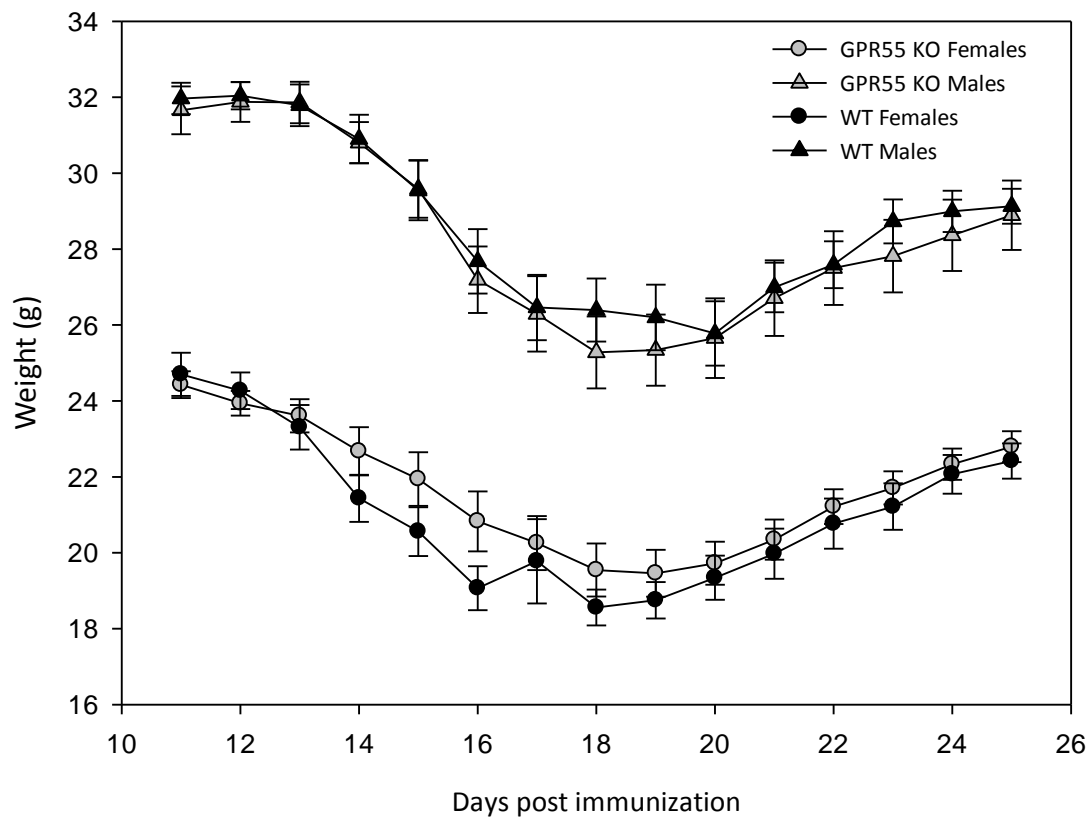
Mice	EAE/Total No°	EAE Group acute Score \pm SEM	EAE 1 st relapse Score \pm SEM	Day of Onset \pm SD
Initial Acute Phase				
GPR55 ^{-/-} : Females	21/21	3.1 \pm 0.2*	3.1 \pm 0.2*	16.6 \pm 2.4
GPR55 ^{-/-} : Males	12/13	3.2 \pm 0.3	3.5 \pm 0.1	17.1 \pm 0.2
GPR55 ^{+/+} : Females	12/12	3.8 \pm 0.1	3.8 \pm 0.0	15.2 \pm 1.2
GPR55 ^{+/+} : Males	16/16	3.6 \pm 0.1	3.6 \pm 0.1	16.6 \pm 2.2
Induced Relapse				
GPR55 ^{-/-} : Females	21/21	3.8 \pm 0.1	3.8 \pm 0.1	34.8 \pm 1.0
GPR55 ^{-/-} : Males	13/13	3.7 \pm 0.2	3.7 \pm 0.2	34.7 \pm 1.4
GPR55 ^{+/+} : Females	12/12	3.9 \pm 0.1	3.9 \pm 0.1	35.4 \pm 1.3
GPR55 ^{+/+} : Males	16/16	3.9 \pm 0.1	3.9 \pm 0.1	34.9 \pm 1.4

EAE was induced in ABH.GPR55^{-/-} knockout mice and wildtype littermates. These were immunized with spinal cord homogenate in Freund's adjuvant on day 0 and 7 and a relapse was induced by a further injection on day 28. Animals were scored 0 = normal 1= limptail, 2= impaired righting reflex, 3= paresis and 4= complete hindlimb paralysis, 5= moribund/death. The results represent disease incidence, the mean maximal clinical scores animals \pm SEM of all animals in the group, the mean maximal score \pm SEM of all animals that developed EAE and the day of onset \pm SD. * P<0.05 compared to wildtype littermates.

6.2.16 Weight losses and function of GPR55 during relapse remitting EAE in ABH animals

Although the severity of the acute disease was marginal it was not statistically significantly reduced in the GPR55 knockout mice on the ABH background (Figure 6.14; Table 6.2), this observation was however not reflected by significant weight differences (Figure 6.16). This showed a clear sexual dimorphism with males heavier than females however there was no influence of the genotype.

Figure 6.16 EAE- weight losses in ABH mice

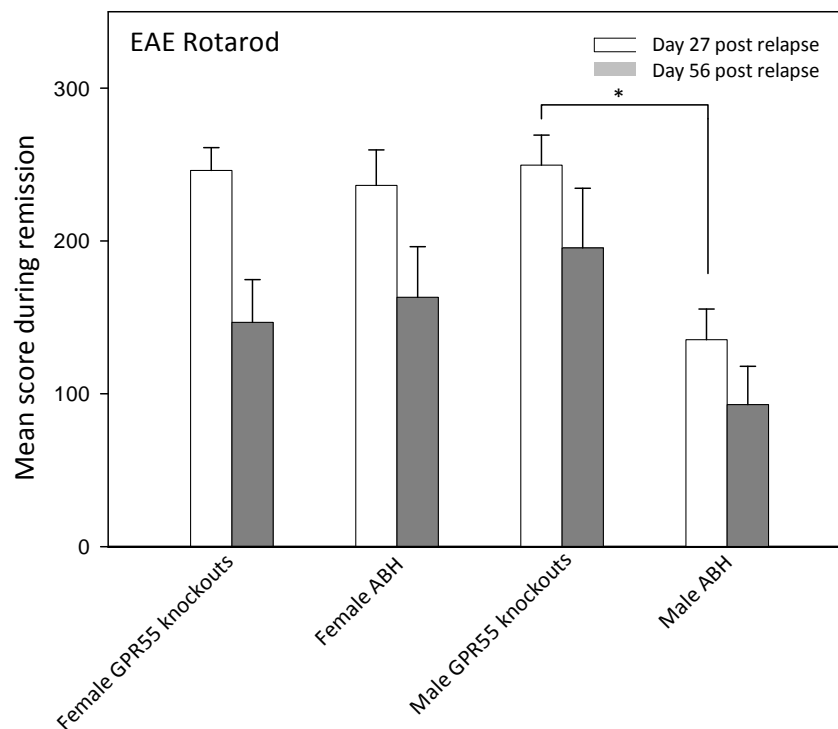


EAE was induced in ABH.GPR55^{-/-} knockout mice and wild-type littermates. These were immunized with spinal cord homogenate in Freund's adjuvant on day 0 and 7. Animals were weighed from day 10. The results represent the mean \pm SEM daily weight

6.2.17 Measurement of motor performance in relapsing EAE in ABH mice

The Accelerating Rotarod treadmill was used to assess the motor control and coordination in both strains. Assessment was done during the remission phases of the disease, over a maximum 5 minute observation period. The first assessment was done on day 27 after animals had recovered from the initial attack. Following the development of acute disease a relapse was induced to determine whether significant disability indicative of nerve loss (Al-Izki *et al.*, 2012) would be observed. Second assessment was done on day 56 post first relapse. It was found that there was no statistical significant difference in the incidence of relapse or maximum severity of relapse (Figure 6.15). When comparing female GPR55 knockout females with wild-type littermates there was no difference observed. However, when comparing GPR55 knockout males with wild-type males it was found that the wild-type males had statistically significant ($P < 0.05$) reduced motor coordination after acute attack. Wild-type males also showed a trend toward significant motor deficit after first relapse (Figure 6.17).

Figure 6.17 Neurological deficits in ABH mice



EAE was induced with spinal cord homogenate in Freund's adjuvant in ABH mice on day 0 and 7. Animals were allowed to undergo an acute phase inflammatory attack and relapse was induced by re-immunization with spinal cord homogenate in Freund's adjuvant at day 28. Motor co-ordination was assessed by an accelerating Rotarod performance measurement post-acute phase in remission at day 27 and post-1st relapse in remission phase at day 56.

6.3 Discussion

The results of this study suggest that there may be some immune deficit, particularly in female C57BL/6 mice in relation to the development of EAE. However, analysis of the thymus, lymph nodes and T and B cell numbers and function did not reveal the nature of the defect. In these experiments there was essentially no antigen-specific T cell proliferation detected when cells were stimulated with MOG 35-55 peptide *in vitro*. It has previously been reported that peptides that induce pathogenic response often give a non-existent T cell proliferative response (Amor *et al.*, 1993; Heijmans *et al.*, 2005). However, MOG peptide induced responses have been reported in many studies (Graham *et al.*, 2010; Heijmans *et al.*, 2005; Issazadeh *et al.*, 2000). The lack of responses therefore probably relates to the inconsistent level of sensitization as shown by the inconsistent induction of EAE. The immunophenotype in C57BL/6.GPR55^{-/-} may also have contributed to the difficulties in generating monoclonal antibodies (chapter 4).

C57BL/6.GPR55^{-/-} knockout and C57BL/6^{+/+} wild-type mice were initially immunophenotyped and there was no obvious difference in the immunophenotype in naïve animals and there was no significant difference in the T cell proliferative response to MOG or Con A mitogenic stimulation. C57BL/6.GPR55^{-/-} knockout and C57BL/6^{+/+} wild-type mice were also immunophenotyped post MOG *in vivo* stimulation and *in vitro* re-stimulation and no significant differences were observed when comparing the two strains.

C57BL/6^{+/+} wildtype and C57BL/6.GPR55^{-/-} knockout mice were injected with MOG35-55 peptide in Freund's adjuvant in order to induce EAE. The disease was markedly reduced in the GPR55 knockout mice on the C57BL/6 mice suggesting that GPR55 controls immune function. This would suggest that GPR55 antagonism would be anti-inflammatory, however it has been reported that the non-selective GPR55 agonist O-1602 modulates the inflammatory response in a number of conditions (Li *et al.*, 2013; Lin *et al.*, 2011; Schicho *et al.*, 2012). However, O-1602 may act on GPR18 which is expressed by immune cells (McHugh 2012) as the ligand has also been reported to be a GPR18 agonist (Caldwell *et al.*, 2013). Although the low susceptibility was consistently observed in two additional experiments one of the difficulties with EAE in C57BL/6 mice is that the disease in controls is variable and the severity of disease may be high or low dependent on the experiment (Axtell *et al.* 2011 (Coquet *et al.*, 2013)). As such in two experiments the wildtype controls likewise failed, as found in the GPR55 knockout animals, to get disease and thus failed quality control that justifies analysing data from these failures. When the sexes were compared it seemed that females were marginally less susceptible than males. This would suggest some sex hormone influence on the immune response.

To eliminate the influence of low grade disease induction associated with MOG-induced disease in C57BL/6 mice GPR55 knockout mice were generated on the ABH background as this strain gives consistent disease incidence and severity (Baker et al. 1990, Al-Izki et al. 2012). Knockout mice were generated following a cross of GPR55 knockout mice on the C57BL/6 background (C57BL6.GPR55^{-/-}) x (ABH^{+/+}) with ABH wildtype mice. EAE was induced in the animals by injections with spinal cord homogenate in Freund's adjuvant. Although a marginally lower susceptibility remained in the GPR55 knockout (ABH.GPR55^{-/-}) mice compared to wild-type littermates this difference was not as obvious as on the C57BL/6 background. The lower susceptibility was mainly observed in the first attack and the incidence and severity of disease increased and no significant differences between the two strains were observed in the first relapse (Figure 6.14). This observed disease susceptibility differences may be due to differences in strain backgrounds therefore the lower susceptibility might be due to minor influences of GPR55 receptor. This study demonstrates that the influence of GPR55 is largely dependent on the genetic background of the mouse and when on a fully EAE susceptible background GPR55 exhibits minor influence. Similar effects have been noted with CB₂ receptor where Cnr2-deficiency leads to enhanced susceptibility in C57BL/6 background mice (Maresz et al., 2007; Palazuelos et al., 2008). However, on the ABH background the influence of CB₂ deficiency is lost and CB₂ agonists exhibit no influence on EAE susceptibility (Croxford et al., 2008) (G.Pryce unpublished observations). This is lack of immune phenotype is also apparent in differences between ABH.CB₁ and C57BL/6.CB₁ deficient mice (Pryce et al. 2003, Rossi et al. 2011) and ABH.Trpv1 and C57BL/6.Trpv1 knockout mice (Pryce 2010, Musumeci et al 2010) As most EAE studies uses gene knockout animals on the C57BL/6 background it is of concern that many studies may not translate even to other mouse strains. The chances of this then translating to humans is unlikely. This may be a further reason for the failure to translate treatments of rodent EAE to human benefit (Vesterinen et al., 2010). Therefore many treatments are essentially tried in one individual inbred mouse strain, which may not be the typical response of the outbred population. The difference found in the C57BL/6 may be as much to do with the inconsistent disease susceptibility and the influence of the transgene therefore it is important that disease the susceptible in the control group is stable. As such it is often the case that when a transgene enhances EAE susceptibility the control group shows weak EAE (Bettelli et al., 2003; Elhofy et al., 2005) and when the transgene inhibits EAE the susceptibility of the control group is strong (Das et al., 2000; Sinha et al., 2011). The level of susceptibility in spinal cord-induced EAE has remained consistent over many years (Baker et al., 1990; Al-izki et al., 2012).

Both strains also had comparable weight losses. A Rotarod treadmill was used to assess the motor control and coordination in both strains. No significant difference was observed when comparing

both female groups (ABH^{+/+}, ABH.GPR55^{-/-}). ABH wild-type males were found to be the most neurologically impaired in comparison to the different groups. Although a statistical difference was observed after the initial attack there was no statistical difference after the first relapse even though the ABH wild-type male performance was reduced overall compared to all the other groups on both days. Likewise it has been found that males are more likely to develop progressive neurodegeneration after onset (Runmarker *et al.*, 1993). Recently it has been reported that GPR55 knockout mice exhibit significant motor coordination deficits compared to wild-type littermates (Wu *et al.*, 2013). This view is not supported by our studies where no differences in Rotarod performance were observed when comparing GPR55 knockout females with wild-type females. In our studies GPR55 knockout males performed better than wild-type males in the Rotarod motor co-ordination test.

CHAPTER 7

Spasticity

7.1 Introduction

The cannabinoid system has been demonstrated to exhibit tonic control of spasticity using EAE models of MS (Baker *et al.*, 2001). The phytocannabinoid THC and CB₁ receptor have been reported to act as important mediators for the control of spasticity by cannabis (Pryce *et al.*, 2007; Wilkinson *et al.*, 2003). The use of THC is associated with unwanted, psychotropic effects of cannabis due to CB₁ receptor stimulation in certain cognitive-control centres in the brain (Howlett *et al.*, 2002; Varvel *et al.*, 2005). Cannabis therefore has a small therapeutic window in spasticity because THC and CB₁ receptors mediate both the therapeutic and adverse effects of cannabis (Pryce *et al.*, 2007; Varvel *et al.*, 2005). Although disease symptoms of MS are generated by lesions within the CNS aberrant neurotransmission must traverse the peripheral nervous system and neuromuscular junction to cause spasticity (Baker *et al.*, 2012). Likewise sensory and positional signals must be transmitted back to the CNS through synapses expressing CB₁ receptors (Baker *et al.*, 2012). Spasticity results from lack of inhibition of excessive neurotransmission in the CNS, resulting in excessive contraction of muscles. It was hypothesised it may be possible to maintain therapeutic activity, whilst limiting psychoactive potential (Baker *et al.*, 2012; Pryce, 2010). It was believed altered neurotransmission could be controlled between muscles and the spinal cords by targeting CB₁ in peripheral sensory and motor pathways (Baker *et al.*, 2012). In attempt to generate CNS-excluded CB₁ receptor agonists, VSN16 series compounds were made (Hoi *et al.*, 2006), based around some cyclic anandamide compounds (Berglund *et al.*, 1998; Tong *et al.*, 1998). These were found to be anti-spastic but had a mechanism of action that was independent of CB₁ receptor (Hoi *et al.*, 2006; Pryce, 2010). The presence of novel cannabinoid receptor(s) in the vasculature has been suggested by many studies (White *et al.*, 1997). In a recent study, anandamide showed to cause vasorelaxation that is sensitive to rimonabant and is insensitive to PTX, suggesting a non-CB₁ receptor-mediated vasorelaxation (White *et al.*, 1997). VSN16R has also shown to relax rat mesenteric arteries in an endothelium-dependent manner, via a PTX-insensitive mechanisms (Hoi *et al.*, 2006). Importantly the vasorelaxation induced by VSN16R was reduced by rimonabant, AM251 and O-1918 which were reported to influence GPR55 function (Baker *et al.*, 2006b; Hoi *et al.*, 2007a; Ryberg *et al.*, 2007). In addition, the mechanism of action was found to be CB₁ receptor-independent and VSN16R failed to bind or agonise to the CB₁ cannabinoid receptor when tested up to 300µM (Pryce, 2010).

These molecules may also influence the abnormal cannabidiol receptor, thought to be GPR18, however activation of this receptor is reported to be PTX-sensitive (Kohn *et al.*, 2006). GPR55 has been reported to be expressed in dorsal root ganglion (Lauckner *et al.*, 2008) and has a reported influence on neurotransmission (Lauckner *et al.*, 2008; Staton *et al.*, 2008; Sylantyev *et al.*, 2013). It has been suggested that VSN16R may act via GPR55 (Hoi *et al.*, 2007b; Pryce *et al.*, 2007). Whilst VSN16R had a pharmacological influence on GPR55 function, it was important to determine to what extent GPR55 was involved in the control of spasticity. Having established a method to generate EAE-susceptible mice that could develop EAE, it was hypothesised that GPR55 would be the mediator of the therapeutic action of VSN16 in spasticity.

7.2 Results

7.2.1 VSN16- a water soluble compound without cannabimimetic effects in the CNS

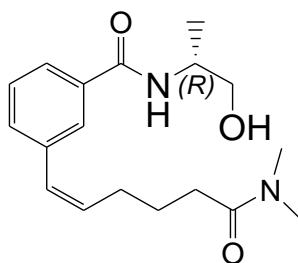
VSN16R (Figure 7.1, Table 7.1) is a water soluble (>30mg/ml) compound that can cause sympathetic muscular relaxation in the vas deferens (Table 7.1) at a dose of 1mg/kg i.v. (Pryce, 2010). This failed to induce any obvious cannabimimetic effects including the visible sedative effects, or motor outcomes such as hypomotility or resultant hypothermic responses, in contrast to that observed following administration of CNS-penetrant cannabinoid receptor agonists or high doses of the GABA_B-agonist (Pryce, 2010). 5mg/kg i.v. VSN16R induced comparable level of control of spasticity as found following administration of baclofen or the botanical drug substances found in Sativex (Figure 7.2), but did not induce sedative effects as found with administration of baclofen and Sativex® as reported previously (Hilliard *et al.*, 2012). Previous studies demonstrated that VSN16 is orally bioavailable (about 30%) with a C_{max} within 15 minutes of administration (Pryce, 2010). Doses of 40mg/kg p.o. for 24 days were well tolerated (Pryce, 2010). Following administration of 100mg/kg, 500mg/kg and 1000mg/kg p.o. there were no obvious abnormal behavioral responses of animals. Mice appeared alert and mobile during an observation period for up to 2h following drug administration. There was no evidence of immobility when assessed visually and the temperature of mice receiving 1g/kg was 37.5°C ± 0.4 (n =3) 90 minutes after drug administration. This was within the normal range and was consistent with lack of a hypomotile phenotype. There was no evidence of toxicity of VSN16R as shown by no weight loss following 5 daily treatments (Table 7.2). There was however a significant (P<0.05) weight gain (growth) of mice treated with both 100mg/kg and 500mg/kg p.o. by the fifth day of treatment (Day 4) compared to baseline (Day 0), which only appeared to occur in 1/3 mice treated with 1000mg/kg p.o. However there was no significant difference in the weight of mice treated with either 1g/kg or 0.1g/kg VSN16R at the start (29.0 ± 2.0g vs. 27.7 ± 0.6g. p=0.33) or end (30.2 ± 1.1g vs. 31.1 ± 0.5g. p=0.26) of treatment (Pryce, 2010).

VSN16R was found to be orally active and whilst 0.5mg/kg p.o. administered in water failed to inhibit spasticity in EAE. It was however found that 5mg/kg p.o. and 40mg/kg p.o. inhibited spasticity (Pryce, 2010). In an attempt to generate more additional therapeutically active compounds, following analysis of the original series of compounds (Hoi *et al.*, 2007b; Pryce, 2010), more compounds were synthesised by Prof D.L. Selwood (Figure 7.1). These included VSN17 enantiomers and VSN40R (Figure 7.1, Table 7.1). It was found that VSN16R, VSN16S, VSN17R and

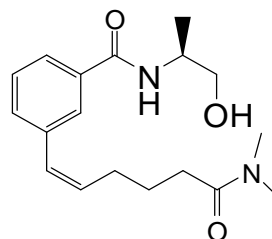
VSN17S and VSN40R all had potent activity in the low nM range in relaxation of mouse vas deferens with VSN16R being the most potent (EC_{50} = around 10nM (Table 7.1). VSN16R is about 85% CNS excluded (Pryce, 2010) and it was therefore of interest that VSN40R was as potent in the vas deferens assay (Table 7.1), but had a CLogP, which is logarithm of its partition coefficient between n-octanol and water as a marker of lipophilicity, of 3.5 that would suggest the potential for entry into the CNS. However, upon *in vitro* estimation of pharmacokinetic potential, it was found that VSN40R was rapidly metabolised by liver cells, which indicated it would have limited merit in investigating this compound *in vivo* (Table 7.1). It was therefore not studied further. However, it was found that VSN16R, VSN16S and VSN17R and VSN17S were sufficiently metabolically stable *in vitro* (Table 7.1). As there were insufficient animals to perform extensive dose-response studies, an oral dose of 10mg/kg was arbitrarily selected for initial studies using oral delivery of agents. This was based on doses that were active with VSN16R and their *in vitro* pharmacokinetics (Table 7.1).

Figure 7.1 Chemical structure of VSN series compounds

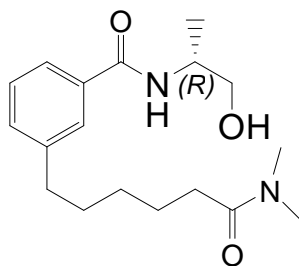
VSN16R



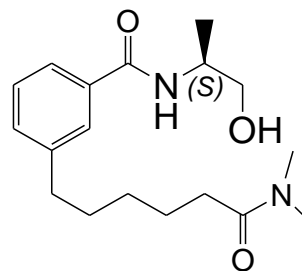
VSN16S



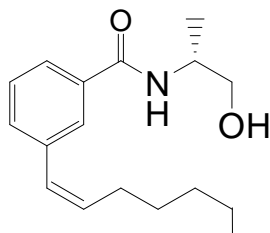
VSN17R



VSN17S



VSN40R



VSN44R

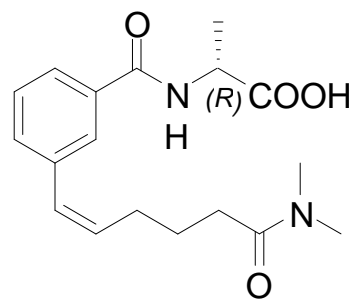


Table 7.1 *Physiochemical properties of compounds*

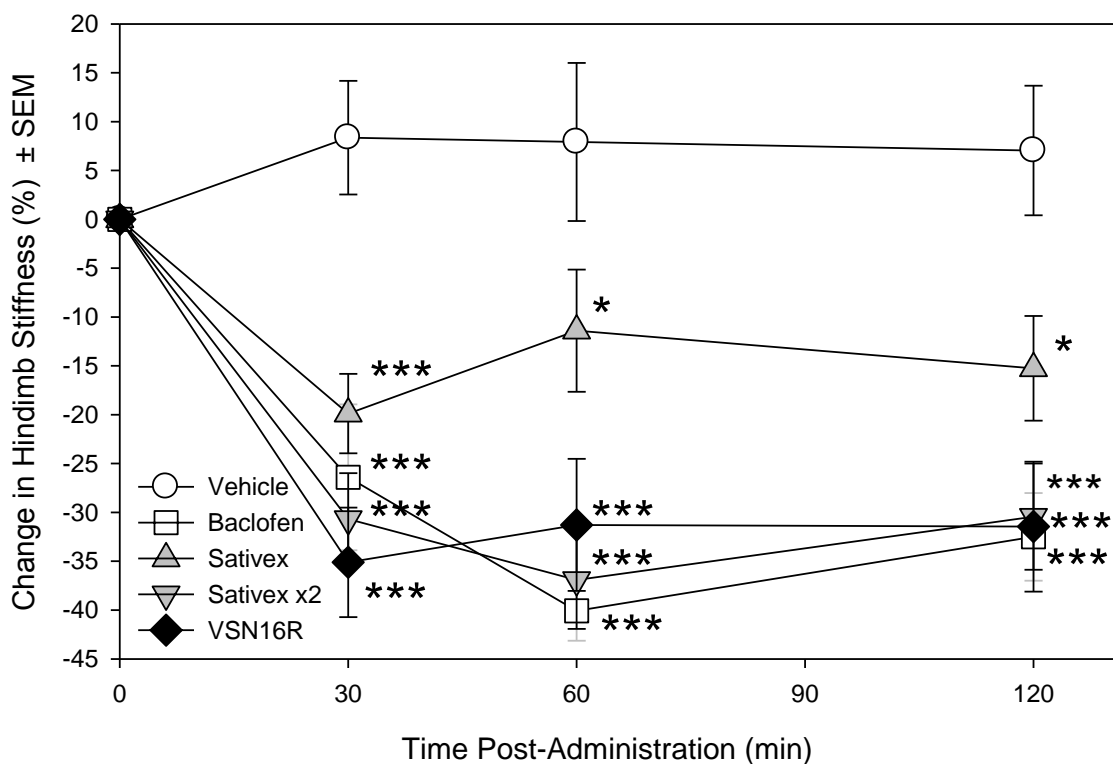
Compound	CLogP	Vas Deferens (LogEC ₅₀)	Cyp Inhibition	Hepatocyte Stability
VSN16R	0.9	-7.98 (10.5nm)	>10 μ M	>200min
VSN16S	0.9	-7.44 (36.3nm)	>>3 μ M	>200min
VSN17R	1.2	-6.95 (112nm)	>>3 μ M	>200min
VSN17S	1.2	-6.95 (112nm)	>>3 μ M	>200min
VSN40R	3.5	-7.22 (60.3nm)	>>3 μ M	2 min
VSN44R	1.2	-8.85 (1.4nm)	N.D.	N.D.

Compounds were synthesized by Prof. David Selwood, London who estimated the CLogP ,a measurement of a compound's hydrophilicity, based on the structure of the molecule. The cytochrome P450 activity and hepatocyte stability was assessed on a variety of Cyp enzymes in rat hepatocytes, both performed by Cyprotex Ltd. The vas deferens relaxation assays were performed by Prof. Ruth Ross, Aberdeen

7.2.2 VSN16R anti-spastic effects

Following the development of spasticity animals were treated with VSN16R, Sativex, Baclofen and vehicle. Animals were treated with 5mg/kg of each compound. The effects of VSN16R was compared to baclofen and showed similar effects when comparing the two anti-spastic agents. However, a double dose of Sativex was required in order to obtain similar effects as with baclofen or VSN16R.

Figure 7.2 VSN16R is as at least as effective as current anti-spastic agents



ABH mice were immunized with spinal cord antigens in Freund's adjuvant to induce relapsing EAE. Following the development of spasticity, animals received a single intravenous administration of 0.1ml of vehicle (ethanol:cremaphor:PBS) or 5mg/kg of either (+)baclofen, 5mg/kg VSN16R or the botanical drug substances within Sativex® containing 5mg/kg tetrahydrocannabinol and 5mg/kg cannabidiol or twice the amount (Sativex® x 2) with 10mg/kg tetrahydrocannabinol and 10mg/kg cannabidiol. These experiments were run in separate groups of animals and caution should be made when comparing effects between groups. * $P < 0.05$, ** $P < 0.01$, *** $P < 0.001$ compared to baseline in pair wise analysis. The studies involving baclofen and/or Sativex have been reported previously (Hilliard *et al.*, 2012) and were performed by G. Pryce.

Table 7.2 *VSN16R Does not induce weight loss following repeated administration*

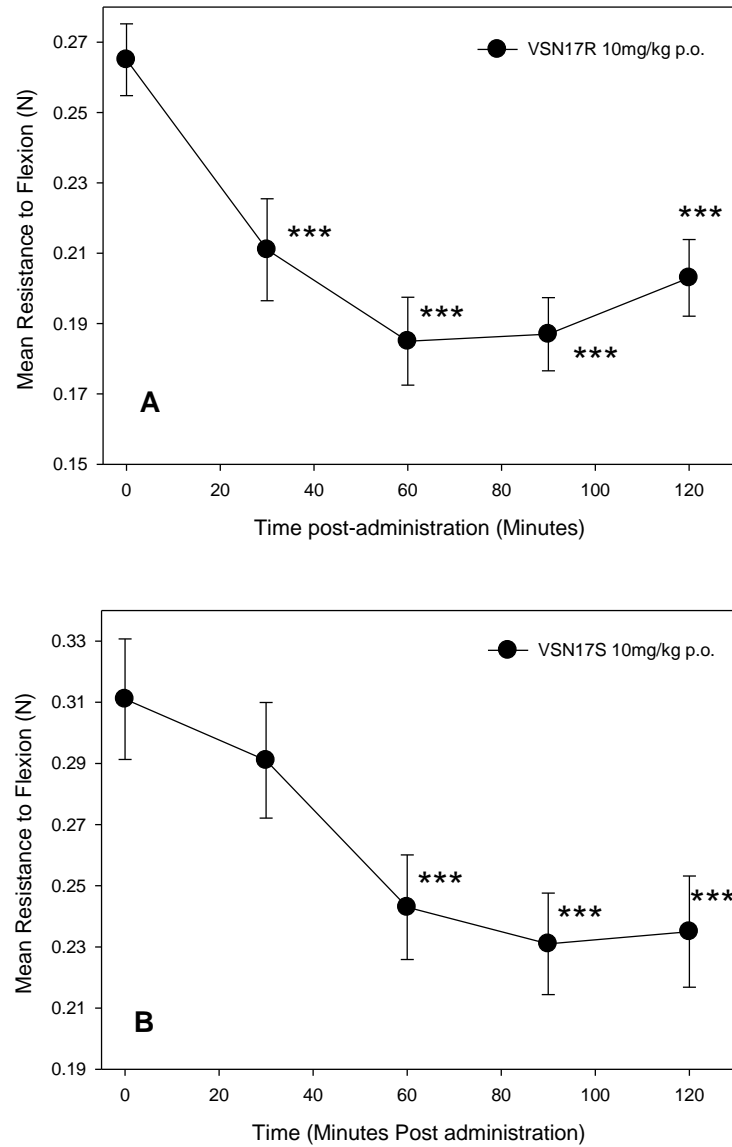
Drug Treatment	Weight (g)				
	Baseline	Day 1	Day 2	Day 3	Day 4
1000mg/kg p.o.	27.0	28.8	29.4	30.8	30.6
	29.0	28.9	28.1	28.1	28.9
	31.0	30.9	30.8	29.8	31.0
Mean \pm SD	29.0 \pm 2.0	29.5 \pm 1.2	29.4 \pm 1.4	29.6 \pm 1.4	30.2 \pm 1.1
500mg/kg p.o.	27.8	27.1	28.3	29.0	31.5
	27.4	28.3	28.8	28.7	30.8
	28.0	29.5	29.9	28.2	29.8
Mean \pm SD	27.7 \pm 0.3	28.3 \pm 1.2	29.0 \pm 0.8	28.6 \pm 0.4	30.7 \pm 0.9
100mg/kg p.o.	28.0	28.5	29.2	30.1	30.9
	28.0	31.3	31.8	31.8	31.7
	27.0	28.8	29.2	29.4	30.7
Mean \pm SD	27.7 \pm 0.6	29.5 \pm 1.5	30.1 \pm 1.5	30.4 \pm 1.2	31.1 \pm 0.5

Animals were weighed and then administered daily with 100mg/kg, 500mg/kg or 1000mg/kg p.o. VSN16R in water for 5 consecutive days. The results represent the individual weights and mean \pm SD of the group.

7.2.3 VSN17 enantiomers anti-spastic effects

It was found that the VSN17 enantiomers had potent activity in the low nM range in relaxation of mouse vas deferens (Table 7.1). VSN17 enantiomers exhibited significant ($P<0.001$) anti-spastic activity in EAE (Figure 7.3).

Figure 7.3 VSN17R and VSN17S are novel anti-spastic agents

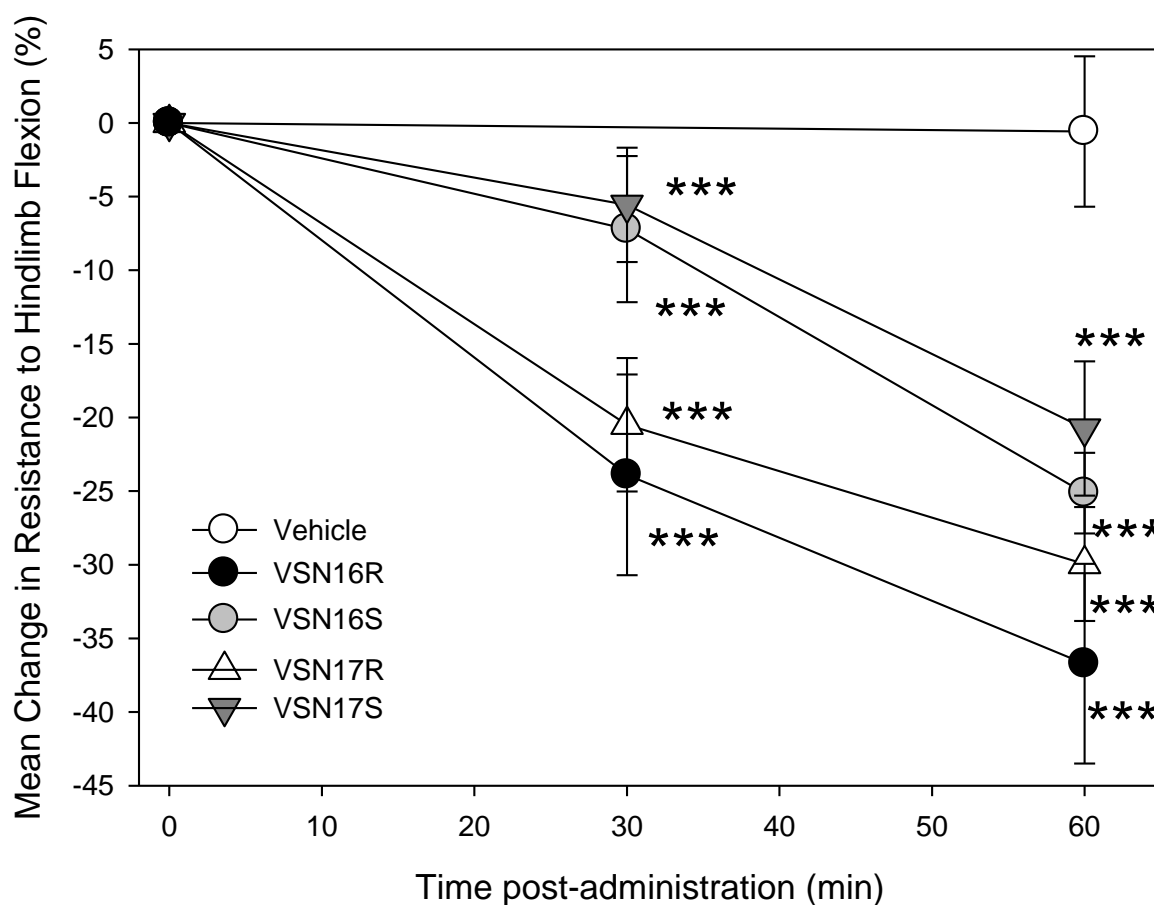


ABH mice were immunized with spinal cord antigens in Freund's adjuvant to induce relapsing EAE. Following the development of spasticity (3-4 months after disease induction), animals were administered orally with 10mg/kg (A) VSN17R ($n=13$ limbs) or (B) VSN17S ($n=16$ limbs) in water. The level of limb spasticity was assessed by the resistance to hind limb flexion force when the limb was placed against a strain gauge. Results represent the \pm SEM resistance to hind limb flexion of individual limbs ($n=16$ hind limbs/group). *** $P<0.001$ compared to baseline. This was performed in collaboration with G. Pryce.

7.2.4 Comparison of VSN16 and VSN17 enantiomers anti-spastic effects

It was found that VSN16R, VSN16S, VSN17R and VSN17S all had potent activity in the low nM range in relaxation of mouse vas deferens with VSN16R being the most potent (EC_{50} = around 10nM (Table 7.1). All VSN16 and VSN17 enantiomers exhibited significant ($P<0.001$) anti-spastic activity. In this series of experiments VSN16R seemed to perform better than VSN16S and VSN17 compounds (Figure 7.4).

Figure 7.4 VSN16 and VSN17 compounds are novel anti-spastic agents

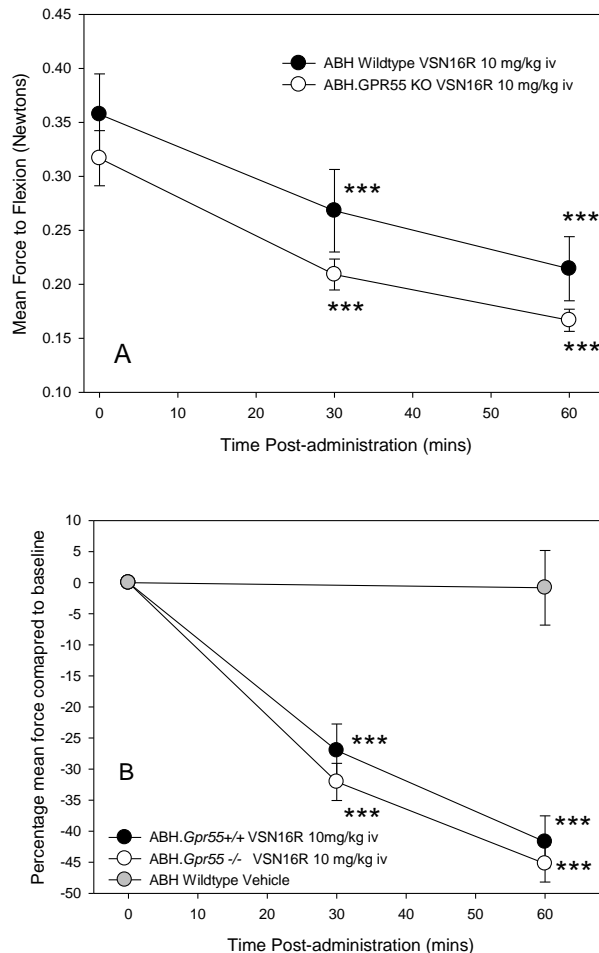


ABH mice were immunized with spinal cord antigens in Freund's adjuvant to induce relapsing EAE. Following the development of spasticity (3-4 months after disease induction), compounds were administered at 10mg/kg. These were administered orally in water. Animals were administered with VSN16R (n= 16 limbs), VSN16S (n=15 hind limbs), VSN17R (n=13 limbs) or (B) VSN17S (n=16limbs) in water. The level of limb spasticity was assessed by the resistance to hind limb flexion force when the limb was placed against a strain gauge. The data was normalised to baseline readings and results represent the mean \pm SEM percentage change from baseline. *** $P<0.001$ compared to baseline. This was performed in collaboration with G. Pryce.

7.2.5 VSN16R anti-spastic effects in GPR55 knockout mice

It has been previously shown that VSN16R is active in CB₁ receptor knockout mice (Pryce, 2010). VSN16R was administered intravenously to spasticity GPR55-deficient mice and surprisingly the compound was still active (Figure 7.5A) and demonstrated comparable levels of activity to that found following administration of VSN16R to wild-type mice (Figure 7.5B).

Figure 7.5 *VSN16R inhibits spasticity in GPR55 knockout mice*

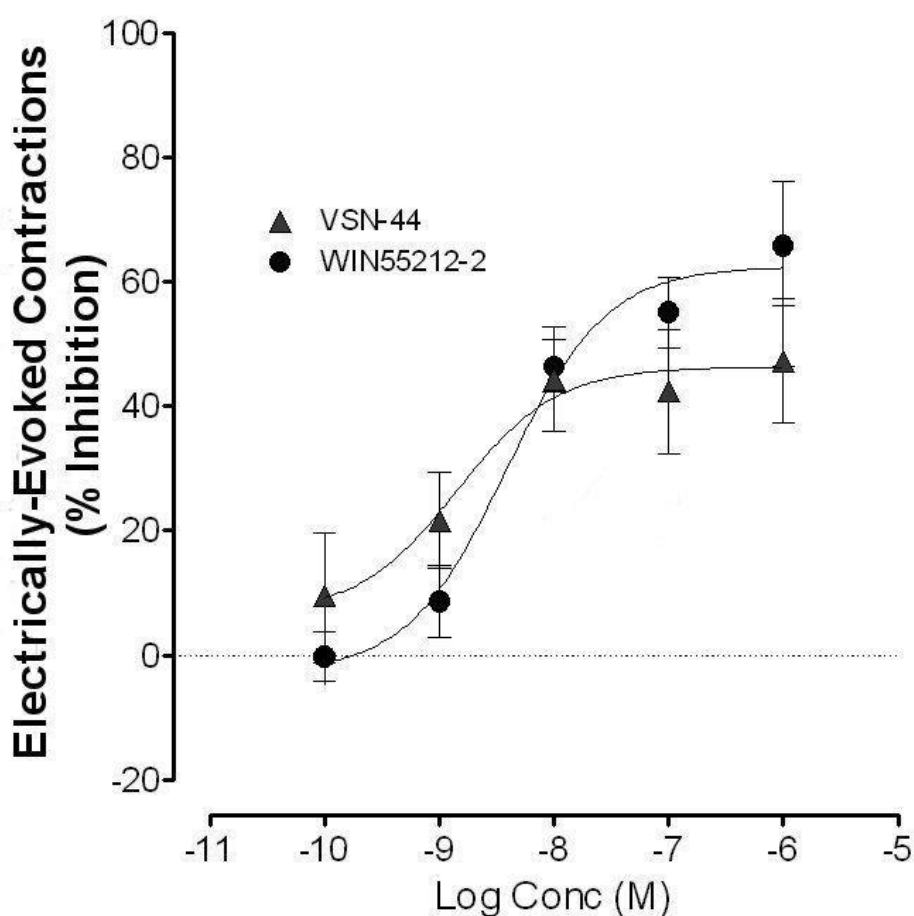


ABH mice were immunized with spinal cord antigens in Freund's adjuvant to induce relapsing EAE. Following the development of spasticity (3-4months after disease induction), animals were administered intravenously with 10mg/kg VSN16R. The level of limb spasticity was assessed by the resistance to hind limb flexion force when the limb was placed against a strain gauge. Spastic ABH animals received VSN16R in water or vehicle (into either wildtype ABH or ABH.GPR55 knockouts) and (A) resistance to flexion against a strain gauge was assessed. All animals were genotyped prior to use in the assay and were confirmed to be either wildtype homozygous or fully GPR55 deficient. (B) Results of resistance of the limb to flexion were converted to a percentage change from baseline. The results represent the mean \pm SEM. n=16 limbs per group. ***P<0.001 compared to baseline. This was performed in collaboration with G. Pryce.

7.2.6 VSN44 anti-contratile effects

An additional compound was also synthesised. This was termed VSN44R (Figure 7.1). This was based on analysis of mass spectroscopy of plasma samples obtained during pharmacokinetic analysis performed at a contract research organization, and VSN44 was predicted to be acid metabolite of VSN16R. This was highly active in the vas deferens assay with EC_{50} of 1.4 nM compared with 3.9nM for R-(+) WIN55,212-2 (Table 7.1, Figure 7.6). VSN44 was highly active causing an anti-contratile effect in the vas deferens assay with EC_{50} of 1.4 nM compared with 3.9nM for R-(+) the cannabinoid agonist WIN55, 212-2 (Table 7.1, Figure 7.6).

Figure 7.6 *VSN44R induces relaxation of the mouse vas deferens*

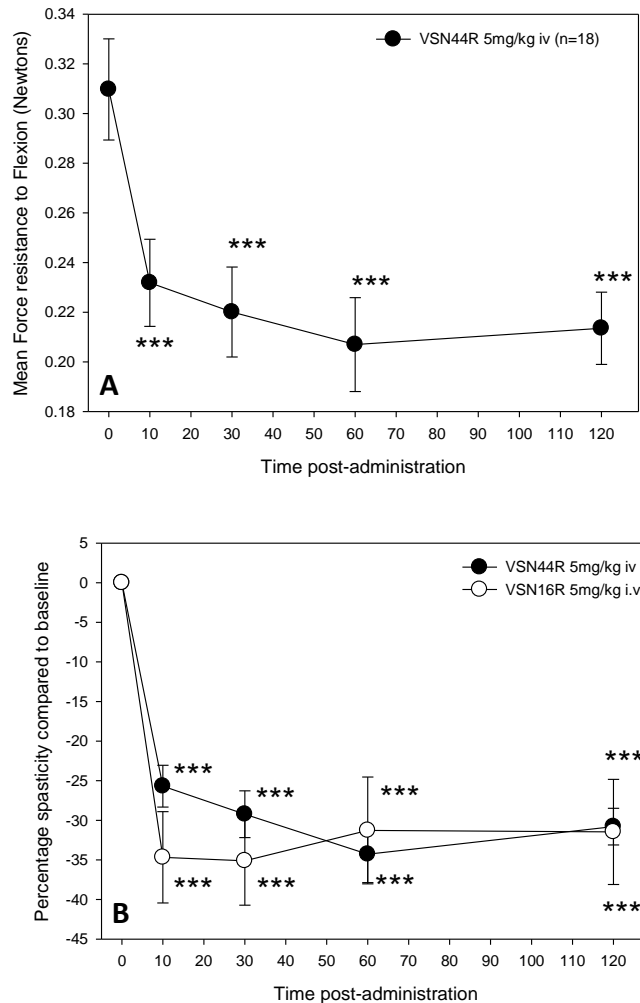


The vas deferens from C57BL/6 mice were isolated and contractions were monitored following incubation with various concentrations of VSN44R or WIN55212-2. The results represent the mean \pm SEM of 5-6 replicates. The study was performed by Ruth Ross, University of Aberdeen.

7.2.6 VSN44 and VSN16R anti-spastic effects

As formal pharmacokinetics have yet to be performed, VSN44 was administered intravenously in spastic EAE animals in the first instance to avoid any issue with poor oral bioavailability. It was found that VSN44 significantly ($P<0.001$) inhibited spasticity (Figure 7.7A) and induced an inhibition of spasticity to a comparable level to that obtained with VSN16R (Figure 7.7B).

Figure 7.7 Inhibition of Spasticity with VSN44

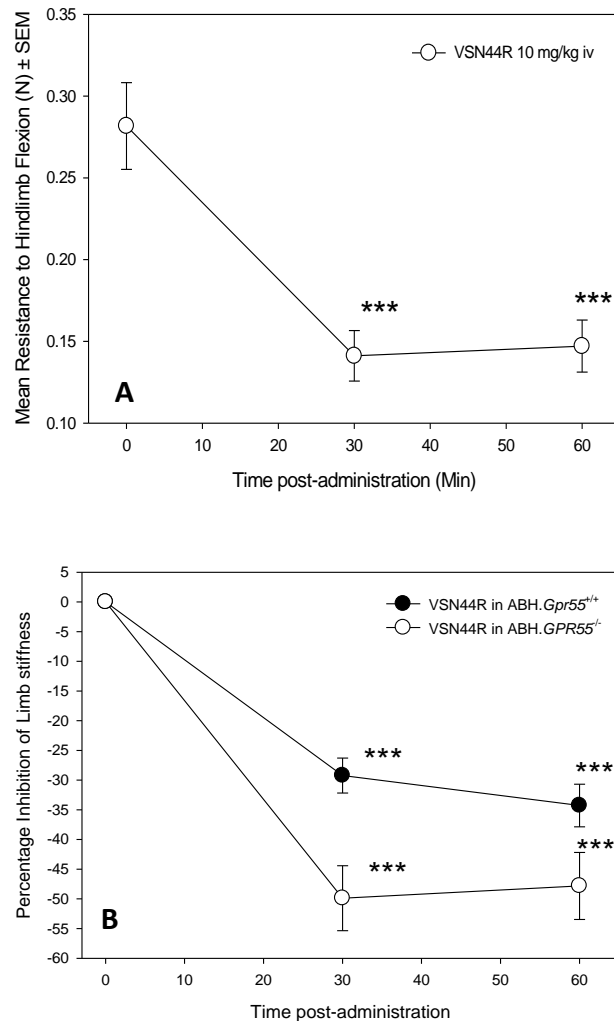


ABH mice were immunized with spinal cord antigens in Freund's adjuvant to induce relapsing EAE. Following the development of spasticity, animals were received a single intravenous administration of (A, B) VSN44R (n=18 limbs) or (B) VSN16 in saline (n= x . (A) The results represent the mean \pm SEM forces to bend hind limbs to full flexion against a strain gauge or (B) the percentage change from baseline. * $P<0.05$, ** $P<0.01$, *** $P<0.001$ compared to baseline. These studies were performed in collaboration with G. Pryce.

7.2.7 VSN16R and VSN44 anti-spastic effects in GPR55 knockout mice

VSN16R and VSN44 was administered intravenously to spasticity GPR55-deficient mice and the compounds were still active (Figure 7.8). This suggests that while VSN16R may be a pro-drug, the mechanism of action is clearly not via GPR55 and another target candidate is now sought.

Figure 7.8 VSN44R inhibits spasticity in GPR55 knockout mice



Wildtype ABH (closed circles) and GPR55 Knockout (open circles) mice were immunized with spinal cord antigens in Freund's adjuvant to induce relapsing EAE. Following the development of spasticity, animals were received a single intravenous administration of 10mg/kg i.v. of VSN44R in saline (n=18 limbs) or (B) VSN16R in saline (n= 12hindlimbs). (A) The results represent the mean \pm SEM forces to bend hindlimbs to full flexion against a strain gauge (n=12 limbs) or (B) the percentage change from baseline in wildtype (n=18) or GPR55 knockout (n=12). * $P < 0.05$, ** $P < 0.01$, *** $P < 0.001$ compared to baseline. These studies were performed in collaboration with G. Pryce.

7.3 Discussion

The study further demonstrates the activity in controlling spasticity by VSN16R. Although the initial chemical series failed to identify many active compounds besides VSN15 and VSN16 that exhibited activity (Hoi *et al.*, 2007b) additional chemical entities were synthesised that had efficacy in a similar manner to VSN16R. VSN16R was slightly more active than VSN16S as found previously in *in vivo* rodent (mouse and rat) studies (Pryce, 2010) *in vitro* in rat (Hoi *et al.*, 2007b). However, VSN16S had 100% bioavailability compared to about 30% for VSN16R (D.Selwood Unpublished), though this could perhaps influence toxicology profiles. VSN16R is clearly very well tolerated. There were no behavioural effects when administered up to 120mg/kg p.o. in rats (Pryce, 2010) and it was demonstrated here that there is no overt toxicity when administered at 40mg/kg p.o. for nearly one month. Furthermore, there were no apparent effects when administered up to 1000mg/kg/day, which is the regulatory maximum for toxicology purposes for such small molecules. As the compound is active as an anti-spastic drug at 5mg/kg (Pryce, 2010) or less then there is a minimum 200 fold therapeutic window. Additional studies in Sprague Dawley rats have confirmed a No Observable Effect Level (NOEL) of 1g/kg p.o. in 28 day toxicology studies (Charles Rivers, Edinburgh UK. D.Selwood/D.Baker unpublished)

VSN16R could potentially act on GPR55 within neural circuits. This is because it has been shown that GPR55 is expressed in nervous tissue including dorsal root ganglion (Lauckner *et al.*, 2008; Sylantsev *et al.*, 2013; Wu *et al.*, 2013) and can influence nerve transmission (Kargl *et al.*, 2011; Sylantsev *et al.*, 2013; Waldeck-Weiermair *et al.*, 2008; Wu *et al.*, 2013). Allosteric modulators of the cannabinoid receptors have been reported previously (Price., 2005). VSN16R may act at an allosteric site of GPR55 to augment the action of GPR55 agonism such as that occurring following co-incubation with LPI, as shown here in mouse cells. This has previously been seen with CB₁ receptor-agonists in human cells (Pryce, 2010). However, this activity was only found at high concentrations above 1µM compared to the low nanomolar range for biological activity found in rat vasculature (Hoi *et al.*, 2007b; Pryce, 2010). This may reflect a problem with the cell lines used in *in vitro* binding assays compared to normal cells. It is clear that where GPR55 is expressed in tissues it is expressed at low levels. In contrast, in transfected GPR55 over-expressing cells, there are high levels of surface GPR55, therefore second messenger systems may become more quickly exhausted and thus limit the biological activity of GPR55 binding molecules (Ross, 2009). Alternatively, VSN16R may need to be metabolically altered to form an active compound. This could have helped to explain why VSN16R fails to bind to receptors in *in vitro* tests, including CB₁, CB₂ and GPR55, but shows a nM level affinity in tissue-based assays. VSN44 also showed similar

anti-spastic effects in both GPR55 knockout mice and wild-type littermates. Perhaps future studies could confirm whether the metabolite can directly bind to receptors in *in vitro* assays.

As found previous in rat mesentery artery relaxation studies (Hoi *et al.*, 2007b), VSN16R was slightly more active than VSN16S in the relaxation of the vas deferens. This appeared to be the case for the anti-spastic effect of VSN16S found here and shown previously following intravenous administration (Pryce, 2010). However, caution needs to be made when making such a conclusion. This is because the compounds were tested in different cohorts of animals. Animals with spasticity show significant variability in the degree of limb stiffness (Baker *et al.*, 2000) and the level of relaxation that can be achieved therefore may be variable between limbs. Therefore, further analysis of drug efficacies in the same animals will be needed to directly compare the level of efficacy of one drug vs. another. However, the level of inhibition of spasticity with VSN compounds was similar to that achievable with cannabinoids (Baker *et al.*, 2000) and baclofen and Sativex botanical drug substances (Hilliard *et al.*, 2012). The advantage of VSN16 compounds were that they were very well tolerated and caused no obvious sedative effects in mice as seen here or in an Irwin behavioral test, which is a panel of behavioural studies for CNS side-effects in rats up to 150mg/kg p.o. (Pryce, 2010). Levels of THC above 2.5mg/kg i.p. induced cannabimimetic effects in mice (Croxford *et al.* 2008) and VSN16R was at least as active as Sativex botanical drug substances at 5mg/kg THC doses that also causes cannabimimetic effects (Hilliard *et al.*, 2012).

Although studies in vas deferens may suggest that VSN16 is an allosteric modulator of the GPR55 receptor it is possible that the effects of the compound acts on a possible co-receptor. The molecular target has proved elusive and in comparison to positive controls. It has been shown that there is a lack of direct agonism of VSN16R at concentrations $>10\mu\text{M}$ on a large number of receptors (Pryce, 2010). These include A_1 , A_{2A} , A_3 , α_1 (non-selective), α_2 (non-selective), β_1 , AT_1 , BZD, β_2 , CCK_A , $Cnr1$, $Cnr2$, $D1$, $D2S$, ET_A , GABA (non-selective), Glycine, $GAL2$, $CXCR2$, $CCR1$, H_1 , H_2 , MC_4 , ML_1 , M_1 , M_2 , M_3 , NK_2 , NK_3 , Y_1 , Y_2 , NT_1 , δ_2 , κ , μ , $ORL1$, $5-HT_{1A}$, $5-HT_{1B}$, $5-HT_{2A}$, $5-HT_3$, $5-HT_{5A}$, $5-HT_6$, $5-HT_7$, somatostatin (non-selective), $TRPV1$, VIP_1 , V_{1a} , Ca^{2+} channel (L verapamil site), K^+ channel, SK^+Ca channel, Na^+ channel (site 2), Cl^- channel, FAAH, NE transporter, DA transporter, Nav 1.5 Na^+ channel, hERG $Kv11.1$ K^+ channel, GPR6, GPR12, GPR35, GPR55, GPR119 (Pryce, 2010). There has been a weak activity at lysophosphatidic acid receptors such as $LPA1$ $EC_{50} = 1.1\mu\text{M}$, $LPA2 = 3.4\mu\text{M}$, $LPA3 = 0.96\mu\text{M}$, $LPA4$ (GPR23) $= 3.4\mu\text{M}$ based on calcium responses in B10, LPA-receptor transfected cells (D. Selwood, London, J. Chang, La Jolla USA), which are higher than the 1-10nm affinity of VSN16R in vas deferens and mesenteric artery relaxation (Hoi *et al.*, 2007b; Pryce, 2010).

CHAPTER 8

Final conclusions

GPR55 was essentially an uncharacterized orphan receptor at the beginning of this project. There were only a few papers that described the identification of the receptor and mRNA expression levels in a few tissues. The existence of a new cannabinoid-like receptor in the cardiovascular system was proposed on the basis of previously reported findings on the Abn-cbd (Johns *et al.*, 2007) as the atypical cannabinoid had demonstrated vasodilator effects in earlier studies (Jarai *et al.*, 1999). Further studies determined that the observed vasodilatory effect of abnormal cannabidiol was not mediated by GPR55 (Johns *et al.*, 2007). Likewise a pronociceptive influence of GPR55 has been inconsistent (Breen *et al.*, 2012; Schuelert *et al.*, 2011; Staton *et al.*, 2008; Wu *et al.*, 2013). GPR55 was identified as a cannabinoid receptor in 2006 as it was suggested to interact with cannabinoids (Baker *et al.*, 2006). Since then a series of data has been published describing the functions of the receptor using a number of non-selective, putative GPR55 agonists and antagonists in various expression assays however the pharmacology remains diverse and inconsistent (Pertwee, 2005; Ross, 2009). Although O-1602 and O-1918 have shown to exert effects that are GPR55 dependent, these molecules also mediate notably vascular effects that are independent of GPR55 (Johns *et al.*, 2007). LPI is the only ligand that has been consistently reported as an endogenous ligand that possesses agonistic effects on GPR55 in a number of expression systems (Anavi-Goffer *et al.*, 2012; Henstridge *et al.*, 2009; Kotsikorou *et al.*, 2011; Lauckner *et al.*, 2008; Oka *et al.*, 2007).

One of the main hurdles in the characterization of the GPR55 receptor was a lack of validated commercially available reagents to probe GPR55 function. During this project a number of polyclonal antibodies have become available and we and other groups (unpublished) have tested several of them however these have been shown to contain significant GPR55 non-specific activities. This means that staining profiles may be unreliable in identifying true tissue distribution; this observation has been previously reported with other cannabinoid receptors (Graham *et al.*, 2010; Grimsey *et al.*, 2008). There are a number of studies that have demonstrated the use of GPR55 antibodies for staining various tissues and cell lines (Fonseca *et al.*, 2011; Henstridge *et al.*, 2011; Romero-Zerbo *et al.*, 2011). Blockade of antigen binding is a control that is used to validate antibodies. However, whilst this might confirm that binding is via the antigen-binding site of the antibody, it would not prove that the antibody could not detect more than one protein, which may share peptide epitopes. Knockdown of the target antigen or the use of knockout mice are essential

controls that are often lacking in many cannabinoid receptor staining studies. In this study different approaches using either recombinant protein/peptide fragments of mouse GPR55 or GPR55 transfected cell lines were used to generate hybridomas from GPR55 knockout mice. However, none of them were found to bind specifically, without reactivity to other targets, to the native GPR55 protein. As earlier mentioned one of the hybridoma (4D12) antibodies showed a band at around 37kDa corresponding to the size of the GPR55 protein therefore there might have been some reactivity to the native protein. However, due to reactivity of the hybridoma antibodies (4D12) to other targets as well we did not observe any specific GPR55 staining when comparing staining of GPR55 transfected and untransfected cells. The inability to develop antibodies may have been a problem with the immunizing peptides and not adopting a conformation that exists in the native protein, which is a transmembrane G protein coupled receptor. Alternatively this may have reflected some form of immune defect that appears to be present in some GPR55 knockout mice.

At the beginning of this study the biological role of GPR55 was mainly unreported with a few exceptions. Earlier studies revealed that GPR55 signaling pathways differ from CB₁ and CB₂ receptors. In one of the studies an increase of calcium was found in the stimulated GPR55 transfected cells involving G_q, G₁₂, RhoA, actin, phospholipase C, and calcium release from inositol 1,4,5-trisphosphate receptors-gated stores (Lauckner *et al.*, 2008). GPR55 has also been suggested to play an important role in mechanical hyperalgesia as GPR55 knockout mice lacked an increased sensitivity to pain (Staton *et al.*, 2008). The GPR55 knockout mice also had increased levels of the anti-inflammatory cytokines IL-4 and IL-10 which have previously been described to exert anti-nociceptive effects (Staton *et al.*, 2008; Vale *et al.*, 2003).

More recent studies have identified various other functions of GPR55. GPR55 has been shown to be expressed in various gastrointestinal tissues (Li *et al.*, 2013; Lin *et al.*, 2011; Ross, 2009; Ryberg *et al.*, 2007; Schicho *et al.*, 2012). The precise function of this receptor in these tissues is not clear (Duncan *et al.*, 2005), although it appears that GPR55 agonism can alter gut motility (Li *et al.*, 2013; Ross, 2009). GPR55 is detected in enteric neurons of the rat ileum and GPR55 expression was increased in these cells upon the development of LPS-induced inflammation (Lin *et al.* 2011). This suggests that GPR55 may be involved in the response of the gut to intestinal inflammation (Lin *et al.*, 2011). Although CB₁ receptor activation has been shown to reduce gastrointestinal motility and affect lower esophageal sphincter relaxations (Izzo *et al.*, 2010; Martin *et al.*, 2004), recently, O-1602 was shown to inhibit neurogenic contractions in the gut, an effect mediated by GPR55 and independent of CB₁ or CB₂ receptors (Li *et al.*, 2013; Ross *et al.*, 2012). O-1602 has also

previously been shown to reduce spontaneous contractions in the rat ileum and LPS induced contractions in the colon (Lin *et al.*, 2011; Ross *et al.*, 2012). O-1602 as well as CBD has been shown to have anti-inflammatory properties in acute pancreatitis possibly mediated by GPR55 (Li *et al.*, 2013; Schicho *et al.*, 2012). Activation of CB₂ receptors has been shown to reduce inflammation (Maresz *et al.*, 2007; Palazuelos *et al.*, 2008).

One example of a cannabinoid ligand that has shown to inhibit EAE is the phytocannabinoid CBD (Kozela *et al.*, 2011). Although CBD has been reported to be a GPR55 antagonist, the mechanisms of action of this ligand are unclear (Whyte *et al.*, 2009; Li *et al.*, 2013). CBD has been previously suggested to be a transient receptor potential vanilloid two receptor agonist and a CB₁ receptor antagonist (Li *et al.*, 2013; Pertwee, 2008; Qin *et al.*, 2008). While it has been reported that CBD can inhibit EAE in C57BL/6 mice (Kozela *et al.*, 2011), this compound exhibited no inhibitory effect in EAE in Biozzi ABH mice (Maresz *et al.*, 2007).

As GPR55 knockout EAE animals in this current study developed less severe disease, GPR55 antagonism could potentially be an approach to inhibit EAE as the receptor might be predicted to influence T cell-driven neuroinflammation. It is interesting that the reduced susceptibility of EAE shown here in this study was observed in both C57BL/6 and ABH GPR55 knockout mice. The mechanism of action of this has not been clear and although the inhibitory effect in EAE suggests that it may inhibit T cell function, this could not be verified. Therefore, there may be an effect on antigen presenting cell function. Further studies will be required to find changes in immune function that can account for this small effect.

Other explanations in susceptibility to EAE have also previously been reported (Bolton *et al.*, 2013). There may be some gender influence in susceptibility to EAE suggesting that there may be a hormonal effect. Differences in sex hormone levels could account for different susceptibilities to disease. Although females develop more MS than males (Compston *et al.*, 2002) studies in EAE show that this can be a complex relationship with females sometimes more susceptible to males and *vice versa* (Okuda *et al.*, 2002; Smith-Bouvier *et al.*, 2008; Spach *et al.*, 2009). Vitamin D levels may be a risk factor in multiple sclerosis and many susceptibility genes, notably the major histocompatibility complex, might have vitamin D response elements in their promoters (Disanto *et al.*, 2012). It has been found that the sex and age specific effects of calcifediol, a vitamin D prehormone, differ between C57BL/6 and ABH mice (Bolton *et al.*, 2013). In our study it was found that mainly GPR55 knockout female mice were less susceptible to EAE on the C57BL/6 background compared to GPR55 knockout males suggesting some gender influence in susceptibility.

Endocannabinoids have been suggested to mediate some of their additional effects through GPR55 (Ryberg *et al.*, 2007). Virodamine has previously shown to act as a partial agonist at CB₁ and full agonist at CB₂ (Porter *et al.*, 2002) and has been shown to act as a partial GPR55 agonist at low concentrations and a partial antagonist at higher concentrations (Sharir *et al.*, 2012). These findings suggest a role for virodamine in modulating cannabinoid receptor function (Porter *et al.*, 2002).

Increased levels of LPI have also been observed during a number of pathological conditions (Ford *et al.*, 2010; Moreno-Navarrete *et al.*, 2012). For instance, levels of endocannabinoids and the GPR55 agonist LPI have been shown to be increased during inflammation (Walter and Stella 2004; Ford *et al.* 2010) and it has been suggested that GPR55 activity may play a pivotal role in balancing the involvement of the endocannabinoids during inflammation (Sharir *et al.*, 2012). Increased LPI levels have also recently been observed in obese patients and the same study also demonstrated higher GPR55 expression levels in adipose tissue in diabetic obese patients than in the control group (Moreno-Navarrete *et al.*, 2012). Another GPR55 agonist O-1602 has been reported to promote enhancement of glucose-stimulated insulin secretion in isolated rat pancreatic islets via a GPR55 mediated mechanism (Romero-Zerbo *et al.*, 2011).

GPR55 has also been shown to form heteromers with CB₁ receptors in HEK293 cell line expressing both receptors (Kargl *et al.*, 2012). Whilst GPR55-mediated signalling was shown to be inhibited in the presence of CB₁ receptor, in contrast, CB₁ signalling properties were found to be increased in the presence of GPR55 (Kargl *et al.*, 2012). The three-dimensional structure of GPR55 was recently examined and the involvement of hydrogen bonding and hydrophobic interactions for ligand binding has been described. In that study the amino acid residue Lys80 was identified as the main residue for receptor recognition (Elbegdorj *et al.*, 2012). In human endothelial cells CB₁ and GPR55 receptors have been shown to mediate signalling induced by anandamide activation. Furthermore, the activation status of integrins determines whether CB₁ receptor or GPR55 signalling cascades are stimulated (Waldeck-Weiermair *et al.*, 2008). The endogenous ligand LPI has previously been reported to activate the ERK MAP-kinase pathway, Ca²⁺ signalling and the downstream target CREB (Balenga *et al.*, 2011a; Henstridge *et al.*, 2011; Henstridge *et al.*, 2010; Oka *et al.*, 2007). In our study LPI was found to induce intracellular Ca²⁺ release in the GPR55 transfected cells compared to non-transfected cells. The augmentation of calcium levels in the GPR55 transfected cells upon stimulation by agonists is consistent with previous findings (Waldeck-Weiermair *et al.*, 2008).

Most recently a signalling role for GPR55 in synaptic circuits of the brain was reported (Sylantsev *et al.*, 2013). By combining pre-synaptic and post-synaptic imaging GPR55 function at the single synapse level has been confirmed using GPR55 knockout animals as a control. The authors also described the receptor to activate both inositol triphosphate (IP3) and non-IP3 stores although previous studies have only shown activation of IP3-dependent Ca^{2+} stores (Sylantsev *et al.*, 2013). Therefore, this suggests that GPR55 may influence neurotransmission both in the CNS (Sylantsev *et al.*, 2013) and peripheral nervous system as shown by the relaxation of the vas deferens (Pryce, 2010). Molecules that stimulate GPR55 may have the potential role to modulate neurotransmission.

GPR55 is a “lipid-receptor” that is mainly stimulated by LPI and atypical cannabinoids (Kapur *et al.*, 2009; Oka *et al.*, 2007). The receptor may be functionally related to the cannabinoid receptors as it appears to be bound and modulated by some endocannabinoids (Baker *et al.*, 2006; Sharir *et al.*, 2012). VSN16R is a water soluble drug that has shown to inhibit experimental spasticity and modulate GPR55. VSN16R has been demonstrated to inhibit neurogenic contraction in the vas deferens of the testis and is relatively CNS excluded. The spasticity was significantly inhibited in EAE animals treated with VSN16R at a concentration of 1-40mg/kg (Pryce, 2010), however treatment with the compound did not influence susceptibility to EAE. VSN16R has been shown to act as an allosteric modulator and not as a direct agonist or antagonist. Although the initial experiment with VSN16R in the vas deferens assay indicated that the anti-contraction effect was mediated by the GPR55 receptor, results from this study demonstrated an anti-spastic effect in GPR55-deficient mice treated with VSN16R. These results conclude that the anti-spastic effect of VSN16R in EAE is not mediated by the GPR55 receptor.

As VSN16R was potentially mediating its effects via GPR55 as suggested by the vas deferens assay (Pryce, 2010), further work was conducted in cell cultures. GPR55 transfected and untransfected astrocytoma cell lines treated with VSN16R on its own did not induce activation of CREB. It has previously shown that the compound does not induce calcium responses in GPR55 transfected HEK cells (Pryce, 2010). However, the combination of 1 μM LPI and 10 μM VSN16R did however induce CREB activation. This suggests that VSN16R functions as a GPR55 modulator rather than being a direct agonist. The GPR55 transfected and untransfected astrocytoma cell lines were stimulated with LPI and the cytoskeletal rearrangement was assessed using Phalloidin staining. Results showed GPR55 mediated cytoskeletal morphology rearrangement in the GPR55 transfected cell line upon stimulation with 1 μM of LPI; consistent with previously reported findings (Balenga *et al.*, 2011a; Obara *et al.*, 2011). The studies shown here in mouse GPR55 transfected

astrocytoma cells confirms previous observations in assays where human GPR55 HEK cells have been stimulated by LPI (Pryce, 2010). However, the concentrations required to modulate GPR55 function were substantially higher in these cell based assays than in the low nanomolar activity tissue based cell assays such as mesenteric artery bed and vas deferens (Hoi *et al.*, 2007; Pryce, 2010). This suggests that maybe VSN16R requires metabolism for activity, it has weak affinity for another receptor that interacts with GPR55 or that transfected cell lines that have supranormal and supraphysiological levels of GPR55 may not have sufficient intracellular signalling molecules to accommodate the high level of expression of GPR55. The difference in GPR55 expression levels might also explain the variations in pharmacological responses when comparing cell based assays with tissue based assays. Although VSN16R augmented the responses induced by AM251 in GPR55-transfected cells, the action of VSN16R was antagonized by AM251 and O-1918 in tissue-based assays (Hoi *et al.*, 2007; Pryce, 2010). However, whilst there may be some activity via GPR55 in some *in vitro* assays, the activity of VSN16R in spastic GPR55-deficient animals clearly shows that that VSN16R has an activity that is not GPR55-dependent. As mentioned earlier, screening against a large panel of receptors has been performed (*see discussion chapter 7*). However, there was some weak agonist activity on LPA1 (EC_{50} 1.1 μ M), LPA2 (EC_{50} 3.4 μ M), LPA3 (EC_{50} = 0.9 μ M), LPA4 (EC_{50} 3.4 μ M) receptors (D. Selwood, Multispan Inc, J. Chung, Scripps Institute USA. Unpublished). Whether these lipid receptors contribute to the biological activity of VSN16R requires further study.

The cannabinoid system has previously shown to regulate various immune functions including suppression of immune cell activation and cytokine production; it has also shown to alter cell proliferation and enhance apoptosis (Klein *et al.*, 2003). CB₁ receptor expression by neurons, but not T cells, has been demonstrated to be necessary for cannabinoid-mediated EAE suppression (Croxford *et al.*, 2008; Maresz *et al.*, 2007). However, encephalitogenic T cells have been shown to be essential for the control of EAE associated inflammation (Maresz *et al.*, 2007). CB₂-deficient T-cells in the CNS during EAE has shown to exhibit a higher rate of proliferation and increased production of inflammatory cytokines; these findings were associated with a more severe clinical disease (Maresz *et al.*, 2007). It has been found that the disease was more severe in the CB₂ knockout mice, this prompted the idea that the encephalitogenic CD4 T-cell effector functions are regulated via the CB₂ receptor (Maresz *et al.*, 2007; Palazuelos *et al.*, 2008). T-cells from the CB₂-deficient mice were reactivated *in vitro* and the cytokine production of IFN- γ and IL-2 was examined. Upon adding a CB₂ receptor agonist a reduction in proliferation and production of both cytokines was observed only in the T-cells from the wild-type mice indicating that the T-cell

effector functions were mediated by CB₂ (Maresz *et al.*, 2007). However, whilst we have been able to confirm augmentation of MOG35-55 induced EAE disease in two CB₂ knockout strains on the C57BL/6 background (C57BL/6.*Cnr2*^{TgZim1} and C57BL.*Cnr2Tg*^{Delt1}) when the CB₂ deficiency is on the ABH mouse background, which is highly susceptible to spinal cord-induced EAE, there is no phenotype (G.Pryce Unpublished). This may explain the consistent finding that CB₂ receptor agonists or antagonists exhibit no influence on the development or severity of EAE (Croxford *et al.*, 2008). These observations that the immunophenotypes seem to become minimal when the gene deficiency is introduced into a highly susceptible background might also suggest that GPR55 ligands might not have much influence on the development of EAE.

The immunophenotypes of our GPR55 knockout mice on the C57BL/6 background was compared with wild-type littermates prior to the EAE experiments to investigate potential differences. Overall, no significant variation between the two strains was observed. *In vitro* stimulation with Con A or MOG peptide was used to induce proliferation in our GPR55 knockout mice and wild-type mice and no significant differences was observed when comparing the two animal groups. MOG35-55 peptide in Freund's adjuvant was used to induce EAE in GPR55 knockout and wild-type mice on the C57BL/6 background where GPR55 knockout mice were found to develop a much milder disease than wild-type littermates. GPR55 knockout mice were also generated on the ABH background and although a lower disease susceptibility remained in the GPR55 knockout mice on the ABH background this difference was not as obvious as on the C57BL/6 background. The lower susceptibility was only observed in the first attack. The two strains had comparable weight losses. Motor control and coordination was assessed using a Rotarod and no apparent difference was observed when comparing both female groups however, ABH wild-type males were found to be the most neurologically impaired when comparing the two male groups.

EAE induced in gene knockout mice on the C57BL/6 mouse background, which is a relatively resistant strain (Levine *et al.*, 1973; Tuohy *et al.*, 1988), gives a markedly augmented phenotype in CB₂ deficient mice (Maresz *et al.*, 2007) and a reduced phenotype in GPR55 deficient mice that is either marginal or absent in EAE induced in knockout mice in the ABH background, which is highly susceptible to EAE induction (Baker *et al.*, 1990). These observations suggest that many phenotypes observed in EAE in C57BL/6 background knockout mice may not be reproducible if the gene deficiency is on a different genetic background. Spinal cord-induced EAE in ABH mice has been remarkably consistent over a number of years and these experiments provides a level of quality of control of expected susceptibility (Al-Izki *et al.*, 2012; Baker *et al.*, 1990). MOG-induced disease in C57BL/6 mice is remarkably inconsistent, in our and others hands. As such there is more confidence in the data generated on the ABH background. Whilst in our experiments

C57BL/6.Gpr55^{-/-} deficient mice typically developed less severe disease, positive controls sometimes failed to become sensitized. In the case of the C57BL/6.*Cnr2* knockout mice experiments the controls gave poor disease, whereas CB₂ knockout mice exhibited good disease (see supplementary Figure 9, G.Pryce Unpublished). Therefore the phenotype is in part dictated by the disease severity in controls. This inconsistency of disease in C57BL/6 mice has been shown repeatedly within the EAE literature and the type of phenotype appears often as a product of the susceptibility in wild-type animals in individual experiments (Axtell *et al.*, 2010; Coquet *et al.*, 2013). This may in part account for the poor translatability of studies from rodents to humans (Baker *et al.*, 2012; Vesterinen *et al.*, 2010).

Future studies

Future studies would be required to investigate the possible mechanisms behind the milder EAE disease in the GPR55 knockout animals possibly mediated by protective anti-inflammatory properties as previously been suggested (Staton *et al.*, 2008). It would also been interesting to further investigate cells belonging to the immune system such the functional role of antigen presenting cells including the role of macrophages and dendritic cells in other systems using eg. cell migration assays. Furthermore neutrophil function should be explored. Polymorphonuclear neutrophils express GPR55 which may influence the GPR55-mediated activity (Balenga *et al.*, 2011b; Schicho *et al.*, 2012) and may have a phenotype associated with altered neutrophil migration (Johns *et al.*, 2007; Schicho *et al.*, 2012). It is also interesting that neutrophils have limited role in multiple sclerosis and are a minor component of EAE lesions in ABH mice (Baker *et al.*, 1990), although they are maybe more abundant in EAE in C57BL/6 mice (Wu *et al.*, 2010). Interestingly, GPR55 deletion exhibits a greater activity in EAE susceptibility in C57BL/6 rather than ABH mice. Furthermore, different forms of inflammation should be examined to determine whether there is a consistent immune inhibition in GPR55 knockout mice.

There is a need for development of specific antibodies in order to detect GPR55 and further optimize other techniques such as *in situ* hybridization for detection in tissues. Antibody production may be achieved following immunization with native protein in its natural conformation in the membrane eg. with GPR55 transfected cells. Other receptors such as GPR18 have been suggested to mediate some of the atypical cannabinoid effects in various systems that are not mediated by GPR55. GPR18 assays have become commercially available and therefore future studies will soon examine the action of VSN16R and its metabolites on GPR18. However, GPR18 is reported to be PTX-sensitive indicating signalling via Gi/Go (McHugh *et al.*, 2012),

whereas the activity of VSN16R has been found to be insensitive to PTX (Hoi *et al.*, 2007). Further GPR55-dependent activities should be assessed such that lack of activity of VSN16R in GPR55 can be confirmed or refuted. In addition it will be important to address the function and receptor binding activity of any metabolites of VSN16 compounds. In this study we also tested VSN44, a VSN16R metabolite, and it was found to have anti-spastic effects in both GPR55 knockout EAE mice on the ABH background and in wild-type littermates. However, the function of VSN44 would still need to be tested in other functional assays and it must be determined whether its activity is similar if only more potent to VSN16R as its metabolite.

There is also a need to identify the target for VSN16R so that the anti-spastic mechanisms mediated by the chemical agent can be further investigated and identified. This unidentified receptor may be a target for future development of anti-spastic drugs. VSN16R has proved exceptionally safe in rodents with no detectable toxic effect up to 1g/kg p.o./day. Rodent and dog 28 day *in vivo* toxicology have been completed (D.Selwood, D.Baker, Unpublished) and future studies will examine the safety of VSN16R for human use.

Abood ME, Ditto KE, Noel MA, Showalter VM, Tao Q (1997). Isolation and expression of a mouse CB1 cannabinoid receptor gene. Comparison of binding properties with those of native CB1 receptors in mouse brain and N18TG2 neuroblastoma cells. *Biochem Pharmacol* **53**(2): 207-214.

Adams MM, Hicks AL (2005). Spasticity after spinal cord injury. *Spinal cord* **43**(10): 577-586.

Al-Izki S, Pryce G, O'Neill J, Butter C, Giovannoni G, Amor S (2012). Practical guide to the induction of relapsing progressive experimental autoimmune encephalomyelitis in the Biozzi ABH mouse. *Multiple Sclerosis and Related Disorders* **1**: 29-38.

Allen SJ, Baker D, O'Neill JK, Davison AN, Turk JL (1993). Isolation and characterization of cells infiltrating the spinal cord during the course of chronic relapsing experimental allergic encephalomyelitis in the Biozzi AB/H mouse. *Cellular immunology* **146**(2): 335-350.

Alnemri ES, Livingston DJ, Nicholson DW, Salvesen G, Thornberry NA, Wong WW, *et al.* (1996). Human ICE/CED-3 protease nomenclature. *Cell* **87**(2): 171.

Amor S, Baker D, Groome N, Turk JL (1993). Identification of a major encephalitogenic epitope of proteolipid protein (residues 56-70) for the induction of experimental allergic encephalomyelitis in Biozzi AB/H and nonobese diabetic mice. *Journal of immunology (Baltimore, Md. : 1950)* **150**(12): 5666-5672.

Amor S, Smith PA, Hart B, Baker D (2005). Biozzi mice: of mice and human neurological diseases. *Journal of neuroimmunology* **165**(1-2): 1-10.

Anavi-Goffer S, Baillie G, Irving AJ, Gertsch J, Greig IR, Pertwee RG, *et al.* (2012). Modulation of L-alpha-lysophosphatidylinositol/GPR55 mitogen-activated protein kinase (MAPK) signaling by cannabinoids. *The Journal of biological chemistry* **287**(1): 91-104.

Anderson JM, Hampton DW, Patani R, Pryce G, Crowther RA, Reynolds R, *et al.* (2008). Abnormally phosphorylated tau is associated with neuronal and axonal loss in experimental autoimmune encephalomyelitis and multiple sclerosis. *Brain : a journal of neurology* **131**(Pt 7): 1736-1748.

Andradas C, Caffarel MM, Perez-Gomez E, Salazar M, Lorente M, Velasco G, *et al.* (2011). The orphan G protein-coupled receptor GPR55 promotes cancer cell proliferation via ERK. *Oncogene*.

Andre A, Gonthier MP (2010). The endocannabinoid system: its roles in energy balance and potential as a target for obesity treatment. *Int J Biochem Cell Biol* **42**(11): 1788-1801.

Ashton JC (2011). Knockout controls and the specificity of cannabinoid CB2 receptor antibodies. *Br J Pharmacol* **163**(6): 1113; author reply 1114.

Ashton JC, Friberg D, Darlington CL, Smith PF (2006). Expression of the cannabinoid CB2 receptor in the rat cerebellum: an immunohistochemical study. *Neuroscience letters* **396**(2): 113-116.

Atwood BK, Mackie K (2010). CB2: a cannabinoid receptor with an identity crisis. *Br J Pharmacol* **160**(3): 467-479.

Axtell RC, de Jong BA, Boniface K, van der Voort LF, Bhat R, De Sarno P, *et al.* (2010). T helper type 1 and 17 cells determine efficacy of interferon-beta in multiple sclerosis and experimental encephalomyelitis. *Nature medicine* **16**(4): 406-412.

Baker D, Gerritsen W, Rundle J, Amor S (2011). Critical appraisal of animal models of multiple sclerosis. *Multiple sclerosis (Houndmills, Basingstoke, England)* **17**(6): 647-657.

Baker D, Hankey DJ (2003). Gene therapy in autoimmune, demyelinating disease of the central nervous system. *Gene therapy* **10**(10): 844-853.

Baker D, O'Neill JK, Gschmeissner SE, Wilcox CE, Butter C, Turk JL (1990). Induction of chronic relapsing experimental allergic encephalomyelitis in Biozzi mice. *Journal of neuroimmunology* **28**(3): 261-270.

Baker D, Pryce G, Croxford JL, Brown P, Pertwee RG, Huffman JW, *et al.* (2000). Cannabinoids control spasticity and tremor in a multiple sclerosis model. *Nature* **404**(6773): 84-87.

Baker D, Pryce G, Croxford JL, Brown P, Pertwee RG, Makriyannis A, *et al.* (2001). Endocannabinoids control spasticity in a multiple sclerosis model. *Faseb J* **15**(2): 300-302.

Baker D, Pryce G, Davies WL, Hiley CR (2006a). In silico patent searching reveals a new cannabinoid receptor. *Trends in pharmacological sciences* **27**(1): 1-4.

Baker D, Pryce G, Davies WL, Hiley CR (2006b). In silico patent searching reveals a new cannabinoid receptor. *Trends in Pharmacological Sciences* **27**(1): 1-4.

Baker D, Pryce G, Jackson JS, Bolton C, Giovannoni G (2012). The biology that underpins the therapeutic potential of cannabis-based medicines for the control of spasticity in multiple sclerosis. *Multiple Sclerosis and Related Disorders* **Volume 1**(Issue 2): 64-75.

Balenga NA, Aflaki E, Kargl J, Platzer W, Schroder R, Blattermann S, *et al.* (2011a). GPR55 regulates cannabinoid 2 receptor-mediated responses in human neutrophils. *Cell research* **21**(10): 1452-1469.

Balenga NA, Henstridge CM, Kargl J, Waldhoer M (2011b). Pharmacology, signaling and physiological relevance of the G protein-coupled receptor 55. *Adv Pharmacol* **62**: 251-277.

Barak LS, Ferguson SS, Zhang J, Caron MG (1997). A beta-arrestin/green fluorescent protein biosensor for detecting G protein-coupled receptor activation. *The Journal of biological chemistry* **272**(44): 27497-27500.

Barcellos LF, Oksenberg JR, Begovich AB, Martin ER, Schmidt S, Vittinghoff E, *et al.* (2003). HLA-DR2 dose effect on susceptibility to multiple sclerosis and influence on disease course. *Am J Hum Genet* **72**(3): 710-716.

Barnett MH, Prineas JW (2004). Relapsing and remitting multiple sclerosis: pathology of the newly forming lesion. *Annals of neurology* **55**(4): 458-468.

Battista N, Di Tommaso M, Bari M, Maccarrone M (2012). The endocannabinoid system: an overview. *Frontiers in behavioral neuroscience* **6**: 9.

Begg M, Pacher P, Batkai S, Osei-Hyiaman D, Offertaler L, Mo FM, *et al.* (2005). Evidence for novel cannabinoid receptors. *Pharmacology & therapeutics* **106**(2): 133-145.

Berglund BA, Boring DL, Wilken GH, Makriyannis A, Howlett AC, Lin S (1998). Structural requirements for arachidonylethanolamide interaction with CB1 and CB2 cannabinoid receptors: pharmacology of the carbonyl and ethanolamide groups. *Prostaglandins, leukotrienes, and essential fatty acids* **59**(2): 111-118.

Bettelli E, Baeten D, Jager A, Sobel RA, Kuchroo VK (2006). Myelin oligodendrocyte glycoprotein-specific T and B cells cooperate to induce a Devic-like disease in mice. *The Journal of clinical investigation* **116**(9): 2393-2402.

Bettelli E, Pagany M, Weiner HL, Linington C, Sobel RA, Kuchroo VK (2003). Myelin oligodendrocyte glycoprotein-specific T cell receptor transgenic mice develop spontaneous autoimmune optic neuritis. *The Journal of experimental medicine* **197**(9): 1073-1081.

Bielekova B (2012). Daclizumab Therapy for Multiple Sclerosis. *Neurotherapeutics : the journal of the American Society for Experimental NeuroTherapeutics*.

Bisogno T, Howell F, Williams G, Minassi A, Cascio MG, Ligresti A, *et al.* (2003). Cloning of the first sn1-DAG lipases points to the spatial and temporal regulation of endocannabinoid signaling in the brain. *J Cell Biol* **163**(3): 463-468.

Blankman JL, Simon GM, Cravatt BF (2007). A comprehensive profile of brain enzymes that hydrolyze the endocannabinoid 2-arachidonoylglycerol. *Chem Biol* **14**(12): 1347-1356.

Bloomgren G, Richman S, Hotermans C, Subramanyam M, Goelz S, Natarajan A, *et al.* (2012). Risk of natalizumab-associated progressive multifocal leukoencephalopathy. *The New England journal of medicine* **366**(20): 1870-1880.

Bo L, Peterson JW, Mork S, Hoffman PA, Gallatin WM, Ransohoff RM, *et al.* (1996). Distribution of immunoglobulin superfamily members ICAM-1, -2, -3, and the beta 2 integrin LFA-1 in multiple sclerosis lesions. *Journal of neuropathology and experimental neurology* **55**(10): 1060-1072.

Bolton C, Gates J, Giovannoni G (2013). Serum levels of 25-hydroxy vitamin D in normal Biozzi and C57BL/6 mice and during the course of chronic relapsing experimental autoimmune encephalomyelitis (CR EAE). *Inflammation research : official journal of the European Histamine Research Society ... [et al.]*.

Bondarenko A, Waldeck-Weiermair M, Naghdi S, Poteser M, Malli R, Graier WF (2010). GPR55-dependent and -independent ion signalling in response to lysophosphatidylinositol in endothelial cells. *Br J Pharmacol* **161**(2): 308-320.

Breen C, Brownjohn PW, Ashton JC (2012). The atypical cannabinoid O-1602 increases hind paw sensitisation in the chronic constriction injury model of neuropathic pain. *Neuroscience letters* **508**(2): 119-122.

Brinkmann V (2009). FTY720 (fingolimod) in Multiple Sclerosis: therapeutic effects in the immune and the central nervous system. *Br J Pharmacol* **158**(5): 1173-1182.

Brinkmann V, Billich A, Baumruker T, Heining P, Schmouder R, Francis G, *et al.* (2010). Fingolimod (FTY720): discovery and development of an oral drug to treat multiple sclerosis. *Nat Rev Drug Discov* **9**(11): 883-897.

Broman T (1964). BLOOD-BRAIN BARRIER DAMAGE IN MULTIPLE SCLEROSIS SUPRAVITAL TEST-OBSERVATIONS. *Acta neurologica Scandinavica. Supplementum* **40**: SUPPL 10:21-14.

Brown A, Wise A (2001). Identification of modulators of GPR55 activity *Patent WO00186305 GlaxoSmithKline*.

Brown AJ, Daniels DA, Kassim M, Brown S, Haslam CP, Terrell VR, *et al.* (2011). Pharmacology of GPR55 in yeast and identification of GSK494581A as a mixed-activity glycine transporter subtype 1 inhibitor and GPR55 agonist. *The Journal of pharmacology and experimental therapeutics* **337**(1): 236-246.

Brown AJ, Robin Hiley C (2009). Is GPR55 an anandamide receptor? *Vitamins and hormones* **81**: 111-137.

Brown et al. AB, Alan Wise (2003). Identification of modulators of gpr55 activity.

Brown P (1994). Pathophysiology of spasticity. *Journal of neurology, neurosurgery, and psychiatry* **57**(7): 773-777.

Butter C, Baker D, O'Neill JK, Turk JL (1991). Mononuclear cell trafficking and plasma protein extravasation into the CNS during chronic relapsing experimental allergic encephalomyelitis in Biozzi AB/H mice. *Journal of the neurological sciences* **104**(1): 9-12.

Buttmann M (2010). Treating multiple sclerosis with monoclonal antibodies: a 2010 update. *Expert Rev Neurother* **10**(5): 791-809.

Caldwell MD, Hu SS, Viswanathan S, Bradshaw H, Kelly ME, Straiker A (2013). A GPR18-based signaling system regulates IOP in murine eye. *Br J Pharmacol*.

Capobianco M, Rizzo A, Malucchi S, Sperli F, Di Sapio A, Oggero A, *et al.* (2008). Glatiramer acetate is a treatment option in neutralising antibodies to interferon-beta-positive patients. *Neurol Sci* **29 Suppl 2**: S227-229.

Chang A, Staugaitis SM, Dutta R, Batt CE, Easley KE, Chomyk AM, *et al.* (2012). Cortical remyelination: a new target for repair therapies in multiple sclerosis. *Annals of neurology* **72**(6): 918-926.

Chazotte B (2010). Labeling cytoskeletal F-actin with rhodamine phalloidin or fluorescein phalloidin for imaging. *Cold Spring Harbor protocols* **2010**(5): pdb prot4947.

Chiba T, Ueno S, Obara Y, Nakahata N (2011). A synthetic cannabinoid, CP55940, inhibits lipopolysaccharide-induced cytokine mRNA expression in a cannabinoid receptor-independent mechanism in rat cerebellar granule cells. *The Journal of pharmacy and pharmacology* **63**(5): 636-647.

Choi JW, Gardell SE, Herr DR, Rivera R, Lee CW, Noguchi K, *et al.* (2010). FTY720 (fingolimod) efficacy in an animal model of multiple sclerosis requires astrocyte sphingosine 1-phosphate receptor 1 (S1P1) modulation. *Proc Natl Acad Sci U S A* **108**(2): 751-756.

Chun J, Hartung HP (2010). Mechanism of action of oral fingolimod (FTY720) in multiple sclerosis. *Clinical neuropharmacology* **33**(2): 91-101.

Coles AJ, Wing M, Smith S, Coraddu F, Greer S, Taylor C, *et al.* (1999a). Pulsed monoclonal antibody treatment and autoimmune thyroid disease in multiple sclerosis. *Lancet* **354**(9191): 1691-1695.

Coles AJ, Wing MG, Molyneux P, Paolillo A, Davie CM, Hale G, *et al.* (1999b). Monoclonal antibody treatment exposes three mechanisms underlying the clinical course of multiple sclerosis. *Annals of neurology* **46**(3): 296-304.

Colombo C, Cutson JJ, Yamauchi T, Vinson C, Kadowaki T, Gavrilova O, *et al.* (2002). Transplantation of adipose tissue lacking leptin is unable to reverse the metabolic abnormalities associated with lipoatrophy. *Diabetes* **51**(9): 2727-2733.

Compston A, Coles A (2002a). Multiple sclerosis. *Lancet* **359**(9313): 1221-1231.

Compston A, Coles A (2008). Multiple sclerosis. *Lancet* **372**(9648): 1502-1517.

Compston A, Coles A (2002b). Multiple sclerosis. *The Lancet* **359**(9313): 1221-1231.

Confavreux C, Vukusic S (2004). Non-specific immunosuppressants in the treatment of multiple sclerosis. *Clinical neurology and neurosurgery* **106**(3): 263-269.

Constantinescu CS, Farooqi N, O'Brien K, Gran B (2011). Experimental autoimmune encephalomyelitis (EAE) as a model for multiple sclerosis (MS). *Br J Pharmacol* **164**(4): 1079-1106.

Coquet JM, Middendorp S, van der Horst G, Kind J, Veraar EA, Xiao Y, *et al.* (2013). The CD27 and CD70 costimulatory pathway inhibits effector function of T helper 17 cells and attenuates associated autoimmunity. *Immunity* **38**(1): 53-65.

Corey-Bloom J, Wolfson T, Gamst A, Jin S, Marcotte TD, Bentley H, *et al.* (2012). Smoked cannabis for spasticity in multiple sclerosis: a randomized, placebo-controlled trial. *CMAJ : Canadian Medical Association journal = journal de l'Association medicale canadienne* **184**(10): 1143-1150.

Coward DM (1994). Tizanidine: neuropharmacology and mechanism of action. *Neurology* **44**(11 Suppl 9): S6-10; discussion S10-11.

Cravatt BF, Demarest K, Patricelli MP, Bracey MH, Giang DK, Martin BR, *et al.* (2001). Supersensitivity to anandamide and enhanced endogenous cannabinoid signaling in mice lacking fatty acid amide hydrolase. *Proceedings of the National Academy of Sciences of the United States of America* **98**(16): 9371-9376.

Croning MD, Fricker DG, Komiyama NH, Grant SG (2010). Automated design of genomic Southern blot probes. *BMC genomics* **11**: 74.

Croxford JL (2010). Gene therapy for experimental allergic encephalomyelitis by delivery of inhibitory cytokines or cytokine inhibitors *Thesis*: 258.

Croxford JL, Pryce G, Jackson SJ, Ledent C, Giovannoni G, Pertwee RG, *et al.* (2008). Cannabinoid-mediated neuroprotection, not immunosuppression, may be more relevant to multiple sclerosis. *Journal of neuroimmunology* **193**(1-2): 120-129.

Cudaback E, Marrs W, Moeller T, Stella N (2010). The expression level of CB1 and CB2 receptors determines their efficacy at inducing apoptosis in astrocytomas. *PLoS One* **5**(1): e8702.

Das P, Drescher KM, Geluk A, Bradley DS, Rodriguez M, David CS (2000). Complementation between specific HLA-DR and HLA-DQ genes in transgenic mice determines susceptibility to experimental autoimmune encephalomyelitis. *Human immunology* **61**(3): 279-289.

De Jager PL, Jia X, Wang J, de Bakker PI, Ottoboni L, Aggarwal NT, *et al.* (2009). Meta-analysis of genome scans and replication identify CD6, IRF8 and TNFRSF1A as new multiple sclerosis susceptibility loci. *Nat Genet* **41**(7): 776-782.

DeMorrow S, Glaser S, Francis H, Venter J, Vaculin B, Vaculin S, *et al.* (2007). Opposing actions of endocannabinoids on cholangiocarcinoma growth: recruitment of Fas and Fas ligand to lipid rafts. *The Journal of biological chemistry* **282**(17): 13098-13113.

Denic A, Johnson AJ, Bieber AJ, Warrington AE, Rodriguez M, Pirko I (2011). The relevance of animal models in multiple sclerosis research. *Pathophysiology : the official journal of the International Society for Pathophysiology / ISP* **18**(1): 21-29.

Deutsch SI, Rosse RB, Connor JM, Burket JA, Murphy ME, Fox FJ (2008). Current status of cannabis treatment of multiple sclerosis with an illustrative case presentation of a patient with MS, complex vocal tics, paroxysmal dystonia, and marijuana dependence treated with dronabinol. *CNS Spectr* **13**(5): 393-403.

Devane WA, Hanus L, Breuer A, Pertwee RG, Stevenson LA, Griffin G, *et al.* (1992). Isolation and structure of a brain constituent that binds to the cannabinoid receptor. *Science* **258**(5090): 1946-1949.

Di Marzo V (2008). Targeting the endocannabinoid system: to enhance or reduce? *Nature reviews. Drug discovery* **7**(5): 438-455.

Di Marzo V, De Petrocellis L, Bisogno T (2005). The biosynthesis, fate and pharmacological properties of endocannabinoids. *Handb Exp Pharmacol*(168): 147-185.

Dinh TP, Freund TF, Piomelli D (2002). A role for monoglyceride lipase in 2-arachidonoylglycerol inactivation. *Chem Phys Lipids* **121**(1-2): 149-158.

Dinh TP, Kathuria S, Piomelli D (2004). RNA interference suggests a primary role for monoacylglycerol lipase in the degradation of the endocannabinoid 2-arachidonoylglycerol. *Molecular pharmacology* **66**(5): 1260-1264.

Disanto G, Sandve GK, Berlanga-Taylor AJ, Ragnedda G, Morahan JM, Watson CT, *et al.* (2012). Vitamin D receptor binding, chromatin states and association with multiple sclerosis. *Human molecular genetics* **21**(16): 3575-3586.

- Dobson RGG (2013). Visual guide for Clinicians; Multiple sclerosis. *Clinical publishing*.
- Drmota GP, Groblewski T (2004). *Screening assays for cannabinoid-ligand type modulators of GPR55*.
- Drmota T, Greasley P, Groblewski T (2004). Screening assays for cannabinoid-ligand type modulators of GPR55. *Patent WO2004/074844. AstraZeneca*.
- Duncan M, Davison JS, Sharkey KA (2005). Review article: endocannabinoids and their receptors in the enteric nervous system. *Alimentary pharmacology & therapeutics* **22**(8): 667-683.
- Dutta R, Trapp BD (2011). Mechanisms of neuronal dysfunction and degeneration in multiple sclerosis. *Progress in neurobiology* **93**(1): 1-12.
- Dyment DA, Ebers GC, Sadovnick AD (2004). Genetics of multiple sclerosis. *Lancet neurology* **3**(2): 104-110.
- Eckel RH, Grundy SM, Zimmet PZ (2005). The metabolic syndrome. *Lancet* **365**(9468): 1415-1428.
- Edan G, Miller D, Clanet M, Confavreux C, Lyon-Caen O, Lubetzki C, *et al.* (1997). Therapeutic effect of mitoxantrone combined with methylprednisolone in multiple sclerosis: a randomised multicentre study of active disease using MRI and clinical criteria. *Journal of neurology, neurosurgery, and psychiatry* **62**(2): 112-118.
- Egertova M, Elphick MR (2000). Localisation of cannabinoid receptors in the rat brain using antibodies to the intracellular C-terminal tail of CB. *The Journal of comparative neurology* **422**(2): 159-171.
- Elbegdorj O, Westkaemper RB, Zhang Y (2012). A homology modeling study toward the understanding of three-dimensional structure and putative pharmacological profile of the G-protein coupled receptor GPR55. *Journal of molecular graphics & modelling* **39C**: 50-60.
- Elhofy A, Wang J, Tani M, Fife BT, Kennedy KJ, Bennett J, *et al.* (2005). Transgenic expression of CCL2 in the central nervous system prevents experimental autoimmune encephalomyelitis. *Journal of leukocyte biology* **77**(2): 229-237.
- Ellmerich S, Mycko M, Takacs K, Waldner H, Wahid FN, Boyton RJ, *et al.* (2005). High incidence of spontaneous disease in an HLA-DR15 and TCR transgenic multiple sclerosis model. *Journal of immunology (Baltimore, Md. : 1950)* **174**(4): 1938-1946.
- Elphick MR (2002). Evolution of cannabinoid receptors in vertebrates: identification of a CB(2) gene in the puffer fish *Fugu rubripes*. *Biol Bull* **202**(2): 104-107.

Farina C, Weber MS, Meinl E, Wekerle H, Hohlfeld R (2005). Glatiramer acetate in multiple sclerosis: update on potential mechanisms of action. *Lancet neurology* **4**(9): 567-575.

Farooqi N, Gran B, Constantinescu CS (2010). Are current disease-modifying therapeutics in multiple sclerosis justified on the basis of studies in experimental autoimmune encephalomyelitis? *Journal of neurochemistry* **115**(4): 829-844.

Felder CC, Joyce KE, Briley EM, Mansouri J, Mackie K, Blond O, *et al.* (1995). Comparison of the pharmacology and signal transduction of the human cannabinoid CB1 and CB2 receptors. *Molecular pharmacology* **48**(3): 443-450.

Flechter S, Vardi J, Pollak L, Rabey JM (2002). Comparison of glatiramer acetate (Copaxone) and interferon beta-1b (Betaferon) in multiple sclerosis patients: an open-label 2-year follow-up. *Journal of the neurological sciences* **197**(1-2): 51-55.

Fonseca BM, Teixeira NA, Almada M, Taylor AH, Konje JC, Correia-da-Silva G (2011). Modulation of the novel cannabinoid receptor - GPR55 - during rat fetoplacental development. *Placenta* **32**(6): 462-469.

Ford LA, Roelofs AJ, Anavi-Goffer S, Mowat L, Simpson DG, Irving AJ, *et al.* (2010). A role for L-alpha-lysophosphatidylinositol and GPR55 in the modulation of migration, orientation and polarization of human breast cancer cells. *Br J Pharmacol* **160**(3): 762-771.

Fox RJ, Thompson A, Baker D, Baneke P, Brown D, Browne P, *et al.* (2012). Setting a research agenda for progressive multiple sclerosis: the International Collaborative on Progressive MS. *Multiple sclerosis (Houndmills, Basingstoke, England)* **18**(11): 1534-1540.

Fredriksson R, Lagerstrom MC, Lundin LG, Schioth HB (2003). The G-protein-coupled receptors in the human genome form five main families. Phylogenetic analysis, paralogon groups, and fingerprints. *Molecular pharmacology* **63**(6): 1256-1272.

Freund J, Stern ER, Pisani TM (1947). Isoallergic encephalomyelitis and radiculitis in guinea pigs after one injection of brain and Mycobacteria in water-in-oil emulsion. *Journal of immunology (Baltimore, Md. : 1950)* **57**(2): 179-194.

Friese MA, Montalban X, Willcox N, Bell JI, Martin R, Fugger L (2006). The value of animal models for drug development in multiple sclerosis. *Brain : a journal of neurology* **129**(Pt 8): 1940-1952.

Galiegue S, Mary S, Marchand J, Dussossoy D, Carriere D, Carayon P, *et al.* (1995). Expression of central and peripheral cannabinoid receptors in human immune tissues and leukocyte subpopulations. *Eur J Biochem* **232**(1): 54-61.

Gantz I, Muraoka A, Yang YK, Samuelson LC, Zimmerman EM, Cook H, *et al.* (1997). Cloning and chromosomal localization of a gene (GPR18) encoding a novel seven transmembrane receptor highly expressed in spleen and testis. *Genomics* **42**(3): 462-466.

Gao Y, Vasilyev DV, Goncalves MB, Howell FV, Hobbs C, Reisenberg M, *et al.* (2010). Loss of retrograde endocannabinoid signaling and reduced adult neurogenesis in diacylglycerol lipase knock-out mice. *The Journal of neuroscience : the official journal of the Society for Neuroscience* **30**(6): 2017-2024.

Gaoni Y, Mechoulam R (1964). Isolation, Structure, and Partial Synthesis of an Active Constituent of Hashish. *Journal of the American Chemical Society* **86**(8): 1646-1647.

Genain CP, Nguyen MH, Letvin NL, Pearl R, Davis RL, Adelman M, *et al.* (1995). Antibody facilitation of multiple sclerosis-like lesions in a nonhuman primate. *The Journal of clinical investigation* **96**(6): 2966-2974.

Geurts JJ, Kooi EJ, Witte ME, van der Valk P (2010). Multiple sclerosis as an "inside-out" disease. *Annals of neurology* **68**(5): 767-768; author reply 768.

Glass M, Dragunow M, Faull RL (1997a). Cannabinoid receptors in the human brain: a detailed anatomical and quantitative autoradiographic study in the fetal, neonatal and adult human brain. *Neuroscience* **77**(2): 299-318.

Glass M, Felder CC (1997b). Concurrent stimulation of cannabinoid CB1 and dopamine D2 receptors augments cAMP accumulation in striatal neurons: evidence for a Gs linkage to the CB1 receptor. *The Journal of neuroscience : the official journal of the Society for Neuroscience* **17**(14): 5327-5333.

Gold R, Linington C, Lassmann H (2006). Understanding pathogenesis and therapy of multiple sclerosis via animal models: 70 years of merits and culprits in experimental autoimmune encephalomyelitis research. *Brain : a journal of neurology* **129**(Pt 8): 1953-1971.

Goldenberg MM (2012). Multiple Sclerosis Review. *P T* **37**(3): 175-184.

Gong JP, Onaivi ES, Ishiguro H, Liu QR, Tagliaferro PA, Brusco A, *et al.* (2006). Cannabinoid CB2 receptors: immunohistochemical localization in rat brain. *Brain research* **1071**(1): 10-23.

Goodman AD, Brown TR, Krupp LB, Schapiro RT, Schwid SR, Cohen R, *et al.* (2009). Sustained-release oral fampridine in multiple sclerosis: a randomised, double-blind, controlled trial. *Lancet* **373**(9665): 732-738.

Graham DB, Akilesh HM, Gmyrek GB, Piccio L, Gilfillan S, Sim J, *et al.* (2010). ITAM signaling in dendritic cells controls T helper cell priming by regulating MHC class II recycling. *Blood* **116**(17): 3208-3218.

Gran OBK, Fitzgerald D, Rostami A (2007). *Experimental Autoimmune Encephalomyelitis*.: Springer: Heidelberg, p. 19.

Grimsey NL, Goodfellow CE, Scotter EL, Dowie MJ, Glass M, Graham ES (2008). Specific detection of CB1 receptors; cannabinoid CB1 receptor antibodies are not all created equal! *J Neurosci Methods* **171**(1): 78-86.

Grossman RI, Gonzalez-Scarano F, Atlas SW, Galetta S, Silberberg DH (1986). Multiple sclerosis: gadolinium enhancement in MR imaging. *Radiology* **161**(3): 721-725.

Hajos N, Katona I, Naiem SS, MacKie K, Ledent C, Mody I, *et al.* (2000). Cannabinoids inhibit hippocampal GABAergic transmission and network oscillations. *The European journal of neuroscience* **12**(9): 3239-3249.

Hajos N, Ledent C, Freund TF (2001). Novel cannabinoid-sensitive receptor mediates inhibition of glutamatergic synaptic transmission in the hippocampus. *Neuroscience* **106**(1): 1-4.

Hall GL, Compston A, Scolding NJ (1997). Beta-interferon and multiple sclerosis. *Trends Neurosci* **20**(2): 63-67.

Hammond SR, English DR, McLeod JG (2000). The age-range of risk of developing multiple sclerosis: evidence from a migrant population in Australia. *Brain : a journal of neurology* **123** (Pt 5): 968-974.

Hauser SL, Oksenberg JR (2006). The neurobiology of multiple sclerosis: genes, inflammation, and neurodegeneration. *Neuron* **52**(1): 61-76.

Healey DG, Baker D, Gschmeissner SE, Turk JL (1987). An antigenic determinant common to lymphocytes and Langerhans cells of the guinea pig. *Int Arch Allergy Appl Immunol* **82**(2): 120-124.

Heijmans N, Smith PA, Morris-Downes MM, Pryce G, Baker D, Donaldson AV, *et al.* (2005). Encephalitogenic and tolerogenic potential of altered peptide ligands of MOG and PLP in Biozzi ABH mice. *Journal of neuroimmunology* **167**(1-2): 23-33.

Heinemann A, Shahbazian A, Holzer P (1999). Cannabinoid inhibition of guinea-pig intestinal peristalsis via inhibition of excitatory and activation of inhibitory neural pathways. *Neuropharmacology* **38**(9): 1289-1297.

Hemmer B, Stuve O, Kieseier B, Schellekens H, Hartung HP (2005). Immune response to immunotherapy: the role of neutralising antibodies to interferon beta in the treatment of multiple sclerosis. *Lancet neurology* **4**(7): 403-412.

Henstridge CM, Balenga NA, Ford LA, Ross RA, Waldhoer M, Irving AJ (2009). The GPR55 ligand L-alpha-lysophosphatidylinositol promotes RhoA-dependent Ca²⁺ signaling and NFAT activation. *FASEB J* **23**(1): 183-193.

Henstridge CM, Balenga NA, Kargl J, Andradas C, Brown AJ, Irving A, *et al.* (2011). Minireview: recent developments in the physiology and pathology of the lysophosphatidylinositol-sensitive receptor GPR55. *Mol Endocrinol* **25**(11): 1835-1848.

Henstridge CM, Balenga NA, Schroder R, Kargl JK, Platzer W, Martini L, *et al.* (2010). GPR55 ligands promote receptor coupling to multiple signalling pathways. *Br J Pharmacol*.

Herkenham M, Lynn AB, Little MD, Johnson MR, Melvin LS, de Costa BR, *et al.* (1990). Cannabinoid receptor localization in brain. *Proceedings of the National Academy of Sciences of the United States of America* **87**(5): 1932-1936.

Heynen-Genel S, Dahl R, Shi S, Milan L, Hariharan S, Bravo Y, *et al.* (2010a). Screening for Selective Ligands for GPR55 - Agonists. In: (ed)[^](eds). *Probe Reports from the NIH Molecular Libraries Program*, edn. Bethesda MD. p[^]pp.

Heynen-Genel S, Dahl R, Shi S, Milan L, Hariharan S, Sergienko E, *et al.* (2010b). Screening for Selective Ligands for GPR55 - Antagonists. In: (ed)[^](eds). *Probe Reports from the NIH Molecular Libraries Program*, edn. Bethesda MD. p[^]pp.

Hiley CR, Kaup SS (2007). GPR55 and the vascular receptors for cannabinoids. *Br J Pharmacol* **152**(5): 559-561.

Hilliard A, Stott C, Wright S, Guy G, Pryce G, Al-Izki S, *et al.* (2012). Evaluation of the Effects of Sativex (THC BDS: CBD BDS) on Inhibition of Spasticity in a Chronic Relapsing Experimental Allergic Autoimmune Encephalomyelitis: A Model of Multiple Sclerosis. *ISRN neurology* **2012**: 802649.

Ho WS (2010). Angiogenesis: a new physiological role for N-arachidonoyl serine and GPR55? *Br J Pharmacol* **160**(7): 1580-1582.

Ho WS, Hiley CR (2004). Vasorelaxant activities of the putative endocannabinoid virodhamine in rat isolated small mesenteric artery. *The Journal of pharmacy and pharmacology* **56**(7): 869-875.

Hoi PM, Hiley CR (2006). Vasorelaxant effects of oleamide in rat small mesenteric artery indicate action at a novel cannabinoid receptor. *Br J Pharmacol* **147**(5): 560-568.

Hoi PM, Visintin C, Okuyama M, Gardiner SM, Kaup SS, Bennett T, *et al.* (2007a). Vascular pharmacology of a novel cannabinoid-like compound, 3-(5-dimethylcarbamoyl-pent-1-enyl)-N-(2-hydroxy-1-methyl-ethyl)benzamide (VSN16) in the rat. *British Journal of Pharmacology* **152**(5): 751-764.

Hoi PM, Visintin C, Okuyama M, Gardiner SM, Kaup SS, Bennett T, *et al.* (2007b). Vascular pharmacology of a novel cannabinoid-like compound, 3-(5-dimethylcarbamoyl-pent-1-enyl)-N-(2-hydroxy-1-methyl-ethyl)benzamide (VSN16) in the rat. *Br J Pharmacol* **152**(5): 751-764.

Hong J, Tejada-Simon MV, Rivera VM, Zang YC, Zhang JZ (2002). Anti-viral properties of interferon beta treatment in patients with multiple sclerosis. *Multiple sclerosis (Houndmills, Basingstoke, England)* **8**(3): 237-242.

Howlett AC, Barth F, Bonner TI, Cabral G, Casellas P, Devane WA, *et al.* (2002). International Union of Pharmacology. XXVII. Classification of cannabinoid receptors. *Pharmacol Rev* **54**(2): 161-202.

Howlett AC, Blume LC, Dalton GD (2010). CB(1) cannabinoid receptors and their associated proteins. *Current medicinal chemistry* **17**(14): 1382-1393.

Howlett AC, Breivogel CS, Childers SR, Deadwyler SA, Hampson RE, Porrino LJ (2004). Cannabinoid physiology and pharmacology: 30 years of progress. *Neuropharmacology* **47 Suppl 1**: 345-358.

Howlett AC, Fleming RM (1984). Cannabinoid inhibition of adenylate cyclase. Pharmacology of the response in neuroblastoma cell membranes. *Molecular pharmacology* **26**(3): 532-538.

Huang L, Ramirez JC, Frampton GA, Golden LE, Quinn MA, Pae HY, *et al.* (2011). Anandamide exerts its antiproliferative actions on cholangiocarcinoma by activation of the GPR55 receptor. *Lab Invest* **91**(7): 1007-1017.

Hutchinson M, Kappos L, Calabresi PA, Confavreux C, Giovannoni G, Galetta SL, *et al.* (2009). The efficacy of natalizumab in patients with relapsing multiple sclerosis: subgroup analyses of AFFIRM and SENTINEL. *J Neurol* **256**(3): 405-415.

Hwang AS, Wilcox GL (1989). Baclofen, gamma-aminobutyric acidB receptors and substance P in the mouse spinal cord. *The Journal of pharmacology and experimental therapeutics* **248**(3): 1026-1033.

Idris AI, Ralston SH (2010). Cannabinoids and bone: friend or foe? *Calcified tissue international* **87**(4): 285-297.

Idris AI, Sophocleous A, Landao-Bassonga E, van't Hof RJ, Ralston SH (2008). Regulation of bone mass, osteoclast function, and ovariectomy-induced bone loss by the type 2 cannabinoid receptor. *Endocrinology* **149**(11): 5619-5626.

Informatics MG (2012). TIGM.

Inglese M, Mancardi GL, Pagani E, Rocca MA, Murialdo A, Saccardi R, *et al.* (2004). Brain tissue loss occurs after suppression of enhancement in patients with multiple sclerosis treated with autologous haematopoietic stem cell transplantation. *Journal of neurology, neurosurgery, and psychiatry* **75**(4): 643-644.

Innes JR (1951). Experimental "allergic" encephalitis: attempts to produce the disease in sheep and goats. *Journal of comparative pathology* **61**(4): 241-250.

Issazadeh S, Abdallah K, Chitnis T, Chandraker A, Wells AD, Turka LA, *et al.* (2000). Role of passive T-cell death in chronic experimental autoimmune encephalomyelitis. *The Journal of clinical investigation* **105**(8): 1109-1116.

Izzo AA, Sharkey KA (2010). Cannabinoids and the gut: new developments and emerging concepts. *Pharmacology & therapeutics* **126**(1): 21-38.

Jarai Z, Wagner JA, Varga K, Lake KD, Compton DR, Martin BR, *et al.* (1999). Cannabinoid-induced mesenteric vasodilation through an endothelial site distinct from CB1 or CB2 receptors. *Proceedings of the National Academy of Sciences of the United States of America* **96**(24): 14136-14141.

Jenkin KA, McAinch AJ, Grinfeld E, Hryciw DH (2010). Role for cannabinoid receptors in human proximal tubular hypertrophy. *Cell Physiol Biochem* **26**(6): 879-886.

Johns DG, Behm DJ, Walker DJ, Ao Z, Shapland EM, Daniels DA, *et al.* (2007). The novel endocannabinoid receptor GPR55 is activated by atypical cannabinoids but does not mediate their vasodilator effects. *Br J Pharmacol* **152**(5): 825-831.

Kaczocha M, Glaser ST, Deutsch DG (2009). Identification of intracellular carriers for the endocannabinoid anandamide. *Proceedings of the National Academy of Sciences of the United States of America* **106**(15): 6375-6380.

Kamen L, Henney HR, 3rd, Runyan JD (2008). A practical overview of tizanidine use for spasticity secondary to multiple sclerosis, stroke, and spinal cord injury. *Current medical research and opinion* **24**(2): 425-439.

Kammermeier PJ, Davis MI, Ikeda SR (2003). Specificity of metabotropic glutamate receptor 2 coupling to G proteins. *Molecular pharmacology* **63**(1): 183-191.

Kappos L, Gold R, Miller DH, Macmanus DG, Havrdova E, Limmroth V, *et al.* (2008). Efficacy and safety of oral fumarate in patients with relapsing-remitting multiple sclerosis: a multicentre, randomised, double-blind, placebo-controlled phase IIb study. *Lancet* **372**(9648): 1463-1472.

Kapur A, Zhao P, Sharir H, Bai Y, Caron MG, Barak LS, *et al.* (2009). Atypical responsiveness of the orphan receptor GPR55 to cannabinoid ligands. *The Journal of biological chemistry* **284**(43): 29817-29827.

Kargl J, Balenga N, Parzmair GP, Brown AJ, Heinemann A, Waldhoer M (2012). The Cannabinoid Receptor CB1 Modulates the Signaling Properties of the Lysophosphatidylinositol Receptor GPR55. *The Journal of biological chemistry* **287**(53): 44234-44248.

Kargl J, Balenga NA, Platzer W, Martini L, Whistler JL, Waldhoer M (2011). The GPCR-associated sorting protein 1 regulates ligand-induced down-regulation of GPR55. *Br J Pharmacol* **165**(8): 2611-2619.

Katona I, Freund TF (2012). Multiple functions of endocannabinoid signaling in the brain. *Annual review of neuroscience* **35**: 529-558.

Kaur G, Trowsdale J, Fugger L (2012). Natural killer cells and their receptors in multiple sclerosis. *Brain : a journal of neurology*.

Kiene M, Marzi A, Urbanczyk A, Bertram S, Fisch T, Nehlmeier I, *et al.* (2012). The role of the alternative coreceptor GPR15 in SIV tropism for human cells. *Virology* **433**(1): 73-84.

Klein TW, Newton C, Larsen K, Lu L, Perkins I, Nong L, *et al.* (2003). The cannabinoid system and immune modulation. *Journal of leukocyte biology* **74**(4): 486-496.

Kmietowicz Z (2010). Cannabis based drug is licensed for spasticity in patients with MS. *BMJ* **340**: c3363.

Kobayashi Y, Arai S, Waku K, Sugiura T (2001). Activation by 2-arachidonoylglycerol, an endogenous cannabinoid receptor ligand, of p42/44 mitogen-activated protein kinase in HL-60 cells. *J Biochem* **129**(5): 665-669.

Kofler DM, Severson CA, Mousissian N, De Jager PL, Hafler DA (2011). The CD6 multiple sclerosis susceptibility allele is associated with alterations in CD4+ T cell proliferation. *Journal of immunology (Baltimore, Md. : 1950)* **187**(6): 3286-3291.

Kohno M, Hasegawa H, Inoue A, Muraoka M, Miyazaki T, Oka K, *et al.* (2006). Identification of N-arachidonylglycine as the endogenous ligand for orphan G-protein-coupled receptor GPR18. *Biochemical and biophysical research communications* **347**(3): 827-832.

Kotsikorou E, Madrigal KE, Hurst DP, Sharir H, Lynch DL, Heynen-Genel S, *et al.* (2011). Identification of the GPR55 agonist binding site using a novel set of high-potency GPR55 selective ligands. *Biochemistry* **50**(25): 5633-5647.

Kozela E, Lev N, Kaushansky N, Eilam R, Rimmerman N, Levy R, *et al.* (2011). Cannabidiol inhibits pathogenic T cells, decreases spinal microglial activation and ameliorates multiple sclerosis-like disease in C57BL/6 mice. *Br J Pharmacol* **163**(7): 1507-1519.

Kroeze WK, Sheffler DJ, Roth BL (2003). G-protein-coupled receptors at a glance. *J Cell Sci* **116**(Pt 24): 4867-4869.

Kurtzke JF (1993). Epidemiologic evidence for multiple sclerosis as an infection. *Clinical microbiology reviews* **6**(4): 382-427.

Kurtzke JF (1975). A reassessment of the distribution of multiple sclerosis. Part one. *Acta neurologica Scandinavica* **51**(2): 110-136.

Larionov A, Krause A, Miller W (2005). A standard curve based method for relative real time PCR data processing. *BMC Bioinformatics* **6**: 62.

Lauckner JE, Jensen JB, Chen HY, Lu HC, Hille B, Mackie K (2008). GPR55 is a cannabinoid receptor that increases intracellular calcium and inhibits M current. *Proceedings of the National Academy of Sciences of the United States of America* **105**(7): 2699-2704.

Lauffer L, Iakoubov R, Brubaker PL (2008). GPR119: "double-dipping" for better glycemic control. *Endocrinology* **149**(5): 2035-2037.

Leung D, Saghatelian A, Simon GM, Cravatt BF (2006). Inactivation of N-acyl phosphatidylethanolamine phospholipase D reveals multiple mechanisms for the biosynthesis of endocannabinoids. *Biochemistry* **45**(15): 4720-4726.

Levine S, Sowinski R (1973). Experimental allergic encephalomyelitis in inbred and outbred mice. *Journal of immunology (Baltimore, Md. : 1950)* **110**(1): 139-143.

Li K, Feng JY, Li YY, Yuece B, Lin XH, Yu LY, *et al.* (2013). Anti-inflammatory role of cannabidiol and o-1602 in cerulein-induced acute pancreatitis in mice. *Pancreas* **42**(1): 123-129.

Liblau RS, Singer SM, McDevitt HO (1995). Th1 and Th2 CD4+ T cells in the pathogenesis of organ-specific autoimmune diseases. *Immunol Today* **16**(1): 34-38.

Limmroth V (2012). Multiple sclerosis: Oral BG12 for treatment of relapsing-remitting MS. *Nature reviews. Neurology* **9**(1): 8-10.

Lin XH, Yuece B, Li YY, Feng YJ, Feng JY, Yu LY, *et al.* (2011). A novel CB receptor GPR55 and its ligands are involved in regulation of gut movement in rodents. *Neurogastroenterol Motil* **23**(9): 862-e342.

Lipina C, Rastedt W, Irving AJ, Hundal HS (2012). New vistas for treatment of obesity and diabetes? Endocannabinoid signalling and metabolism in the modulation of energy balance. *BioEssays : news and reviews in molecular, cellular and developmental biology* **34**(8): 681-691.

Lipton MM, Freund J (1952). Encephalomyelitis in the rat following intracutaneous injection of central nervous system tissue with adjuvant. *Proc Soc Exp Biol Med* **81**(1): 260-261.

Lulu S, Waubant E (2012). Humoral-Targeted Immunotherapies in Multiple Sclerosis. *Neurotherapeutics : the journal of the American Society for Experimental NeuroTherapeutics*.

Lumsden CE (1949). Experimental allergic encephalomyelitis. *Brain : a journal of neurology* **72**(Pt. 2): 198-226.

Mackie K, Lai Y, Westenbroek R, Mitchell R (1995). Cannabinoids activate an inwardly rectifying potassium conductance and inhibit Q-type calcium currents in AtT20 cells transfected with rat brain cannabinoid receptor. *The Journal of neuroscience : the official journal of the Society for Neuroscience* **15**(10): 6552-6561.

Maresz K, Pryce G, Ponomarev ED, Marsicano G, Croxford JL, Shriver LP, *et al.* (2007). Direct suppression of CNS autoimmune inflammation via the cannabinoid receptor CB1 on neurons and CB2 on autoreactive T cells. *Nature medicine* **13**(4): 492-497.

Martin BR, Wiley JL (2004). Mechanism of action of cannabinoids: how it may lead to treatment of cachexia, emesis, and pain. *The journal of supportive oncology* **2**(4): 305-314; discussion 314-306.

Martinelli Boneschi F, Rovaris M, Capra R, Comi G (2005). Mitoxantrone for multiple sclerosis. *Cochrane database of systematic reviews (Online)*(4): CD002127.

Mathey EK, Derfuss T, Storch MK, Williams KR, Hales K, Woolley DR, *et al.* (2007). Neurofascin as a novel target for autoantibody-mediated axonal injury. *The Journal of experimental medicine* **204**(10): 2363-2372.

Matsuda LA, Lolait SJ, Brownstein MJ, Young AC, Bonner TI (1990). Structure of a cannabinoid receptor and functional expression of the cloned cDNA. *Nature* **346**(6284): 561-564.

McHugh D, Hu SS, Rimmerman N, Juknat A, Vogel Z, Walker JM, *et al.* (2010). N-arachidonoyl glycine, an abundant endogenous lipid, potently drives directed cellular migration through GPR18, the putative abnormal cannabidiol receptor. *BMC neuroscience* **11**: 44.

McQualter JL, Bernard CC (2007). Multiple sclerosis: a battle between destruction and repair. *Journal of neurochemistry* **100**(2): 295-306.

Mechoulam R, Peters M, Murillo-Rodriguez E, Hanus LO (2007). Cannabidiol--recent advances. *Chemistry & biodiversity* **4**(8): 1678-1692.

Melck D, Bisogno T, De Petrocellis L, Chuang H-h, Julius D, Bifulco M, *et al.* (1999). Unsaturated Long-Chain N-Acyl-vanillyl-amides (N-AVAMs): Vanilloid Receptor Ligands That Inhibit Anandamide-Facilitated Transport and Bind to CB1 Cannabinoid Receptors. *Biochemical and Biophysical Research Communications* **262**(1): 275-284.

Meleger AL (2006). Muscle relaxants and antispasticity agents. *Physical medicine and rehabilitation clinics of North America* **17**(2): 401-413.

Milanov IG (1992). Mechanisms of baclofen action on spasticity. *Acta neurologica Scandinavica* **85**(5): 305-310.

Mokhtarian F, McFarlin DE, Raine CS (1984). Adoptive transfer of myelin basic protein-sensitized T cells produces chronic relapsing demyelinating disease in mice. *Nature* **309**(5966): 356-358.

Moreno-Navarrete JM, Catalan V, Whyte L, Diaz-Arteaga A, Vazquez-Martinez R, Rotellar F, *et al.* (2012). The L-alpha-lysophosphatidylinositol/GPR55 system and its potential role in human obesity. *Diabetes* **61**(2): 281-291.

Morrison LR (1947). Disseminated encephalomyelitis experimentally produced by the use of homologous antigen. *Archives of neurology and psychiatry* **58**(4): 391-416.

Muir VJ, Plosker GL (2011). Cladribine tablets: in relapsing-remitting multiple sclerosis. *CNS Drugs* **25**(3): 239-249.

Mulroy E, Joyce E, Scott J, Melling J, Goggin C, Mahon N, *et al.* (2012). Long-term risk of leukaemia or cardiomyopathy after mitoxantrone therapy for multiple sclerosis. *European neurology* **67**(1): 45-47.

Munro S, Thomas KL, Abu-Shaar M (1993). Molecular characterization of a peripheral receptor for cannabinoids. *Nature* **365**(6441): 61-65.

Nelson PN, Reynolds GM, Waldron EE, Ward E, Giannopoulos K, Murray PG (2000). Monoclonal antibodies. *Molecular pathology : MP* **53**(3): 111-117.

Neuhaus O, Farina C, Wekerle H, Hohlfeld R (2001). Mechanisms of action of glatiramer acetate in multiple sclerosis. *Neurology* **56**(6): 702-708.

Nguyen T, Nioi P, Pickett CB (2009). The Nrf2-antioxidant response element signaling pathway and its activation by oxidative stress. *The Journal of biological chemistry* **284**(20): 13291-13295.

Nielsen JB, Crone C, Hultborn H (2007). The spinal pathophysiology of spasticity--from a basic science point of view. *Acta physiologica (Oxford, England)* **189**(2): 171-180.

Novotna A, Mares J, Ratcliffe S, Novakova I, Vachova M, Zapletalova O, *et al.* (2011). A randomized, double-blind, placebo-controlled, parallel-group, enriched-design study of nabiximols* (Sativex((R))), as add-on therapy, in subjects with refractory spasticity caused by multiple sclerosis. *Eur J Neurol*.

Nunez E, Benito C, Pazos MR, Barbachano A, Fajardo O, Gonzalez S, *et al.* (2004). Cannabinoid CB2 receptors are expressed by perivascular microglial cells in the human brain: an immunohistochemical study. *Synapse* **53**(4): 208-213.

O'Dowd BF, Nguyen T, Marchese A, Cheng R, Lynch KR, Heng HH, *et al.* (1998). Discovery of three novel G-protein-coupled receptor genes. *Genomics* **47**(2): 310-313.

O'Neill JK, Baker D, Davison AN, Allen SJ, Butter C, Waldmann H, *et al.* (1993). Control of immune-mediated disease of the central nervous system with monoclonal (CD4-specific) antibodies. *Journal of neuroimmunology* **45**(1-2): 1-14.

Obara Y, Ueno S, Yanagihata Y, Nakahata N (2011). Lysophosphatidylinositol causes neurite retraction via GPR55, G13 and RhoA in PC12 cells. *PLoS One* **6**(8): e24284.

Ofek O, Karsak M, Leclerc N, Fogel M, Frenkel B, Wright K, *et al.* (2006). Peripheral cannabinoid receptor, CB2, regulates bone mass. *Proceedings of the National Academy of Sciences of the United States of America* **103**(3): 696-701.

Offertaler L, Mo FM, Batkai S, Liu J, Begg M, Razdan RK, *et al.* (2003). Selective ligands and cellular effectors of a G protein-coupled endothelial cannabinoid receptor. *Molecular pharmacology* **63**(3): 699-705.

Oka S, Nakajima K, Yamashita A, Kishimoto S, Sugiura T (2007). Identification of GPR55 as a lysophosphatidylinositol receptor. *Biochemical and biophysical research communications* **362**(4): 928-934.

Oka S, Ota R, Shima M, Yamashita A, Sugiura T (2010). GPR35 is a novel lysophosphatidic acid receptor. *Biochemical and biophysical research communications* **395**(2): 232-237.

Oka S, Toshida T, Maruyama K, Nakajima K, Yamashita A, Sugiura T (2009). 2-Arachidonoyl-sn-glycero-3-phosphoinositol: a possible natural ligand for GPR55. *J Biochem* **145**(1): 13-20.

Okamoto Y, Tsuboi K, Ueda N (2009). Enzymatic formation of anandamide. *Vitamins and hormones* **81**: 1-24.

Oksenberg JR, Barcellos LF, Cree BA, Baranzini SE, Bugawan TL, Khan O, *et al.* (2004). Mapping multiple sclerosis susceptibility to the HLA-DR locus in African Americans. *Am J Hum Genet* **74**(1): 160-167.

Okuda Y, Okuda M, Bernard CC (2002). Gender does not influence the susceptibility of C57BL/6 mice to develop chronic experimental autoimmune encephalomyelitis induced by myelin oligodendrocyte glycoprotein. *Immunology letters* **81**(1): 25-29.

Onaivi ES, Ishiguro H, Gu S, Liu QR (2012). CNS effects of CB2 cannabinoid receptors: beyond neuro-immuno-cannabinoid activity. *J Psychopharmacol* **26**(1): 92-103.

Oreja-Guevara C (2012). Clinical efficacy and effectiveness of Sativex, a combined cannabinoid medicine, in multiple sclerosis-related spasticity. *Expert review of neurotherapeutics* **12**(4 Suppl): 3-8.

Overton HA, Babbs AJ, Doel SM, Fyfe MC, Gardner LS, Griffin G, *et al.* (2006). Deorphanization of a G protein-coupled receptor for oleoylethanolamide and its use in the discovery of small-molecule hypophagic agents. *Cell Metab* **3**(3): 167-175.

Palazuelos J, Davoust N, Julien B, Hatterer E, Aguado T, Mechoulam R, *et al.* (2008). The CB(2) cannabinoid receptor controls myeloid progenitor trafficking: involvement in the pathogenesis of an animal model of multiple sclerosis. *The Journal of biological chemistry* **283**(19): 13320-13329.

Papadopoulou A, Kappos L, Sprenger T (2012). Teriflunomide for oral therapy in multiple sclerosis. *Expert review of clinical pharmacology* **5**(6): 617-628.

Parmar HW (2009). International Cannabinoid Research Society meeting. *J Biol Chem*, **283**: 21054-21064.

Patrikios P, Stadelmann C, Kutzelnigg A, Rauschka H, Schmidbauer M, Laursen H, *et al.* (2006). Remyelination is extensive in a subset of multiple sclerosis patients. *Brain : a journal of neurology* **129**(Pt 12): 3165-3172.

Paul F, Dorr J, Wurfel J, Vogel HP, Zipp F (2009). Early mitoxantrone-induced cardiotoxicity in secondary progressive multiple sclerosis. *BMJ case reports* **2009**.

Pearson G, Robinson F, Beers Gibson T, Xu BE, Karandikar M, Berman K, *et al.* (2001). Mitogen-activated protein (MAP) kinase pathways: regulation and physiological functions. *Endocr Rev* **22**(2): 153-183.

Perez-Gomez E, Andradas C, Flores JM, Quintanilla M, Paramio JM, Guzman M, *et al.* (2012). The orphan receptor GPR55 drives skin carcinogenesis and is upregulated in human squamous cell carcinomas. *Oncogene*.

Perry JS, Han S, Xu Q, Herman ML, Kennedy LB, Csako G, *et al.* (2012). Inhibition of LT α cell development by CD25 blockade is associated with decreased intrathecal inflammation in multiple sclerosis. *Science translational medicine* **4**(145): 145ra106.

Pertwee RG (2002). Cannabinoids and multiple sclerosis. *Pharmacology & therapeutics* **95**(2): 165-174.

Pertwee RG (2008). The diverse CB $_1$ and CB $_2$ receptor pharmacology of three plant cannabinoids: delta9-tetrahydrocannabinol, cannabidiol and delta9-tetrahydrocannabivarin. *Br J Pharmacol* **153**(2): 199-215.

Pertwee RG (2009). Emerging strategies for exploiting cannabinoid receptor agonists as medicines. *Br J Pharmacol* **156**(3): 397-411.

Pertwee RG (2007). GPR55: a new member of the cannabinoid receptor clan? *Br J Pharmacol* **152**(7): 984-986.

Pertwee RG (2005a). Pharmacological actions of cannabinoids. *Handb Exp Pharmacol*(168): 1-51.

Pertwee RG (2005b). The therapeutic potential of drugs that target cannabinoid receptors or modulate the tissue levels or actions of endocannabinoids. *AAPS J* **7**(3): E625-654.

Pertwee RG, Gibson TM, Stevenson LA, Ross RA, Banner WK, Saha B, *et al.* (2000). O-1057, a potent water-soluble cannabinoid receptor agonist with antinociceptive properties. *Br J Pharmacol* **129**(8): 1577-1584.

Pertwee RG, Howlett AC, Abood ME, Alexander SP, Di Marzo V, Elphick MR, *et al.* (2010). International Union of Basic and Clinical Pharmacology. LXXIX. Cannabinoid receptors and their ligands: beyond CB $_1$ and CB $_2$. *Pharmacol Rev* **62**(4): 588-631.

Pettit DA, Harrison MP, Olson JM, Spencer RF, Cabral GA (1998). Immunohistochemical localization of the neural cannabinoid receptor in rat brain. *Journal of neuroscience research* **51**(3): 391-402.

Pierrot-Deseilligny C (2009). Clinical implications of a possible role of vitamin D in multiple sclerosis. *J Neurol* **256**(9): 1468-1479.

Pierson E, Simmons SB, Castelli L, Goverman JM (2012). Mechanisms regulating regional localization of inflammation during CNS autoimmunity. *Immunological reviews* **248**(1): 205-215.

Pietr M, Kozela E, Levy R, Rimmerman N, Lin YH, Stella N, *et al.* (2009). Differential changes in GPR55 during microglial cell activation. *FEBS Lett* **583**(12): 2071-2076.

Pineiro R, Falasca M (2012). Lysophosphatidylinositol signalling: new wine from an old bottle. *Biochimica et biophysica acta* **1821**(4): 694-705.

Pineiro R, Maffucci T, Falasca M (2011). The putative cannabinoid receptor GPR55 defines a novel autocrine loop in cancer cell proliferation. *Oncogene*.

Pineiro R, Maffucci T, Falasca M (2010). The putative cannabinoid receptor GPR55 defines a novel autocrine loop in cancer cell proliferation. *Oncogene*.

Piomelli D (2003). The molecular logic of endocannabinoid signalling. *Nat Rev Neurosci* **4**(11): 873-884.

Polman CH, Reingold SC, Banwell B, Clanet M, Cohen JA, Filippi M, *et al.* (2011). Diagnostic criteria for multiple sclerosis: 2010 revisions to the McDonald criteria. *Annals of neurology* **69**(2): 292-302.

Porter AC, Sauer JM, Knierman MD, Becker GW, Berna MJ, Bao J, *et al.* (2002). Characterization of a novel endocannabinoid, virodhamine, with antagonist activity at the CB1 receptor. *The Journal of pharmacology and experimental therapeutics* **301**(3): 1020-1024.

Price MR, Baillie GL, Thomas A, Stevenson LA, Easson M, Goodwin R, *et al.* (2005). Allosteric modulation of the cannabinoid CB1 receptor. *Molecular pharmacology* **68**(5): 1484-1495.

Pryce (2010). Cannabinoids for the control of experimental multiple sclerosis. *Thesis*.

Pryce G, Baker D (2007). Control of spasticity in a multiple sclerosis model is mediated by CB1, not CB2, cannabinoid receptors. *Br J Pharmacol* **150**(4): 519-525.

Qin N, Neeper MP, Liu Y, Hutchinson TL, Lubin ML, Flores CM (2008). TRPV2 is activated by cannabidiol and mediates CGRP release in cultured rat dorsal root ganglion neurons. *The Journal of neuroscience : the official journal of the Society for Neuroscience* **28**(24): 6231-6238.

Raine CS (1994). The Dale E. McFarlin Memorial Lecture: the immunology of the multiple sclerosis lesion. *Annals of neurology* **36 Suppl**: S61-72.

Ramagopalan SV, Maugeri NJ, Handunnetthi L, Lincoln MR, Orton SM, Dymment DA, *et al.* (2009). Expression of the multiple sclerosis-associated MHC class II Allele HLA-DRB1*1501 is regulated by vitamin D. *PLoS Genet* **5**(2): e1000369.

Ranzenhofer ER, Lipton MM, Steigman AJ (1958). Effect of homologous spinal cord in Freund's adjuvant on cockerel comb, testicular and body growth. *Proc Soc Exp Biol Med* **99**(2): 280-282.

Rice GP, Filippi M, Comi G (2000). Cladribine and progressive MS: clinical and MRI outcomes of a multicenter controlled trial. Cladribine MRI Study Group. *Neurology* **54**(5): 1145-1155.

Rice GP, Incorvaia B, Munari L, Ebers G, Polman C, D'Amico R, *et al.* (2001). Interferon in relapsing-remitting multiple sclerosis. *Cochrane database of systematic reviews (Online)*(4): CD002002.

Rog DJ (2010). Cannabis-based medicines in multiple sclerosis--a review of clinical studies. *Immunobiology* **215**(8): 658-672.

Rog DJ, Nurmikko TJ, Young CA (2007). Oromucosal delta9-tetrahydrocannabinol/cannabidiol for neuropathic pain associated with multiple sclerosis: an uncontrolled, open-label, 2-year extension trial. *Clin Ther* **29**(9): 2068-2079.

Romero-Zerbo SY, Rafacho A, Diaz-Arteaga A, Suarez J, Quesada I, Imbernon M, *et al.* (2011). A role for the putative cannabinoid receptor GPR55 in the islets of Langerhans. *J Endocrinol* **211**(2): 177-185.

Ross GR, Lichtman A, Dewey WL, Akbarali HI (2012). Evidence for the putative cannabinoid receptor (GPR55)-mediated inhibitory effects on intestinal contractility in mice. *Pharmacology* **90**(1-2): 55-65.

Ross RA (2009). The enigmatic pharmacology of GPR55. *Trends in pharmacological sciences* **30**(3): 156-163.

Roth SH (1978). Stereospecific presynaptic inhibitory effect of delta9-tetrahydrocannabinol on cholinergic transmission in the myenteric plexus of the guinea pig. *Canadian journal of physiology and pharmacology* **56**(6): 968-975.

Runmarker B, Andersen O (1993). Prognostic factors in a multiple sclerosis incidence cohort with twenty-five years of follow-up. *Brain : a journal of neurology* **116** (Pt 1): 117-134.

Ryberg E, Larsson N, Sjogren S, Hjorth S, Hermansson NO, Leonova J, *et al.* (2007). The orphan receptor GPR55 is a novel cannabinoid receptor. *Br J Pharmacol* **152**(7): 1092-1101.

Sanudo-Pena MC, Strangman NM, Mackie K, Walker JM, Tsou K (1999). CB1 receptor localization in rat spinal cord and roots, dorsal root ganglion, and peripheral nerve. *Zhongguo yao li xue bao = Acta pharmacologica Sinica* **20**(12): 1115-1120.

Sawcer S, Hellenthal G, Pirinen M, Spencer CC, Patsopoulos NA, Moutsianas L, *et al.* (2011). Genetic risk and a primary role for cell-mediated immune mechanisms in multiple sclerosis. *Nature* **476**(7359): 214-219.

Sawzdargo M, Nguyen T, Lee DK, Lynch KR, Cheng R, Heng HH, *et al.* (1999). Identification and cloning of three novel human G protein-coupled receptor genes GPR52, PsiGPR53 and GPR55: GPR55 is extensively expressed in human brain. *Brain Res Mol Brain Res* **64**(2): 193-198.

Schicho R, Bashashati M, Bawa M, McHugh D, Saur D, Hu HM, *et al.* (2011). The atypical cannabinoid O-1602 protects against experimental colitis and inhibits neutrophil recruitment. *Inflammatory bowel diseases* **17**(8): 1651-1664.

Schicho R, Storr M (2012). A potential role for GPR55 in gastrointestinal functions. *Current opinion in pharmacology* **12**(6): 653-658.

Schuelert N, McDougall JJ (2011). The abnormal cannabidiol analogue O-1602 reduces nociception in a rat model of acute arthritis via the putative cannabinoid receptor GPR55. *Neuroscience letters* **500**(1): 72-76.

Selewski DT, Shah GV, Segal BM, Rajdev PA, Mukherji SK (2010). Natalizumab (Tysabri). *AJNR. American journal of neuroradiology* **31**(9): 1588-1590.

Sharir H, Console-Bram L, Mundy C, Popoff SN, Kapur A, Abood ME (2012). The Endocannabinoids Anandamide and Virodhamine Modulate the Activity of the Candidate Cannabinoid Receptor GPR55. *J Neuroimmune Pharmacol.*

Sinha S, Miller LM, Subramanian S, Burrows GG, Vandenbark AA, Offner H (2011). RTL551 treatment of EAE reduces CD226 and T-bet+ CD4 T cells in periphery and prevents infiltration of T-bet+ IL-17, IFN-gamma producing T cells into CNS. *PLoS One* **6**(7): e21868.

Smith-Bouvier DL, Divekar AA, Sasidhar M, Du S, Tiwari-Woodruff SK, King JK, *et al.* (2008). A role for sex chromosome complement in the female bias in autoimmune disease. *The Journal of experimental medicine* **205**(5): 1099-1108.

Smith PF (2007). Symptomatic treatment of multiple sclerosis using cannabinoids: recent advances. *Expert review of neurotherapeutics* **7**(9): 1157-1163.

Spach KM, Blake M, Bunn JY, McElvany B, Noubade R, Blankenhorn EP, *et al.* (2009). Cutting edge: the Y chromosome controls the age-dependent experimental allergic encephalomyelitis sexual dimorphism in SJL/J mice. *Journal of immunology (Baltimore, Md. : 1950)* **182**(4): 1789-1793.

Staton PC, Hatcher JP, Walker DJ, Morrison AD, Shapland EM, Hughes JP, *et al.* (2008). The putative cannabinoid receptor GPR55 plays a role in mechanical hyperalgesia associated with inflammatory and neuropathic pain. *Pain* **139**(1): 225-236.

Steinman L, Martin R, Bernard C, Conlon P, Oksenberg JR (2002). Multiple sclerosis: deeper understanding of its pathogenesis reveals new targets for therapy. *Annual review of neuroscience* **25**: 491-505.

Steinman L, Zamvil SS (2005). Virtues and pitfalls of EAE for the development of therapies for multiple sclerosis. *Trends in immunology* **26**(11): 565-571.

Suarez J, Bermudez-Silva FJ, Mackie K, Ledent C, Zimmer A, Cravatt BF, *et al.* (2008). Immunohistochemical description of the endogenous cannabinoid system in the rat cerebellum and functionally related nuclei. *The Journal of comparative neurology* **509**(4): 400-421.

Suarez J, Llorente R, Romero-Zerbo SY, Mateos B, Bermudez-Silva FJ, de Fonseca FR, *et al.* (2009). Early maternal deprivation induces gender-dependent changes on the expression of hippocampal CB(1) and CB(2) cannabinoid receptors of neonatal rats. *Hippocampus* **19**(7): 623-632.

Sutphen R, Xu Y, Wilbanks GD, Fiorica J, Grendys EC, Jr., LaPolla JP, *et al.* (2004). Lysophospholipids are potential biomarkers of ovarian cancer. *Cancer Epidemiol Biomarkers Prev* **13**(7): 1185-1191.

Sylantsev S, Jensen TP, Ross RA, Rusakov DA (2013). Cannabinoid- and lysophosphatidylinositol-sensitive receptor GPR55 boosts neurotransmitter release at central synapses. *Proceedings of the National Academy of Sciences of the United States of America* **110**(13): 5193-5198.

Tal C, Laufer A, Behar AJ (1958). An experimental demyelinating disease in the Syrian hamster. *British journal of experimental pathology* **39**(2): 158-164.

Tanimura A, Yamazaki M, Hashimoto-dani Y, Uchigashima M, Kawata S, Abe M, *et al.* (2010). The endocannabinoid 2-arachidonoylglycerol produced by diacylglycerol lipase α mediates retrograde suppression of synaptic transmission. *Neuron* **65**(3): 320-327.

Thomas L, Paterson PY, Smithwick B (1950). Acute disseminated encephalomyelitis following immunization with homologous brain extracts; studies on the role of a circulating antibody in the production of the condition in dogs. *The Journal of experimental medicine* **92**(2): 133-152.

Thrower BW (2009). Relapse management in multiple sclerosis. *The neurologist* **15**(1): 1-5.

Tischner D, Reichardt HM (2007). Glucocorticoids in the control of neuroinflammation. *Molecular and cellular endocrinology* **275**(1-2): 62-70.

Tong W, Collantes ER, Welsh WJ, Berglund BA, Howlett AC (1998). Derivation of a pharmacophore model for anandamide using constrained conformational searching and comparative molecular field analysis. *Journal of medicinal chemistry* **41**(22): 4207-4215.

Toubi E, Nussbaum S, Staun-Ram E, Snir A, Melamed D, Hayardeny L, *et al.* (2012). Laquinimod modulates B cells and their regulatory effects on T cells in multiple sclerosis. *Journal of neuroimmunology* **251**(1-2): 45-54.

Trapp B, RICHARD M. RANSOHOFF, ELIZABETH FISHER and RICHARD A. RUDICK (1999). Neurodegeneration in Multiple Sclerosis:Relationship to Neurological Disability. *Neuroscientist* 1999 5: 48.

Trapp BD (2012). Lessons from Jack Griffin and the "pathogenesis of peripheral nerve disease". *Journal of the peripheral nervous system : JPNS* 17 Suppl 3: 20-23.

Trapp BD, Peterson J, Ransohoff RM, Rudick R, Mork S, Bo L (1998). Axonal transection in the lesions of multiple sclerosis. *The New England journal of medicine* 338(5): 278-285.

Tsou K, Brown S, Sanudo-Pena MC, Mackie K, Walker JM (1998). Immunohistochemical distribution of cannabinoid CB1 receptors in the rat central nervous system. *Neuroscience* 83(2): 393-411.

Tsunoda I, Fujinami RS (2002). Inside-Out versus Outside-In models for virus induced demyelination: axonal damage triggering demyelination. *Springer seminars in immunopathology* 24(2): 105-125.

Tsunoda I, Terry EJ, Marble BJ, Lazarides E, Woods C, Fujinami RS (2007). Modulation of experimental autoimmune encephalomyelitis by VLA-2 blockade. *Brain Pathol* 17(1): 45-55.

Tuohy VK, Sobel RA, Lees MB (1988). Myelin proteolipid protein-induced experimental allergic encephalomyelitis. Variations of disease expression in different strains of mice. *Journal of immunology (Baltimore, Md. : 1950)* 140(6): 1868-1873.

Uma Devi KR, Ramalingam B, Brennan PJ, Narayanan PR, Raja A (2001). Specific and early detection of IgG, IgA and IgM antibodies to Mycobacterium tuberculosis 38kDa antigen in pulmonary tuberculosis. *Tuberculosis (Edinburgh, Scotland)* 81(3): 249-253.

Vale ML, Marques JB, Moreira CA, Rocha FA, Ferreira SH, Poole S, *et al.* (2003). Antinociceptive effects of interleukin-4, -10, and -13 on the writhing response in mice and zymosan-induced knee joint incapacitation in rats. *The Journal of pharmacology and experimental therapeutics* 304(1): 102-108.

van Noort JM, Baker D, Amor S (2012). Mechanisms in the development of multiple sclerosis lesions: reconciling autoimmune and neurodegenerative factors. *CNS & neurological disorders drug targets* 11(5): 556-569.

van Noort JM, van Sechel AC, Bajramovic JJ, el Ouagmiri M, Polman CH, Lassmann H, *et al.* (1995). The small heat-shock protein alpha B-crystallin as candidate autoantigen in multiple sclerosis. *Nature* 375(6534): 798-801.

Varvel SA, Bridgen DT, Tao Q, Thomas BF, Martin BR, Lichtman AH (2005). Delta9-tetrahydrocannabinol accounts for the antinociceptive, hypothermic, and cataleptic effects of marijuana in mice. *The Journal of pharmacology and experimental therapeutics* **314**(1): 329-337.

Vesterinen HM, Sena ES, ffrench-Constant C, Williams A, Chandran S, Macleod MR (2010). Improving the translational hit of experimental treatments in multiple sclerosis. *Multiple sclerosis (Houndmills, Basingstoke, England)* **16**(9): 1044-1055.

Visser EM, Wilde K, Wilson JF, Yong KK, Counsell CE (2012). A new prevalence study of multiple sclerosis in Orkney, Shetland and Aberdeen city. *Journal of neurology, neurosurgery, and psychiatry* **83**(7): 719-724.

Wade DT, Makela PM, House H, Bateman C, Robson P (2006). Long-term use of a cannabis-based medicine in the treatment of spasticity and other symptoms in multiple sclerosis. *Multiple sclerosis (Houndmills, Basingstoke, England)* **12**(5): 639-645.

Waldeck-Weiermair M, Zoratti C, Osibow K, Balenga N, Goessnitzer E, Waldhoer M, *et al.* (2008). Integrin clustering enables anandamide-induced Ca²⁺ signaling in endothelial cells via GPR55 by protection against CB1-receptor-triggered repression. *J Cell Sci* **121**(Pt 10): 1704-1717.

Walters CE, Pryce G, Hankey DJ, Sebt SM, Hamilton AD, Baker D, *et al.* (2002). Inhibition of Rho GTPases with protein prenyltransferase inhibitors prevents leukocyte recruitment to the central nervous system and attenuates clinical signs of disease in an animal model of multiple sclerosis. *Journal of immunology (Baltimore, Md. : 1950)* **168**(8): 4087-4094.

Wandstrat A, Wakeland E (2001). The genetics of complex autoimmune diseases: non-MHC susceptibility genes. *Nature immunology* **2**(9): 802-809.

Wang J, Simonavicius N, Wu X, Swaminath G, Reagan J, Tian H, *et al.* (2006). Kynurenic acid as a ligand for orphan G protein-coupled receptor GPR35. *The Journal of biological chemistry* **281**(31): 22021-22028.

Wang J, Ueda N (2009). Biology of endocannabinoid synthesis system. *Prostaglandins Other Lipid Mediat* **89**(3-4): 112-119.

Weiner HL (2004). Multiple sclerosis is an inflammatory T-cell-mediated autoimmune disease. *Archives of neurology* **61**(10): 1613-1615.

Wheeler A, Smith HS (2013). Botulinum toxins: Mechanisms of action, antinociception and clinical applications. *Toxicology*.

Whitaker JN (1994). Rationale for immunotherapy in multiple sclerosis. *Annals of neurology* **36 Suppl**: S103-107.

White R, Hiley CR (1997). A comparison of EDHF-mediated and anandamide-induced relaxations in the rat isolated mesenteric artery. *Br J Pharmacol* **122**(8): 1573-1584.

Whittle B, Guy, G., Robson, P.R (2001). Prospects for new cannabis-based prescription medicines. *Journal of Cannabis Therapeutics* **1**: 183-205.

Whyte LS, Ryberg E, Sims NA, Ridge SA, Mackie K, Greasley PJ, *et al.* (2009). The putative cannabinoid receptor GPR55 affects osteoclast function in vitro and bone mass in vivo. *Proceedings of the National Academy of Sciences of the United States of America* **106**(38): 16511-16516.

Wilkinson JD, Whalley BJ, Baker D, Pryce G, Constanti A, Gibbons S, *et al.* (2003). Medicinal cannabis: is delta9-tetrahydrocannabinol necessary for all its effects? *The Journal of pharmacy and pharmacology* **55**(12): 1687-1694.

Wilson RI, Nicoll RA (2002). Endocannabinoid signaling in the brain. *Science* **296**(5568): 678-682.

Wilson RI, Nicoll RA (2001). Endogenous cannabinoids mediate retrograde signalling at hippocampal synapses. *Nature* **410**(6828): 588-592.

Wu CS, Chen H, Sun H, Zhu J, Jew CP, Wager-Miller J, *et al.* (2013). GPR55, a G-Protein Coupled Receptor for Lysophosphatidylinositol, Plays a Role in Motor Coordination. *PLoS One* **8**(4): e60314.

Wu CS, Zhu J, Wager-Miller J, Wang S, O'Leary D, Monory K, *et al.* (2010a). Requirement of cannabinoid CB(1) receptors in cortical pyramidal neurons for appropriate development of corticothalamic and thalamocortical projections. *The European journal of neuroscience* **32**(5): 693-706.

Wu F, Cao W, Yang Y, Liu A (2010b). Extensive infiltration of neutrophils in the acute phase of experimental autoimmune encephalomyelitis in C57BL/6 mice. *Histochemistry and cell biology* **133**(3): 313-322.

Wu GF, Alvarez E (2011). The immunopathophysiology of multiple sclerosis. *Neurologic clinics* **29**(2): 257-278.

Xiao YJ, Schwartz B, Washington M, Kennedy A, Webster K, Belinson J, *et al.* (2001). Electrospray ionization mass spectrometry analysis of lysophospholipids in human ascitic fluids: comparison of the lysophospholipid contents in malignant vs nonmalignant ascitic fluids. *Anal Biochem* **290**(2): 302-313.

Yin H, Chu A, Li W, Wang B, Shelton F, Otero F, *et al.* (2009). Lipid G protein-coupled receptor ligand identification using beta-arrestin PathHunter assay. *The Journal of biological chemistry* **284**(18): 12328-12338.

Yoshida T, Fukaya M, Uchigashima M, Miura E, Kamiya H, Kano M, *et al.* (2006). Localization of diacylglycerol lipase- α around postsynaptic spine suggests close proximity between production site of an endocannabinoid, 2-arachidonoyl-glycerol, and presynaptic cannabinoid CB1 receptor. *The Journal of neuroscience : the official journal of the Society for Neuroscience* **26**(18): 4740-4751.

Yousry TA, Major EO, Ryschkewitsch C, Fahle G, Fischer S, Hou J, *et al.* (2006). Evaluation of patients treated with natalizumab for progressive multifocal leukoencephalopathy. *The New England journal of medicine* **354**(9): 924-933.

Zafonte R, Lombard L, Elovic E (2004). Antispasticity medications: uses and limitations of enteral therapy. *American journal of physical medicine & rehabilitation / Association of Academic Physiatrists* **83**(10 Suppl): S50-58.

Zajicek J (2005). Diagnosis and disease modifying treatments in multiple sclerosis. *Postgrad Med J* **81**(959): 556-561.

Zajicek J, Fox P, Sanders H, Wright D, Vickery J, Nunn A, *et al.* (2003). Cannabinoids for treatment of spasticity and other symptoms related to multiple sclerosis (CAMS study): multicentre randomised placebo-controlled trial. *Lancet* **362**(9395): 1517-1526.

Zajicek J. RM, Schnelle M (2009). Cannabis extract in the treatment of muscle stiffness and other symptoms in multiple sclerosis - results of the MUSEC study. *In: Proceeding of the 25th Congress of the European Committee for Treatment and Research in Multiple Sclerosis.*

Zajicek JP, Apostu VI (2011). Role of cannabinoids in multiple sclerosis. *CNS Drugs* **25**(3): 187-201.

Zajicek JP, Hobart JC, Slade A, Barnes D, Mattison PG (2012). Multiple sclerosis and extract of cannabis: results of the MUSEC trial. *Journal of neurology, neurosurgery, and psychiatry* **83**(11): 1125-1132.

Zajicek JP, Wing M, Scolding NJ, Compston DA (1992). Interactions between oligodendrocytes and microglia. A major role for complement and tumour necrosis factor in oligodendrocyte adherence and killing. *Brain : a journal of neurology* **115** (Pt 6): 1611-1631.

Zhang X, Maor Y, Wang JF, Kunos G, Groopman JE (2010). Endocannabinoid-like N-arachidonoyl serine is a novel pro-angiogenic mediator. *Br J Pharmacol* **160**(7): 1583-1594.

Zhao P, Abood ME (2012). GPR55 and GPR35 and their relationship to cannabinoid and lysophospholipid receptors. *Life sciences.*

Zhu B, Symonds AL, Martin J, Wraith DC, Li S, Wang P (2013). Early growth response gene 2 (Egr-2) controls the self-tolerance of T cells and prevents the development of lupuslike autoimmune disease. *The Journal of Experimental Medicine J. Exp. Med.* Vol. 205 No. 10 2295-2307.

Zimmer A, Zimmer AM, Hohmann AG, Herkenham M, Bonner TI (1999). Increased mortality, hypoactivity, and hypoalgesia in cannabinoid CB1 receptor knockout mice. *Proceedings of the National Academy of Sciences of the United States of America* **96**(10): 5780-5785.

APPENDIX
Supplementary data

Supplementary Figure 1 : TG0039 Project Materials- GPR55 mouse deletion sequence

Genomic Sequence Deleted:

ATGAGCCAGCCAGAGCGTGACAACTGCTCATTGCTCCGTGGATAAGCTTACCAGAACCTTGACAGCTGGCAGTCCATATCCCCACCTTCTCCTTGGC
CTGGTTCTCAACCTACTGGCCATCCGAGGCTTCAGTGCCTTCTAAAGAAGAGGAAGCTGGACTATATCGCCACTTCTATCTACATGATCAACTTGGCTG
TTTTCGATTTACTGCTGGTGCTCTCCCTCCATTCAAGATGGTCTGCCACAAGTGGAGTCCCCCTTGCCGTCCTTCTGCACTCTGGTGGAGTGCCTCTAC
TTCATCAGCATGTATGGGAGTGTCTTACCATCTGCTTCATCAGCTGGACAGTTCCTGGCCATCCAGTACCCGATCCTGGCTAGCCATCTCCGGTCGC
CCAGGAAGACCTTTGGGATCTGCTGCATCATCTGGATGCTGGTCTGGATCGGAAGCATCCCCATCTACACCTTCCACAGGGAAGTGGAGAGATACAAG
TGCTTTCACAACATGTCGGATGTACCTGGAGTGCCAGTGTCTTCTCCCTGGAGATCTTTGGCTTCTCCTTCCCATGGGCATCATGGGCTTCTGTTT
CTATAGGAGTATTACATCCTGCTGCGCGTCCAGACAGCACTGAGGACTGGGTCCAACAGAGAGACACTAAGGGCTGGGTACAAAAGAGAGCCTGC
ATCTGGACCATGCTACCAATCTTGTATCTTGTGGTCTCCTTCTCCAGTGCACTTGGGCTTCTCCTGCAATCTGGTGGAGAACCGCTTTATCTT
GGACTGCAGAATGAAGCAGGGCATCAGCTTGTCTGCACTTGTCTGTGTTTCTCAACATCAACTGCTGCCTTGTATGTTTTTGTACTACTTTGTCT
TCAAAGAATTTGCGATGCGCATCAAGGCCACCGGCCCTCCCAATCAAGCTGGTCAACCAGGATACCATGCTCCAGGGGCTAAGAGAAGGTACCT
CTCTCAAGGGAAGGAAAACACAGTCTAAATCTCATAAAGACCCTCCTGGGCTTGGCTTGGCTTTGACACTCGCTGAGTACCATCTCTGTTCTTTATA
CTCTACAACCTTT

**Genomic Locus: (The deleted sequence represents nt 19548-20658 in the sequence below. The
KOS clone used to generate the FTV represents nt 15760-26029 in the sequence below.)**

CTGTGCTTTGGCAATGTTAAGGGGATCAGGGATGGCATCAGAGATGAGAAAATGTGCTGGATTAGACAGAGGCGGAGTCACTGGTTCACTCCAG
GATTCTTCTCTTCACTTCAAGTCAGACCTCCCTCAGCTCCAGTAGAAACCGAAGAAGATGAAGCCAGTGGTGTTAATGCAGGAGCCTGAATGCAGGA
GGCCACCACAGTGACACAAGAGCAGGAGGTCTCACACAGATGTCTAGAACTTCTCCTTCTTTGAGCTCTCAGTCAACTTCCAGGAAGGGAGAGGA
GAGGCGGGGATTCTAAGCGGCTGCTGTCCCTGCCTTGACATGAACATCAACACTTTGCTCTCTGAAGCCGCTCATGTACTGCTCTCAAGGTGGC
CAGGCATCTTCACTCTCCGTTGGTGGAGAATGTGGTCCACCTAGAGGGCAGGAAAGGGGACTTCTCTTGGAGACTTCAAGGCTGGGACTCATTGGTAC
TCCTAAGCTGTCTGACCACTCATGGGAACCATCTGGGCTTGGGGACAGAAGTGTGACCAATCTGGGATTGGAGCAGAGGTGAGACGTGTAGCTAC
TGTGTGGAGTAAAGGGTCTTCCCCACCTTCTCCCTTGTCTTCTCCTAGTTATCTCTGCTTCCCTTCCCTTCTGCTGAGCTGAGCTTCAAGGCAAGT
ACCCTGCTACTCAGGATGATGCTGTATCAATCCCAGCCTTTTCCCTCCTCAGACACAAGCTCTAAGGAGACAATGGCAGACTGACATATATCCATG
GGGAGGAAGAGTCTGAATCTTGTAGTGAGTTGCTGGGTGTTGTTATCTGTCTCTCACTCCATCTGGTTTTGAGAAAGTTTCTACTGTCCGCTTGGAC
AGACAGTAGACAAGCTGCAGAACAGGAACAGCAAGCACTTATTGATCAATGAACCTTCTGACCCAGGTTATCGATGAGGAAGTTGACTAGGAGG
AATTACAGAGACTTGTCAAAGGGTGGGGCCACTCTCTGTTTGTGGGCTTCTTAGGAATCAGGGTGCCACTGGTGACCTATGACTTTCTCTCAG
TCACCCCATCTCCACTTCTGTCCCAATCTTCTCAGCATGGCTGTTTCTTCTCCGACCTTCTCTGCCCCTGTATCCAGCCCCACGCTGCCCATC
CACTGAGTTGATCTGGGTTAGAGATGAGGTAAGGAACATCAAGGTTTCTTTTATTGGTCAGCTTCAATATGATGTTCTGTTCACTGTGTTGT
TCAAGGTGACCTTTGAGCAGCTCTACTCCTGGCTGACTGGCTTGTAGCCTCTGCTTGTGCTGCAATCTTAGACTTCACTACACAGAGGCAACC
CACCCCTGTCTTCAAGAGACAGTCCCACTCTGTCCCCAGAGACACCTCTATGTTTGGTCTTCTGAATGTCAAGCAACCTTGTGTGTGAGAAGACCTC
TTAAGCTATTCTTGTACCTCTGGCCTCTCTGCTCCCTGCCTCCTGCTGCCCCGCTTAGGGTTAGCCTCTAAGCCTACACCCCTTAGGTTAATCCTT
ACCCCTTAGGTGAACCCCTGCTGGGGCAAGTCTATCCCTCTGAATAGGTGCTGGGCCCTGATGGCTGAAGGGGTGAATGGAGTAGTGTCAAGGAG
GATGTGGTAGTGAGAACTCTTAGGTAAAGCAGTCAGAAAGAGCTTGTCTTGCGCCGAGAAGGAAGTCTTCTGGAGCTCTCTGATGCTGGTGCA
CTTGATGAAGTTGGAGGTATGTGCTCCAGTATCATCTTTAGAACCCCTTGAAGGAGGCGAGGGAGCCAGCTGTCAAAGCTTCTAGCTTGTCT
CTTAGGAAGAGAGGGTAGGACGGATCAAGGCAGTGATCCCAAGGCTTAGGAACTCCCAAGAACTTTTTTATTATGCTTTTTCTGGTTTCAAAGGG
AGCTAGAGAGAGAGGGCTCTGAACCATGGGCAGGTCTTGTCTGCTGCTACAGAGATAGATATTCTATCTTCCAGGTTTTAGAGAGCACTTGGGG
AGGTGGGACAGTGATTGTTACATAGCTTTACGAAATGTCTCTGTGTTTTTGAATCATGACCAAGCAATTTAAGCATTTAAAGACAAGCAACAG
CAAGGCATTTCTTGAAGAAACATATATGAAGGAGGACGGTACACACCCCAATGCCATCTGTATGGTGAACCTGAGAGCAGCCTGGGGTACCTGAGA
GCTTGTCTCCCAACCTGTCCCCGTGCACAAGAAAAAGAAAGTAGCAAGACCAAGGTGTGTGAGCCCCCTTGTAGTAGCAGCAGGACGGTGTAG
ACCCCTTGTGGGTTTCCAGCCCCATGCTCTGGGTAACATGGCGGGTATGGGACACCTGTGTGCTCTTGCCTGTCAAGCTTCCAGCTGCCCTGATCTTA
TGCCCTGGTCTAGACACTGCTTGTGTGTACAGCCAGGCTCTGGCTAGGGTGTGGCTAGGAACATGAAGGTATCTCACTTAAGGAAGTTCTGCTCCA
GGACTCGTCTTGGCTCTAGGACAGCTTGTCTCTGTCCCGGTAAGAGAATGTACGTAGCGTTACCCATCCACAGCCTGGGGTTGATCAGAATGA
AAGACAGTGGGGCTTGAATGGCTGTACAGATCTGCCATCTGTACATTGAACACTGGGAAGTGTAGCTCTGGAGGACCCCTGCTTACACAGAAGC
CGATATGTATTCAAGGAGCACCCTGTACCAGGATGAATCACTCAGACCCACCTTAGGGAGTTTCTATTCTGTAGACACATGAAAGTCACAGCATGCA
TGATCTATAAAAAATAGCCTTGCCTTGTCTCGGAGGGGCCCCCTAGCTCTCCTGGCTCAAGTGTGCACTGACGCTGGCTTTCTAATTGCCTGAGCC
GTATGAGGGCTCCTTGTGAGCATCTGAGGGGCTGGCTTGTCTTCTTGAAGAAGAGCCCCAGGAAAAACATCTGCTCATCATCTTTCGACACACC
TGTGTGGGTCTGACATAAGCCAGACTGCATCAGGAGCACTGCTCATATTACGCTTTCAATATGAAAGTTTCCATTAACCCAGTCTCTGTGCCAG
GGGTTCCCTGCTGAACCAATGTGCTAAATGTCCCTGATGATGCTCCTCTGTCTTGTAGTGATGCTTGTGAGAGAAGAAGGCTTCTCACTG
GACAGCCTCCCTCTCATCTCATCTCATCTCATGCTGCCCTGCCCCATTCTTGACTTATATTTGGGAGCTGGGTGAGTGTACATCTAAGGGGATGG

CCTCCAGGGACCCATTGGTGGCGATTCAGGGCTATGCAGACCTGAGAAATGAGGTTCCAGCCTTGGATGCTGTTTTGTCCCATTGCTGTCTTGGACAG
 AGATAATACCTGTGACACCGGATAGACAGCTGCTTCAGGTTACCCATGAGTGGGGTAGGCTTGGAAACCACTCTCTGTGTTCTCTGTAAAAAGG
 AGCTGTTACCCATCCAACAGAGTCAAGTGGTCCCTCCATGTGCAAGTGTGTCTGCCAGGCAAGATGACCCAGAGCAAAGGCTTTAGTAGGCTGAAT
 AGCCACCTTCCCATGGATGACCAAGAGCTAAACCTGGTGTGTGTATAGCAACGCTCTATGCTGGAAAGATCTCTAGTGCCCAAGAGTACCAATTACAA
 AGAGGGCAGGAAATCTAAAGCCATAAACTGGGGAAGGTAAAGCAGGGCTCCTGGAGTTGTACAGCTGTCTCAGATTGGTGACCTGGACCCAG
 GAGATTGGGGGTGGGGATAGGGTTTGAGAACCACTGATTCATCCCAAAATAGTGAGTGAAGGAGACTTGGCTGGTGTGTGTACCAAGTCCCAATGGT
 GGCTCAAGTGGCAGTTGGCTCAGCAGTACCAGAAATGGGGAGGATCACTGTTAGTGTGAAGTACAGCAGAATGCAGCCAGCGAGTGTGGGAAACC
 CAGCACTTAGTTGTGAAAAAGCCAGATTCTGTTACTAAAGCCAGTGGGGCTAGGAGCTATTGTTAGCCATAATGTGACCTTATTCTGACTCAGCCT
 TGGAAAACTGACACACTGGCTACACGTACAGCTGCAAGATCTAGCAAAAATTAATTGGAAAAACCAATTCGATTAACATGACTGACCAATAAATTCAT
 ACAATGTACTGTGACCTTGTCTCAGGCTTCACTTCTGGCTCCAGAGAAGAACTGGTATTTAATGGCCCTGCCAAGGGATTGAACAATGTGACCCCTG
 GGTATCAGGTATGATGTTATAGGGTCTTATCTGTAACAAGTAGGTACAGGTGGTTATCAGGTGCATAGCTGGTCTTCCAGTTGGTGAGGATCCAG
 ACCCTGTGCAGTTTGTGCTCAGTCAGTGGTGTCTAATTGTCTGTGAAGCCACTGGGTCTCAAAGGCCCCACACACTTGGACTCAGTCCCTTTCAGCC
 TGCTCTTCCATCTCCCACTGACACTGGCTGTGTCCATGAGAGGCCAATTCAAGAGACCTGTTGACTACACATCTCTACTGGTGTGCTCCCT
 TCTGGGTCTAGTTATGGTGTAAATGTATCTCTTTACAGGGAACCTCCTCCTACCTACCAGCAGCACTTGACAGGCATTTCCTATAGGCTTAGGTCCAA
 GTCACCCCTTTTCTAAGTTCCAAGGCCTGACCTGGATGTGGAAGGCTGATCAGGGACATCCTTGTCCCTTAACAGACATTTTTCGGTTAACCCAGCT
 AACTGGTGGGTGGGTCTATCCCTTGGCTCCAGAGGATTGACTGGAGAGCACCTATTCAAACTGCATTCACTCAGCCCTGTTAGAGTCCCTCC
 CTGTAGACCTTTGAAGTTGGAGTCATTACAGTAACACAGTGAAGATGCCCTGGGCTTCTGAGAACCCACATAGAAAATTCACCTACAGAAAGTT
 ACTGTGAATAACCAAGTAATTTCAAAGATGCTTGAAGTACTGTAGGCCAGTAGCAGCTGCAGAGACTCAAAGGATGTGAAAGGACTAGCTTGATAT
 GTCAACGAGGAAAAGATAGGATGAGCTTTCTAGCCTGGGATGAAAAGAGTATCAACCAAGCAGGGGTAGACACATCCCTAAGGACCTATATGGAGAT
 GCTACTACAAAATCTCCATGCTCTCCGAGGGCCAGCTCCATTGGGACAATATCCTTTGGGGCAACAGAGTGGCTGACAAAAGGTACCGTGAGA
 ATCCATCTTGAGGACAGGGGACTAAAAGACTATAAAGGTGTTGATTTGAGGTACACACCCTGAAACTACTACTAGTACCTCTCAGCTTCTCAGCT
 GTGCTTCTGGTAAGGCCAGGCGAGAGACACAGGCACTGAAGGTGAGCAAGTGCCCTGTCTCTCTTCCCTTTGTGAACAGTGTCTGTGTGGGA
 GTGTGGTGTGTTGGTGGTGGTGGTGGTGGGACATTCACTGTGAGATATAGCAGAAGTGAGGCCTTGTCTCTTGTGTCTGCAGAGGAGACTGG
 AAGGTGTCACTTCAAAGGAATGCTTGAGGGAGCAAGCCAGCAGCTCACCTTGAGGCCCCAGACCCTGCCTTTGTTCTGAGGCAGTCACCTGAGAAACA
 ACCAAAATCTATGTCACGGAGTGGGGGTGGGAGGAGGAGTGGGAGAGAGTGGGAGGGGTGTTGTACAGCACAGTCACACACACACACACA
 CACACACACACACACCCCACTCGCATGTGGTGCATGCACAATAGACTGATGTTCTTAGGCTTTGGGAAGGACTATCTCCAGCAGCTGGAAGCCCTGCC
 ATATTTTCAACAGGCCCCCACTCCCGCAGCCACTCTCGCCCTGAAACAACGTTTCTTCCCTGAAGGAGCAGCTGAGGCTTGTCTTCTG
 GAGGCCACCAAGTACAATCAGTTGCTATAGAGTAAGGCAGGGACAGGTGCCAACACAGTGGCGCTTGGTAGGCTTGCCTGCACCTGCTGGACCAGAG
 GGTGAGAAACCTTTCAGAACCAAGCAGGCAATGGACTTCTGGCATTACGGAGGGTGGCATCAGGCCAGCATCTCGGAGTGTAAAGTCAATTTAA
 CTGCAGAGGCTAGGTGTTTAAACATTTTGACAAACACAGATGTAGTAGGTGTTAATAGAGCTTAGAGCTGTTGCTATTCTCCTGGGATGTCACT
 CTGGGGAACAGTCAGATATCAGAGGTACAGCCAGGGGCTGATGGAGGGTCTGGGGTATGGCGTCAGTGGCAGAAAGACATTTCTACTACCTGGA
 GGCTGAATGTTACGGTCTGGCTGGCTGTGTCTGGTCTGGTGGAGAGCTTCTCTGCTTTTGCCTGGGTCTGTACAAGAAGTTTTCTGATTCCTT
 CTGATAGGGACAGTCAACTGTCTGGGTGACAGAGTTAGCATTTTACCTTAATGGCCCCCTAAGGTCCAGGGTGGGGTTCAATGCCTGAAT
 TTAAGTGGGAGCATCCAGTCCACAAGGCTTTTACTCTGTGAACCTGAATAGAACATGTGTGTTTCTCTAGTTTCTTAACCTGAATACCCCGCTCTGA
 GCTCAGGACATTTTACAAAGACTTGCTAACCCTGTTGCCCTAAACATCTCTAGCTCCGGGAATCTGCATGAATCTAGAAAGAGAGGCTCCTCAA
 GACCTACAGAGAGGGCTCAGCAGTAAAGAGCACTGTCTCTTCCAGAGACCTGGCTTCCATTCCAGTGACCACACGGTGGGTACAGCAGTCTG
 GAAGTCTAGTCTGAGGTATCTAGTCCCTCTTCTGGCCTTTTCAAGGAATACGTGAGCATGATGCAAGACCCAGACACATATAACAAATAAAATGA
 AATAAAGAAATAAGAGAGTGCCCTTGATAGGGGAATGGGGCCGCAAGATTGGGTGGCTAAGAACCAGGCTATGAATGTAGACTCTCTATTACATG
 GACACAAGACTTTGTCTACAGTTCCTCATGGCTGCAAGCTGCCCTCCACCACTGCTGGTGTCTTCCAGAGAGCTCATACCAAAATCATGCTCTG
 GAGTCTAGCCACCTTCCCTGAACATTGCCATGCCCTCCCTTACAGATCCTGTGGCACTTCTCATCTAGGCTGGGGCTCCAAAGCCTGGCTTTCTTC
 AAGGTAGGGTGAAGCCTGGAGATGTTCAAAGCAGACGCTTCTAGCATCCATTCTCATAATTGTATCCTGGGGAAGATAATAGATGCATGGTGTGAG
 GATGACATGGGGAAGCGCCAGCATCTTCAATCAAAATCAACAGGCATTGTGCTTCTGGGCAATGCCACATGCCCACTTGTAGTGGGACAAGAAA
 GACAGAGAGGGCTTACAAGTACCAGTGGTCTGAAAAGGAGAGAATAGGCTAATTAGGAGCCATGTCTGCCACCATCTGGCTTGTGCTGAGGT
 GACTGCAATAGTACCCTGCCACCTTCCATAGGCTAGTGTCTTAACTTAAAGGAGAATTACATCAGCAGCTTAAAGCAGGAGGACACAGTGTCTG
 GTACTTTAAAGATGAAGGAGAAGCTGCTGTGGTGGTGGGTCTCAGTTTGCCTGCCCTGTGCTTCTCAAAGAGCCCTCTCACTTGCCAGCGACACT
 TAGCTGCGGTAGGTATCCACAGGGGTTCTGGGGTCTGCGGTGTGAGCAATGGGACTGTGGGGTCTGGTCTGAAGCCGGCAGCCCTCTGTTGTAT
 ATTATGGTCTAGTGTCCCTCTCCCTGAAGAGATCCAGGCTGGAGCTCGAGGATGACAGCATAGAGAAGTCGTTTGTCTTCTCAGGGGTGAGCAA
 GCAAAGCTGACTTTCCATTGGGCTCTTTGACTAGGAGGACCTGGGGATTTGAATAATTAGGGACTATCTCTGTCTGAAGAACACGTAAGGAC
 CCAAGCAATGAATTGTGGCAATACGAATAAGGTGAGGAGTTTACAATCTAGGCCAGTGAGCAGGTCACTCGTACCTTGTATGTTATTTATGAT
 ATTTATGTCTTTGTCTCTTCTAGGAGCTGATGTCAATTCATCTCCAGGATGTCTTATCTGACCTGCCATGGAAGCTCCTGGGGGCTCTAACTG
 TCGTCTCCAGAGTCCCTCAAAGGCCCTCCCACTCCCTGAAGACTGTCTTGGCTCAGCTGTGATCAGAGTTTCTCCTTCCAGAAGATTCCCTCTTC
 AGTCTTCTCTCTCACTGTTCCCTCCCTCAGCGCTTCTGTCTTCTGCTCTGCACTGTCAACCTGTTTTAGGAGAGGGTCCCTCATGAGGGGTCT
 TTGATTCCTCTGCTTCTGCTTCTAGGGCTGTTTCCATGGAACCAAGCAAGAGGTCATTCAAAGGAAACCAAGAGACAGTCTGTGGA
 CAGCCCCATCCCTCGCAGTTTAAACAGCGGCTGCACAGCGAGAGACTGTCTCTTCCGAGCTAGGCTGCAGTGAAATAATCAAACTCCAGAG
 GACAGCATGGGGGAGATTGTCAGGGATGGCGTGGGGTGGGGCTAGGGTGGGGGAGGTGGGAAGAGTCTTCAAGAACAGTGAACCCGGATGCA
 TGTTACATTGTTATTCATTAGAGCCCTTTCCCATATCTGTCTGCACTAAGTCTCCAGCTTAGCCTGTTATTTCTCTTCCGGTGAGAAAGAGCCGG
 AGTGTAGAGCCAGGAAACAGAACTCCAAGACCAAGTTATGAGAGGCTGGGGGAGGGGGGCGTCTTACACTCGCCCACTCCCAAGCTC
 AAGTCCCTCTGACCTGTGCTTTTTATTATCTATTCAAGTGGCAGAATAGACTTGCACATGCCTTGTCTTCTGGTCCCACAGAGAATCATTTACAAA
 CCACTGTCTACTTTATGACCCGTGAGACTGTCTCTGGGCTGTGTATATGCTCAACGCTCATTAGGTTCCCTTAAAGTACATATGAGTCATCTCAA
 AATTGTCTCACTCTCTCTCCCAACAGGAGTGGGGTGTGCTTTTTTGCACCCCACTGAGCTGGTGGGTGGCCAGCACTGTGACTTTCTGTGTT
 TGGTTTTTCCGTGTTTGCACATTACAGATCTGTATATCTTTCTCGGTTTCTGTTGTCTTGTGAGTTTGTTCAGGAGAAGGTCCAGATGATAGAGGG
 GAAAAATGCTTTTGTACACGGGGTACAGACAGGGGAGGGGAGGGGAGGGGAGGGGAGGGGAGGGGAGGGGAGGGGAGGGGAGGGGAGGGG
 GAGGGGAGGCGAGATTCTTTGACTTTGGGTGAGAAGCATATTAGCCAGTTTCCCTTAGAGCTTGTGGGGAAGAGGAACGCGGAGTGTATTTCAA

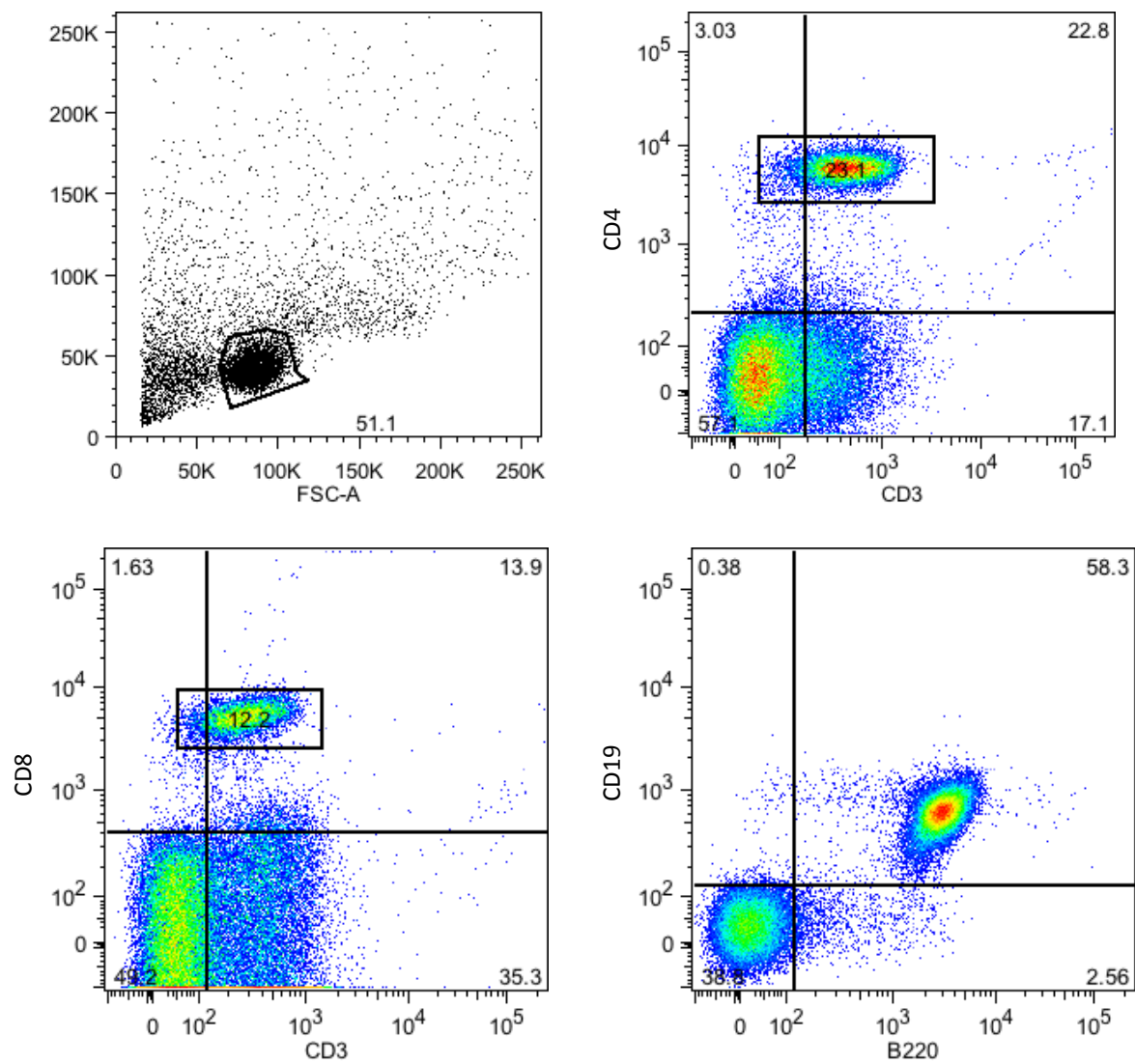
TGTC AATTGTTGGATCGGCCAGCTACCAAGATCAGGGAAGCTGGGGACATATAAAATACCACAAGGCCACCTACTGAGCTTCAGCAGGGGCCTGAC
CGGTATCCTGAGGTCTTGTGTTGTTTCAACTCTGCTCTAAGCCATTGCCATAAAGCCATATTGGTACATGGCCACAACCTACCCACGCTGTCTGTG
GTTGCCCTAGAGGCAACAACATAGATTTAGGGGGTTTCAACCTACCGTAAGCTTCACAACATCTCAATGATTATATTCTGGTCTTTGAAAGGATCTT
CCAACCTAAAAAGTTTTACAGGCAGAGACCCCTGGAAGTTCAAACTTCACAGAACACTTGACACATAGTAGGAGCTAAATATCCATGTTGCCTGGCTA
TGAAGCTGGACCTTGGTGAATCTATACAGTCTGTGCCTTCACTTTGGAAGGGGGATCCTCCATGGTAGCACTTACCTCATAACTCTGCCACTGAACA
CAGCCAATTTCTGGTTGCATTTCTGGTTGCTGAGATAGAAGTGGCTCGTGGTCAAAGAGGATACAGTCCTTTATGGTGGGGTAATCATACTGTATAGT
GTTAGAATCAGTTCCTGCTGTGGCCAGGACATAGTAGGAGCATGAAGCATCCAGCTCTTTATATTTCCATGGATCAAGGAGTAGAAAGCTAAGCT
GGGTGGCAGATGCATTTAATCTGCACTTGGGAGGCAGAAGCAGGCAGCTCTGTGAGTTCAAGGTCAAGTCTGGTTTACATAGTAAGATCCAGACCA
GCTGTGCCTACATATTGAGAGACTGTCTCAAATAAACAAACAAACAAATAAAACAAACAAACAAACAAACAAACAAACAAACAAACAAACAAACAA
AGAAGAAGATGAAAAAGACAAAGAAGGAGGAGGAAGAGGAGAAGGAAGGAGAAGGAAGGAAGGAAGGAAGGAAGGAAGGAAGGAAGGAAGGAAG
GAAGAAGAAGGAAGGAAGGAAGGAAGGAAGGAAGGAAGGAAGGAGGAGGAGGAGGAGGAGGAGGAGGAGGAGGAGGAGGAGGAGGAGGAGGAGGAG
GGGCTATAATCCTCGAAGCCTGTCCCTGTGCCTCATCAGCCAGCTGGGTCTATATTCTAGAGGTTTTATAACTCTTATAATGATACCACTAGCTGG
GAACCAATGTTCAAAAAAACACATGAGCCTGCAGGGGATACTTTACATTTAAACATTAAACCAATTGTCCTGTGCGGTGGAGCAGAGAGGTTCTCT
CAACAGGCAGAGTATAGCACCTAAGAGCCTGGAAGTCTATAGGCAAAAGGAACGGATGGCATTGTCACTCAGGGTGGACTCTGGCCTCTCTCTGT
GTAGGAACATCTGTCGCGCTATTGTTGTCATTGATCCACCCTAGGTTACCAAGGCAGAACAGATATATGTGTAACCTGGCTACCCAATAATGACCACTTCT
AACCCTGCAACAAGAGAATGGTGTGTACATGGCAATTGCAAGGGGGGGGGGGGAGGGGACGGGACCTGTGTGTGGGAGTCTGGTGGTAAGT
GTGTTACTTCTTACT

Selection Cassette:

GGCGCGCCGGATCCCGGGCCGCTCTAGCTAGACTAGTCTAGCTAGAGAATTCCGCCCCCCCCCCCCCCCCCTCTCCCTCCCCCCCCCTAACGTTACT
GGCCGAAGCCGCTTGAATAAGGCCGGTGTGCGTTTGTCTATGTTATTTCCACCATTGCGCGTCTTTGGCAATGTGAGGGCCCGGAAACCTGGC
CCTGTCTTCTGACGAGCATTCTAGGGGTCTTCCCTCTCGCCAAAGGAATGCAAGGTCTGTTGAATGTCGTGAAGGAAGCAGTTCCTCTGGAAGCT
TCTTGAAAGACAAACACGTCTGTAGCGACCTTTGCAAGGCAGCGGAACCCCCACCTGGCGACAGGTGCCTCTGCGGCCAAAGCCACGTGTATAAGA
TACACCTGCAAAAGCGGCACAACCCAGTGCCACGTTGTGAGTTGGATAGTTGTGAAAGAGTCAAATGGCTCTCCTCAAGCGTATTCAACAAGGGGG
TGAAGGATGCCAGAAAGGTACCCATTGTATGGGATCTGATCTGGGGCTCGGTGCACATGCTTACATGTGTTAGTCGAGGTTAAAAAACGTTCTA
GGCCCCCGAACCACGGGGACGTGGTTTTCTTTGAAAAACAGATGATAAGCTTGCCACAACCATGGAAGATCCCGTCTGTTTACACGTCGTGACT
GGGAAAACCTGGCGTTACCCAACTAATCGCCTTGCAGCACATCCCCCTTTCGCCAGCTGGCGTAATAGCGAAGAGGCCGACCGATCGCCCTTCCC
AACAGTTGCGCAGCCTGAATGGCGAATGGCGCTTTGCTGTTTCCGGCACCAAGAGCGGTGCCGGAAGCTGGCTGGAGTGCATCTTCTGAGGC
CGATACTGTCGTGCTCCCTCAAACCTGGCAGATGCACGGTTACGATGCGCCATCTACACCAACGTGACCTATCCATTACGGTCAATCCGCGTTTGT
CCCAGGGAGAATCCGACGGGTGTTACTCGCTCACATTTAATGTTGATGAAAGCTGGCTACAGGAAGGCCAGACGCAATATTTTATGATGGCGTTAA
CTCGCGTTTTCATCTGTGTTGCAACGGGCGCTGGGTGCTTACGGCCAGGACAGTCTGTTGCGGTCTGAATTTGACCTGAGCGCATTTTACGCGCCG
GAGAAAACCGCTCGCGGTGATGGTGTGCGCTGGAGTGACGGCAGTTATCTGGAAGATCAGGATATGTGGCGGATGAGCGGCATTTTCCGTGACGT
CTCGTTGCTGCATAAACCGACTACACAAATCAGCGATTTCCATGTTGCCACTCGCTTAAATGATGATTTACGCGCGCTGTACTGGAGGCTGAAGTTCA
GATGTGCGGCGAGTTGCGTGACTACCTACGGGTAACAGTTTCTTATGCGAGGGTGAACGCGAGGTGCCAGCGGCACCGCGCTTTCGCGGGTGAA
ATTATCGATGAGCGTGGTGGTTATGCCGATCGCGTCACACTACGTCTGAACGTGCAAAACCGGAACTGTGGAGCGCGGAAATCCCGAATCTCTATCG
TGCGGTGGTTGAAGTGCACACCGCCGACGGCAGCTGATTGAAGCAGAAGCTGCGATGTCGGTTTCCGCGAGGTGCGGATTGAAAATGGTCTGCTG
CTGCTGAACGGCAAGCCGTTGCTGATTGAGGCGTTAACCCTCAGCAGCATCATCTCTCATGGTCAGGTGATGGATGAGCAGACGATGGTGCAGG
ATATCTGCTGATGAAGCAGAACTTTAACGCCGTGCGCTGTTGCAATTATCGAACCATCCGCTGTGGTACACGCTGTGCGACCGCTACGGCTGT
ATGTGGTGGATGAAGCAATATTGAAACCCACGGCATGGTGCAATGAATCGTCTGACCGATGATCCGCGCTGGCTACCGCGCATGAGCGAACCGGT
AACCGCAATGGTGCAGCGCATGTAATCACCCGAGTGTGATCATCTGGTCTGGGGAATGAATCAGGCCACGGCGCTAATCACGACGCGCTGTAT
CGCTGGATCAATCTGTGATCTTCCCGCCCGTGCAAGTATGAAGGCGGGGAGCCGACACCACGGCCACCGATATTATTTGCCGATGTACGCGCG
CGTGGATGAAGACGACGCTTCCCGCTGTGCCGAAATGGTCCATCAAAAAATGGCTTTGCTACCTGGAGAGACGCGCCCGCTGATCTTTGCGAAT
ACGCCACGCGATGGGTAACAGTCTTGGCGGTTTCGCTAAATACTGGCAGGCGTTTCGTGATATCCCGTTTACAGGGCGGCTTCTGTGGGACTGG
GTGGATCAGTCGCTGATTAATATGATGAAAACGGCAACCCGTGGTGGCTTACGGCGGTGATTTTGGCGATACGCCGAACGATCGCCAGTTCTGTAT
GAACGGTCTGGTCTTTGCCGACCGCACGCCGATCCAGCGCTGACGGAAGCAAAACACCAGCAGCAGTTTTCCAGTTCCGTTATCCGGGCAACCA
TCGAAGTGACCGCAATACCTGTTCCGTATAGCGATAACGAGCTCTGCTGAGTGGTGGCGCTGGATGGTAAGCCGCTGGCAAGCGGTGAAGT
GCCCTGAGTGTGCTCCACAAGGTAACAGTTGATTGAACCTGCTGACTACCGAGCGGAGAGCGCGCGCAACTCTGCTCAGCTACAGTACGCGTAG
TGCAACCGAACGCGACCGCATGGTCAAGAGCCGGGCACATCAGCGCCTGGCAGCAGTGGCGTCTGGCGGAAAACCTCAGTGTGACGCTCCCCGCCG
GTCCACGCCATCCGCTATGACCACAGCGAAATGGATTTTTGCATCGAGCTGGGTAATAAGCGTTGGCAATTAACCGCAGTCAGGCTTTCTTTC
ACAGATGTGGATTGGCGATAAAAAACAAGTCTGACGCCGCTGCGCGATCAGTTACCCGTGACCGCTGGATAACGACATTGGCGTAAGTGAAGCG
ACCCGCTTACCCCTAACGCTGGGTGCAACGCTGGAAGGCGGCGGGCCATTACCAGGCCGAAGCAGCGTTGTTGAGTGCACGGCAGATACACTTG
CTGATGCGGTGCTGATTACGACCGCTCAGCGTGGCAGCATCAGGGGAAAACCTTATTTACAGCCGAAAACCTACCGGATTGATGGTAGTGGTCAA
ATGGCGATTACCGTTGATGTTGAAGTGGCGAGCGATACCCGATCCGGCGCGGATTGGCTGAACTGCCAGCTGGCGCAGGTAGCAGAGCGGGTA
AACTGGCTCGGATTAGGGCCGCAAGAAAACCTATCCGACCGCTTACTGCGCGCTGTTTACCGCTGGGATCTGCCATTGTGACAGATGTATACCCG
TACGTCTCCGAGCGAAAACGGTGTGCGCTGCGGGACGCGCAATTAATTATGGCCACACCAAGTGGCGCGGCACTTCAAGTTCAACATACGCCG
CTACAGTCAACAGCAACTGATGGAACCAAGCCATCGCCATCTGCTGCACGCGGAAGAAAGGCACATGGCTGAATATCGACGTTTCCATATGGGGATTG
GTGGCGACGACTCTGGAGCCGTCAGTATCGGCGGAATTCAGCTGAGCGCGGTGCTACCATACAGTTGGTCTGGTGTCAAAAAATAATAATAA
CCGGGACAGGCATGTCTGCCGTATTTCCGCTAAGGAAATCCATTATGTACTATTTAAAAACACAACTTTTGGATGTTCCGGTTATCTTTTCTTTTA

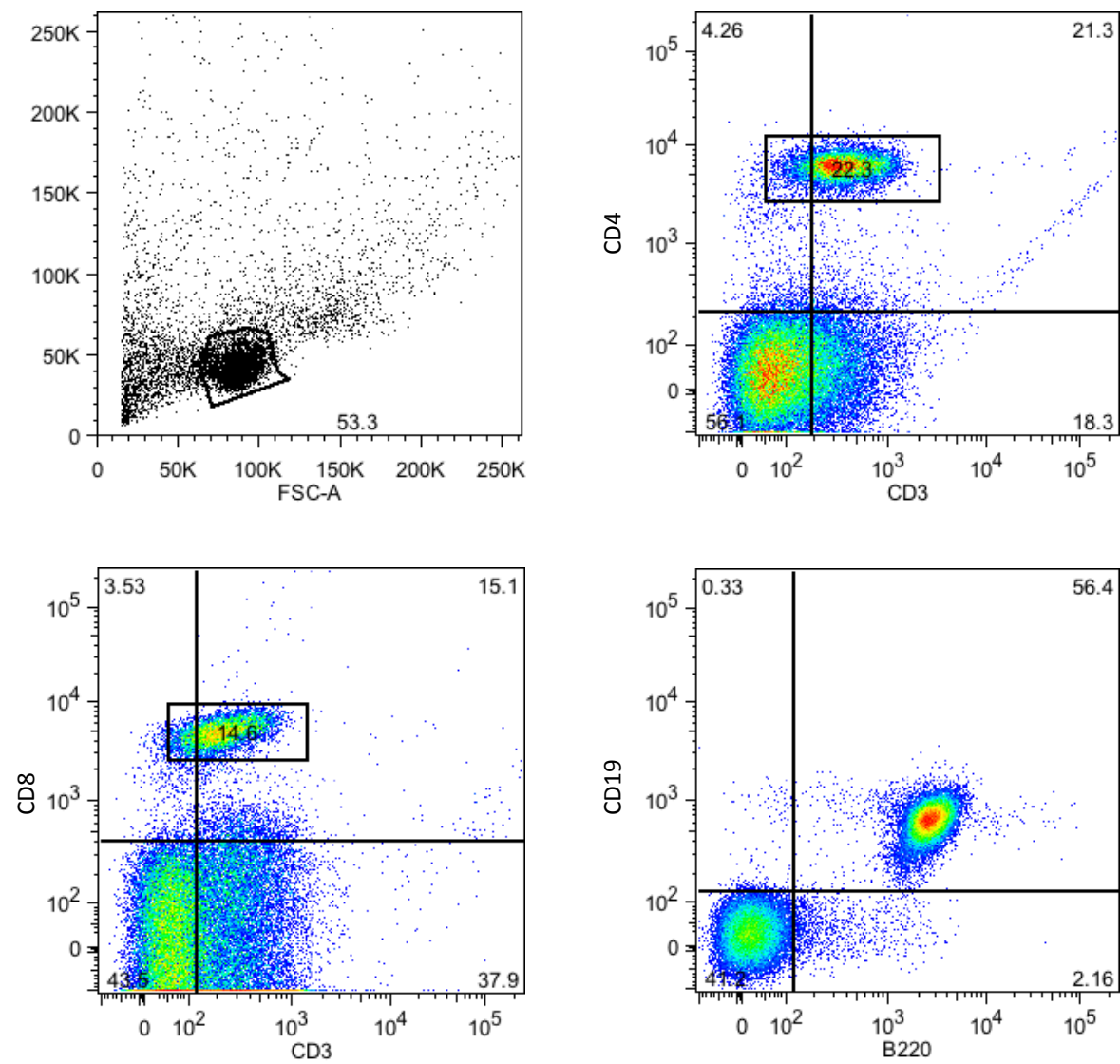
[illegible]

AGCATTCTAGGGGCTTTCCCTCTCGCCAAAGGAATGCAAGGTCTGTTGAATGTCGTGAAGGAAGCAGTTCCTCTGGAAGCTTCTTGAAGACAAAC
 AACGTCTGTAGCGACCCCTTTGCAGGCAGCGGAACCCCCACCTGGCGACAGGTGCCTCTGCGGCCAAAAGCCACGTGTATAAGATACACCTGCAAAG
 GCGGCACAACCCAGTGCCACGTTGTGAGTTGGATAGTTGTGGAAAGAGTCAAATGGCTCTCTCAAGCGTATTCAACAAGGGGCTGAAGGATGCCC
 AGAAGGTACCCATTGTATGGGATCTGATCTGGGGCTCGGTGCACATGCTTTACATGTGTTTAGTCGAGGTTAAAAAACGCTAGGCCCCCGAAC
 CACGGGGACGTGGTGTCTTTGAAAAACAGATGATAAGCTTGCCACAACCATGGAAGATCCCGTCTGTTTACAACGTGCTGACTGGGAAAAACCTTG
 GCGTTACCCCAATTAATCGCTTGCAGCACATCCCCCTTTCCGCACTGGCGTAATAGCGAAGAGGCCGACCCGATCGCCCTTCCCAACAGTTGCGCA
 GCCTGAATGGCAATGGCGCTTGTGCTGGTTCCGGCACCAAGAGCGGTGCCGAAAGCTGGCTGGAGTGCATCTCTGAGGCCGATACTGTCGT
 CGTCCCTCAAACCTGGCAGATGCACGGTTACGATGCGCCATCTACCAACCTGACCTATCCATTACGGTCAATCCGCCGTTTGTCCACGAGAGAA
 TCCGACGGGTTGTTACTCGCTCACATTAATGTTGATGAAAGCTGGCTACAGGAAGGCCAGACGCGAATTATTTTGTGGCGTTAACTCGGCGTTTCA
 TCTGTGGTGAACGGGCGCTGGGTGCGTTACGGCCAGGACAGTCTGTTGCCGTCTGAATTTGACCTGAGCGCATTTTACGCGCCGAGAAAAACCGC
 TCGCGGTGATGGTGTGCGTGGAGTGACGGCAGTTATCTGGAAGATCAGGATATGTGGCGGATGAGCGGCATTTCCGTGACGTCTCGTGTGCA
 TAAACCGACTACACAAATCAGCGATTCCATGTTGCCACTCGCTTAAATGATGATTGAGCCGCGCTGTAAGTGGAGGCTGAAGTTCAGATGTGCGGCGA
 GTTGTGCTGACTACCTACGGGTAAAGTTTCTTATGGCAGGGTGAACGCGAGGTGCCAGCGGCACCGCGCTTTCGGCGGTGAAATTATCGATGAGC
 GTGGTGGTTATGCCGATCGCGTCACACTACGTCTGAACGTGAAAACCCGAAACTGTGGAGCGCCGAAATCCCGAATCTCTATCGTGGGTGGTTGAA
 CTGCACACCGCCGACGGCAGCGTGATTGAAGCAGAAGCTGCGATGTCGGTTCCGCGAGGTGCGGATTGAAAATGGTCTGCTGCTGTAACGGCA
 AGCCGTTGCTGATTTCGAGGCGTTAACCGTCACGAGCATCATCTCTGCATGGTCAGGTGATGGATGAGCAGACGATGGTGCAGGATATCTGCTGATG
 AAGCAGAAACCTTAACGCGGTGCGCTGTTGCGATTATCCGAACCATCGCTGTGGTACACGCTGTGCGACCGCTACGGCTGTATGTGGTGGATGA
 AGCCAATATTGAAACCCAGGCATGGTGCCAATGAATCGTCTGACCGATGATCCGCGCTGGCTACCGCGGATGAGCGAACCGGTAAACGGAATGGTG
 CAGCGCGATCGTAATCACCGAGTGTGATCATCTGGTCTGGGGAATGAATCAGGCCACGGCGCTAATCAGCAGCGCTGTATCGCTGGATCAAATC
 TGTGATCTTCCCGCCCGGTGCAGTATGAAGGCGCGGAGCCGACACCGCCAGCGATATTATTTGCCGATGACGCGCGCTGGATGAAGACC
 AGCCCTTCCCGGCTGCGGAAATGTCATCAAAAATGCTTTCGCTACCTGGAGAGACGCGCCGCTGATCTTTCGGAATACGCCACCGCGATG
 GGTAACAGTCTTGGCGGTTTCTGCTAAATACTGCGCAGGCGTTTTCGTCAGTATCCCCGTTTACAGGGCGGCTTCTGCTGGGACTGGGTGGATCAGTCTGCT
 GATTAATATGATGAAAACGGCAACCCGTGGTGGCTTACGGCGGTGATTTGGCGATACGCCGAACGATCGCCAGTTCTGTATGAACGGTCTGGTCT
 TTGCCAGCCGACGCCGATCCAGCGCTGACGGAAGCAAAACACCAGCAGCAGTTTTTCCAGTTCCGTTTATCCGGGCAAAACCATCGAAGTGACCAGC
 GAATACCTGTTCCGTCATAGCGATAACGAGCTCTGCACTGGATGGTGGCGCTGGATGGTAAGCCGCTGGCAAGCGGTGAAGTGCTCTGGATGTCG
 CTCCACAAGGTAACAGTTGATTGAAGTCTGAACTACCGCAGCGGAGAGCGCCGGCAACTCTGGCTCACAGTACGCGTAGTGAACCGAACGC
 GACCGCATGTCAGAAAGCGGGCACATCAGCGCTGGCAGCAGTGGCGTCTGGCGGAAAACCTCAGTGTGACGCTCCCCCGCGCTCCACGCCATC
 CCGCATCTGACCACAGCGAAATGGATTTTGCATCGAGCTGGTAATAAGCGTTGGCAATTAACCGCCAGTCAGGCTTTCTTTCACAGATGTGGATT
 GGCATAAAAAACAACTGCTGACGCCGCTGCGCGATCAGTTACCCGTGACCGCTGGATAACGACATTGGCGTAAGTGAAGCGACCCGATTGACC
 CTAACGCCTGGGTGGAACGCTGGAAGCGCGGGGCCATTACAGGCCGAAGCAGCGTTGTTGAGTGCACGGCAGATACATTGCTGATGCGGTGCT
 GATTACGACCGCTCACGCGTGGCAGCATCAGGGGAAAACCTATTATCAGCCGGAACCTACCGGATTGATGGTAGTGGTCAAATGGCGATTACCG
 TTGATGTTGAAGTGGCGAGCGATACACCGCATCCGGCGCGGATTGGCTGAACTGCCAGCTGGCGCAGGTAGCAGAGCGGGTAAACTGGCTCGGATT
 AGGGCCGCAAGAAAATATCCGACCGCTTACTGCCGCTGTTTGAACCGTGGGATCTGCCATTGTGAGACATGTATACCCCGTACGCTTCCCGAG
 CGAAAACGGTCTGCGCTGCGGGACGCGCGAATTGAATTATGGCCACACCAAGTGGCGCGGCGACTTCCAGTTCAACATCAGCCGCTACAGTCAACAG
 CAACTGATGGAAACAGCCATCGCCATCTGCTGCACGCGGAAGAAGGCACATGGCTGAATATCGACGGTTTCCATATGGGGATTGGTGGCGACGACT
 CCTGGAGCCCGTCAGTATCGCGGAATCCAGCTGAGCGCCGGTCTGCTACCATACCAAGTGGTCTGGTGTCAAAAATAATAAACCGGGCAGGCCA
 TGTGTCCCGTATTTCCGTAAGGAAATCCATTATGTACTATTTAAAAAACCAAACTTTTGGATGTTGCTGTTTCTTTTACTTTTTTATCATG
 GAGCTTCCGCTTTTCCGATTGGCTACATGACATCAACCATACAGCAAAAGTGATACGGGATTATTTTGGCGCTATTTCTCTGTTCTCGCT
 ATTATTCAACCGCTGTTTGGTCTGTTTCTGACAACTCGAACTGTTTATTGCGACTTATAATGGTTACAATAAAGCAATAGCATCACAATTTTCA
 AAATTTAATTAAGGCCGCGGGATCGATCCCGTCGAGCAGTGTGGTTTTCAAGAGGAAGCAAAAGCCTCTCCACCCAGGCTGGAATGTTTCCACCCA
 ATGTCGAGCAGTGTGGTTTTGCAAGAGGAAGCAAAAGCCTCTCCACCCAGGCTGGAATGTTTCCACCAATGTCGAGCAAAACCCGCCAGCGTCT
 TGTCTTGGCGAATTGCAACACGAGATGAGTGGGGCGCGCGGTCCAGGTCCACTTCGCATATTAAGGTGACGCGTGTGGCTCGAACCCGA
 GCGACCTGACGCAATATGGGATCGGCCATTGAACAAGATGGATTGCACGAGGTTCTCGGCCGCTTGGGTGGAGAGGCTATTCGGCTATGACTG
 GGCACAACAGACAATCGGCTGCTGATGCCGCGTGTCCGGCTGTGAGCGAGGGGCGCCGGTCTTTTGTCAAGACCGACCTGTCGGGTGCC
 TGAATGAATGCAGGACGAGGACGCGCGCTATCTGGCTGGCCACGAGCGGCTTCTTGCAGCTGTGCTCGACGTTGTACTGAAGCGGGAAG
 GGACTGGCTGCTATTGGCGAAGTGCCGGGGCAGGATCTCTGTCTACCTGCTCTGCCGAGAAAGTATCCATCATGGCTGATGCAATGCGGC
 GGCTGCATACGCTTATCCGGCTACCTGCCATTGACACCAAGCGAAACATCGCATCGAGCGAGCAGTACTCGGATGGAAGCCGGTCTTGTGAT
 CAGGATGATCTGGACGAAGAGCATCAGGGGCTCGCGCCAGCCGAAGTGTGCCAGGCTCAAGGCGCGCATGCCGACGGCGAGGATCTCGTGTG
 ACCATGGCGATGCTGCTTCCGCAATATCATGGTGGAAAATGGCCGCTTTCTGGATTATCGACTGTGGCCGGCTGGGTGTGGCGGACCGCTATCA
 GGACATAGCGTTTGGTACCCGTGATATTGCTGAAGAGCTTGGCGCGAATGGGCTGACCGCTTCTCTGCTTACGGTATCGCCGCTCCGATTCTGC
 AGCGCATCGCTTCTATCGCTTCTTGACGAGTCTTCTGAGGGGATCGGCAATAAAAAGACAGAATAAACGCACGGGTGTTGGGTGTTTGTTCGG
 ATCCGAATCTCTGAGGGCGCGCCGCGGAGCGAGGCGGTTACCAATTTGCCCTATGACCATCACCTGGATGGGTGACAGATGTACATCTGTTTGT
 AGTTTGGTAAGAACAGGTGAATTTCTATTCTAAGTCTAAATGTATGAAGCAGAAAGAACCAAAACAAACAAACCAAAACAGAGTAG
 CTGAAAAGTCTGTATCTCAGCTTCCCATCTTCCATTCTGTTGGAGAGTCTAGAAAGGAAGCGAAAGGCGAGGGAATTAGAGTGGTTTTGTGGC
 ATTACGGGCTAGGGAAGAAATATGCTTCAAGATGGAGCAAGCTTGTACTATTTTCCAGTCTCTTCTGAAGCTCTTGGCGATTACCTCACAGAAAT
 GAGGACAAAGAGGGCTTTTAAAGGCTGAGAAGGATTAGGTGGAGGGAGGGGGGCTGTGTGAAGCAGGTTGTGTGGAACAGGAGACATGACAG
 AGCCAATGGGGACACAGTGGAAGGGGAGAGTAGCAAGGAGTAAAGTATACCCCGGAAGGAAGAGACATGCTAGAGTTGGAAGTGTGCC
 CCTCTCTATTGCCATCTGGTAGCGATGCTGTCCAGGACTAAGCAAGATTTAGCCTAAAAAGAGAGCTTTTGAAGGTGGCCAGCCTCTGACTTGG
 ACAGCCTAGGAAGGAGTGCATTACACAGTATGAAGGGGATGAGGAAGAGCTGGTCTTCACTTGGTTCAGCTCAACGGTAACAGAATGAAGTTGTCC
 TTATTGTGCTGTTGGGTGACTCTATCTAAGAAGCTGGCCAGGATGGGGGCTGGGAAAGGCTATCTTACCAAGCAGCACAAGGCTGCAATTTG
 AGGAAGGTGGTAGGGCTACCAAGTTCTGAGGGAAATGCGAGACAGCTGAACAGCGTGGGAACCTTCATCGGCTCTCTGCTCAGGAGAGG
 AGCTCCACGCGACAGCTGAAAGCTCACTCTCATGGCTCAGCGTAGGGGAGAGTAAATAATTAGAAGGATAAATTGTGGGGTGTGTTTGAAGAC
 GGAAGGAGTGGGACAGGAAGATCCAGGAGACTTCATGTGCTTAGGAAGAAAAGTAACTAGGTAGAATATCCAGGGTCAAGGGCCAGGGGTG

Supplementary Figure 2A: FACS raw data –immunophenotyping of naïve animals**KO animal 1**

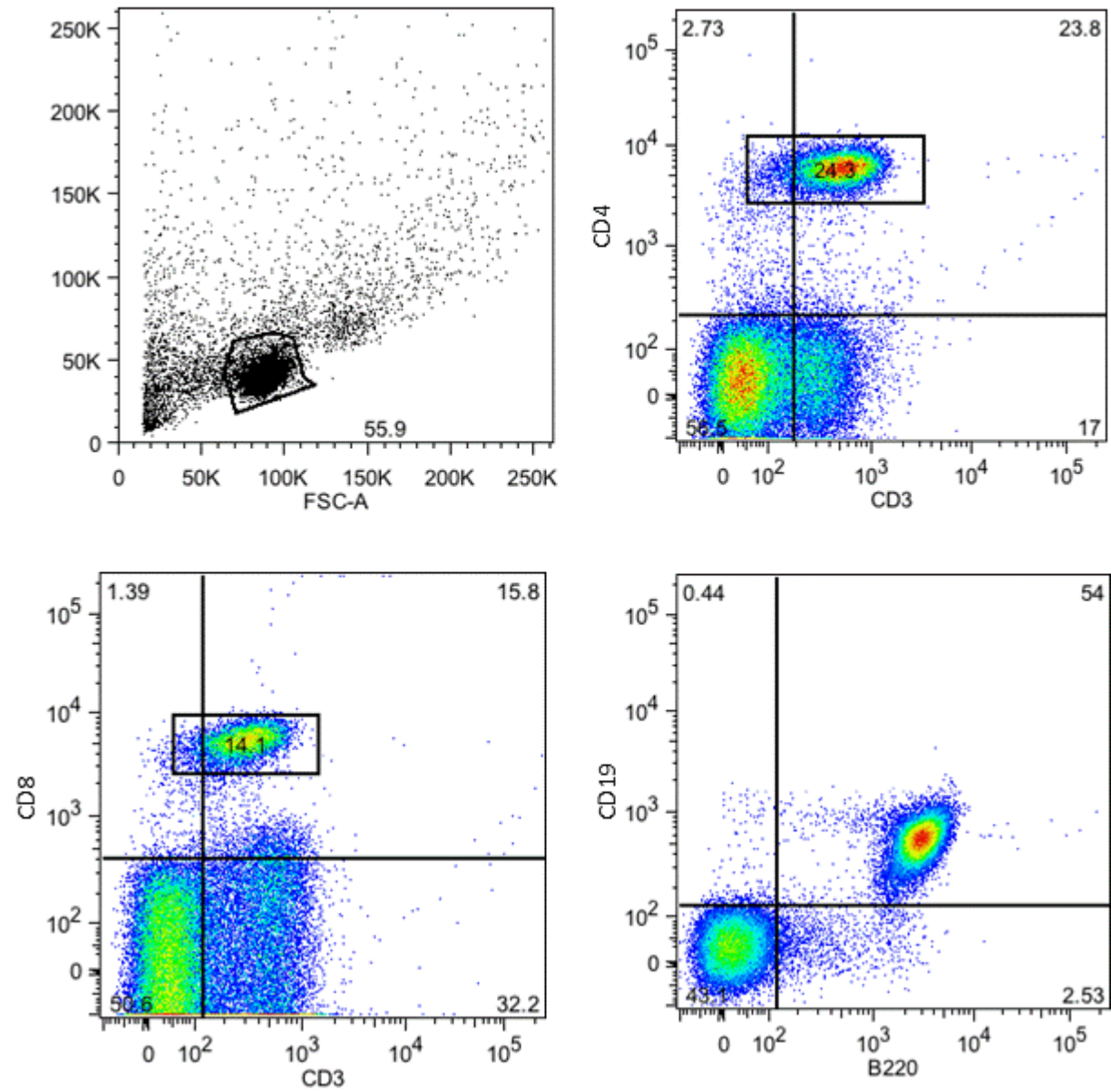
Supplementary Figure 3B: *FACS raw data –immunophenotyping of naïve animals*

KO animal 2



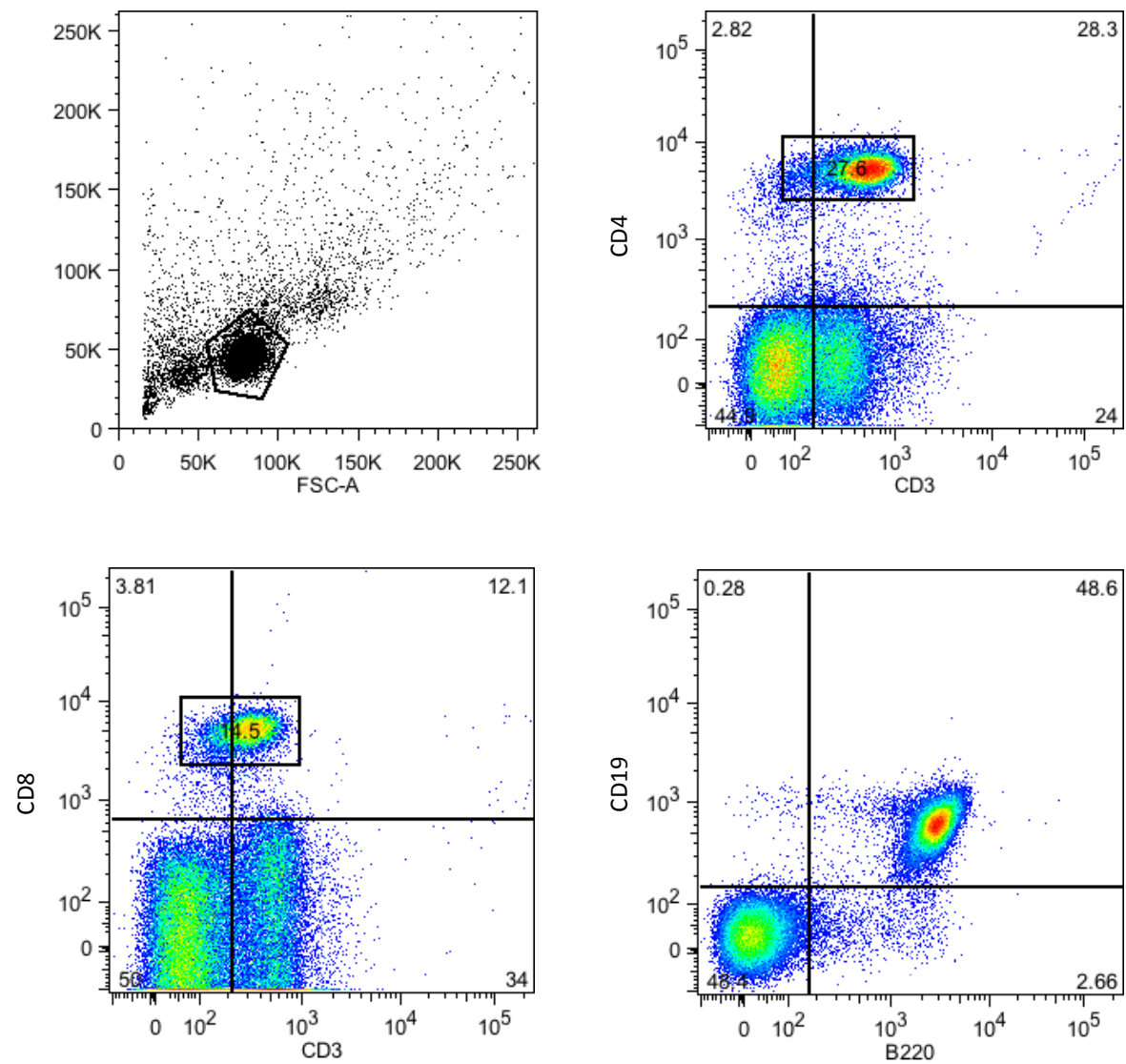
Supplementary Figure 4C: FACS raw data –immunophenotyping of naïve animals

KO animal 3



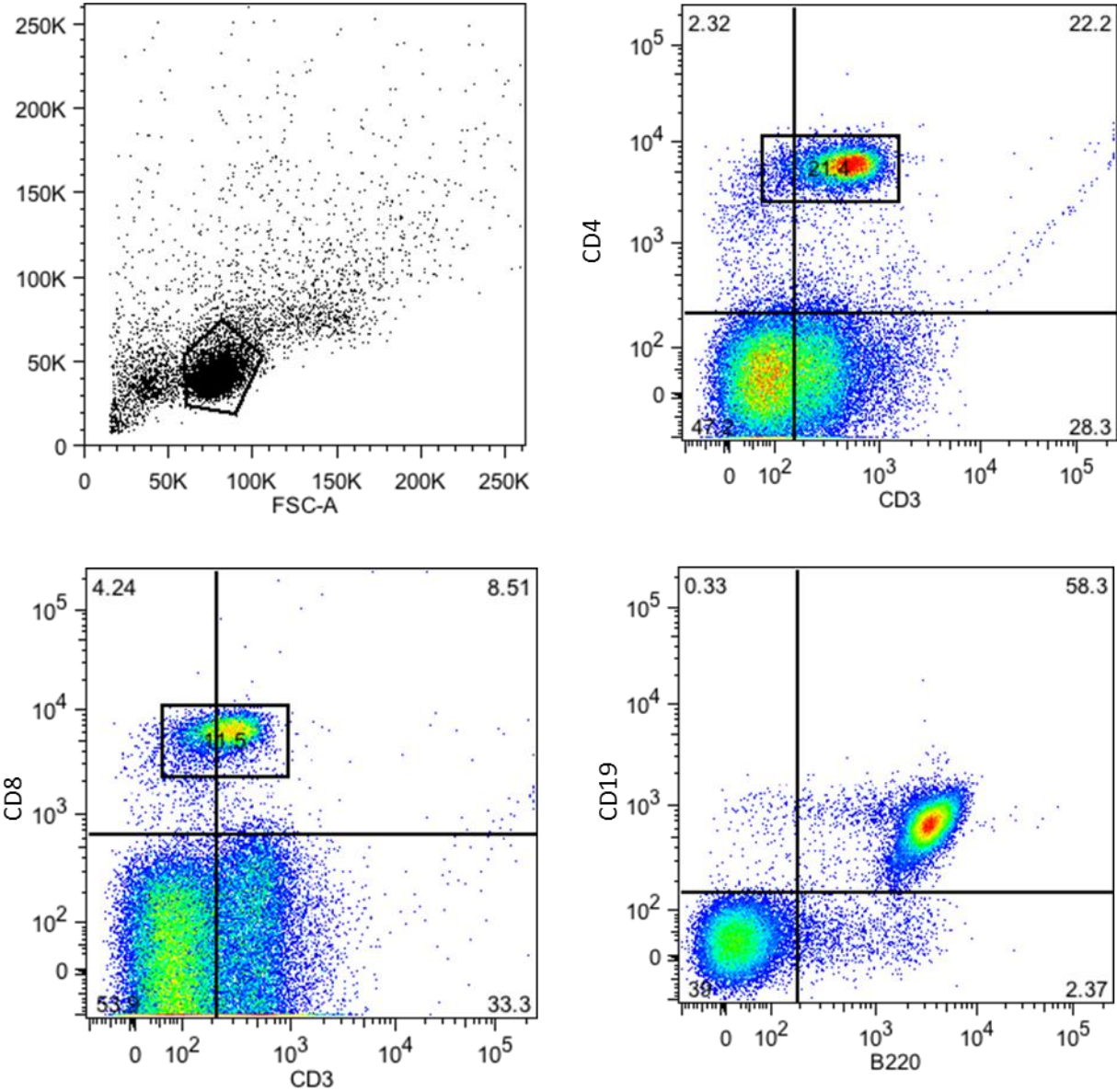
Supplementary Figure 5D: FACS raw data –immunophenotyping of naïve animals

WT animal 1



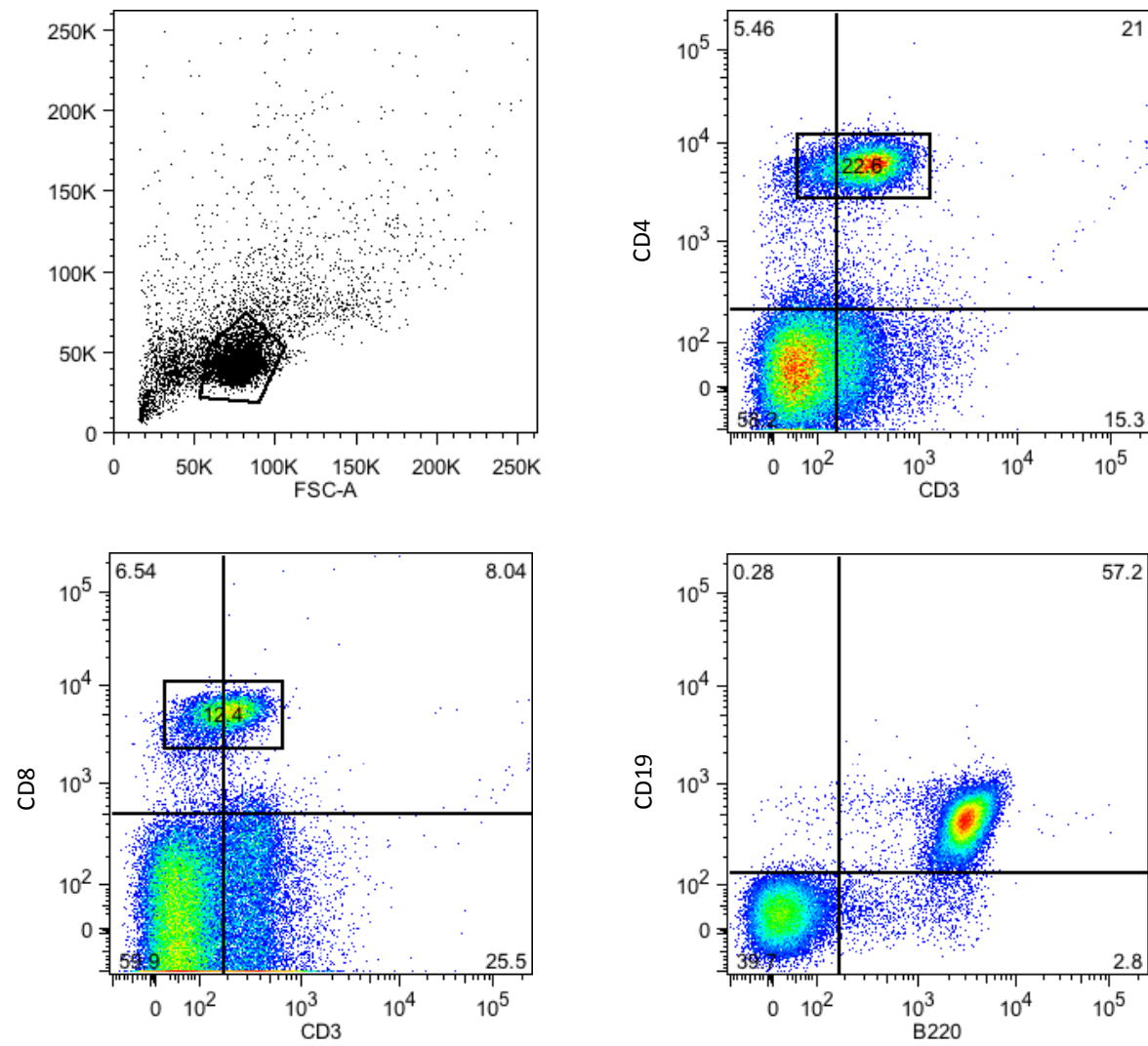
Supplementary Figure 6E: FACS raw data –immunophenotyping of naïve animals

WT animal 2



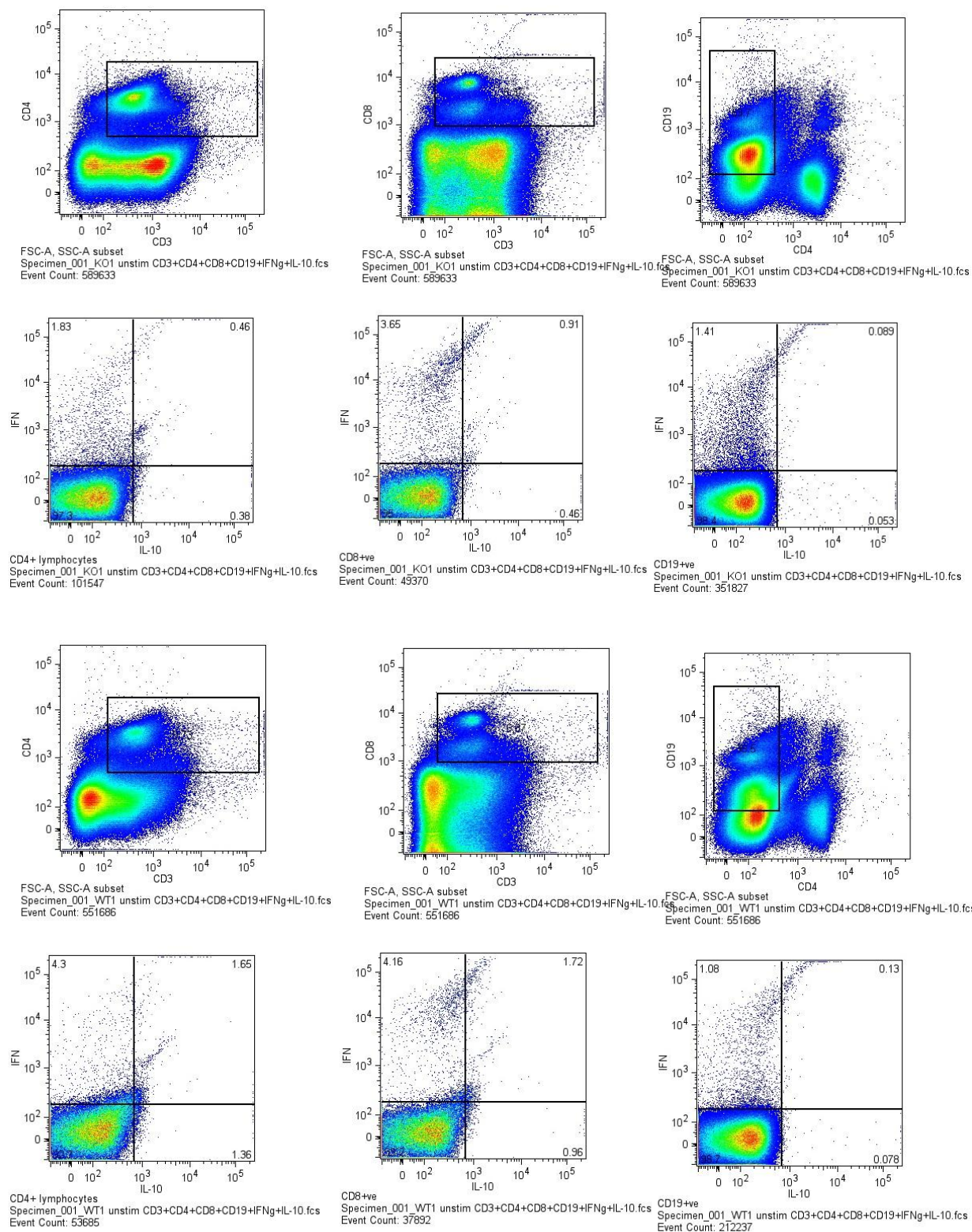
Supplementary Figure 7F: FACS raw data –immunophenotyping of naïve animals

WT animal 3

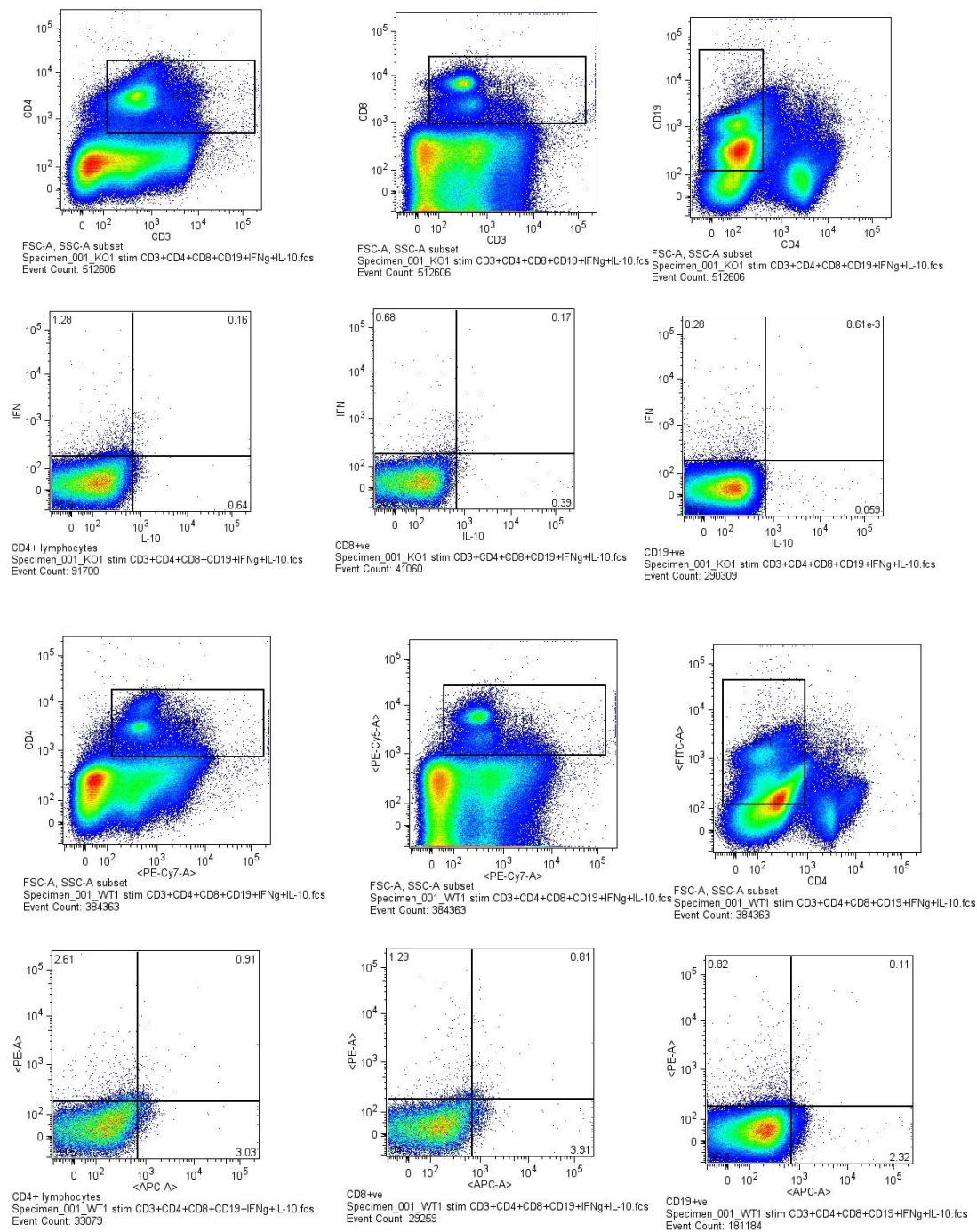


Supplementary Figure 3: FACS raw data – IFN γ and IL-10 cytokine responses in T- and B-cells

from MOG *in vivo* stimulated C57BL/6.GPR55^{-/-} and C57BL/6^{+/+} mice

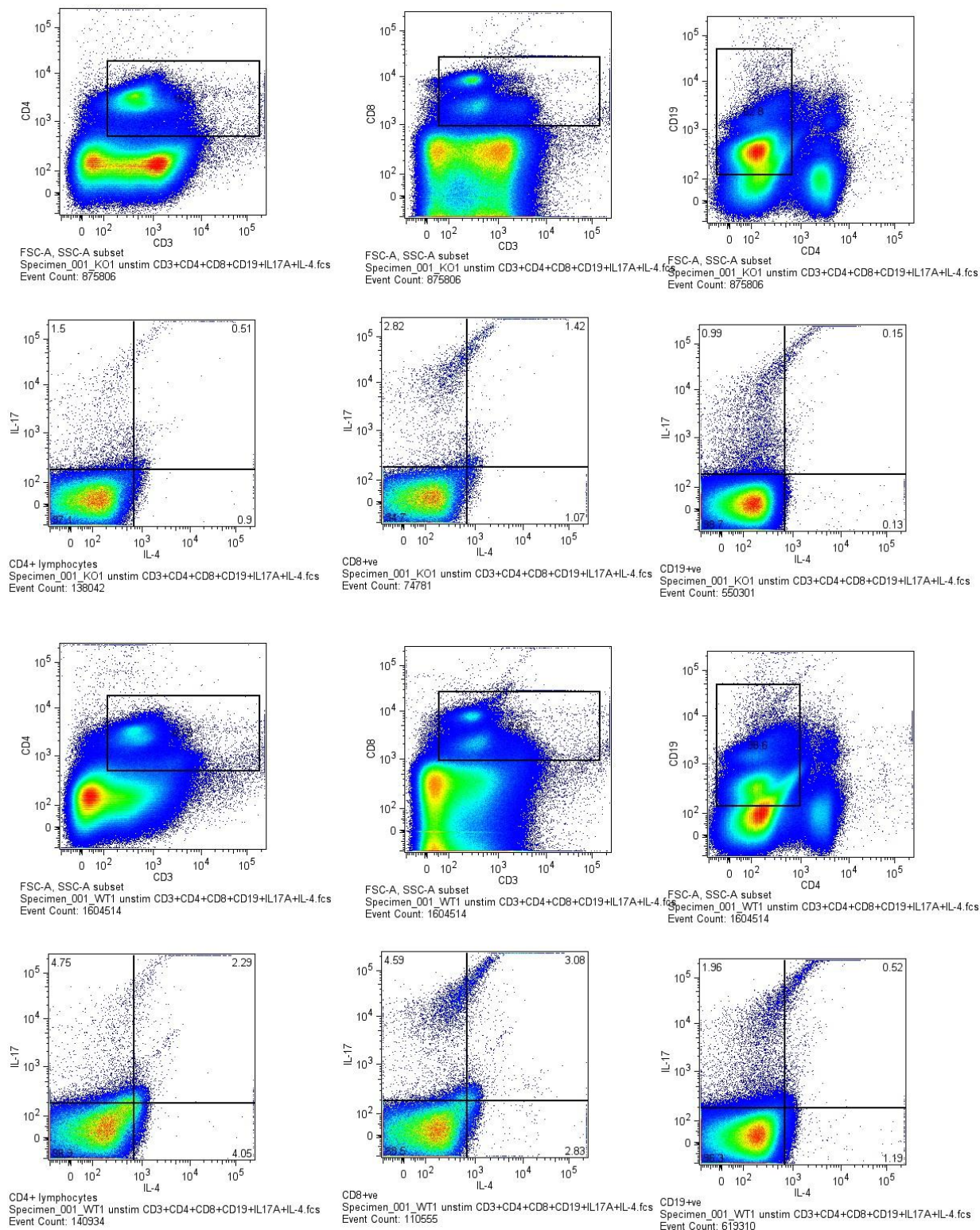


Supplementary Figure 4: FACS raw data – IFN γ and IL-10 cytokine responses in T- and B-cells
from MOG in vivo and in vitro stimulated C57BL/6.GPR55^{-/-} and C57BL/6^{+/+} mice



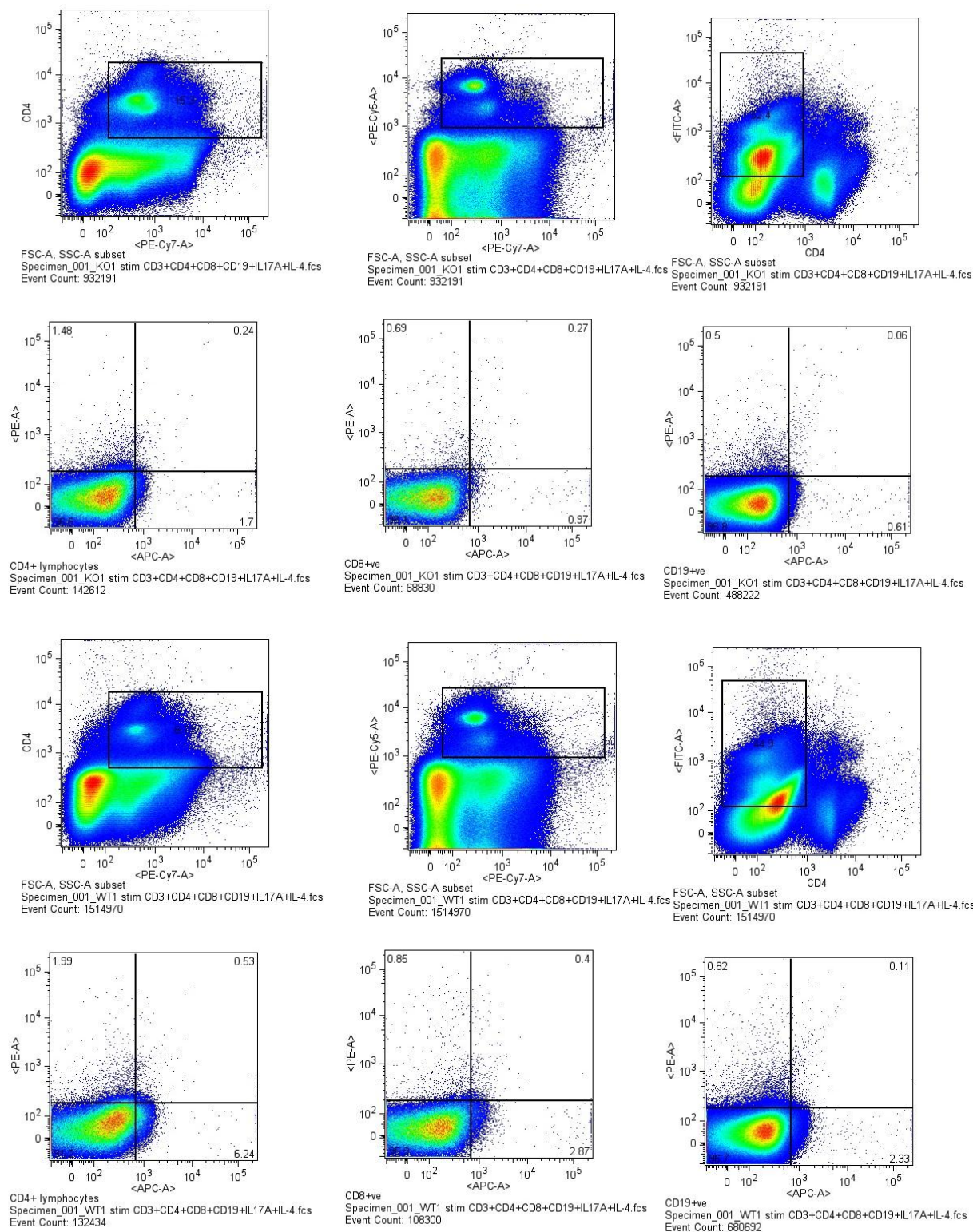
Supplementary Figure 5: FACS raw data – IL-4 and IL-17A cytokine responses in T- and B-cells

from MOG *in vivo* stimulated C57BL/6.GPR55^{-/-} and C57BL/6^{+/+} mice

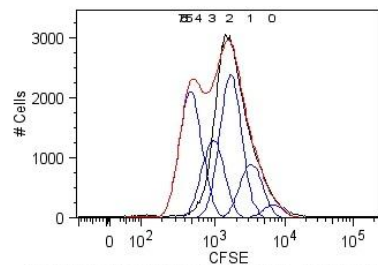


Supplementary Figure 6: FACS raw data – IL-4 and IL-17A cytokine responses in T- and B-cells

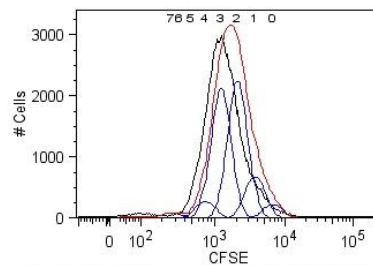
from MOG *in vivo* and *in vitro* stimulated C57BL/6.GPR55^{-/-} and C57BL/6^{+/+} mice



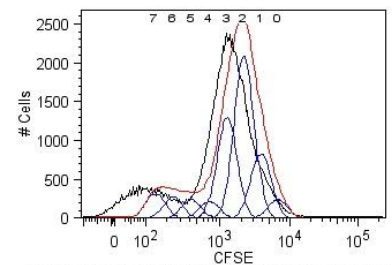
Supplementary Figure 7: FACS raw data –CFSE proliferation assay



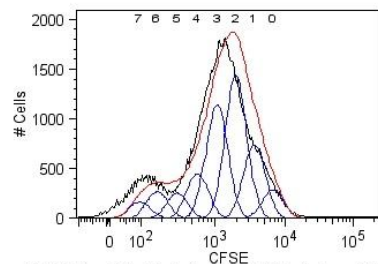
%Divided = 85.2; Div. Index = 1.64; Prol. Index = 1.93.
Proliferation
Specimen_001_CFSE unstimulated KO1.fcs
Event Count: 106461



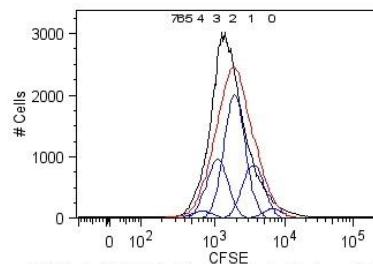
%Divided = 83.4; Div. Index = 1.64; Prol. Index = 1.97.
Proliferation
Specimen_001_CFSE unstimulated KO2.fcs
Event Count: 107482



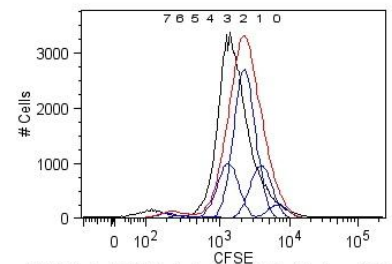
%Divided = 82.1; Div. Index = 1.51; Prol. Index = 1.85.
Proliferation
Specimen_001_CFSE unstimulated KO3.fcs
Event Count: 108804



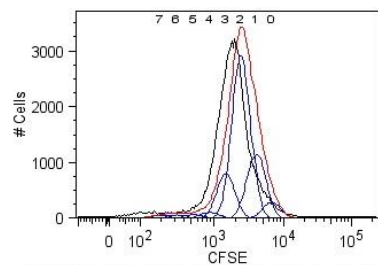
%Divided = 75.8; Div. Index = 1.42; Prol. Index = 1.87.
Proliferation
Specimen_001_CFSE unstimulated WT1.fcs
Event Count: 103504



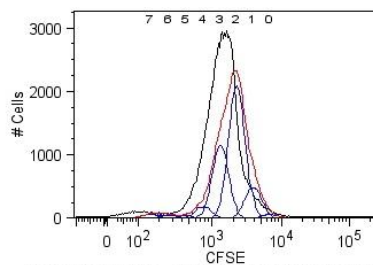
%Divided = 86.7; Div. Index = 1.49; Prol. Index = 1.72.
Proliferation
Specimen_001_CFSE unstimulated WT2.fcs
Event Count: 104452



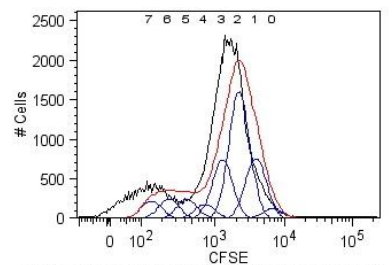
%Divided = 83.8; Div. Index = 1.46; Prol. Index = 1.74.
Proliferation
Specimen_001_CFSE unstimulated WT3.fcs
Event Count: 107150



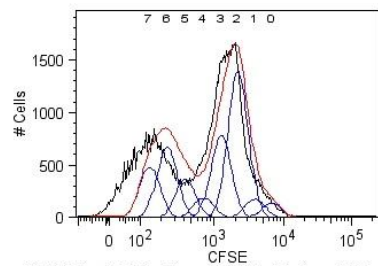
%Divided = 82.8; Div. Index = 1.4; Prol. Index = 1.69.
Proliferation
Specimen_001_CFSE stimulated KO1.fcs
Event Count: 101131



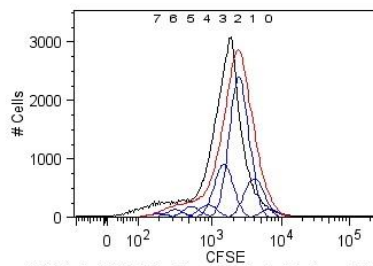
%Divided = 92.5; Div. Index = 1.79; Prol. Index = 1.93.
Proliferation
Specimen_001_CFSE stimulated KO2.fcs
Event Count: 97077



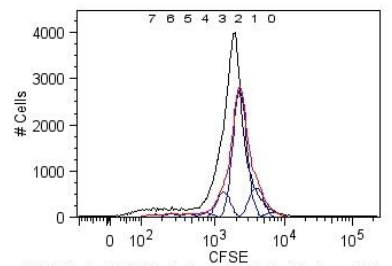
%Divided = 87.4; Div. Index = 1.54; Prol. Index = 1.76.
Proliferation
Specimen_001_CFSE stimulated KO3.fcs
Event Count: 95481



%Divided = 80; Div. Index = 1.78; Prol. Index = 2.22.
Proliferation
Specimen_001_CFSE stimulated WT1.fcs
Event Count: 92800



%Divided = 87.3; Div. Index = 1.61; Prol. Index = 1.85.
Proliferation
Specimen_001_CFSE stimulated WT2.fcs
Event Count: 96261

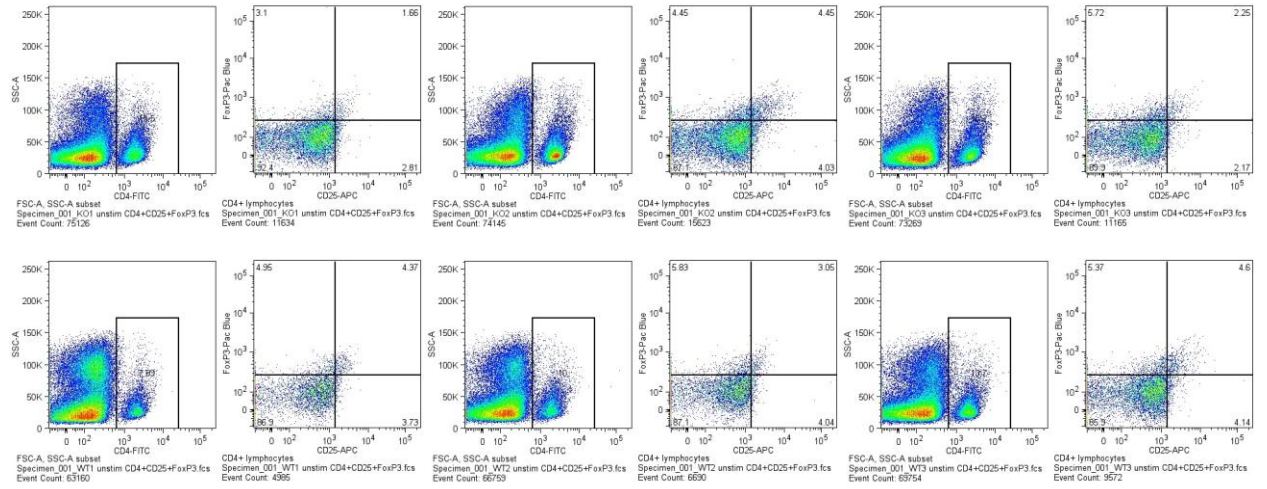


%Divided = 88.5; Div. Index = 1.59; Prol. Index = 1.8.
Proliferation
Specimen_001_CFSE stimulated WT3.fcs
Event Count: 97212

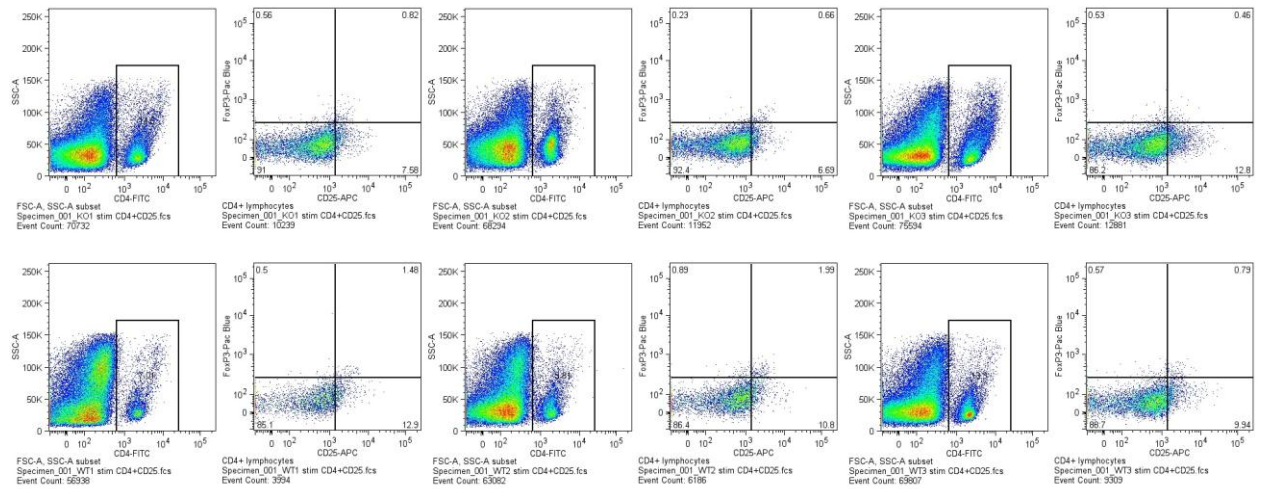
Supplementary Figure 8: FACS raw data – Fox 3P responses in T- and B-cells from MOG

stimulated C57BL/6.GPR55^{-/-} and C57BL/6^{+/+} mice

A. In vivo MOG stimulation

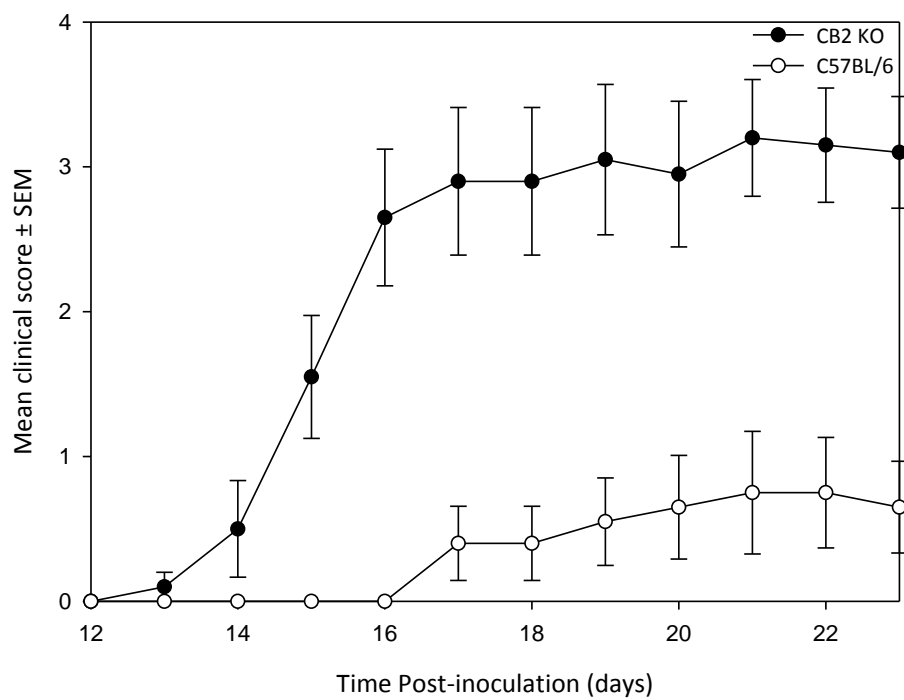


B. In vivo and in vitro MOG stimulation



Supplementary Figure 9: Experimental autoimmune encephalomyelitis in CB₂ knockout animals

A. C57BL/6 mice



B. ABH mice

